

MARIAN VAN DER WIEL

**UPLIFT AND VOLCANISM OF THE SE COLOMBIAN
ANDES IN RELATION TO
NEOGENE SEDIMENTATION IN THE
UPPER MAGDALENA VALLEY**

CENTRALE LANDBOUWCATALOGUS



0000 0456 5624

18n 546064

80951

BIBLIOTHEEK
LANDBOUWUNIVERSITEIT
WAGENINGEN

promotoren: Dr. S.B. Kroonenberg, hoogleraar in de geologie
Dr. H.N.A. Priem, hoogleraar in de isotopen-geochronologie
en planetaire geologie aan de Rijksuniversiteit Utrecht

NN08201, 1452

A.M. VAN DER WIEL

**UPLIFT AND VOLCANISM OF THE SE COLOMBIAN
ANDES IN RELATION TO NEOGENE SEDIMENTATION
IN THE UPPER MAGDALENA VALLEY**

PROEFSCHRIFT

TER VERKRIJGING VAN DE GRAAD VAN
DOCTOR IN DE LANDBOUW- EN MILIEUWETENSCHAPPEN,
OP GEZAG VAN DE RECTOR MAGNIFICUS,
DR. H.C. VAN DER PLAS,
IN HET OPENBAAR TE VERDEDIGEN OP
DINSDAG 26 NOVEMBER 1991
DES NAMIDDAGS TE VIER UUR
IN DE AULA VAN DE LANDBOUWUNIVERSITEIT
TE WAGENINGEN

isn: 546064

Curriculum vitae

Anne Marian van der Wiel was born on the 24th of October 1952 in Amsterdam, The Netherlands. After obtaining her Gymnasium-beta certificate at the Amsterdams Lyceum, she started to study biology at the University of Amsterdam. In September 1979 the Masters degree was obtained with specialization in palynology, and paleontology and plant physiology as additional subjects.

From 1981 to 1983 she performed post-graduate palynological research at the Department of Palynology and Paleo/Actuo-ecology of the Hugo de Vries Laboratory of the University of Amsterdam, under supervision of Prof. Dr. Th. van der Hammen.

In 1983 she obtained a scholarship from the Colombian government for carrying out nine months of post-graduate stratigraphical research on the Highplain of Bogotá in Colombia.

In 1984 she started with the study of geology at the University of Amsterdam, for which she received her degree in February 1987.

In September 1986 she was awarded a scholarship by WOTRO (Netherlands Foundation for the Advancement of Tropical Research) for doing a Ph.D.-project in geology at the Agricultural University of Wageningen in collaboration with the Isotope Laboratory in Amsterdam. The investigation forms part of the ECO-ANDES project.

Stellingen, behorende bij het proefschrift van A.M. van der Wiel

*

1. Een correcte interpretatie van stratigrafische sekties in termen van fossiele riviersystemen is alleen mogelijk wanneer de invloed van de verschillende allocyclische factoren, die bepalend zijn geweest voor de sedimentaire processen, bekend is.

Dit proefschrift

Miall, A.D. (1980) Cyclicity and the facies model concept in fluvial deposits. *Bull. Can. Petrol. Geol.* 281, 59-80.

*

2. Het riviertype dat zich ontwikkelt in actieve, vulkanische gebieden is voornamelijk een functie van de hoeveelheid sediment die aangevoerd wordt en van het tijdsbestek waarin dit gebeurt.

Dit proefschrift

Vessell, R.K. and Davies, D.K. (1981) Nonmarine sedimentation in an active fore arc basin. In: *Recent and ancient nonmarine depositional environments: models for exploration*, (Edited by Ethridge, F.G. and Flores, R.M.), *Soc. Econ. Pal. Mineral. Spec. Publ.* 31, 31-49.

*

3. Het concept van een Partial Annealing Zone is goed bruikbaar bij de interpretatie van splijtingssporen-ouderdommen van zirkoon en titaniet.

Dit proefschrift

*

4. Het samenvallen van de verschillende Neogene opheffingspuls van het Garzón Massief met pauzes in de activiteit van de vulkanische boog (de Centrale Cordillera) is het best te verklaren door vlakke subductie van de Nazca Plaat gedurende die periodes.

Dit proefschrift

*

5. De ouderdom van strike-slip bewegingen langs de East Andean Frontal Fault Zone en de totale horizontale verplaatsing langs de breukzone worden door diverse auteurs overschat.

Dit proefschrift

Giegengack, R. (1984) Late Cenozoic tectonic environments of the Central Venezuelan Andes. In: *The Caribbean-South American plate boundary and regional tectonics*, (Edited by Bonini, W.E. and others), *Geol. Soc. Am. Mem.* 162, 343-364.

Meissnar, R.O., Flueh, E.R., Sibane, F. and Berg, E. (1976) Dynamics of the active plate boundary in southwest Colombia according to recent geophysical measurements. *Tectonophysics* 53, 115-136.

*

6. Bij de interpretatie van pollendiagrammen wordt de rol van de tektoniek vaak ondergewaardeerd.

*

7. Er dient één standaardmodel te komen voor referentielijsten in wetenschappelijke publikaties.

*

8. "Oorlogen zijn de aardbevingen van de geschiedenis, ze ontstaan schijnbaar even onverwacht en ze hebben even diepliggende, onvermijdelijke oorzaken."

A. den Doolaard in een interview in de Volkskrant van vrijdag 19 juli 1991.

*

9. "It is chance and not perfection that rules the world."

Judith Guest, Ordinary people.

*

10. De organisatie van veel grote bedrijven in Nederland lijkt te voldoen aan de tweede hoofdwet van de thermodynamica: de wanorde neemt voortdurend toe.

*

11. Het is kenmerkend voor de arrogantie van het Westen dat Afrika en Zuid-Amerika geen enkele rol spelen in de "nieuwe wereldorde" van Bush.

*

12. Het afbeelden van blote lichaamsdelen van vrouwen in advertenties als middel om de verkoop van bepaalde produkten te stimuleren is inderdaad goedkoop, zoals de nieuwste reclame van een bekend zeepmerk ("goedkoper kan het niet" bij een afbeelding van twee vrouwenborsten) al aangeeft.

*

13. Experimenten moeten reproduceerbaar zijn, dat wil zeggen: ze moeten altijd op dezelfde manier mis gaan.

Wetten van Finagle.

*

NW082201, 1452

Errata

Page 104, fig. 31, and page 123, fig. 35. To the subscript of these figures should be added: Present-day situation is indicated in grey.

Page 158. Table XXIV. First column of numbers, given below the different locations, represents x; second column represents G.

Page 161. Second ainea: (fig. 48, to the right) should be: (fig. 49, to the right).

Page 180. Fig. 54. is fig. 56.

Aan Frans
Aan mijn ouders

A los geólogos de
Ingeominas, Bogotá y
Ingeominas, Ibagué

Contents

ACKNOWLEDGEMENTS

ABSTRACT	1
SAMENVATTING	3
RESUMEN	5

PART 1: INTRODUCTION 9

Chapter I: General information 9

1. Introduction	9
1.1. Scope of the investigation	9
1.2. Background of the investigation	11
2. Location and geography of the study area	13
3. Regional geology	13
3.1. Plate tectonic setting	13
3.2. Regional tectonic setting	14
3.3. Regional geologic history	15
4. Previous literature	18
5. Aerial photographs and topographical sheets	19
5.1. The S. Neiva Basin	19
5.2. Ignimbrite plateau west of the S. Neiva Basin	19
5.3. Volcaniclastic terraces along the Río Páez	19
5.4. Other areas	20

PART 2: THE GARZON MASSIF 21

Chapter II: Precambrian to Recent thermotectonic history of the Garzón Massif (Eastern Cordillera of the Colombian Andes) as revealed by fission track analysis 21 A.M. van der Wiel and P.A.M. Andriessen

1. Introduction	21
2. Analytical Procedures	23
3. Results and discussion	24
3.1. Precambrian history of the massif	28
3.2. Mesozoic history of the massif	28
3.3. Cenozoic history of the massif	35
4. Conclusions	39

PART 3: DEPOSITS OF THE S. NEIVA BASIN 41

Chapter III: Neogene infill of the S. Neiva Basin 41

1. Introduction	41
2. Lithostratigraphy of the Neogene formal and informal rock units	41

2.1. Introduction	41
2.2. La Cira Formation	42
2.3. Honda Formation	42
2.4. Gigante Formation	47
2.5. Las Vueltas formation	59
2.6. Quaternary alluvial fan deposits	60
2.7. Quaternary terraces	62
2.8. Youngest Quaternary alluvial deposits	64
Chapter IV: Geochronology of the Neogene deposits of the S. Neiva Basin	65
A.M. van der Wiel, E.H. Hebeda and P.A.M. Andriessen	
1. Methods	65
2. Results and discussion	66
Chapter V: Petrology of the Honda, Gigante and Las Vueltas formations	71
1. Petrology of the conglomerates and sandstones	71
1.1. Introduction	71
1.2. The pebble counts: method	71
1.3. Results of the pebble counts	73
1.4. The point counts: method	75
1.5. Results of the point counts	78
1.6. Discussion and conclusions	80
2. Petrology of the volcanic deposits of the Gigante Formation	81
2.1. Microscopical description of the volcanic deposits	81
2.2. Chemical composition and classification of the volcanic deposits	83
2.2.1. Methods	83
2.2.2. Results and discussion	83
2.3. Conclusions	88
Chapter VI: Sedimentation patterns of the Honda Formation: influence of uplift and basin subsidence on fluvial deposition	89
A.M. van der Wiel and G.D. van den Bergh	
1. Introduction	89
2. Facies types and facies associations of the Honda Formation	89
2.1. Introduction	89
2.2. Lithofacies types of the Honda Formation	89
2.3. Interpretation of the data in terms of facies associations	91
3. Depositional environments	93
3.1. Distinction of four large-scale sequences in the Honda Formation	93
3.2. Paleocurrent directions	95
3.3. Depositional environments of sequences A and B	95
3.4. Depositional environments of sequence C	96
3.5. Depositional environment of sequence D	97
4. Discussion	98
4.1. Uplift, basin subsidence and volcanism	101
4.2. Climate	103
4.3. Paleogeographic reconstruction and interpretation of river systems	103
5. Conclusions	105

Chapter VII: Sedimentation patterns of the Gigante Formation: influence of volcanism and uplift of the Garzón Massif on fluvial deposition	107
A.M. van der Wiel and G.D. van den Bergh	
1. Introduction	107
2. Facies types and facies associations of the Gigante Formation	107
2.1. Introduction	107
2.2. Lithofacies types of the Gigante Formation	107
2.3. Interpretation of the data in terms of facies associations	109
3. Depositional environments	112
3.1. Paleocurrent directions	115
3.2. Depositional environment of the Neiva Member	115
3.3. Depositional environment of the Los Altares Member	119
3.4. Depositional environment of the Garzón Member	122
4. Discussion	124
5. Paleogeographic reconstruction and conclusions	125
Chapter VIII: Tectonics of the S. Neiva Basin	127
1. Faulting of the basinal sediments	127
2. Folding of the basinal sediments	128
3. Conclusions	128
PART 4: DEPOSITS OUTSIDE THE S. NEIVA BASIN	131
Chapter IX: Deposits of the Gigante Formation outside the S. Neiva Basin	133
1. Introduction	133
2. Lithostratigraphy, geochronology and petrology of the deposits	133
2.1. Quebrada El Arrayán	133
2.1.1. Description	133
2.1.2. Discussion and conclusions	135
2.2. Suaza Valley: "Picuma conglomerate"	135
2.2.1. Description	135
2.2.2. Conclusions	137
Chapter X: Deposits west of the S. Neiva Basin: the Guacacallo and El Carmen formations	139
1. Location of the Guacacallo Formation	139
2. Structure of the ignimbrites	139
2.1. Distinction between flow units and cooling units	139
2.2. Structure of the flow units	140
3. Stratigraphy and field relations of the Guacacallo Formation	143
3.1. Guacacallo-Saladoblanco area	143
3.1.1. Field relations of the Guacacallo and El Carmen formations	143
3.1.2. Descriptions	144
3.1.3. Interpretation	147
3.2. La Argentina-La Plata area	149
3.2.1. Introduction	149
3.2.2. Descriptions	151
3.2.3. Interpretation	152
4. Petrography of the Guacacallo Formation	152
4.1. Welding and devitrification: microscopical and macroscopical observations	152
4.2. Microscopical description of the ignimbrites	153

5. Geochronology of the Guacacallo Formation	153
6. Geochemistry of the Guacacallo Formation	156
6.1. Introduction	156
6.2. Results and discussion	158
7. Possible sources of the ignimbrites	165
8. Conclusions	167
Chapter XI: The volcanoclastic terraces along the Río Páez and downstream part of the Río La Plata	169
1. Introduction	169
2. Location and field relations	169
3. Stratigraphy of the terraces	170
3.1. Stratigraphy of the highest terrace	170
3.2. Stratigraphy of the high, middle and low terraces	172
3.3. Interpretation	172
4. Geochronology of the deposits	176
5. Geochemistry of the deposits	179
6. Conclusions	181
PART V: SYNTHESIS	183
Chapter XII: Overview of the geological history of the S. Neiva Basin and adjacent areas	183
1. Tectonics and sedimentation in the S. Neiva Basin	183
2. Possible causes for the scarcity of erosional products from the Garzón Massif in the sediments of the Honda Formation	185
3. Geological histories of the areas outside the S. Neiva Basin	185
3.1. The area west of the S. Neiva Basin	185
3.2. The Suaza Valley	186
4. Uplift of the Garzón Massif in the light of the plate tectonic setting	186
4.1. Strike-slip movements	186
4.2. Uplift of the massif in relation to igneous activity	188
REFERENCES	191
APPENDICES	199
Appendix 1. Geological map of the S. Neiva Basin	
Appendix 2. Lithology and mineralogy of the dated samples	199
Appendix 3. Gigante Formation, XRFS analyses	203
Appendix 4. Guacacallo Formation, XRFS analyses	205
Appendix 5. Río Páez and Río La Plata terraces, XRFS analyses	207

Acknowledgements

This study was made possible by a grant (W75-265) of the Netherlands Foundation for the Advancement of Tropical Research (WOTRO). The execution of the geological map was financed partly by an extra grant of WOTRO, partly by a grant from the LEB-Fonds (Landbouw Export Bureau 1916/1918) in Wageningen and partly by the Department of Soil Science and Geology of the Agricultural University of Wageningen.

I would like to express my gratitude to all persons who, directly or indirectly, contributed to this study:

In Wageningen, I wish to thank in the very first place the people from the Drafting Department (Sectorale Dienst Produkt- en Biotechnologie). I am very grateful to Pieter Versteeg for drafting the majority of the figures, as well as the topographical base of the geological map, and for making such a nice job of it. I understand that the Drafting Department is looking forward to new orders.

I would like to thank my first promotor, Prof. Dr. S.B. Kroonenberg, for his interest and cooperation and him and his wife, Corry, for the many pleasant evenings I spent at their house. I wish to thank my second promotor Prof. Dr. H.N.A. Priem for critically reading the manuscript.

Furthermore, I wish to express thanks to the staff of the department of Soil Science and Geology of the Agricultural University for their cooperation and for the provision of facilities. In particular I would like to thank Mr. O.D. Jeronimus for making the thin sections, Bram Kuijper for the XRFS analyses, Norbert Lukkezen for taking care of the financial aspects of the investigation, Ton Engelsma for the preparation of the XRFS samples, and Marjan Noordhoek and Joke Cobben for looking after administrative matters.

Preliminary field-work in Colombia was performed by students of the Agricultural University: Angelique, Anne Marie, Ed, Gerard, Joost, Marleen and Pauline. I am much indebted to them for the data, and for their help and enthusiasm.

Also I want to thank the people from the Kartografen Collectief Wageningen, and especially Theo Jacobs and Ko Onderstal, for preparing the final version of the geological map, and the people from the Photography Department (Sectorale Dienst Produkt- en Biotechnologie) for the copy proofs of the figures.

I am grateful to Jos Bakker for his help during my second fieldwork period and for all the times he drove boxes with samples to and from Amsterdam.

In Amsterdam, I would like to thank the staff of the Isotope Laboratory of the Free University, the former NWO-Laboratory for Isotope Geology, for their hospitality and their help with the sample preparation and the chemical analyses, the more so as these activities had to be carried out in a period of great stress and incertitude, caused by the uncertain future of the laboratory.

My sincere thanks go to Paul Andriessen for performing the fission track age determinations, for his interest in the work and for the discussions on the ins and outs of fission track dating and the uplift history of the Garzón Massif.

I would like to thank Erhard Hebeda, John König and Rob Scheveers for performing the K-Ar analyses, Lodewijk Ijlst for his help with the mineral separation, Nel Slimmen and Tineke Vogel for preparing part of the samples for fission track and K-Ar analysis, Piet Remkes, Coos van Belle and Richard Smeets for their help with the K-determinations, Ed Verdurmen for

performing the preliminary K-determinations and Rossana Jong-Loy for taking care of administrative matters.

The lunches with Mary-Ann Broekema, Nel Slimmen and Tineke Vogel, as well as the lunches and outings with the other Ph.D.-students working at the laboratory: Geert-Jan, Jan, José, Jurian, Kay, Paul, Peter and Pieter greatly helped and encouraged me. I wish the Ph.D.-students much success with their work.

Henk Helmers of the Institute for Earth Sciences of the Free University is gratefully acknowledged for critically reading chapters V, X and XI, and for his constructive suggestions to improve them, as well as for his help with some thin sections. Also, I am indebted to Frank Beunk for his assistance with the processing of the XRFS data, to Piet Maaskant for performing the microprobe analyses on Cl and F in apatite, discussed in chapter II, and to Ton Roep for his assistance with some of the point counts.

I am indebted to the people of the Photography Department of the Free University, for the reproduction of the photographs and the people from the Polished Sections Preparation Laboratory for preparing additional thin sections.

I would like to thank Mr. C.R. Snabilié from the Laboratory of Physical Geography (University of Amsterdam) for his advice with regard to the geological map and for designing and drawing figure 35.

I would like to express my gratitude to Sonia Salamanca of the Hugo de Vries Laboratory (University of Amsterdam) for the Spanish translation of the abstract and for all her help and hospitality in Colombia. Furthermore, I am thankful to Jody Dos Santos for her assistance with administrative matters and to Guido van Reenen for his help with MS Word 4.

I am very grateful to Hans Diederix of the ITC in Enschede for his supervision and assistance in the field. Also, I want to thank Ing. J.W. Pikaar of the Photogrammetry Department for the preparation of a topographical base of the eastern part of the fieldwork area.

At the Institute for Earth Sciences in Utrecht I would like to thank my "veldwerkmaatje" Gert van den Bergh for the pleasant and constructive time we spent together in Colombia, and for the many discussions on the sedimentology of the Honda and Gigante Formations. Poppe de Boer is gratefully acknowledged for critically reading chapter VI and for his helpful comments to improve it.

I am much indebted to Prof. Dr. H.-U. Schmincke from Institut für Mineralogie at the Ruhr Universität, Bochum (presently professor at the University of Kiel) for enabling me to participate in two of his courses on volcanoclastic rocks, and to him and Armin Freundt for helping me with the interpretation of several of the thin sections. Also I would like to thank Frank Nadermann for introducing me to the geology of ignimbrites in Gran Canaria, and Peter Bitschene, Jon Dehn and Klaus Mehl for their hospitality during one of my stays in Bochum.

En Colombia me gustaría agradecer sobre todo a la familia de Alba a y Doña Gustavita por considerarme como un miembro de su familia y por toda la ayuda y calor humano que me dieron durante las diferentes épocas en que residí en Bogotá. También querría agradecer a la familia de Espejo, y especialmente a Nohora, por su hospitalidad y por su amistad.

Además, me gustaría agradecer a los geólogos de Ingeominas, Bogotá y Ingeominas, Ibagué por su ayuda, por su interés en mi trabajo y por haber coleccionado muestras de huellas de fisión para mí.

Estoy en deuda con el personal del Centro Interamericano de Fotointerpretación (CIAF), hoy en día parte del Instituto Geográfico de Agustín Codazzi (IGAC), por la hospitalidad que me brindaron y por haberme prestado equipo de campo, y al Dr. R. Pardo por haber preparado parte de la base topográfica del mapa geológico.

Quiero dar las gracias al Sr. Chepe Carillo por haberme transportado en el campo y por su ayuda en los conteos de grasas.

Finally, I wish to express my gratitude to the people who are most near to me: Frans, my parents, my sisters and my friends, for their support. I like to thank Frans also for his patience and forbearance during the last few months, when the work had to be finished.

Abstract

The present study deals with the relation between Neogene uplift and volcanism of the SE Colombian Andes and sedimentation processes in the Upper Magdalena Valley. The southernmost part of the Upper Magdalena Valley, the S. Neiva Basin, is located between latitudes 2°08'-2°31'N and longitudes 75°22'-75°37'W. To the east, the basin borders the Garzón Massif, the southernmost part of the Eastern Cordillera. To the west, the basin borders the terrain of a fold and thrust belt that was active from the Eocene to the L.Miocene. The Central Cordillera is located W of the fold and thrust belt.

Three subinvestigations were carried out. A fission track study was performed on rocks from the Garzón Massif. Sedimentological, stratigraphical and geochronological investigations were accomplished in the S. Neiva Basin as well as in the area of the fold and thrust belt and part of the Central Cordillera. For the sake of clarity, these subinvestigations are discussed in different parts of the thesis.

In part 1 (chapter I) the goals of the investigation are presented. Furthermore, information is given on the regional geology and tectonic setting and on published literature, aerial photographs and topographical sheets, used during the present study.

Part 2 (chapter II) discusses the results of the fission track study of the Precambrian Garzón Massif. Fission track age determinations of apatites, zircons and sphenes revealed that three major uplift and cooling phases occurred. Around 900 Ma ago, an orogeny resulted in ≥ 10 km uplift. Some 100 Ma ago block faulting and differential uplift took place and between ≥ 12 Ma ago and the present time, the Garzón Massif was uplifted some 6.5 km.

Part 3 (chapters III to VIII) deals with the Neogene deposits in the S. Neiva Basin. In chapter III the stratigraphy of the different rock units is discussed. Emphasis is on the Honda Formation, the Gigante Formation and the informal Las Vueltas formation.

In chapter IV the age of these formations is given, established by means of K-Ar and fission track age determinations. The age of the Honda Formation ranges approximately from ≥ 16 Ma to 10-9 Ma; the age of the Gigante Formation from 10-9 Ma to ≤ 6 Ma. The age of the volcanoclastic middle member of the Gigante Formation could be more accurately determined and ranges from 8 Ma to 6.4 Ma. The age of the Las Vueltas formation could not be established, because the rocks do not contain volcanic material. On the grounds of the age of the Gigante Formation and a K-Ar age of ± 1 Ma for the oldest Quaternary terrace, the formation is thought to have an Upper Miocene to Pliocene age.

Chapter V is dedicated to the petrology of the three formations mentioned above. Pebble and point counts show that the sandstones and conglomerates of the Honda Formation and the lower two members of the Gigante Formation have a western provenance. The upper member of the Gigante Formation, however, shows strong admixing of material with an eastern provenance and the Las Vueltas formation consists entirely of erosional products from the Garzón Massif. These facts suggest that the first Neogene uplift phase of the massif ≥ 12 Ma ago had little influence on the deposits of the Honda Formation. They also suggest that a second uplift phase took place, which started during deposition of the upper member of the Gigante Formation and culminated during deposition of the Las Vueltas formation.

In chapter VI the sedimentological characteristics of the Honda Formation are discussed. It appears that during periods of active uplift or volcanism, sediments were deposited by different alluvial fan systems and volcanic aprons, prograding on a broad alluvial plain. During intervening periods of greater volcanic and tectonic quiescence, the alluvial fans or volcanic aprons became much reduced in size, and sediments were laid down by braided and meandering river systems, flowing toward the east on the alluvial plain.

In chapter VII the sedimentological characteristics of the Gigante Formation are treated. The lower and upper members of the formation were deposited by an ancestral Magdalena River, flowing toward the N. During deposition of the middle member, enormous quantities of volcanics flooded the basin, forcing the paleo-Magdalena River to a more eastward position.

Chapter VIII deals with the tectonics of the S. Neiva Basin. The second Neogene uplift pulse of the Garzón Massif, which started around 6.4 Ma ago, coincided with strong SE-NW compression, leading to folding and faulting of the basinal sediments. It is likely that deposition of the upper unit of the Las Vueltas formation resulted from strike-slip movements along the faults in the massif. On the basis of the approximate age of the sediments that underwent wrench-faulting, it is concluded that these movements began in the Pliocene. Wrench faulting appears to have had little influence on the faults within the S. Neiva Basin.

Part 4 of the thesis (chapters IX to XI) is dedicated to deposits outside the S. Neiva Basin, which were investigated during the present study. These deposits comprise two small outcrops of fluvial and volcanoclastic sediments of Gigante age (chapter IX) as well as Pliocene to Quaternary volcanoclastic sediments of the fold and thrust belt area and the Central Cordillera (chapters X and XI).

In chapter IX it is shown that the geological history of the S. Neiva Basin and the Garzón Massif is compatible with the geological history of the Suaza Valley, further to the S, and the Miocene history of the fold and thrust belt area.

Chapter X deals with the Pliocene volcanoclastic deposits in the fold and thrust belt area and the Central Cordillera. These deposits comprise the informal fluvio-volcanic El Carmen formation, with an age of ≥ 3.3 Ma, and the ignimbrites of the Guacacallo Formation, with an age of 2.5 ± 0.2 Ma. The stratigraphical relation between the ignimbrites and the Gigante Formation further to the E, in the S. Neiva Basin, suggests that the basin mainly underwent erosion in the period between ≤ 6 Ma and 2.5 ± 0.2 Ma.

Chapter XI treats the volcanoclastic terraces along the Páez River and the downstream part of the La Plata River. The deposits resulted from two separate influxes of volcanoclastic material, probably from the Nevado del Huila. The older deposits have an age of ± 1 Ma; the younger deposits are dated at < 1 Ma. After deposition, erosional terraces were formed in the sediments. The terraced deposits are lateral equivalents of similar terraces along the part of the Magdalena River, located between Gigante and El Hobo.

In part 5 (chapter XII) a synthesis of the data from the previous chapters is given, and the geological histories of the different areas are integrated in a single model. Furthermore, uplift of the Garzón Massif is discussed in the light of the plate tectonic setting. Neogene uplift phases of the Garzón Massif coincided with cessation of activity of the Central Cordillera volcanic arc. Volcanism was resumed during periods of tectonic quiescence. The fact that Laramide-style uplift was contemporaneous with absence of volcanic activity, suggests that low-angle subduction of part of the Nazca Plate took place. Beside low-angle subduction, however, crustal predisposition to a certain style of uplift probably played a role in determining the style of mountain building. Thus it is likely that Laramide-style uplift of the massif was also influenced by the presence of inherited zones of structural weakness.

Samenvatting

Deze studie houdt zich bezig met de relatie tussen Neogene opheffing en het vulkanisme van de ZO Colombiaanse Andes en sedimentatieprocessen in de Boven Magdalena Vallei. Het zuidelijkste deel van de Boven Magdalena Vallei, het Z. Neiva Bekken, strekt zich uit tussen 2°08'-2°31' Noorderbreedte en 75°22'-75°37' Westerlandte. Aan de oostkant grenst het bekken aan het Garzón Massief, het zuidelijkste deel van de Oostelijke Cordillera. Aan de westzijde begrenst het bekken het terrein van een plooiings- en overschuivingszone die actief was tussen het Eoceen en het Onder Mioceen. De Centrale Cordillera ligt westelijk van deze zone.

Het onderzoek bestaat uit drie deelonderzoeken. Er werd een splijtingssporen analyse gemaakt van gesteenten uit het Garzón Massief. Voorts werd sedimentologisch, stratigrafisch en geochronologisch onderzoek uitgevoerd in the Zuidelijke Neiva Bekken en in een deel van het gebied, dat gevormd wordt door de plooiings- en overschuivingszone en de Centrale Cordillera. Voor de overzichtelijkheid worden deze deelonderzoeken in verschillende delen van het proefschrift behandeld.

In deel 1 (hoofdstuk I) worden de doelstellingen van het onderzoek uiteengezet. Verder wordt informatie gegeven over de regionale geologie en de tektoniek en over bestaande publikaties, gebruikte luchtfoto's en topografische kaarten die bij het onderzoek gebruikt werden.

In deel 2 (hoofdstuk II) worden de resultaten van de splijtingssporen analyses van gesteenten van het Garzón Massief besproken. Ouderdomsbepalingen a.d.h.v. splijtingssporen van apatiet, zircon en titaniet tonen aan, dat er drie grote opheffings- en afkoelingsfasen hebben plaatsgevonden. Rond 900 miljoen jaar geleden resulteerde een orogenese in ≥ 10 km opheffing. Zo'n 100 miljoen jaar geleden vond scholvorming en differentiële opheffing plaats, en tussen ≥ 12 miljoen jaar geleden en het heden werd het Garzón Massief ongeveer 6,5 km opgeheven.

Deel 3 (hoofdstukken III tot en met VIII) behandelt de Neogene afzettingen in het Z. Neiva Bekken. In hoofdstuk III wordt de stratigrafie van de verschillende gesteente eenheden uiteen gezet. De nadruk ligt daarbij op de Honda Formatie, de Gigante Formatie en de informele Las Vueltas formatie.

In hoofdstuk IV worden de ouderdommen van deze formaties gegeven, vastgesteld m.b.v. K-Ar ouderdomsbepalingen en analyses van splijtingssporen. De ouderdom van de Honda Formatie ligt tussen de ≥ 16 en de 10-9 miljoen jaar; de ouderdom van de Gigante Formatie tussen de 10-9 en de ≤ 6 miljoen jaar. De ouderdom van de vulkanoklastische middelste member van de Gigante Formatie kon nauwkeuriger worden bepaald en ligt tussen de 8 en de 6,4 miljoen jaar. De ouderdom van de Las Vueltas formatie kon niet vastgesteld worden, omdat de gesteenten geen vulkanisch materiaal bevatten. Op basis van de ouderdom van de Gigante Formatie en een K-Ar ouderdom van ± 1 miljoen jaar voor het oudste Kwartaire terras, is aangenomen dat de formatie dateert uit het Boven Mioceen en het Pliocceen.

Hoofdstuk V is gewijd aan de petrologie van de drie bovengenoemde formaties. Grind tellingen en punttellingen van zandstenen tonen aan dat de zandstenen en conglomeraten van de Honda Formatie en de onderste twee members van de Gigante Formatie een westelijke herkomst hebben. De gesteenten van de bovenste member van de Gigante Formatie tonen echter duidelijke bijmenging van materiaal uit het oosten en de gesteenten van de Las Vueltas formatie bestaan geheel uit erosieproducten van het Garzón Massief. Deze feiten suggereren dat de eerste Neogene opheffingsfase van het massief, ≥ 12 miljoen jaar geleden, weinig invloed had op de afzettingen van de Honda Formatie. Voorts suggereren ze dat er een tweede opheffingsfase plaatsvond, die begon gedurende afzetting van de bovenste member van de Gigante Formatie en culmineerde gedurende afzetting van de Honda Formatie.

In hoofdstuk VI worden de sedimentologische karakteristieken van de Honda Formatie besproken. Het blijkt dat de sedimenten werden afgezet door verschillende vulkanische en niet-vulkanische puinwaaier-systemen, die zich uitstrekten over een brede alluviale vlakte gedurende periodes van actieve opheffing of vulkanisme. Gedurende tussenliggende periodes van grotere vulkanische en tectonische rust, nam de grootte van de puinwaaiers sterk af, en werd sediment neergelegd door verwilderde en meanderende rivier-systemen, die over de alluviale vlakte naar het oosten stroomden.

In hoofdstuk VII worden de sedimentologische karakteristieken van de Gigante Formatie behandeld. Het blijkt dat de onderste en bovenste members van de formatie zijn afgezet door een paleo-Magdalena Rivier, die naar het N stroomde. Gedurende afzetting van de middelste member overspoelden enorme hoeveelheden vulkanoklastisch sediment het bekken, en dwongen de paleo-Magdalena Rivier om een meer oostelijke positie aan te nemen.

Hoofdstuk VIII behandelt de tektoniek van het Z. Neiva Bekken. De tweede Neogene opheffingspuls van het Garzón Massief, die rond 6,4 miljoen jaar geleden begon, viel samen met sterke ZO-NW compressie, die leidde tot plooiing van en breukvorming in de bekken sedimenten. Het is waarschijnlijk dat de afzetting van de bovenste eenheid van de Las Vueltas formatie het gevolg is van horizontale schuifbewegingen langs breuken in het massief. Op basis van de geschatte ouderdom van de sedimenten, die horizontale schuifbewegingen hebben ondergaan, kan geconcludeerd worden dat de bewegingen in het Pliocen begonnen. De horizontale schuifbewegingen lijken weinig invloed te hebben gehad op de breuken in het Z. Neiva Bekken.

Deel 4 van het proefschrift (hoofdstukken IX tot en met XI) is gewijd aan afzettingen buiten het Z. Neiva Bekken, die gedurende deze studie onderzocht werden. Deze afzettingen omvatten twee kleine ontsluitingen van fluviaatle en vulkanoklastische sedimenten van Gigante ouderdom (hoofdstuk IX) en Pliocene tot Kwartaire vulkanoklastische sedimenten in de plooiings- en overschuivingszone en de Centrale Cordillera (hoofdstukken X en XI).

In hoofdstuk IX wordt aangetoond dat de geologische geschiedenis van het Z. Neiva Bekken en het Garzón Massief compatibel is met de geologische geschiedenis van de Suaza Vallei, verder naar het zuiden, en de Mioceen geschiedenis van de plooiings- en overschuivingszone.

Hoofdstuk X houdt zich bezig met de Pliocene vulkanoklastische afzettingen van de plooiings- en overschuivingszone en de Centrale Cordillera. Deze afzettingen omvatten de informele vulkanoklastische El Carmen formatie, met een ouderdom van $\geq 3,3$ miljoen jaar, en de ignimbrieten van de Guacacallo Formatie, met een ouderdom van $2,5 \pm 0,2$ miljoen jaar. De stratigrafische relatie tussen de ignimbrieten en de Gigante Formatie verder naar het O, in het Z. Neiva Bekken, suggereert dat het bekken voornamelijk erosie heeft ondergaan in de periode tussen ≤ 6 miljoen jaar en $2,5 \pm 0,2$ miljoen jaar geleden.

Hoofdstuk XI behandelt de vulkanoklastische terrassen langs de Páez Rivier en de benedenloop van de La Plata Rivier. De afzettingen zijn het resultaat van twee influxen van vulkanoklastisch materiaal, waarschijnlijk afkomstig van de Huila Vulkaan. De oudere afzettingen hebben een ouderdom van ± 1 miljoen jaar; de jongere zijn gedateerd op ≤ 1 miljoen jaar. Na afzetting van de sedimenten werden er erosieterrassen in gevormd. De geterrasseerde afzettingen zijn het laterale equivalent van gelijksoortige terrassen langs het deel van de Magdalena Rivier dat zich bevindt tussen Gigante en El Hobo.

In deel 5 (hoofdstuk XII) wordt een synthese van de gegevens uit de voorgaande hoofdstukken gegeven en worden de geologische geschiedenissen van de verschillende deelgebieden geïntegreerd in één model. Verder wordt de opheffing van het Garzón Massief besproken in het plaattektonisch kader. De Neogene opheffingsfasen van het massief vielen samen met pauzes in de vulkanische activiteit van de Centrale Cordillera. Vulkanische activiteit vond wel plaats in periodes van tektonische rust. Het feit dat Laramide-stijl opheffing samenviel met afwezigheid van vulkanisme, suggereert dat een deel van de Nazca Plaat onder een lage hoek gesubduceerd werd. Behalve subductie onder een lage hoek lijkt ook predispositie van de korst voor een bepaalde opheffingsstijl mede bepalend voor de stijl van orogenese. Daarom is het waarschijnlijk dat Laramide-stijl opheffing van het massief mede beïnvloed werd door de aanwezigheid van overgeërfde zones van structurele zwakte.

Resumen

El presente estudio trata de la relación entre el levantamiento Neogénico y el volcanismo de la parte SE de los Andes colombianos y los procesos de sedimentación en el valle alto del río Magdalena. El extremo sur del valle alto del Magdalena, es decir la parte sur de la cuenca de Neiva, se encuentra entre las 2°08' y 2°31' de lat. N y 75°22' y 75°37' de long. W. Al oeste la cuenca limita con el Macizo de Garzón, que conforma el extremo sur de la cordillera Oriental. Hacia el este, la cuenca limita con una zona de plegamiento y cabalgamiento que fue activa desde el Eoceno hasta el Mioceno Inferior. La cordillera Central se localiza al W de esta zona.

La investigación se realizó en tres áreas diferentes: En rocas del Macizo de Garzón se llevó a cabo un estudio de huellas de fisión. En la parte S de la cuenca de Neiva se realizaron investigaciones sedimentológicas, estratigráficas y geocronológicas. En un área formada por parte de la zona de plegamiento y cabalgamiento y parte de la cordillera Central se hizo el mismo tipo de estudio. Con el objeto de hacer mayor claridad, cada una de estas regiones se discute en diferentes partes de la tesis.

La primera parte (capítulo 1) presenta los objetivos de la investigación. Además suministra información sobre la geología regional, el contexto tectónico, la literatura disponible y las aerofotografías y los mapas topográficos que se utilizaron.

En la segunda parte se discuten los resultados del estudio de huellas de fisión del Macizo de Garzón de edad Precámbrica. Las dataciones por medio de huellas de fisión de apatitas, zircones y titanitas revelaron la presencia de tres fases principales de levantamiento y enfriamiento. Hace 900 M. A. ciertos procesos orogénicos produjeron un levantamiento de ≥ 10 km. Hace aproximadamente 100 M. A. tuvo lugar un fallamiento en bloques así como un levantamiento diferencial y entre 12 M. A. y el presente el Macizo de Garzón se levantó ± 6.5 km.

La parte 3 (desde el capítulo tercero hasta el octavo inclusive) trata de los depósitos Neogénicos de la parte S de la cuenca de Neiva. En el capítulo III se discute la estratigrafía de las diferentes unidades de roca. Se da especial énfasis a la Formación Honda, la Formación Gigante y la formación (informal) Las Vueltas.

En el capítulo IV se suministran las edades de las formaciones, determinadas por medio de dataciones con K-Ar y por medio de huellas de fisión. La edad de la Formación Honda está entre ≥ 16 M. A. y 10-9 M. A. La edad de la Formación Gigante está entre 10-9 M. A. y ≤ 6 M. A. Fue posible determinar la edad del miembro volcánoclastico intermedio de la Formación Gigante de una forma más precisa, entre 8 y 6.4 M. A. Por el contrario, no fue posible determinar la edad de la formación Las Vueltas debido a que las rocas no contenían material volcánico. Sin embargo, con base en las edades de la Formación Gigante y de la terraza Cuaternaria más vieja, ± 1 M. A., se piensa que la formación Las Vueltas tenga una edad Mioceno Superior a Plioceno.

El capítulo V trata de la petrología de las tres formaciones mencionadas. Los conteos de gravas y de puntos muestran que los conglomerados y las areniscas de la Formación Honda, y de los dos miembros inferiores de la Formación Gigante, tienen una procedencia del oeste. El miembro superior de la Formación Gigante muestra sin embargo una fuerte mezcla de material que procedió tanto del este como del oeste. La formación Las Vueltas consta solamente de productos erosionales del Macizo de Garzón. Estos hechos sugieren que la primera fase del levantamiento Neogénico del Macizo, ≥ 12 M. A., tuvo poca influencia en los depósitos de la Formación Honda. Además sugieren que se inició una segunda fase durante la depositación del miembro superior de la Formación Gigante, la cual culminó durante la sedimentación de la formación Las Vueltas.

En el capítulo VI se discuten las características sedimentológicas de la Formación Honda. Parece ser que los sedimentos se depositaron mediante diferentes sistemas de abanicos aluviales y volcánicos que se progradaron en un amplio plano aluvial durante períodos de levantamiento activo o de volcanismo. Durante períodos de quietud volcánica y tectónica, los abanicos se redujeron mucho en tamaño. Los sedimentos se depositaron mediante sistemas de ríos trezados y meándricos, que corrían hacia el este en el plano aluvial.

En el capítulo VII se tratan las características sedimentológicas de la Formación Gigante. Aparentemente el paleo río Magdalena, que corría hacia el N, depositó los miembros inferior y superior. Durante la depositación del miembro intermedio cantidades enormes de sedimentos volcanoclásticos inundaron la cuenca, forzando el paleo río Magdalena a adoptar una posición más hacia el este.

El capítulo VIII discute la tectónica de la parte sur de la cuenca de Neiva. El segundo pulso Neogénico del levantamiento del Macizo de Garzón, que empezó hace c. 6.4 M. A., coincidió con una compresión fuerte SE-NW, que condujo al plegamiento y fallamiento de los sedimentos de la cuenca. Parece ser que la depositación de la unidad superior de la formación Las Vueltas se produjo debido a movimientos de desplazamiento de rumbo a lo largo de las fallas del Macizo. Con base en la edad aproximada de los sedimentos que estuvieron sujetos a estos movimientos se ha concluido que se iniciaron en el Plioceno. Los movimientos de desplazamiento de rumbo parecen haber tenido poca influencia en el fallamiento dentro de la parte sur de la cuenca de Neiva.

La cuarta parte de esta tesis (capítulos IX a XI) se dedica a algunos depósitos que se encuentran en los alrededores de la parte sur de la cuenca de Neiva. Estos depósitos comprenden dos pequeños afloramientos de sedimentos fluviales y volcanoclásticos de edad Gigante (capítulo IX) así como sedimentos volcanoclásticos de edad Plioceno a Cuaternario, que se encuentran en parte de la zona de plegamiento y cabalgamiento y parte de la cordillera Central (capítulos X y XI).

En el capítulo IX se muestra que la historia geológica de la parte sur de la cuenca de Neiva y del Macizo de Garzón, es compatible con la historia geológica de la cuenca de Suaza, que se encuentra más al sur, y con la historia Miocénica de la zona de plegamiento y cabalgamiento.

El capítulo X concierne a los depósitos volcanoclásticos Pliocénicos que se encuentran en parte de la zona de plegamiento y cabalgamiento y parte de la cordillera Central. Estos depósitos comprenden la formación (informal) fluvio volcánica del Carmen, de edad ≥ 3.3 M. A. y las ignimbritas de la Formación Guacacallo, de edad 2.5 ± 0.2 M. A. La relación estratigráfica entre las ignimbritas y la Formación Gigante más al este, en la parte sur de la cuenca de Neiva, sugiere que esta última estuvo sujeta principalmente a erosión en el período entre ≤ 6 M. A. y 2.5 ± 0.2 M. A.

El capítulo XI trata de las terrazas volcanoclásticas a lo largo del río Páez y de la cuenca inferior del río La Plata. Los depósitos provienen de dos flujos diferentes de material volcanoclástico, probablemente del volcán del Huila. Los depósitos más viejos tienen una edad de ± 1 M. A. Los depósitos más jóvenes tienen una edad de < 1 M. A. Después de la depositación se formaron terrazas erosionales en los sedimentos. Las terrazas son equivalentes laterales de terrazas similares que se encuentran a lo largo de la parte del río Magdalena entre Gigante y El Hobo.

En la quinta parte (capítulo XII) se presenta una síntesis de los datos suministrados en los capítulos anteriores. La historia geológica de las diferentes áreas se integra en un solo modelo. Además se discute el levantamiento del Macizo de Garzón a la luz del contexto de placas tectónicas. Las fases de levantamiento Neogénico del Macizo de Garzón coincidieron con la cesación de la actividad del arco volcánico de la cordillera Central. El volcanismo se reinició durante períodos de quietud tectónica. El hecho de que el levantamiento de estilo Laramide sea contemporáneo con la ausencia de actividad volcánica, sugiere que tuvo lugar una subducción en ángulo bajo de una parte de la placa Nazca. Además de este tipo de subducción la predisposición de la corteza a cierto estilo de levantamiento probablemente juega un papel importante en la determinación del estilo de orogénesis. Parece ser que el estilo Laramide de levantamiento del Macizo estuvo influenciado también por la presencia de zonas de debilidad estructural heredada.

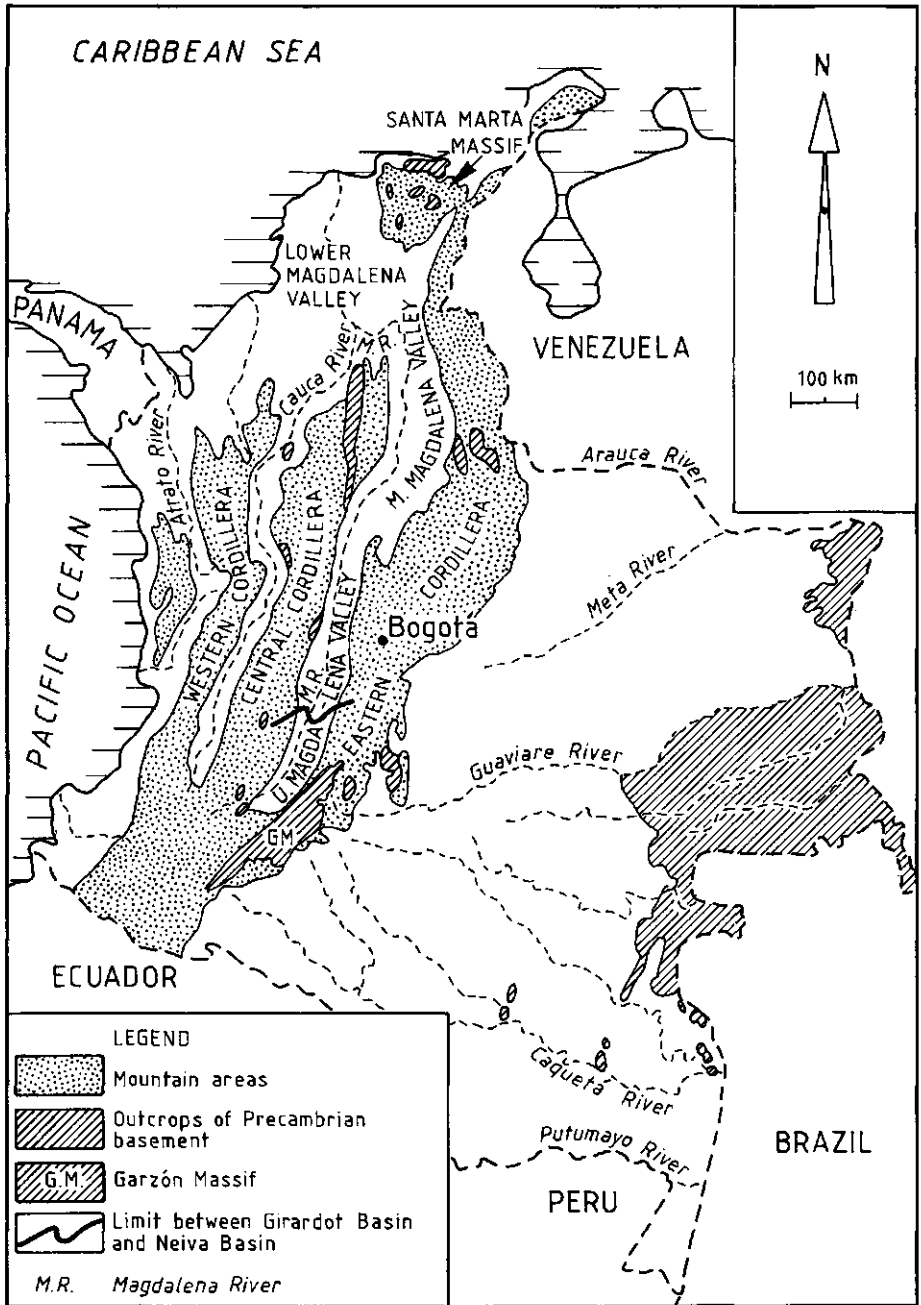


Fig. 1. Location of the Garzón Massif and other Precambrian outcrops in Colombia. Precambrian rocks in the Colombian Andes belong mainly to the Garzón-Santa Marta Granulite Belt. Precambrian outcrops E of this belt belong mainly to the Guiana Shield. Map is based on figures by Kroonenberg (1982a, fig. 1) and Van Houten and Travis (1976, fig. 2).

PART 1

INTRODUCTION

Chapter I

General information

1 Introduction

1.1. Scope of the investigation

This thesis presents the integrated results of a fission track study of the Precambrian Garzón Massif and a sedimentological/geochronological study of the adjacent southern Neiva Basin and surrounding areas, situated in the Department of Huila in the south of Andean Colombia (figs. 1 and 2).

The main goal of the investigation was to reconstruct the Neogene uplift history of the Garzón Massif, which is the southernmost extension of the Eastern Cordillera of the Colombian Andes. In order to fulfill this purpose three subinvestigations were carried out:

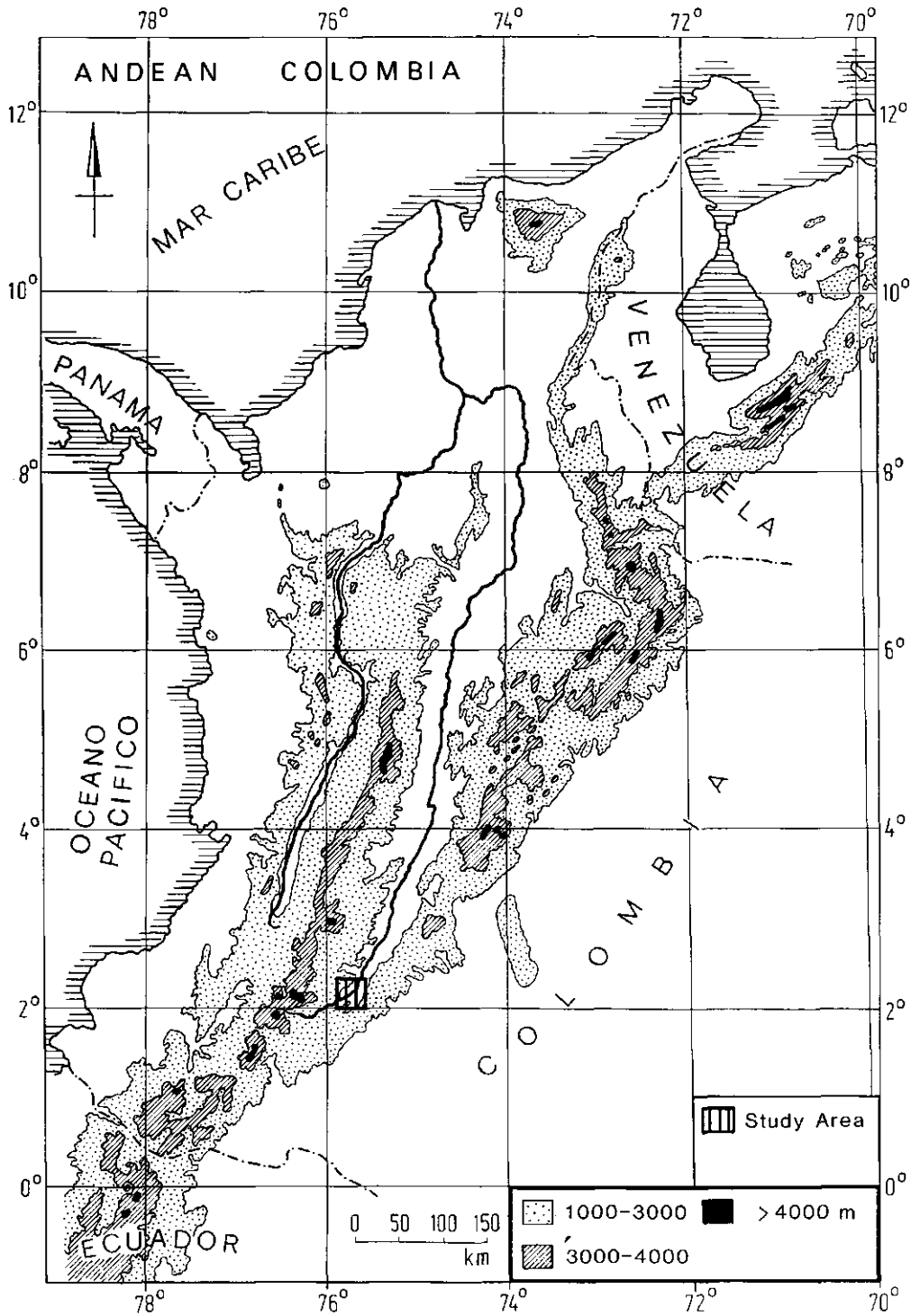
- In the first place the uplift and cooling history of the Garzón Massif was reconstructed on the basis of fission track age determinations of apatites, zircons and sphenes from three series of samples, collected at different localities within the massif. This subinvestigation took place at the Isotope Laboratory of the Institute for Earth Sciences at the Free University in Amsterdam under supervision of Dr. P.A.M. Andriessen.

- To supplement and check the results of the first subinvestigation, the Miocene to Recent sedimentary infill of the adjacent S. Neiva Basin, which forms part of the Upper Magdalena Valley (figs. 1, 2) was studied. In this way the influence of the uplift of the massif on the basin could be assessed.

- Because Pliocene and Pleistocene volcanoclastic deposits are best developed W of the S. Neiva Basin, this area was studied as well, in order to obtain information on the younger geological history of the area. Pliocene volcanoclastic deposits are found W of the La Plata and Páez Valleys, Pleistocene volcanoclastic terraces are present along the downstream part of the La Plata River and along the Páez River (fig. 3).

The latter two subinvestigations were carried out at the Department of Soil Science and Geology of the Agricultural University of Wageningen under supervision of Prof. Dr. S.B. Kroonenberg.

While performing the work on the S. Neiva Basin, it became increasingly clear that Miocene uplift of the Garzón Massif had had relatively little effect on the basin fill, but that sedimentary processes within the basin had been strongly influenced by different Miocene tectonic phases of



the Central Cordillera and by activity of the Central Cordillera volcanic arc. Therefore, the second goal of the investigation became to explain the sedimentation patterns found in the S. Neiva Basin in terms of different combinations and intensities of these external controls and to reconstruct the sedimentary paleo-environments in which the sediments were deposited.

1. 2. Background of the investigation

In Colombia the present-day tropical andean ecosystems show an altitudinal zonation on the slopes of the three cordilleras of the Andes. The distribution of these vegetation belts is largely determined by the mean annual temperature, and, to a lesser extent, by the mean annual precipitation. Cuatrecasas (1958) distinguished two main vegetation belts, *i.e.* a lower neotropical forest belt and a higher páramo belt which is found above the neotropical belt at altitudes above 3300-3800 m. The neotropical forest belt may be further subdivided into a lower tropical forest belt, a subandean forest belt and an andean forest belt, respectively. In fig. 2 the limit between the páramo belt and the neotropical forest belt, as it is found nowadays in the Colombian Andes, approximately coincides with the 3000 m contour line in the E. Cordillera and the 4000 m contour line in the C. Cordillera.

It appears that immigration of species pertaining to either of the two main vegetation belts and the development and evolution of the endemic subandean, andean and páramo elements are strongly correlated with the tectonic and climatic history of the Colombian Andes:

- Immigration of Holarctic species from the North-American continent became possible after the closure of the Panamanian isthmus some 3 Ma ago. This closure resulted from continuous eastward motion of the Caribbean Plate, causing collision of an island arc (the Panamanian isthmus), located at the western border of the Caribbean Plate, with the South American continent (Sykes *et al.*, 1982; Mann and Burke, 1984).

- Van der Hammen and Cleef (1986) suggested that part of the endemic elements of the páramo belt evolved from preexisting neotropical lowland biota which gradually adapted to lower temperatures when uplift of the Andean mountain chains took place and climatic conditions deteriorated as a result of the Pleistocene glaciations.

For these reasons it is of interest to know when the different cordilleras of the Colombian Andes were uplifted. The last few years several publications dealing with the age of the uplift of the Eastern Cordillera at the latitude of the Sabana de Bogotá have appeared (Hooghiemstra, 1984; Helmens *et al.*, 1990; Andriessen *et al.*, in prep.). The latest data indicate that uplift of this part of the Eastern Cordillera took place between 5-3.5 Ma ago (Helmens *et al.*, 1990). Uplift was dated with the aid of radiometric age determinations on syn- and post-uplift sediments and palynological data. In order to supplement these results and to determine whether Neogene uplift of the Eastern Cordillera was simultaneous over its entire length, the uplift history of the southern part of the Eastern Cordillera was reconstructed with geological methods during the present investigation.

The investigation was carried out as part of the ECO-ANDES project, a multidisciplinary cooperative project involving both Colombian and Dutch institutions. The project was started in 1980 as the natural sequel to over thirty years of palynological and paleobotanical research of the Colombian Andes, initiated by Prof. Dr. Th. van der Hammen, former professor of the Department of Palynology and Paleo/Actuo-ecology of the Hugo de Vries Laboratory of the University of Amsterdam. The two main purposes of the project are to reconstruct the Late Tertiary to Quaternary vegetational and climatic history of the Colombian Andes and to obtain a better understanding of the structure, functioning and evolution of tropical montane ecosystems.

In the framework of the ECO-ANDES I project, three E-W transects through the northern part of the Colombian Andes were made. Along these transects, geological, geomorphological,

Fig. 2. Topography of the Colombian Andes. The limit between the neotropical forest belt and the páramo belt coincides with the timber line, which lies at an average elevation of ± 3300 m in the E. Cordillera and an average elevation of ± 3800 m in the C. Cordillera. The entire study area (including part of the Garzón Massif, the S. Neiva Basin and the area W of the S. Neiva Basin) is indicated by the vertically striped square.

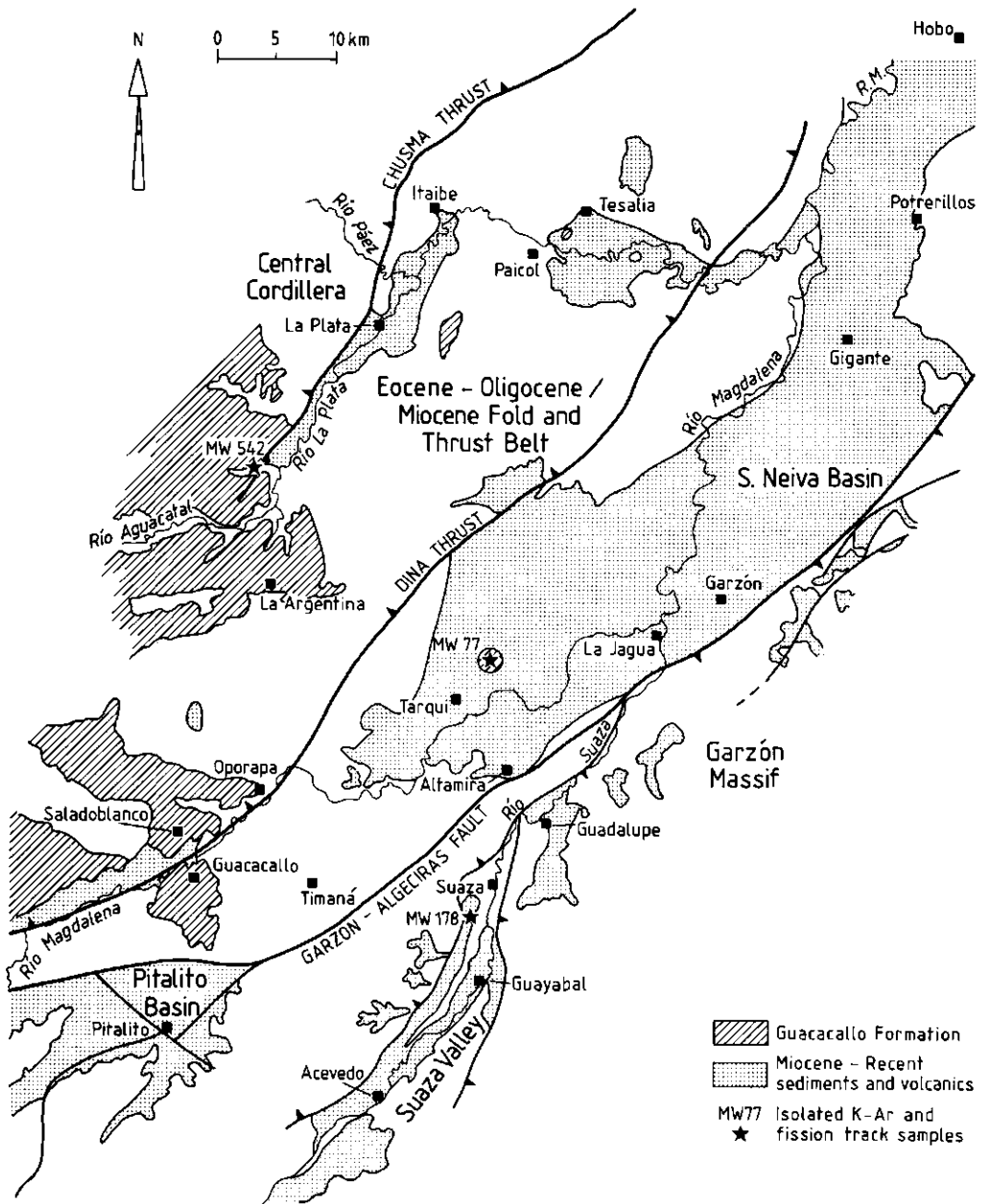


Fig. 3. Neogene deposits of the S. Neiva Basin and adjacent areas. The basin is delimited by the Dina Thrust (easternmost expression of the Chusma fault system) in the west and the Garzón-Algeciras Fault (westernmost expression of the Garzón-Suaza fault system) in the east.

pedological, vegetational, palynological and climatological data were gathered and studied. The present study forms part of the ECO-ANDES II project. The results may be integrated in the planned transect through the southern part of the Colombian Andes.

2. Location and geography of the study area

The Colombian Andes consists of three separate mountain chains, *i.e.* from west to east, the Western, Central and Eastern Cordilleras (fig. 1). In the south of Colombia, the Central and Eastern Cordilleras unite to form a single mountain chain, the Central Cordillera. Further north, the two chains are separated by the Magdalena Valley.

The Garzón Massif forms the southern part of the Eastern Cordillera and borders the upper part of the Magdalena Valley called the Neiva Basin (figs. 1, 2). The massif is located between longitudes 74°30' and 77°30'W and latitudes 1°00' and 3°10'N. The greater part of the massif lies between 1000-2500 m altitude, but in the surroundings of Algeciras, E of the town of Neiva, peaks of more than 3000 m are found.

The second study area covers the southern part of the Neiva Basin, and is approximately delimited by the towns of Potrerillos in the north and La Jagua in the south (fig. 3; lat. 2°08'-2°31'N, long. 75°22'-75°37'W). The total area under study comprises 900 km². The elevation of the area varies between 600-700 m along the Río Magdalena to 1600 m in the mountainous terrains further away from the river.

The third study area covers part of the ignimbrite plateau between the village of Guacacallo and the town of La Plata, as well as the area along the downstream part of the La Plata River and along the Páez River up to its confluence with the Magdalena River. This area is located approximately between longitudes 75°40'-76°10'W and latitudes 2°00'-2°30'N. The volcanoclastic deposits of the ignimbrite plateau are found at elevations ranging between 1300-2000 m; the volcanoclastic terraces along the Páez and La Plata Rivers lie at elevations of 650-1000 m above sea-level.

3. Regional geology

3.1. Plate tectonic setting

The three mountain chains of the Colombian Andes are thought to have formed as a result of the convergence of several subsequently formed oceanic plates and the continental South American Plate in a non-collisional "Andean-type" setting.

Seafloor spreading in the Pacific started at least as early as the Jurassic (Mooney, 1980; Duncan and Hargraves, 1984). On the grounds of geological evidence presented by various authors, Mégard (1984) suggests that in Peru subduction started in the Liassic. In Colombia, data on the initiation of subduction are scarce. Duncan and Hargraves (1984) are of the opinion that at least from 140 Ma onwards the oceanic Phoenix Plate had some kind of interaction with the continental South American Plate. The nature of the interaction between these plates, however, is unclear: either the Phoenix Plate was subducted beneath South America, or right-lateral transcurrent motion took place at the contact between the plates (fig. 4, to the left). Further to the north, the oceanic Farallon Plate was being subducted below the North American Plate. The Farallon Plate and the Phoenix Plate were separated by the Farallon-Phoenix Ridge (fig. 4). Spreading on the ridge stopped ± 119 Ma ago as spreading began in the equatorial Atlantic, and the Farallon and Phoenix Plates together formed a single plate: the Farallon Plate (fig. 4). Since the cessation of spreading on the Farallon-Phoenix Ridge, the South American Plate has converged with the Farallon Plate. Some 25 Ma ago the Farallon Plate split up in the Cocos Plate to the north and the Nazca Plate to the south (Duncan and Hargraves, 1984; fig. 4).

Andean evolution may be divided into long periods of relative tectonic quiescence and short orogenic periods, corresponding with the main phases of intraplate compressive deformation, which alternated or coincided with sedimentation, plutonism and volcanic activity. The main manifestations of this compression are uplift and crustal shortening, leading to folding and faulting. The strong coupling between the oceanic plate and the overriding South American

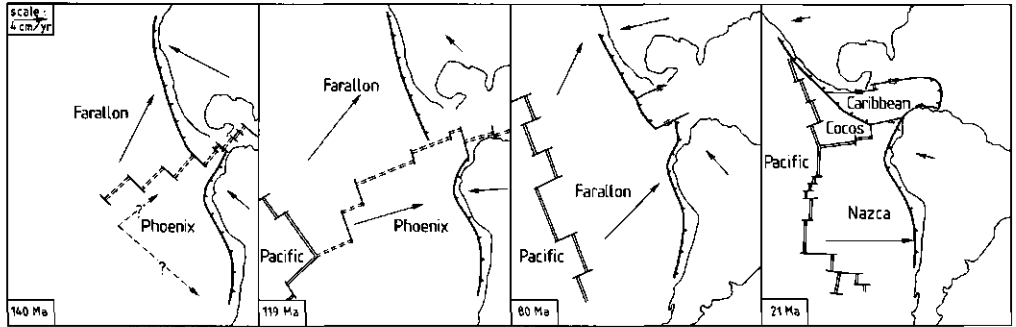


Fig. 4. Reconstruction of the oceanic and continental plate positions around the S. American continent during the last 140 Ma in the hotspot reference frame. Adapted from Duncan and Hargraves (1984).

Plate, caused by the relatively low angle of the subducting plate (at present the dip of the Nazca Plate varies between 5-35°: Meissnar *et al.*, 1976; Pennington, 1981; Jordan *et al.*, 1983a, b), lead to deformation and uplift over distances up to 700 km inland from the original subduction zone.

3. 2 Regional tectonic setting

The Central and Eastern Cordillera of the Colombian Andes are separated by the Magdalena Valley, a broad tectonic depression. Van Houten and Travis (1968) subdivided the upper part of this valley into three basins: from south to north the Neiva Basin, Giradot Basin and Honda Basin respectively, the southernmost two of which have been indicated in fig. 1.

The Neiva Basin is a NE-SW trending basin which is separated from the Girardot Basin by the northeast trending Natagaima intrabasinal fold. To the south, the Neiva Basin ceases to exist as a single tectonic unit south of the town of Timaná, where it is bounded by the convergence of the Central and Eastern Cordilleras (fig. 2). To the east and west, the basin is bounded by reverse faults:

- On the east side the Garzón-Algeciras Fault separates the basin from the Garzón Massif, a large regional basement uplift (figs. 3, 5). The Garzón-Algeciras Fault is an eastward dipping Laramide-style high-angle reverse fault (Butler, 1983) along which right-lateral strike-slip is taking place, probably since the Pliocene. This fault forms part of the Garzón-Suaza fault system (Bakker, 1990). On a larger scale, it is the westernmost fault of the Eastern Andean Frontal Fault Zone which separates the Andean block from the Guiana Shield (Pennington, 1981; see also fig. 57, p.187). This NE-striking fault zone can be followed along the entire length of the Eastern Cordillera up to the Boconó Fault in the Serranía de Mérida (Venezuelan Andes) in the north. To the south, the continuation of the fault zone is found in the Central Cordillera of Ecuador (fig. 57).

- In the west the Neiva Basin is separated from the Central Cordillera by a series of westward dipping thrusts from a Tertiary retro-arc fold and thrust belt, the Chusma fault system (Butler, 1983; Butler and Schamel, 1988; see also fig. 5). This fault system, which developed during the late Eocene-Oligocene, is responsible for some 17-19% of crustal shortening between its westernmost continuation (the Chusma Fault) and the Garzón-Algeciras Fault (Butler and Schamel, 1988).

The Garzón Massif, the southernmost part of the Eastern Cordillera (fig. 1), consists of Precambrian metamorphic rocks which are intruded by Jurassic plutons (Kroonenberg, 1982a, b; Kroonenberg and Diederix, 1982). The massif forms a vertical upthrust block bounded by outward facing thrust belts.

In the southeastern part of the massif and at the convergence of the massif with the Central Cordillera, a series of intramontane basins is found, of which the Suaza Basin is the

southernmost one (fig. 3). The basins are delimited by faults belonging to the Garzón-Suaza fault system. Further to the west another, isolated intramontane basin is present, the Pitalito Basin, a neotectonic strike-slip basin formed by right-lateral movements along the Garzón-Suaza fault system (Bakker, 1990).

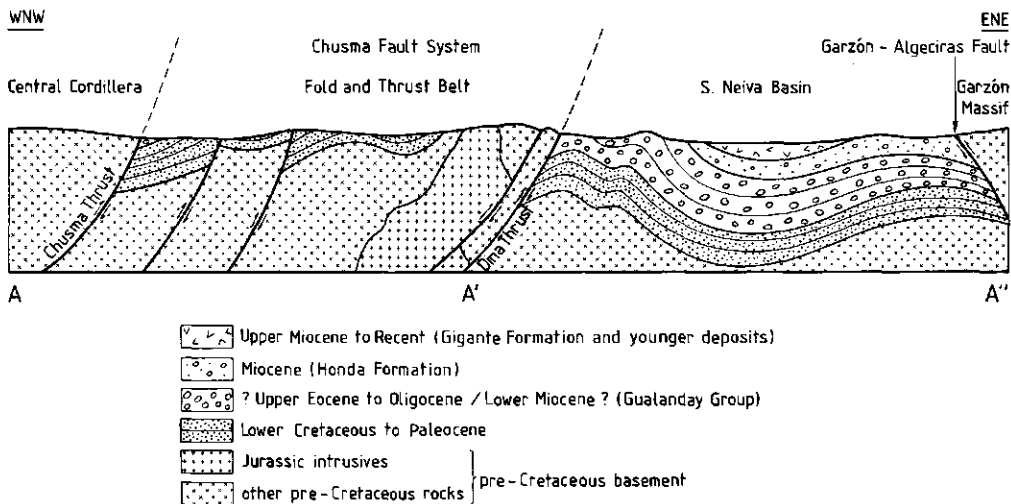


Fig. 5. Schematized profile through the Central Cordillera, the foreland fold and thrust belt, the Neiva Basin and the Garzón Massif. Data are based on the map by Kroonenberg and Diederix (1982), on the sections and geological map by Butler (1983) and on the results of the present field work. The position of A'-A'' is indicated in fig. 28, p. 90; A-A' is located farther to the WNW.

3. 3. Regional geologic history

A schematic representation of the geologic history of the S. Neiva Basin and adjacent areas is given in table I. Formation names in parentheses are introduced in this thesis.

Between 1.2-1.0 Ga ago an orogenic belt formed along the western border of the Guiana Shield (Kroonenberg, 1982a; Priem *et al.*, 1989). This belt, termed the Garzón-Santa Marta granulite belt, underwent granulite facies metamorphism during the Nickerie Metamorphic Episode, a regional tectono-thermal event (Priem *et al.*, 1971, 1982, 1989). On the grounds of similarities in age and rock types, Kroonenberg (1982a) suggested a relation between the Garzón-Santa Marta Belt and the Grenville Province at the eastern margin of the Canadian Shield. The author is of the opinion that both belts may have formed as a result of continental collision between the western side of the Guiana Shield and the eastern side of the Canadian Shield around 1200 Ma. According to Priem *et al.* (1989) granulite facies metamorphism was followed by uplift and cooling between 975-915 Ma ago.

Due to the scarcity of deposits, the Paleozoic history of the area is poorly known. The Lower Paleozoic is characterized by a marine sedimentary series, metamorphosed to schists, metacherts and calcisilicate rocks under low grade to medium grade metamorphic conditions during an orogeny near the end of the Ordovician (Irving, 1975). Outcrops of this age are found west of the present study area (Kroonenberg and Diederix, 1982).

Middle and Upper Paleozoic marine sediments overlie the Precambrian Garzón Massif unconformably. Muscovite-rich shales, sandstones and fossiliferous limestones predominate. The sediments were deposited in a transgressive seaway that extended at least over much of the area of the present Eastern Cordillera. (Irving, 1975). The fossils indicate a Devonian to Upper Carboniferous age (Stibane and Forero, 1969).

Table I. Schematic representation of the geologic history of the S. Neiva Basin and adjacent areas. Formation names in parentheses are introduced in the thesis.

TIME STRAT. UNIT	LITHOSTR. UNIT	DEPOSIT	ENVIRONMENT	EVENT
Quaternary		(volcaniclastic) terraces, alluvial fan deposits	<i>Fluvio-volcanic</i>	
Pliocene	Guacacallo Fm.	ignimbrite deposits	<i>Volcanic</i>	
	(El Carmen fm.)	volcanic debris flow deposits, alluvial fan deposits, torrential congl.	<i>Fluvio-volcanic</i>	
	(Las Vueltas fm.)	alluvial fan deposits	<i>Fluvial</i>	
Miocene	Gigante Fm.	volcaniclastics, fluvial sandstones and conglomerates	<i>Fluvio-volcanic</i>	↑ INTERMITTENT UPLIFT GARZON MASSIF
	Honda Fm.	fluvial sandstones, pebbly sandstones and mudstones, minor volcaniclastics	<i>Fluvial</i> <i>Fluvio-volcanic</i>	
	Eocene-Oligocene	Gualanday Group	fluvial sandstones, mudstones and conglom.	<i>Continental</i>
Maastr.-Paleocene	Guaduas Fm.	marine sandstones and coastal/lagoonal mudst.	<i>Coastal-Lagoonal</i>	
Campanian	Guadalupe Fm.	marine sandstones and "plaeners"	<i>Coastal</i>	REGRESSION
Albian-Santonian	Villeta Fm.	marine anaerobic black shales	<i>Shallow marine</i>	
Aptian-Albian	Caballos Fm.	marine sandstones, locally glauconitic	<i>Coastal</i>	
Norian-Jurassic		acid to intermediate intrusions	<i>Shallow marine</i>	TRANSGRESSION
	Saldaña Fm.	volcaniclastic deposits		ARC VOLCANISM
Upper Paleozoic		marine sandstones, shales and limestones	<i>Marine</i>	EMERGENCE C.CORDILLERA
Lower Paleozoic		schists, metacherts and calcisilicate rocks	<i>Epicontinental</i>	
Upper Precambrian	Garzón Group	granulites, gneisses and amphibolites	<i>Continental</i>	CONTINENTAL COLLISION
		augen gneisses		

Late Paleozoic deformation produced an upland along the site of the present Central Cordillera and a lowland stretching eastward to the Guiana Shield. During this orogenic period the Paleozoic schist belt was formed, which nowadays forms the backbone of the Central Cordillera. Metamorphism was restricted to this western belt; Upper Paleozoic rocks of the present Eastern Cordillera are little metamorphosed (Irving, 1975; McCourt *et al.*, 1984).

In Late Triassic and Jurassic times, thick sequences of volcanoclastic sediments belonging to the Saldaña Formation were deposited east of the Central Cordillera in a continental to shallow marine environment. These extrusives consist of acid to intermediate volcanoclastic rocks like ignimbrites, lavas, agglomerates and tuffaceous sandstones. Granitic to granodioritic plutonism started about 210 Ma ago and continued intermittently to approximately 140 Ma (Aspden *et al.*, 1987). The granitoid rocks intruded the Saldaña Formation to which they are related both spatially and compositionally, suggesting a comagmatic origin (Kroonenberg and Diederix, 1982). Butler (1983) supposes that the extrusion of predominantly intermediate rocks points to activity of a volcanic arc, and thus to the existence of an active subduction system.

In Cretaceous time the sea transgressed from the Pacific and spread northward till it connected with waters of the present Caribbean area (Irving, 1975). The Cretaceous sequence begins with an Aptian-Albian series of thick, locally glauconitic, beds of porous quartz sandstone, which marks the Cretaceous transgression over the eroded Jurassic topography. The sandstone was deposited in a coastal environment (Caballos Formation). Between the Albian and Santonian a thick sequence of black shales was deposited in a shallow marine environment under reducing conditions (Villeta Formation).

At the transition from the Cretaceous to the Tertiary, a world-wide regression took place. In southern Colombia a regressive series of quartzose sandstones, intercalated by thinly-bedded porcelanites ("plaeners") was deposited, partly in a tidal flat and beach environment and partly in a lagoonal environment (Guadalupe Formation). During the Maastrichtian to Paleocene, sedimentation changed from marine sandstones to coastal lagoonal and continental multicoloured mudstones (Guaduas Formation). Deposition of the Guadalupe and Guaduas Formations coincided with uplift of the Western Cordillera and the coeval fold belt along the Caribbean coast, as well as with the emplacement of several large batholiths in the Central Cordillera (Irving, 1975; Bourgois *et al.*, 1987).

In the Eocene, a narrow, east-vergent foreland fold and thrust belt, the Chusma fault system, formed along the eastern margin of the Central Cordillera (fig. 5). The formation of this fold and thrust belt is attributed to the initiation of crustal shortening as a result of changes in the subduction regime of the Benioff zone further to the west (Butler, 1983). On the west side, the fold and thrust belt was bounded by the crystalline basement rocks of the Central Cordillera; in the east, the belt was bounded by the west flank of the Upper Magdalena Valley, which served as foredeep. Foreland folding and thrusting migrated eastward in time, but ended by Latest Oligocene or Lowermost Miocene.

The formation of thrust sheets produced three eastward thinning wedges of conglomerates and sandstones, mainly derived from Cretaceous deposits, that cover the Paleozoic core of the range. The three coarse clastic sequences are separated by mudstone intervals, deposited during periods of low tectonic activity in between thrust phases. Coarse-grained and fine-grained deposits form together the Gualanday Group (Van Houten and Travis, 1968; Anderson, 1970, 1972). The main phase of deformation of the Chusma fault system resulted in an angular unconformity between the Gualanday Group and underlying Cretaceous to Paleocene formations and the younger Neogene formations that were deposited subsequently (fig. 5).

In the Late Tertiary, uplift of the Central Cordillera caused stripping of progressively older layers of cover sediments. Eastward flowing rivers deposited polygenetic conglomerates and sandstones. During phases of relative tectonic quiescence sedimentation of redbrown overbank deposits predominated. These deposits are grouped into the Honda Formation (Van Houten and Travis, 1968; Wellman, 1968, 1970). During deposition of the Honda Formation, initial uplift of the Garzón Massif took place (Van Houten and Travis, 1968; Butler, 1983). This resulted in the formation of a basin between the uplifted Central Cordillera and the emerging Garzón Massif, the Neiva Basin, in which the sediments now started to accumulate.

In Upper Miocene time continuing intermittent uplift of both mountain ranges resulted in the deposition of sandstones and conglomerates (Van Houten and Travis, 1968; Howe, 1969,

1974). Activity of the Central Cordillera volcanic arc produced large amounts of volcanoclastics and volcanics of predominantly intermediate composition. Volcanoclastics and fluvial sediments, which together form the Gigante Formation, were deposited in the Neiva Basin.

Late Miocene to Pliocene uplift of the Garzón Massif was accompanied by folding and faulting of the older sediments in the S. Neiva Basin and in the formation of alluvial fans in the east of the basin. The alluvial fans, which lie unconformably on top of the older deposits, consist of erosional material provening from the massif. This uplift represents the last uplift phase of the southern part of the Garzón Massif: younger deposits were laid down horizontally and are predominantly undeformed. These younger deposits consist of volcanoclastic sediments like volcanic debris flow deposits, rhyolitic ignimbrites and younger, partly alkalibasaltic, volcanics and volcanoclastics (Van Houten, 1976; Kroonenberg *et al.*, 1981; Kroonenberg *et al.*, 1982; Kroonenberg *et al.*, 1987) The sediments partly flooded the Neiva Basin, where they nowadays form erosional terraces along the Magdalena River; in part they were deposited further to the west.

4. Previous literature

Up to the present time, very little work has been done on the geology of the Garzón Massif. The western part of the massif has been studied recently by Kroonenberg as part of a geological mapping project of the CIAF in Bogotá (Colombia). These investigations led to a number of publications on the Precambrian history of the massif (Kroonenberg, 1982a) and the lithology and the origin of the rocks (Kroonenberg, 1980, 1982b). Geochronological studies on rocks from the massif were performed by Alvarez and Cordani (1980), Alvarez (1981), Alvarez and Linares (1985) and Priem *et al.* (1989). No fission track study of the massif has ever been effectuated before.

Detailed maps of the massif are lacking: the geological map of the Uppermost Magdalena Valley (Kroonenberg and Diederix, 1982), at a scale of 1: 200,000, and the geological map of the Department of Huila (Ingeominas, 1989), at a scale of 1: 400,000, include only the westernmost part of the massif. The geological maps of Colombia prepared by Ingeominas (1988) and Geotec (1988) depict the geology of the whole massif, but at a scale of 1: 1,500,000 and 1: 1,200,000 respectively.

Much more information is available on the S. Neiva Basin. Older publications on the regional geology and lithology of the area are listed by Kroonenberg and Diederix (1982). A study of the structural development of the whole Neiva Basin was made by Butler in 1983. A short overview of this investigation was given by Butler and Schamel in 1988.

Reviews of the stratigraphy and the geological history of the S. Neiva Basin are given by Beltrán and Gallo (1968) and Kroonenberg and Diederix (1982). The latter publication includes the already mentioned geological map. A newer geological map of this area, at a scale of 1: 100,000, is in print (Diederix and Gomez, in press). A geomorphological map of the area was prepared by Ruiz (1977) of the IGAC in Bogotá.

In the sixties and seventies, staff and PhD students of Princeton University, New Jersey, performed stratigraphical and petrological studies on the Cenozoic deposits of the basin. Detailed investigations were carried out on the Gualanday Group (Anderson, 1970, 1972), the Honda Formation (Wellman, 1968, 1970) and the Neiva Formation (Howe, 1969, 1974). Regional stratigraphical results were published by Van Houten and Travis (1968) and Van Houten (1976). The latter article by Van Houten (1976) mainly concerns the age and stratigraphy of the younger deposits within the basin.

The geology and geochemistry of the younger deposits which are found west of the S. Neiva Basin were studied by several authors: the lithology and age of the ignimbrites by Kroonenberg *et al.* (1981) and Murcia and Pichler (1986), the volcanic debris flows along the Río Páez by Cepeda *et al.* (1986).

Petrological investigations of the ignimbrites and the young alkalibasaltic volcanics were realized by Kroonenberg *et al.* (1982), Schmitt (1983a, b) and Kroonenberg *et al.* (1987).

5. Aerial photographs and topographical sheets

5.1 *The S. Neiva Basin*

At the Department of Soil Science and Geology of the Agricultural University of Wageningen, a preliminary map was drawn of the S. Neiva Basin on the basis of aerial photographs and existing topographical maps. Two series of aerial photographs were used: the C-series corresponding to a scale of $\pm 1: 35,000$ and the M-series, which is to a scale of $\pm 1: 60,000$. The runs that were used are indicated below:

C-series:	C 1458:	009-012
	C 1587:	218-225
	C 1596:	070-081 and 127-133
	C 1904:	049-052
M-series:	M 1139:	18743-18748 and 39856-39860
	M 1353 (1370):	36717-36728 and 36741-36751

The topographical sheets of the IGAC (Instituto Geográfico de Agustín Codazzi) in Bogotá are to a scale of 1: 25,000. The following maps were used: series 344 no. IVC; series 345 nos. IIIB and IIID; series 366 nos. IIA, IIC, IVA and IVC.

Because topographical maps of the eastern part of the S. Neiva Basin and the Garzón Massif are lacking, additional maps were made by Ing. J.W. Pikaar of the Photogrammetry Department of the ITC in Enschede and by Dr. R. Pardo of the CIAF in Bogotá. For the final map, all topographical maps were brought to a scale of 1: 55,000 and redrawn on a single sheet.

In the field, the preliminary map was checked and the geological data was put on transparent overlays fastened to the aerial photographs. Where available, the 1: 35,000 photos were used in the field in order to get a good resolution. The geological information was transferred from the transparent overlays to the topographical base by means of a pantograph. Both the preliminary map and the final map are semi-controlled mosaics.

5.2 *The ignimbrite plateau west of the S. Neiva Basin.*

For the study of the ignimbrites of the Guacacallo Formation use was made of the following runs of aerial photographs:

C-series:	C 1308:	109-114
	C 1587:	037-041
	C 1941:	149-152
	C 2275:	048-050
M-series:	M 1168:	21253-21256
	M 1261:	25756-25758

Furthermore, the following topographical sheets (at a scale of 1: 25,000) were used:

- Guacacallo-Saladoblanco area: series 388, nos. IIA, IIB, IIC and IID.
- La Argentina-La Plata area: series 365, nos. IID, IVB and, series 366 nos. IA, IC, and IIIA.

5.3 *The volcanoclastic terraces along the Río Páez and Río La Plata*

For the study of the volcanoclastic terraces along the Páez River the following runs of aerial photographs were used:

C-series:	C 1587:	193-198
		212-215
	C 1596:	079-081
	C 1941:	119-122
		246-250
		268-272
	C 1942:	055-058

The numbers of the utilized topographical sheets of the IGAC are: series 344 nos. IIIA, IIIB, IIIC, IIID, IVA and IVC and series 366, nos. IA and IB.

5. 4. Other areas

For the location of the samples in the Garzón Massif, the following runs of aerial photographs were used:

C-series:	C1931:	129-132
	C1937:	008-010
M-series	M1139:	18743-18746

For the study of the Suaza Valley, photonumbers 36731-36734 of series number M 1370 were utilized.

PART 2

THE GARZON MASSIF

Chapter II

Precambrian to Recent thermotectonic history of the Garzón Massif (Eastern Cordillera of the Colombian Andes) as revealed by fission track analysis¹

A.M. van der Wiel and P.A.M. Andriessen²

1. Introduction

The Garzón Massif is a vertical upthrust block bounded by NE-SW high-angle reverse faults. It consists of two main rock groups, *i.e.* the granulite-facies metamorphic rocks of the Garzón Group and the Guapotón and Mancagua augen gneisses (Kroonenberg, 1982a, 1982b). The Garzón Group comprises 1.2-1.0 Ga old granulites, gneisses, amphibolites and minor ultramafic and calcsilicate rocks. These rocks are thought to be of supracrustal origin. The augen gneisses are interpreted as older, Guiana Shield-type basement underlying the Garzón Group and are dated at approximately 1.6 Ga (Priem *et al.*, 1989).

Geochronological and lithological similarities between the Garzón Group granulites within the Garzón Massif and other Andean Precambrian basement outcrops in Colombia led Kroonenberg (1982a) to the suggestion that together they constitute a separate orogenic belt of 1.2-1.0 Ga along the western border of the older Guiana Shield. During the Nickerie Metamorphic Episode, a regional tectono-thermal event, this belt, which is termed the Garzón-Santa Marta Granulite belt (Kroonenberg, 1982a), and extends from the Garzón Massif to the Santa Marta Massif in the N of Colombia (fig. 1) underwent granulite-facies metamorphism and a later, retrogradational low-grade metamorphism. These events are supposedly related to a continental collision period and tentatively correlated with the Grenville Orogeny in North America (Kroonenberg, 1982a; Priem *et al.*, 1989). The intrusion of a set of pegmatite dykes into the granulites and augen gneisses around 895 Ma probably terminated this geological period (Priem *et al.*, 1989).

The next important event is the intrusion of Jurassic granodiorites and associated rocks into the Precambrian rocks of the massif. Aspdén *et al.* (1987) summarize intrusion ages of the plutons

¹ A shorter version of this chapter has been submitted for publication in Earth and Planetary Science Letters.

² Laboratory of Isotope Geology, Institute for Earth Sciences, Free University, De Boelelaan 1085, 1081 HV Amsterdam.

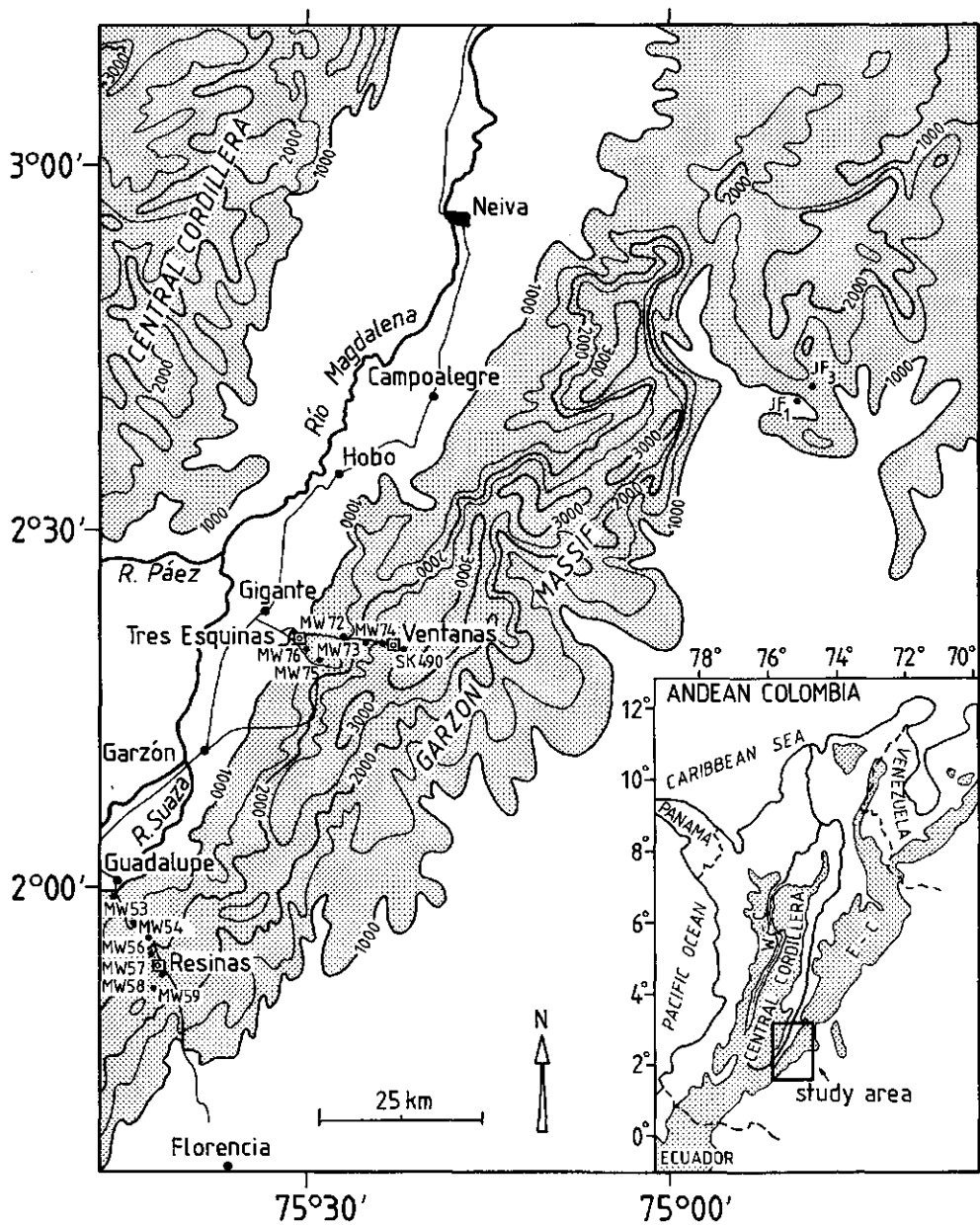


Fig. 6. Location map of the study area. The sample locations of the sections Guadalupe-Florencia, Tres Esquinas and Neiva-San Vicente del Caguán are indicated as well.

in the Colombian Andes: magmatism started about 210 Ma ago and continued intermittently to approximately 140 Ma. According to these authors it is possible that earliest magmatism between 210-180 Ma ago was restricted to a separate eastern province, which coincided approximately with the present Eastern Cordillera, and that this province was subjected to overprinting by the principal Jurassic magmatic event between 180-140 Ma ago.

Minor contact metamorphism appears to be associated with these latter intrusions and their relation to the surrounding rocks suggest that emplacement took place at comparatively low temperatures and shallow depths (Irving, 1975) along major fault zones (Aspden *et al.*, 1987). Furthermore, the intrusives are related both spatially and compositionally to the extrusive Saldaña Formation, suggesting a comagmatic origin. The Saldaña volcanics often form roof pendants of shallow intrusions (Kroonenberg and Diederix, 1982). This intimate association of the intrusives with the volcanics of the Saldaña Formation also points to high-level emplacement conditions.

The Cretaceous is characterized by renewed intrusions of plutonic rocks, ranging in age from 130 to 70 Ma (Aspden *et al.*, 1987; Irving, 1975; Fabre and Delaloye, 1982). Intrusions took place particularly in the Central Cordillera (Aspden *et al.*, 1987), but some small intrusive bodies are present in the Eastern Cordillera, north of Bogotá. The ages of these intrusions range from 120 to 90 Ma (Irving, 1975; Fabre and Delaloye, 1982).

The Cretaceous ended with an orogeny that uplifted and folded the already emergent Central Cordillera and engendered the Caribbean coastal fold belt. The younger intrusions are coeval with this orogeny.

After the Cretaceous period no important thermotectonic event is recognized in the Garzón Massif until its uplift in Middle Cenozoic times.

Indications of Middle Cenozoic to recent uplift are found in the Bolivian Andes, where the period between 15 Ma and the present is characterized by very high uplift rates (Crough, 1983; Benjamin *et al.*, 1987).

The age of the uplift of the central part of the Eastern Cordillera, *i.e.* the area of the Highplain of Bogotá, has been studied extensively by the group of Van der Hammen from the Hugo de Vries Laboratory in Amsterdam. The newest data, which were obtained in collaboration with the Isotope Laboratory of Amsterdam, indicate an uplift age for this part of the Eastern Cordillera of 5-3.5 Ma (Helmens *et al.*, 1990; Andriessen *et al.*, in prep.), which agrees with apatite fission-track data from the Venezuelan Andes published by Kohn *et al.* (1984).

2. Analytical Procedures

Fourteen 5 kilo rock samples were collected from the west and east sides of the Garzón Massif. From the west side six rock samples were collected in roadcuts along the road from Guadalupe to Florencia and another 6 rock samples were collected along the road which enters the Garzón Massif from Tres Esquinas. The maximum differences in altitude within the sections are approximately 1600 m and 1500 m respectively; the horizontal distances over which they were collected are approximately 15 km in both cases (fig. 6). The samples consist of Precambrian gneisses and granulites as well as a Jurassic monzonite (sample MW 56), a Jurassic granite (sample MW 72) and a calcisilicate rock (sample MW 75). An overview of their mineralogy is given in appendix 2.

Two gneiss samples from the east side of the Garzón Massif, taken at altitudes of 950 and 1150 m respectively, were obtained from the Colombian Geological Survey (Ingeominas) and were collected along the road from Neiva to San Vicente del Caguán (Depto. de Meta-Caqueta).

Apatite, zircon and sphene concentrates were recovered by heavy liquids and magnetic separation. The fission track analytical procedures are according to Gleadow *et al.* (1976) and Naeser (1978). The population method was used for dating the majority of the apatites, while the zircons and sphenes and the smallest apatite samples were dated by using the external detector method.

For the population method the apatite concentrates were split into two fractions: the spontaneous fission tracks of one fraction were annealed in an oven at 450°C for 10 hours. This fraction was subsequently irradiated in a reactor. Irradiated and nonirradiated apatites were mounted in epoxy, polished and etched simultaneously in 7% HNO₃ at 20-25°C for 30-40 seconds.

For the external detector method zircon mounts were etched in a eutectic KOH-NaOH melt at 220°C for about 3 hours and then irradiated together with external muscovite detectors, which were subsequently etched for 11-15 minutes in 48% HF at room temperature to reveal the induced tracks. Sphenes were mounted in teflon discs, polished and etched in a mixture of 1 HF: 2 HNO₃: 3 HCl: 6 H₂O at 20°C. Muscovite detectors were etched for 11-15 minutes in 48% HF at room temperature.

Only a limited number of zircon and sphene crystals with sharp polishing scratches were suitable for fission track counting. Counting results from at least 6 grains were combined for each age measurement. Track counting was performed in transmitted light using a oil immersion 100x objective.

Ages were determined using the standard fission track age equation (Hurford and Green, 1982) and the errors for the ages were calculated according to the Poisson distributions of the tracks. Where the pooled data failed the Chi square test at 5%, the ages were calculated from the mean crystal age.

Age calibration of the fission-track dating method was done according to Hurford and Green (1982, 1983) and Andriessen and Bos (1986). Zircons and apatites from the Fish Canyon Tuff and sphenes from Mt. Dromedary were used for calculating mean Zeta values for NBS dosimeter glasses 962 and 963. A single age determination of the Fish Canyon zircons (6 grains) gave an age of 27.2±3.5 Ma, while three age determinations by the external detector method of Fish Canyon apatites gave ages of 28.6±3.8 Ma (16 grains), 30.3±4.2 Ma (17 grains) and 28.2±5.2 Ma (15 grains) respectively. A single age determination of a sphene sample from Mt Dromedary gave an age of 98±11 Ma (6 grains). The ages of the zircons and the apatites determined by the population method were calculated using the mean Zeta value of 308.1 of NBS dosimeter glass 962, whereas the ages of the sphenes and the apatites determined by the external detector method were calculated using the mean Zeta value of 11134 of NBS dosimeter glass 963.

Length measurements were done on 12 apatite mounts using a dry 80x objective. All length measurements were made on horizontal confined tracks in grains with polished-surface orientations approximately parallel to the c-axis of the apatite crystals. The lengths were measured by a projection tube and digitizing arrangement.

A single K-Ar analysis was done on a hornblende separate. Methods used for K-Ar determinations are described in chapter IV, section 1.

3. Results and discussion

The K-Ar mineral age of hornblende grains from sample MW 54 is 902±20 Ma (see table II). Apatite fission track (FT) analytical results are shown in table III and zircon and sphene FT analytical results are shown in table IV, respectively.

Table II. K-Ar mineral data of sample MW 54.

Sample no.	Mineral	K (wt.%)	Radiogenic ⁴⁰ Ar (ppm wt.)	Atmospheric ⁴⁰ Ar (% total ⁴⁰ Ar)	Calculated age ±σ (Ma)
MW 54	Hbl	1.967	156.6	2.79	902±20
		1.977	163.1	6.25	

Since the introduction by Wagner *et al.* (1977) of the use of apparent FT ages of apatites from known elevations as a way to determine the uplift and cooling history of the Central Alps, the FT method has undergone a rapid and extensive evolution. The method has now become indispensable in the reconstruction of the post-crystallization histories of massifs (Gleadow and Fitzgerald, 1987; Fitzgerald and Gleadow, 1988; Omar *et al.*, 1989), particularly so when different U-bearing minerals with a wide range of effective track-retention temperatures are used (Zeitler *et al.*, 1982; Kohn *et al.*, 1984; Shagam *et al.*, 1984; Kamp *et al.*, 1989). It is shown here that in this way it is not only possible to elucidate the more recent uplift and cooling history of mountain chains, but also the older geological record.

In the present study, the post-metamorphic thermotectonic history of the Garzón Massif is reconstructed on the basis of apparent FT ages of apatites, zircons and sphenes, as well as K-Ar ages of various minerals which were determined during the present investigation and obtained from the literature.

Table III. Fission track analytical data of the apatites from the Garzón Massif.

Sample ¹	ρs^2 ($\times 10^4$ μcm^2)	ρi^2 ($\times 10^6$ μcm^2)	t ($\times 10^6$ yr)	1 σ ($\times 10^6$ yr)	Number ³ of grains	ρ_{glass}^2 ($\times 10^5$ μcm^2)	Zeta	Uranium (ppm)	Method	Mean length spont. tracks ² \pm St.dev. (μm) ⁴	P(χ^2) %
MW 59 (2650)	7.0 (118)	4.1 (348)	10.1	2.1	100/100	193534.3 (5927)	308.1	13.1	Pop.	14.11 \pm 1.77 (32)	
MW 58 (2425)	15.94 (154)	84.8 (4097)	11.2	1.4	20	53398.5 (2459)	11134	25.0	Ex.Det.		79
MW 57 (2130)	11 (185)	4.7 (793)	13.9	2.3	100/100	193534.3 (5927)	308.1	15.0	Pop.	14.77 \pm 1.45 (63)	
MW 56 (1755)	0.83 (39)	0.45 (211)	11.0	3.2	100/100	193534.3 (5927)	308.1	1.4	Pop.		
MW 54 (1185)	1.8 (84)	0.12 (543)	9.2	2.0	100/100	193534.3 (5927)	308.1	3.7	Pop.	15.10 \pm 1.43 (38)	
MW 53 (1065)	17.3 (122)	83.9 (2967)	13.9	7.3	15	53641.9 (3368)	11134	24.0	Ex.Det.	14.70 \pm 1.57 (93)	<1
SK 490 (2700)	16 (239)	0.71 (1229)	11.8	1.8	100/100	196235.5 (4327)	308.1	22.2	Pop.	14.97 \pm 1.42 (49)	
MW 74 (2490)	46 (385)	2.2 (1879)	12.2	1.6	100/100	193534.3 (5927)	308.1	70.9	Pop.	14.8 \pm 1.33 (100)	
MW 73 (2110)	3.1 (92)	0.18 (276)	10.1	2.3	100/100	193534.3 (5927)	308.1	5.7	Pop.	14.2 \pm 1.39 (60)	
MW 72 (1750)	2.5 (117)	0.13 (597)	11.7	2.3	100/100	193534.3 (5927)	308.1	4.1	Pop.		
MW 75 (1495)	17.3 (70)	94.0 (1897)	13.6	12.3	10	53641.9 (3368)	11134	27	Ex.Det.	14.51 \pm 1.22 (100)	<1
MW 76 (1220)	67 (565)	3.9 (3307)	10.2	1.2	100/100	193534.3 (5927)	308.1	124.8	Pop.	14.42 \pm 1.40 (100)	
JF 3 (1150)	7.0 (336)	38 (1825)	11.1	1.5	100/100	196235.5 (4327)	308.1	11.9	Pop.	15.06 \pm 1.56 (94)	
JF 1 (950)	16 (499)	0.80 (2583)	12.1	1.5	101/105	196235.5 (4327)	308.1	25.0	Pop.	14.46 \pm 1.18 (32)	

¹ Elevation in meters in parenthesis; ² Number of actually counted or measured tracks in parenthesis

³ The first number refers to counted number of grains with fossil tracks; the second to counted number of grains containing induced tracks

⁴ Mean lengths of induced tracks are indicated in fig.12

Table IV. Fission track analytical data of the zircons and sphenes from the Garzón Massif.

Sample ¹	ρ_s^2 ($\times 10^6$ t/cm ²)	ρ_i^3 ($\times 10^6$ t/cm ²)	t^4 ($\times 10^6$ yr)	1σ ($\times 10^6$ yr)	Number of grains	ρ_{glass}^5 ($\times 10^5$ t/cm ²)	Uranium (ppm)	$P(\chi^2)$ %
Zircon								
MW 59 (2650)	15.36 (1614)	1.18 (62)	715	260	5	198094.9 (2184)	36	<1
MW 57 (2130)	30.40 (1198)	4.26 (84)	421	83	6	198094.9 (2184)	132	66
MW 56 (1755)	5.74 (797)	2.02 (140)	161	44	6	198094.9 (2184)	62	4
MW 54 (1185)	8.96 (1210)	4.38 (296)	124	34	6	198094.9 (2184)	136	1
MW 53 (1065)	17.16 (644)	8.00 (150)	130	23	5	198094.9 (2184)	248	18
SK 490 (2700)	8.02 (737)	4.29 (197)	120	27	6	198094.9 (2184)	133	3
MW 73 (2110)	6.66 (793)	4.55 (271)	89	14	7	198094.9 (2184)	141	46
MW 72 (1750)	14.66 (1210)	8.33 (344)	115	42	6	198094.9 (2184)	259	<1
MW 75 (1495)	13.39 (1231)	8.94 (411)	91	12	6	198094.9 (2184)	278	62
JF 1 (950)	19.0 (1195)	6.82 (214)	169	26	6	198811.8 (4361)	211	22
JF 3 (1150)	25.0 (1258)	7.05 (177)	214	35	6	198811.8 (4361)	218	7
Sphene								
MW 54 (1185)	1365 (999)	22.03 (806)	181	18	6	26644.85 (1632)	130	62
MW 53 (1065)	1135 (937)	18.17 (750)	183	18	6	26644.85 (1632)	108	32
MW 75 (1495)	2005 (1467)	41.74 (1527)	146	20	6	26644.85 (1632)	248	2

1) Elevation in meters in parenthesis

2) ρ_s : density of spontaneous fission tracks; the number of actually counted tracks is given in parenthesis

3) ρ_i : density of induced fission tracks; the number of actually counted tracks is given in parenthesis

4) age calculated according to the Zeta approach with a Zeta value of 308.1; zircon standard used: Fish Canyon with a calculated age of 27.2±3.5 Ma

5) ρ_{glass} : density of fission tracks in standard glass NBS 962; the number of actually counted tracks is given in parenthesis

In order to interpret the obtained data properly, it is necessary to consider the effective track retention temperatures of the different minerals. It has been known for a long time that fission track annealing does not take place at a set temperature, but over a critical temperature interval termed by Wagner (1979) the partial annealing zone (PAZ). Below this zone, in the Total Annealing Zone (TAZ) complete erasure of tracks takes place. The zone above the PAZ is termed the Track Stability Zone (TSZ), where theoretically all tracks are conserved.

The effective track retention temperature is defined as the temperature reigning in the middle of the PAZ where 50% of the tracks are conserved (Wagner and Van den Haute, in prep.). However, the exact temperatures which define the upper and lower limits of the PAZ's of the various minerals are not well known, because the extrapolations of the experimental data generally predict that partial annealing takes place over wider temperature intervals than are inferred from geological settings. This is not the case for apatite: here the experimental data show good agreement with the results from direct studies on fission track retention under geological conditions (Gleadow and Duddy, 1981; Green *et al.*, 1985; Laslett *et al.*, 1987).

According to Wagner and Van den Haute (in prep.) it is likely that the PAZ's of most minerals have a range which is in the order of 70°C. Bearing this in mind, the PAZ of apatite is here taken between 60-120°C, the PAZ of zircon between 180°-240°C and the PAZ of sphene between 215°-285°C on the basis of the existing literature on geologically derived track retention temperatures (Gleadow and Brooks, 1979; Gleadow and Duddy, 1981; Harrison *et al.*, 1979; Zeitler *et al.*, 1982; Zaun and Wagner, 1985; Hurford, 1986; Kamp *et al.*, 1989).

Recent articles by Gleadow *et al.* (1986a, b) and Green *et al.* (1989) have shown that many fission track ages are mixed ages, resulting from complicated thermal histories of the rocks. In contrast to cooling ages, mixed ages do not date a geologic event because they are the result of both track accumulation and track annealing. In the case of mixed ages two types of fission tracks are present: inherited tracks which survived from an older event and new tracks formed during the later geologic event. Cooling ages, on the other hand, result when the mineral experiences cooling from temperatures above the annealing temperature to temperatures below the 100% track stability temperature or in other words, when the mineral passes from the TAZ to the TSZ. The cooling age dates a moment of cooling to a temperature somewhere within the PAZ (Wagner, 1979).

When rock masses, which resided for a geologically long time in the PAZ and the upper part of the TAZ, are brought to the surface as a single structural block by uplift and erosion, apatites from the basement rocks that resided in the PAZ will give mixed ages, with a contribution of tracks from pre-uplift PAZ and from a later set of post-uplift tracks. Apatites that resided in the TAZ will give cooling ages (Gleadow and Fitzgerald, 1987; Omar *et al.*, 1989; Wagner *et al.*, 1989). The mixed ages will decrease with depth because annealing has been stronger in the lower part of the PAZ than in the upper part (Briggs *et al.*, 1981). The cooling ages will also decrease with depth because the apatites which were originally located deep in the former TAZ are the last to enter the PAZ and thus will give the youngest ages.

Apatites, which formerly resided in the TAZ, pass the PAZ during uplift and erosion. These apatites are thus subjected to partial annealing for a much shorter time-span than the apatites coming from the former PAZ. Therefore, cooling ages will lie on a line with a steeper slope than mixed ages (see fig. 3 of Omar *et al.*, 1989). The transition between the two is termed the break in slope. This break in slope has been demonstrated for apparent ages of apatites from a deep drill hole in the Tejon Field, California (Naeser, 1981), the Transantarctic Mountains (Gleadow and Fitzgerald, 1987; Fitzgerald and Gleadow, 1988; Wagner *et al.*, 1989) and the Gulf of Suez Rift (Omar *et al.*, 1989) and dates the initiation of uplift.

For a reconstruction of the cooling and uplift history of basement rocks, it is necessary to differentiate between mixed ages and cooling ages. The sphenes from the Garzón Massif gave apparent FT ages between 183 and 146 Ma and the zircons gave ages between 715 and 89 Ma (table IV). As long as it is uncertain whether these ages are cooling ages or mixed ages it is possible to construct many different cooling pathways of the massif. Therefore geological constraints need to be formulated that rigorously curtail the number of cooling pathways of the rocks and that help to interpret the meaning of the FT ages. The constraints that are used here, are given at the beginning of every section to which they relate.

Finally, it should be stated here that, unless indicated otherwise, a geothermal gradient is employed of 30°C/km. This gradient was chosen on the basis of a published value for the Upper Magdalena Valley of 26°C/km (Butler, 1983) and values from the South American Andes and the Brazilian Shield (Uyeda and Watanabe, 1970).

3. 1. Precambrian history of the massif

The geological constraints used in the present section are the following:

1. According to Kroonenberg (1982a, b) the rocks from the Garzón Group underwent granulite facies metamorphism above the cordierite isograd but below the reaction $OPX + PLAG = CPX + GAR$. This implies that granulite-facies metamorphism took place at a depth of $\pm 22-24$ km. Rb-Sr data by Priem *et al.* (1989) and Alvarez (1981) indicate an age of 1180 Ma for this metamorphism.
2. Hornblende from sample MW 54 gave a K-Ar mineral age of 902 ± 20 Ma (table II). Assuming a closure temperature for hornblende of $\pm 500^\circ\text{C}$ (Andriessen, 1978) and a geothermal gradient of $30^\circ\text{C}/\text{km}$, the sample was located at a depth of some 17 km 900 Ma ago. The granulite, belonging to the Garzón Group, was positioned at a depth of some 23 km 1180 Ma ago (see constraint 1), indicating a relative uplift of 6 km in 280 Ma. This amounts to a relative uplift rate of 0.02 mm/year, corresponding to rates of areal denudation in mountain areas given by Nikonov (1989). On the basis of these data alone, however, it is impossible to establish whether the relative uplift rate was linear and continuous and resulted from denudation and erosion, or discontinuous and resulting from uplift.
3. K-feldspar from a pegmatite vein that intruded into the Precambrian granulites and gneisses was dated at 895 ± 16 Ma by the Rb-Sr method (Priem *et al.*, 1989). The pegmatites show cross-cutting relationships with the older rocks which agrees with the relatively young Precambrian age. The closure temperature of K-feldspar for the Rb-Sr system is approximately $250-200^\circ\text{C}$. The intrusion of the pegmatites represents the last geological activity in the massif before a long period of quiescence.

The apparent zircon FT age of sample MW 59 is 715 ± 260 Ma. As an effective track retention temperature of zircon of 210°C is adopted here (see above), it is apparent that track accumulation in the zircons started around 895 ± 16 Ma, when the rocks had cooled quickly from 500°C to less than 210°C . The old apparent FT age of the zircons indicates that little annealing took place before the zircons reached the TSZ. This fact, in combination with the Jurassic history of the massif (see below), makes it probable that the sample was uplifted to the upper half of the PAZ of zircon around ± 900 Ma and brought gradually to the TSZ by erosion and denudation processes after ± 900 Ma. The rapid cooling from 500°C to 210°C around 900 Ma thus resulted from an uplift from a depth of 17 km to a depth of ≤ 7 km, indicating uplift rates in the order of 1 mm/year or more, which correspond to Tertiary uplift rates of part of the Himalayas (Zeitler *et al.*, 1982).

Priem *et al.* (1989) also give K-Ar mineral ages of Precambrian rocks collected in the Garzón Massif. These mineral ages are comparable to the age given in the present article. The average K-Ar age of two hornblende samples from the Río Suaza, 1 km north of Guadalupe (fig. 6) and a hornblende sample taken in the Quebrada Aguacaliente, some 8 km south of Garzón, is 975 ± 12 Ma. Phlogopite from a nearby sample gave concordant Rb/Sr (mineral/whole rock) and K-Ar ages of 915 ± 21 Ma. These data, together with an closure temperature of the K-Ar system in hornblende of $\pm 500^\circ\text{C}$, a closure temperature of the K-Ar system in phlogopite of $\pm 400^\circ\text{C}$ and a closure temperature of $250-200^\circ\text{C}$ for the Rb-Sr system in K-feldspar indicate a cooling of the samples from 500°C around 975 Ma to 200°C around 895 Ma. Priem *et al.* (1989) explain this cooling in terms of an uplift between 975 and 915 Ma. Considering the mineral ages of sample MW 54 given above, it seems likelier that between 1180-900 Ma the massif was subjected to slow denudation and erosion while major uplift of at least 10 km occurred around 900 Ma. The Precambrian history of the section Guadalupe-Florencia is illustrated in fig. 7.

3. 2. Mesozoic history of the massif

The geological constraint used in this section concerns the shallow intrusion depth of the Jurassic intrusives.

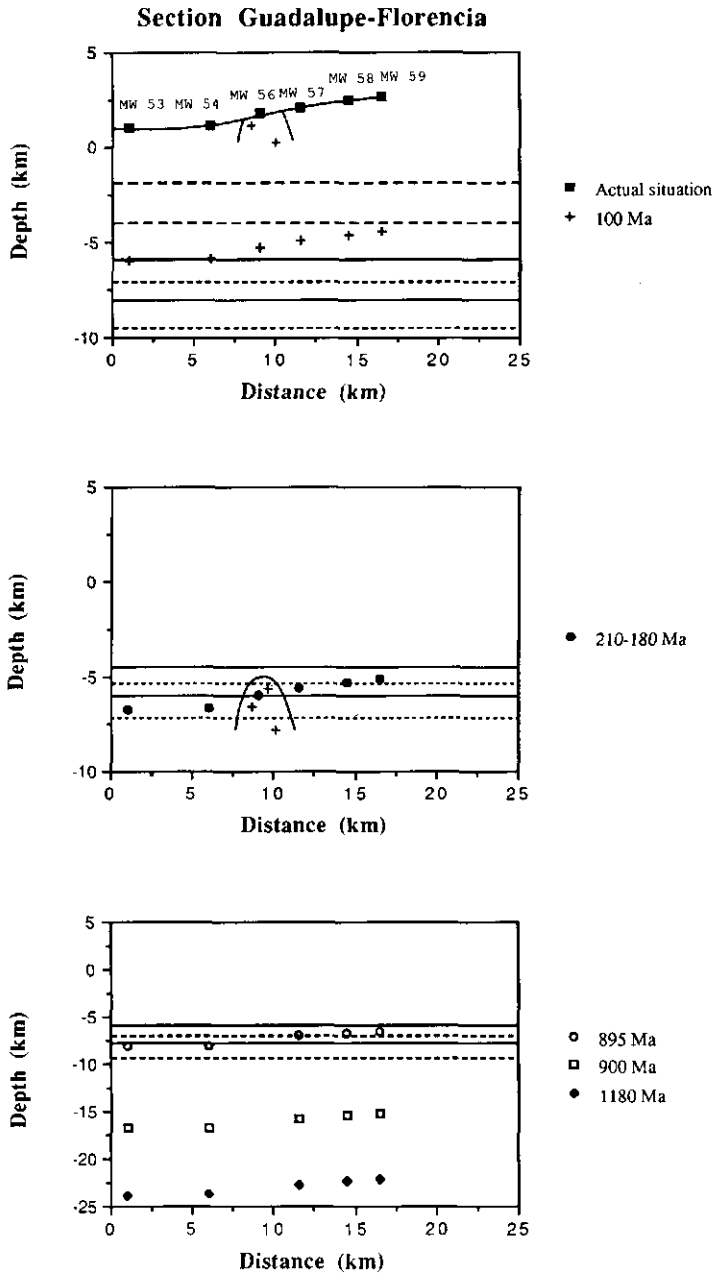


Fig. 7. Interpretation of the zircon, sphene and apatite apparent fission-track ages of the section Guadalupe-Florescia. The cartoons show the cooling and uplift history of the samples by indicating the inferred depth of the different samples of the section at certain moments of the geological past. The boundaries of the PAZ of sphene are indicated by stippled lines, those of zircon by uninterrupted lines and the boundaries of the PAZ of apatite are indicated by interrupted lines.

The occurrence of comagmatic ignimbrites of the Saldaña Formation, associated with the intrusions and the presence of late, anhedral biotite and amphibole in the intrusive rocks indicate that gas expansion took place at shallow depths. Furthermore, the often aphyric or porphyric character of the intrusions and the polygonal structure of the crystals, the presence of groundmass spherulites, as well as the relation with the country rocks, indicates very rapid cooling. The occurrence of muscovite in the recrystallized groundmass spherulites of one of the granodiorites points to cooling at pressures of less than 3 kbar, *i.e.* at a depth of less than 9 km (Winkler, 1979; fig. 15.3).

This is in accordance with the lack of contact metamorphism associated with the intrusions, as described by Irving (1975) and Aspdén *et al.* (1987). Also, Shagam *et al.* (1984) infer intrusion depths of 3-7 km from the age and nature of adjacent country rocks for Triassic/Jurassic intrusives in the Venezuelan Andes, which have a comparable geologic history.

A. Section Guadalupe-Florencia

Sample MW 56 from the section Guadalupe-Florencia is a quartz monzonite. At the time of intrusion the sample must have been located at a depth of less than 9 km. The sample yielded an apparent zircon FT age of 171 ± 31 Ma. As the ages of most intrusives are between 210-170 Ma (Aspdén *et al.*, 1987), the obtained age is thought to approach the actual intrusion age.

As mentioned in the previous section on the Precambrian history of the massif, sample MW 59 was uplifted to the upper half of the PAZ of zircon, *i.e.* to a depth of ≤ 7 km, around 900 Ma. From 900 Ma onward the sample was gradually uplifted to the TSZ, *i.e.* to a depth of some 6-5 km, by erosion and denudation processes. The following arguments plead for this interpretation: - Sample MW 57, located only 500 m below sample MW 59, has an apparent zircon FT age of 421 ± 83 Ma. This age cannot be correlated to any known geologic event in the region. Furthermore, it is intermediate between the zircon ages of the other samples from the same section. Therefore, it is likely that this age is a mixed age and that either its original Precambrian age was partly reset by a later event, or that the sample resided somewhere in the PAZ of zircon from ± 900 Ma onward.

- Samples MW 53 and MW 54 gave apparent sphene FT age of 183 ± 18 and 181 ± 18 Ma respectively. The present elevation difference between MW 59 on the one hand and MW 53 and MW 54 on the other hand is 1600-1500 m. This implies that if sample MW 59 was located at a depth of 5 km after 900 Ma, samples MW 53 and MW 54 were positioned in the lower part of the PAZ of sphene. If sample MW 59 was located much deeper in the PAZ of zircon, the other samples would have been located in the TAZ of sphene. This could agree with the sphene ages but does not agree with the 715 Ma zircon age of MW 59, which should have been much younger in that case. On the other hand, if sample MW 59 were located much higher in the TSZ of zircon, both the sphene and the zircon FT ages of MW 57, MW 53 and 54 should have been much older, because the grains would have been able to collect much more tracks.

These restrictions imply that the sphene and zircon FT ages of the samples and their relation to sample MW 56, the quartz monzonite, can in fact only be explained in the following way (see also fig. 7):

1. Around 210 Ma sample MW 59 was located in the lower part of the TSZ of zircon.
2. Due to the Jurassic plutonic episode, the geothermal gradient of the region was steepened to $40^\circ\text{C}/\text{km}$ between 210-180 Ma. Around 170 Ma ago it returned to $30^\circ\text{C}/\text{km}$. Aspdén *et al.* (1987) are of the opinion that the earliest magmatism between 210 and 190/180 Ma ago was possibly restricted to a separate eastern province that reached from the Santander Massif in the North to the Mocoa Batholith in the South (*i.e.* approximately the region of the present Eastern Cordillera).
3. Due to the steeper geothermal gradient, sample MW 59 was now located in the upper part of the PAZ of zircon and minor annealing of existing tracks took place. MW 57, which is located ± 500 m deeper, underwent a more severe annealing.
4. Somewhere between 210-180 Ma ago sample MW 56 intruded the older rocks at a depth of ± 6 km. Because of the steeper geothermal gradient this depth corresponds to the lower limit of the PAZ of zircon. When the geothermal gradient returned to normal, the sample was positioned near or at the upper limit of the PAZ.

5. Between 210-180 Ma the samples MW 53 and MW 54 were located in the TAZ of zircon, which resulted in complete annealing of all existing tracks. Correspondingly, the sphene ages were severely reduced because the samples were positioned in the lower part of the PAZ of sphene. When the geothermal gradient returned to normal, the zircons entered the PAZ of zircon and started to accumulate tracks once again.

B. Section Tres Esquinas

Sphene grains of sample MW 75 gave an apparent sphene FT age of 146 ± 20 Ma. The apparent zircon FT ages of the section Tres Esquinas range between 120 ± 27 and 89 ± 14 Ma (see table IV). In other words, within error limits all zircon ages are the same, including that of sample MW 72, which comes from a Jurassic biotite granite and has a zircon FT age of 115 ± 42 Ma. Keeping in mind the fact that sample MW 72 must have been located at a depth of less than 9 km at the time of intrusion, there are two alternatives to be considered with regard to the position of the section Tres Esquinas in relation to the section Guadalupe-Florencia:

(1) Both sections, which are nowadays situated at more or less the same altitude, were also located at the same elevation in the past; in other words, they were never separated by cross

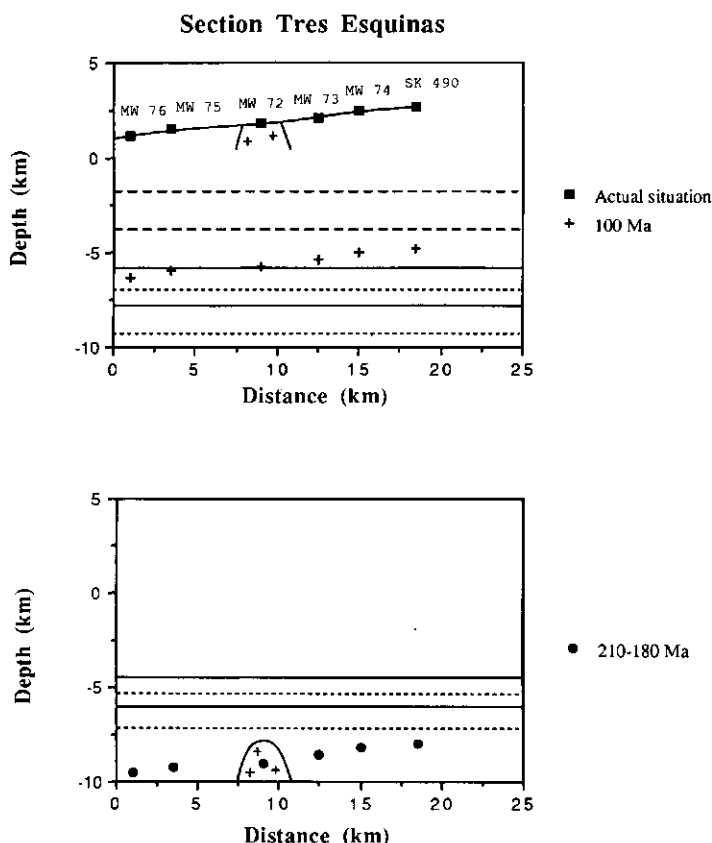


Fig. 8. Interpretation of the zircon, sphene and apatite apparent fission-track ages of the section Tres Esquinas. The cartoons show the cooling and uplift history of the samples by indicating the inferred depth of the different samples of the section at certain moments of the geological past. The boundaries of the PAZ's are indicated as in fig. 7.

faults. The consequence of this supposition would be that between 210-180 Ma the samples of the section Tres Esquinas were located partly in the PAZ and partly in the TAZ of zircon. However, within the error limits, all zircon ages are the same, rendering this hypothesis improbable.

(2) The two sections were separated by cross faults in the past. The very close grouping of the zircon FT ages is most readily explained if it is assumed that section Tres Esquinas was positioned at a greater depth than section Guadalupe-Florencia in such a way that until ± 100 Ma, the average FT age of the zircons, all samples of this section were situated in the TAZ of zircon. This means that before 100 Ma ago section Tres Esquinas was located ± 2900 m lower than section Guadalupe-Florencia.

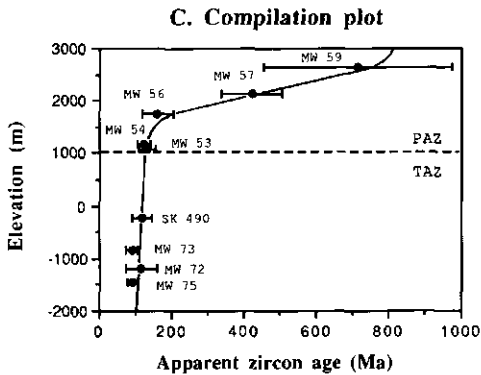
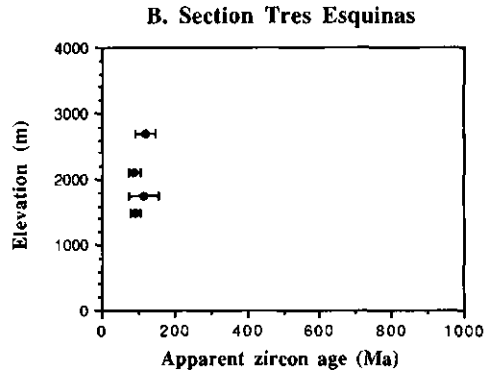
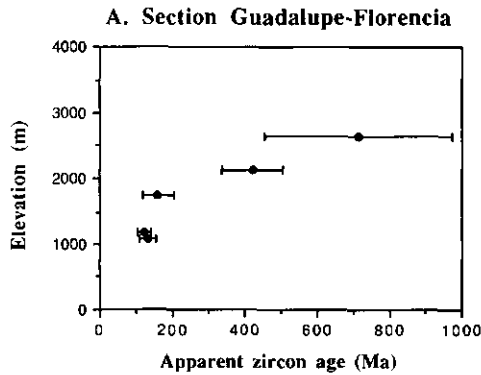
Starting from hypothesis (2), therefore, the following picture emerges (fig. 8): before 210 Ma all samples were situated in the TAZ of zircon, which positions the lowest samples also in the TAZ of sphene. Around 210 Ma the geothermal gradient steepened to $40^\circ\text{C}/\text{km}$ and somewhere between 210-180 Ma ago intrusion of the biotite granite occurred. Because the regional geology gives no indication of faulting within the section, it may be safely assumed that when the biotite granite intruded, sample MW 72 was emplaced at its present position with regard to the other samples, *i.e.* 950 m below sample SK 490. Because sample SK 490 must also have been situated in the TAZ of zircon up to 100 Ma ago, *i.e.* at a depth of at least 8 km, this means that at the time of the intrusion sample MW 72 was positioned at a depth of some 8.9 km. When the geothermal gradient returned to normal around 170 Ma, all samples, including sample MW 72 were still positioned in the TAZ of zircon and no track accumulation took place in the zircon crystals. At the same time sphene from sample MW 75 reached the PAZ of sphene and accumulation of tracks started in this mineral.

Around 100 Ma ago an uplift of some 3.5 km placed all samples at the same time in the TSZ of zircon, resulting in corresponding cooling ages of ± 100 Ma, while sphene from sample MW 75 yielded an apparent age of 146 ± 20 Ma due to its early entrance in the PAZ of sphene.

In figs. 9a and b plots are given of the present elevation of the two sections versus apparent zircon age. In fig. 9c the situation is reconstructed as it is thought to have been before 100 Ma, when section Tres Esquinas was located 2900 m lower relative to section Guadalupe-Florencia. In this figure the real elevation of the sections at that time is left out of consideration. The figure clearly shows a break in slope as indicated in fig. 3 of Omar *et al.* (1989) for apatite. In fig. 9c the lower limit between the former PAZ and TAZ and the age-depth path are also indicated. The close similarity between fig. 3 of Omar *et al.* and fig. 9c of the present article suggests that the interpretation of the zircon and sphene FT ages in terms of cooling ages and mixed ages given above is very likely to be correct and that the 100 Ma zircon ages may be interpreted as an uplift event. It appears that the uplift was a differential uplift, associated with block faulting, because only 700 m of uplift are needed to lift the samples MW 54 and MW 53 to the TSZ of zircon while 3600 m of uplift are needed to lift the Tres Esquinas samples out of the PAZ of zircon. This supposition agrees with the apparent zircon FT ages of the samples JF 1 and JF 3 from the section Neiva-San Vicente del Caguán which are nowadays located at approximately the same elevation as MW 54 and MW 53, but give older ages (169 ± 26 Ma and 214 ± 35 Ma, respectively). It is likely that these ages are mixed ages and that the samples were located somewhere in the PAZ of zircon at the time of the uplift. The uplift of the samples to the TSZ would have amounted to some 1000-1500 m.

The amount of uplift of the different sections cannot have been much greater than indicated above, because otherwise some of the samples would have entered the PAZ of apatite, which would have led to much older apatite ages than the recorded ages (see below). Besides, as it is likely that some erosion took place between 100-12 Ma, the samples must have been positioned at least a few hundreds of meters below the 4 km limit (the lower limit of the PAZ of apatite) after the uplift.

Other arguments for orogenic movements around 100 Ma come from the literature: vertical crustal movements in the Peruvian Andes began in the Albian and reached a maximum in the Santonian (Myers, 1975; Cobbing, 1976, 1978; Mégard, 1984a, b; Mégard *et al.*, 1984). This



Figs. 9a and b Actual elevation of the different samples of the sections Guadalupe-Florencia and Tres Esquinas. **Fig. 9c.** Reconstruction of the relative positions of the two sections as they are thought to have been before ± 100 Ma. In the figure the real elevation of the sections at that time is left out of consideration. The figure shows a clear break-in-slope around 100 Ma. The stippled line indicates the transition from the former TAZ to the former PAZ of zircon.

first phase of the Andean tectonogenic period is called the Peruvian phase and coincides with a peak in magmatic activity between 100-80 Ma. In S. Chile, igneous activity was widespread between 100-85 Ma (Halpern, 1973). Mattson (1984) registered uplift and erosion in the Caribbean region around 100 Ma while Beets *et al.* (1984) interpret an orogenic event (island arc-continental margin collision) between the Coniacian and Campanian in the same region on the grounds of unconformities, high-pressure metamorphism and magmatism.

Furthermore, apparent zircon FT ages between 172 and 60 Ma in the Venezuelan Andes show a strong grouping around 113-81 Ma (Kohn *et al.*, 1984), while apparent zircon FT ages between 126-50 Ma from the circum-Maracaibo Basin region are concentrated around 101-85 Ma (Shagam *et al.*, 1984).

In the introduction it has already been pointed out that intrusions varying in age between 120-93 Ma are recorded in the central part of the Eastern Cordillera of Colombia by Fabre and Delaloye (1982) and intrusions ranging between 131-68 Ma in the Central Cordillera by Irving (1975). In contrast to the intrusions in the Central Cordillera, however, the small plutons found in the Eastern Cordillera have a basic chemistry. Fabre and Delaloye (1983) are of the opinion that these basic dykes intruded during basin subsidence as a result of an extensional regime.

Up to the present time, the above data have never been interpreted in terms of a widespread orogenic event which affected at least the whole northwestern part of the South American continent between 100-80 Ma. For example Kohn *et al.* (1984) and Shagam *et al.* (1984) interpret the majority of their FT ages as mixed ages, although they indicate that the ages may have time significance. They exclude the possibility of a tectonic pulse on the grounds of the inferred subsidence of the area at that time. Their data of the El Carmen Granodiorite are used here to show that an interpretation in terms of a small uplift event may be possible.

C. Section El Carmen Granodiorite, Venezuelan Andes

U-Pb determinations on apatite as well as K-Ar and Rb-Sr analyses of biotite from the El Carmen Granodiorite gave ages, varying between 200 ± 40 and 196 ± 10 Ma (Kohn *et al.*, 1984). These ages are concordant with the primary age of crystallization (225 ± 25 Ma) given by the same authors, indicating rapid cooling of the intrusive body.

For comparison with the previous results, an intrusion age of 210 Ma and an enhanced geothermal gradient of $40^\circ\text{C}/\text{km}$ between 210-180 Ma are assumed here (fig. 10), in correspondance with the assumptions made for the sections Guadalupe-Florencia and Tres Esquinas. Furthermore, it is presumed also that the El Carmen Granodiorite intruded at a depth of less than 9 km, which is in approximate agreement with the inferred intrusion depths of 7-3 km for the Venezuelan Andes (Shagam *et al.*, 1984).

The concordant apparent zircon FT ages of 92 ± 14 and $99 \pm 10/87 \pm 13$ Ma of samples LB 2 and LB 35 respectively, which have an elevation difference of 700 m (see fig. 10), could be

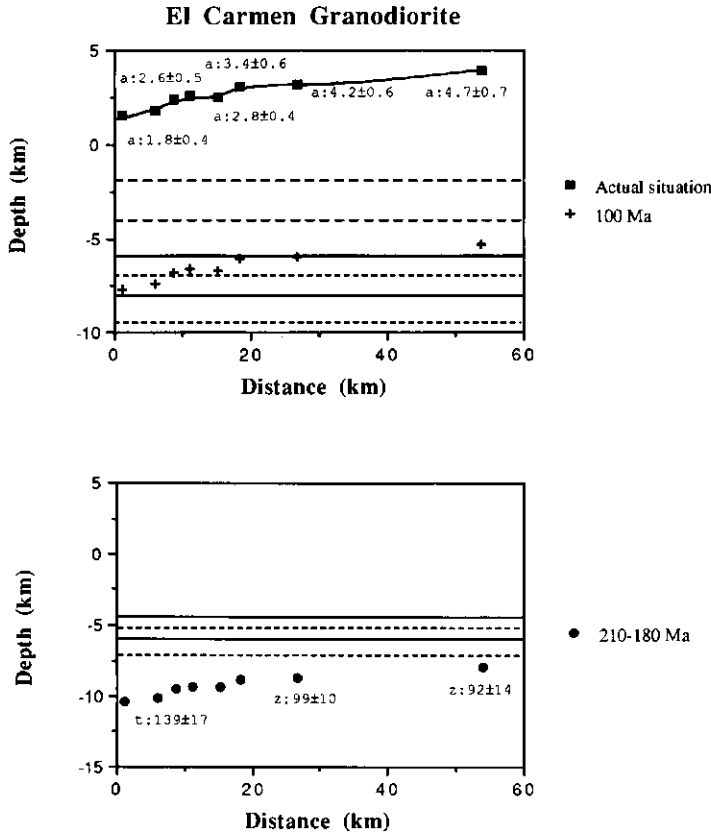


Fig. 10. Possible interpretation of the zircon, sphene and apatite apparent fission-track ages from the El Carmen Granodiorite in Venezuela. The fission-track ages and the relative position of the samples are taken from Kohn *et al.* (1984). Apatite ages are indicated by the letter a, zircon ages by the letter z and sphene ages by the letter s. The cartoons show the cooling and uplift history of the samples by indicating the inferred depth of the different samples of the section at certain moments of the geological past. The boundaries of the PAZ of sphene are indicated by stippled lines, those of zircon by uninterrupted lines and the boundaries of the PAZ of apatite are indicated by interrupted lines.

explained if the samples were located in the TAZ of zircon before 100 Ma, *i.e.* at a depth of 8 km or more. An uplift of ± 2700 m around 100 Ma would enter the samples in the TSZ of zircon, resulting in concordant cooling ages. The sphene FT age of 139 ± 17 Ma of sample SA 2 could well represent a mixed age resulting from tracks which accumulated after the geothermal gradient returned to $30^\circ\text{C}/\text{km}$ some 170 Ma ago, positioning the sample in the PAZ of sphene, and tracks which accumulated after the 100 Ma uplift event.

Both the data presented in this study and the data obtained from the literature indicate a widespread orogenic event and enhanced magmatic activity in the NW of the South American continent around 100-80 Ma. It seems likely that this event is related to a change in the subduction regime at that time. Duncan and Hargraves (1984) are of the opinion that activity of the Galapagos hot-spot started around 100 Ma and led to the formation of an oceanic plateau. Encounter of this plateau with the Greater Antillean trench/arc took place around 80-70 Ma. Because of its buoyancy, the plateau was not subducted but formed the core of the present-day Caribbean plate. Alternatively, a collision of an island arc with the western margin of South and North America 115-105 Ma is suggested, leading to the development of the Caribbean plate 90-85 Ma ago (Beets *et al.*, 1984). Apparently, these changes in the subduction regime lead to compressional deformation in many places and to extensional deformation in other places (Fabre and Delaloye, 1982).

3.3. Cenozoic history of the massif

The apparent apatite FT ages from the sections Guadalupe-Florencia and Tres Esquinas as well as from the samples taken along the road Neiva-San Vicente del Caguán range between 13.9 and 9.2 Ma (table III).

When the ages and their standard errors are plotted against the present elevation of the samples (fig. 11), no correlation seems to exist between the two variables and consequently, no uplift curves can be constructed. This is due to the very low uranium content of the samples which resulted in such great standard errors that even with counts of 100 grains, the ages overlap strongly. It is clear, however, that the apparent apatite ages result from rapid cooling of the apatites from the TAZ to the TSZ with a very limited stay in the PAZ. This implies that before 12 Ma ago the apatites were located at depths greater than 4 km, which is the limit between the TAZ and the PAZ of apatite.

From the fact that all apatite ages lie in the same range of 13.9-9.2 Ma and no younger apatite ages are found, it may be concluded that around 12 Ma ago *all* samples were uplifted to the TSZ. If the samples which are nowadays located at the greatest altitude were situated at a depth of more than 4 km before uplift, this means that the minimum uplift was in the order of 4 km (the uplift necessary to lift the deepest sample from the TAZ to the TSZ). Even accounting for the fact that the tectonic uplift must have been less, because part of the uplift was due to regional isostatic uplift as a result of unloading of the surface by erosion of uplifted crust (Omar *et al.*, 1989), the uplift rate must have amply exceeded the rate of thermal diffusion in rocks (Kohn *et al.*, 1984). This would have resulted in thermal updoming of isotherms and consequent changes in the local geothermal gradient, higher near-surface temperatures and complicated interactions of erosion and distribution of heat generation (Parrish, 1985). Consequently, cooling would have lagged behind uplift. Therefore, the apatite FT ages should be interpreted in terms of cooling following uplift, because they reflect the duration of cooling of the rocks from 120°C to TSZ temperatures ($< 60^\circ\text{C}$). Thus, the ages cannot be used to calculate uplift rates.

Gleadow *et al.* (1986a, b) have shown that the distribution of confined track lengths in apatites gives information on their thermal history. From the moment that the lower temperature limit of the PAZ of apatite is crossed, spontaneous tracks will start to accumulate. As the process of track formation takes place continuously, each track is formed at a different time and, depending on the maximum temperature that each track experiences during track accumulation, each track will undergo a different degree of partial annealing. Tracks that were formed during

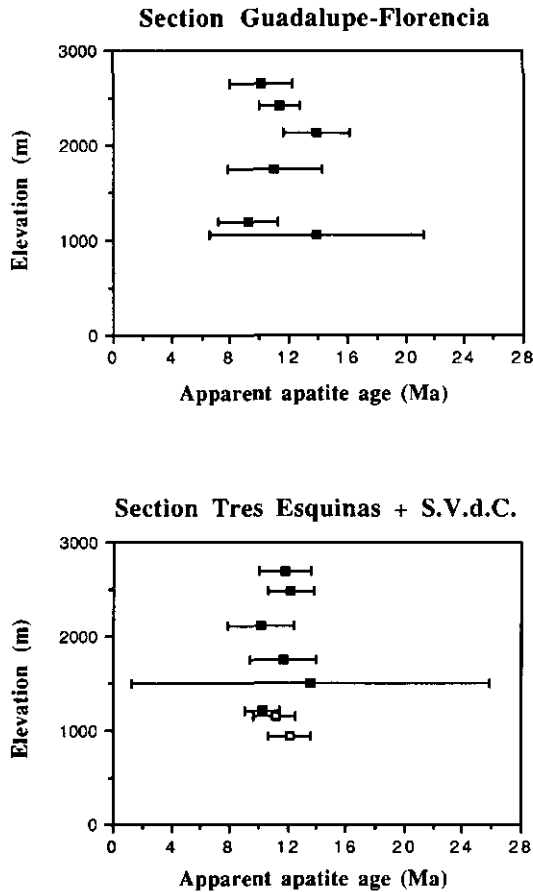


Fig. 11. Age-elevation plots of the apatites from the sections Guadalupe-Florencia, Tres Esquinas and Neiva-San Vicente del Caguán. Open squares represent apatites from the section Neiva-San Vicente del Caguán. Standard deviations are indicated by horizontal bars.

rapid cooling from the TAZ to the TSZ will have experienced relatively little annealing because of their limited residence time in the PAZ. Therefore, these tracks will be relatively long compared to tracks that formed during slow cooling through the PAZ.

As indicated above, apatites from basement rocks record cooling ages when they contain no tracks before uplift and/or cooling, *i.e.* when they cool directly from the TAZ. In that case the distribution of the tracks will be narrow, with high mean values between 12-14 μm (Gleadow *et al.*, 1986b; Gleadow and Fitzgerald, 1987; Omar *et al.*, 1989). Apatites from basement rocks record mixed ages when different generations of tracks are present, *i.e.* when partial annealing of existing tracks takes place in the PAZ. After uplift/cooling, accumulation of newly formed tracks occurs. The distributions of the tracks from these apatites will be negatively skewed and will show a progressive increase in the width of the distribution and a decrease of the mean track length with increasing temperature.

Measurement of confined track lengths in 9 apatite samples (table III, fig. 12) resulted in narrow distributions with mean lengths between 14.11 and 15.10 μm and standard deviations between 1.18-1.77 μm . These mean lengths agree with mean lengths from quickly cooled

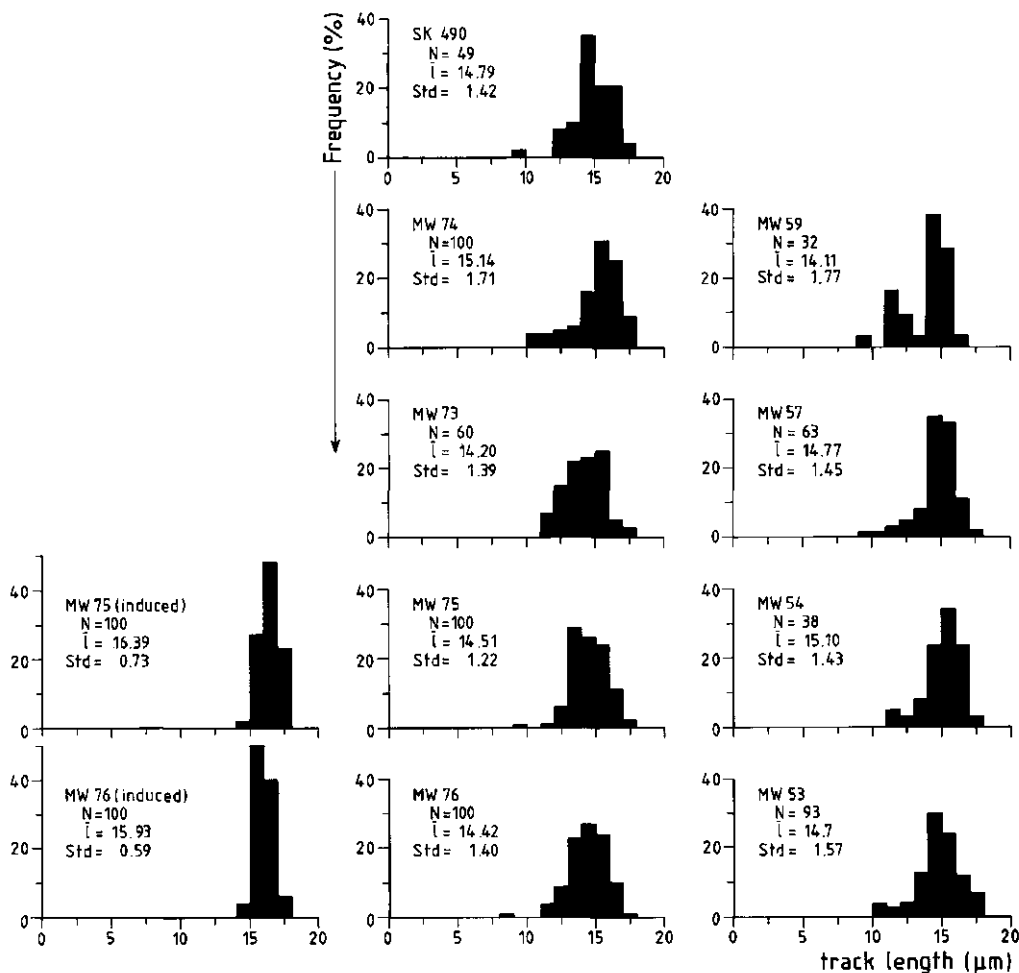


Fig. 12. Length distributions of confined induced and spontaneous tracks of apatite. The induced tracks give narrow symmetrical distributions with mean lengths between 15.05-15.93 μm and standard deviations between 0.59-0.73 μm , while the spontaneous tracks give narrow, negatively skewed distributions with mean lengths between 14.42-15.14 μm and standard deviations between 1.22-1.71 μm .

volcanic rocks of 14.04-15.69 μm (Gleadow *et al.*, 1986b) although the standard deviations are greater (less than 1 μm in the volcanics). They also agree with lengths of 14.1-14.4 μm and standard deviations between 1.2-2.0 μm given by Gleadow and Fitzgerald (1989) for apatites from the Transantarctic Mountains which were uplifted rapidly from the TAZ to the TSZ with short residence times in the PAZ. The higher mean length values of the tracks from the Garzón Massif could be explained by an even shorter residence time in the PAZ, in other words by very fast uplift and cooling.

Green *et al.* (1989) present quantitative modelling techniques for the prediction of fission-track parameters in geological situations from a laboratory-based description of annealing kinetics. Using this modelling, a rapid cooling from 120° to 60°C between 12 and 10 Ma, followed by a

much slower cooling from 60° to 10°C between 10 Ma ago and the present would result in a mean confined track length of 14.87 μm with track lengths varying between 10-17 μm and an apparent apatite FT age of 10.4 Ma. The FT age and length distribution data from the Garzón Massif agree very well with the values obtained from this model.

From the above it is clear that the apparent FT ages of the apatites record cooling from 120°C to ambient temperatures, and that cooling was the result of a very fast uplift which probably took place ≥ 12 Ma ago.

Because all samples from the two sections passed the PAZ during a single uplift pulse, no younger apatite ages are found in the Garzón Massif. It will be shown in the next chapters, however, that geological evidence in the adjacent S. Neiva Basin points to the existence of a younger uplift phase: coarse-grained fault-bounded alluvial fan deposits consisting of erosional material from the massif are found to lie partly unconformably and partly conformably on 6.4 Ma old deposits of the upper part of the Miocene Gigante Formation (Garzón Member). The tectonic relationship between the two types of deposits and the clast composition of the conglomerates indicates that uplift of the massif started during deposition of the Garzón Member (chapters V, VII). The presence of two generations of alluvial fan deposits suggests that uplift was rapid and intermittent rather than continuous and slow. It is probable that uplift stopped some time before 3 Ma ago: the C. Cordillera volcanic arc resumed its activity at ≥ 3.3 Ma, which had stopped ≤ 6 Ma ago and volcanoclastic deposits of this age, found W of the S. Neiva Basin, are undisturbed by folding (chapter X).

Keeping in mind that the lowest sample is located nowadays at an elevation of 1065 m and was positioned at a depth of less than 2 km after the 12 Ma uplift, the maximum uplift between 6-3 Ma must have been in the order of 2.5 km. This much slower and much less pronounced uplift agrees well with the model by Green *et al.* (1989) used above, which predicts slow cooling from 60°C to ambient temperatures between 10 Ma and the present time.

The presence of several uplift phases from 12 Ma onwards is in agreement with data from other parts of the northern Andes found in the literature:

- Further north, in the Venezuelan Andes, Kohn *et al.* (1984) record differential uplift between 11-1.4 Ma. An age of ± 24 Ma was discarded in a later article by Shagam *et al.* (1984). According to Kohn *et al.* (1984) the leading northwestern margin was uplifted first, followed by the trailing southeastern margin between 10-5 Ma, while the central part was uplifted between 5-1.4 Ma.

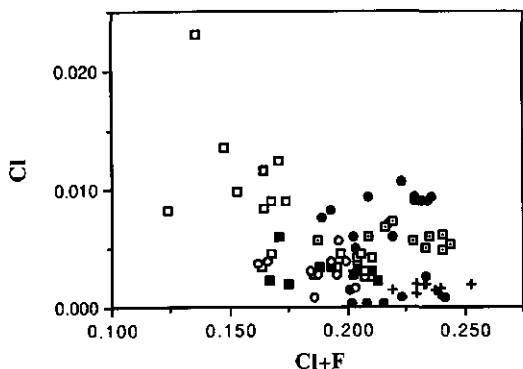
- Shagam *et al.* (1984) are of the opinion that Tertiary uplift in the circum-Maracaibo Basin region started in the Late Oligocene and became progressively greater with higher uplift rates until maximum uplift occurred in Pliocene times.

- In the east of Peru, three Miocene to Pliocene deformation phases can be distinguished, *i.e.* the Quechua 1 (± 20 Ma), Quechua 2 (± 9 Ma) and Quechua 3 (± 6 Ma) phases respectively (Mégard, 1984a, b; Mégard *et al.*, 1984). Of these phases the Quechua 2 phase, which may be considered as the least important one, has little influenced the eastern part of Peru.

- Cooling ages from Bolivia (Crough, 1983; Benjamin *et al.*, 1987) indicate that uplift started 40 Ma ago but that uplift rates increased significantly during the last 15 million years, while uplift in the central part of the Eastern Cordillera of Colombia, *i.e.* the High Plain of Bogotá, took place 5-3.5 Ma ago (Andriessen *et al.*, in prep.; Helmens *et al.*, 1990).

According to Green *et al.* (1985, 1986) annealing in apatite is controlled by the apatite composition: apatites richest in Cl are more resistant to annealing than apatites consisting predominantly of fluorapatite. If the population of apatite grains is very heterogenous, this could lead to broad length distributions because the fluorapatite grains would be more strongly annealed than the chlorapatite grains. Because of the rather large standard deviations of the length distributions of the apatites from the Garzón Massif, electron microprobe analyses were carried out on 6 apatite samples in order to determine the Cl/F ratio.

In fig. 13 the number of Cl atoms per molecule is plotted against the number of Cl+F atoms per molecule. It is apparent that, with the exception of MW 53 and MW 73, the samples have homogeneous Cl/F ratios and that the composition of the majority of the grains is



- Cl (53)
- Cl (57)
- + Cl (59)
- Cl (73)
- Cl (75)
- Cl (76)

Fig. 13. In this diagram the number of chlorine atoms per apatite molecule is plotted against the total number of fluor plus chlorine atoms per apatite molecule.

predominantly fluorapatite with the composition $\text{Ca}_5(\text{PO}_4)_3(\text{F}_{0.98}, \text{Cl}_{0.02})$. Although MW 53 and MW 73 clearly consist of two groups of apatite with different Cl/F ratios, this does not appear to influence their length distributions (fig. 13), nor their apparent ages, which should be somewhat higher than the remaining apatite FT ages, because annealing is less in Cl-rich apatite grains. Possibly this is due to the small differences in composition and the young ages of the apatites.

A complete reconstruction of the cooling history of the Garzón Massif from the Precambrian to the present time can now be plotted in an age-depth diagram. This diagram is given in fig. 14.

4. Conclusions and final remarks

1. After the granulite facies metamorphism, 1180 Ma ago, the Garzón Massif was subjected to a relative uplift of 6 km due to erosion and denudation. Around 900 Ma ago an orogeny resulted in at least 10 km of uplift. Between 850 and 210 Ma ago the geologic history of the Garzón Massif was again determined by erosion and denudation processes.

2. In the Eastern Cordillera and Venezuelan Andes intrusion of granodiorites and associated rocks took place between 210-180 Ma ago at depths between 9-4 km.

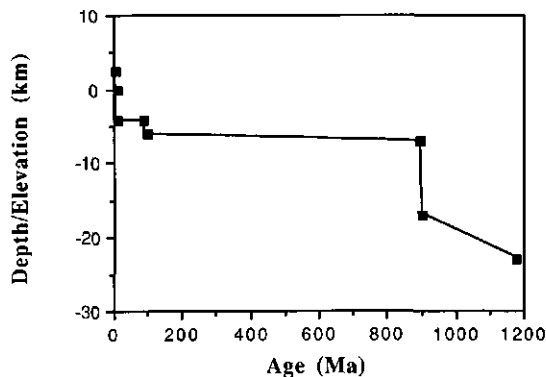


Fig. 14. Plot showing the uplift and cooling history of the Garzón Massif from the Precambrian to the Late Miocene as inferred from the fission track data given in the present chapter.

3. Around 100 Ma block faulting and differential uplift took place in the Garzón Massif. Data obtained from the literature indicate a widespread orogenic event and enhanced magmatic activity in the NW of the South American continent between ± 115 -80 Ma ago.

4. Apatite FT ages and geological evidence from the S. Neiva Basin show that between 12 Ma ago and the present time the Garzón Massif was uplifted some 6.5 km in at least two phases. The oldest phase occurred ≥ 12 Ma ago. It is clear from the track length distribution that both uplift and cooling took place very rapidly during this phase. The youngest phase started around 6.4 Ma and probably stopped before 3.3 Ma ago.

PART 3

DEPOSITS OF THE S. NEIVA BASIN

Chapter III

Neogene infill of the S. Neiva Basin

1. Introduction

In the S. Neiva Basin two sedimentary successions cover the pre-Cretaceous basement rocks (Butler and Schamel, 1988). The older succession is made up of Cretaceous to Oligocene rocks, which form eastward thinning wedges. The total thickness of the succession decreases from ± 6000 m along the edge of the Central Cordillera to 2500 m adjacent to the Garzón Massif (Butler and Schamel, 1988; see also fig. 5). This older succession is separated by an angular unconformity from the younger, Neogene succession.

The younger sedimentary succession consists of a sequence of ± 2600 m of fluvial and volcaniclastic sediments. This sequence was deposited in the S. Neiva Basin as a result of uplift of the Central Cordillera and the Garzón Massif, as well as activity of the Central Cordillera volcanic arc.

Because emphasis of the present study is on the Miocene to Recent deposits, no lithostratigraphical descriptions of the rocks belonging to the older succession will be given. The sediments of the younger succession are subdivided into a number of formal rock units and some informal rock units. The formal rock units comprise the La Cira Formation and the Miocene Honda and Gigante Formations (tables V, VI). The informal rock units are younger, locally developed units. Stratigraphical columns are depicted in figs. 15, 17, 18 and 19; their legend is given in fig. 16. The spatial distribution of all rock units is indicated on the geological map (appendix 1). The La Cira Formation, which is only 35 m thick in the S. Neiva Basin (see chapter VI), is not indicated separately on the map, but has been included in the Honda Formation.

2. Lithostratigraphy of the Neogene formal and informal rock units

2.1. Introduction

From old to young, the Neogene formal and informal rock units can be characterized as follows:

La Cira Formation: 35 m of red-brown and purplish mudstones lying conformably on top of the Upper Gualanday conglomerate.

Honda Formation: principally fluvial sandstones, pebbly sandstones and mudstone intercalations. In the upper part of the formation a polymict orthoconglomerate is present, termed the "Río Seco conglomerate" (Wellman, 1968). The components of this conglomerate are derived from the plutonic and metamorphic basement as well as from the pre-Neogene cover of the Central Cordillera.

Gigante Formation: polymict conglomerates are found at the base and the top of the formation (lower and upper members). The middle member consists of volcanoclastic deposits like tuffaceous sandstones, ignimbrites, and volcanic debris flow and hyperconcentrated flow deposits. The volcanics were erupted by volcanoes of the Central Cordillera volcanic arc. The conglomerates of the lower member, the Neiva Member, originated from erosional material of the Central Cordillera and from contemporaneous volcanism. The components of the conglomerates of the upper member, the Garzón Member, are partly derived from volcanics from the Central Cordillera and partly from the Precambrian Garzón Massif to the east.

Las Vueltas formation: poorly sorted coarse conglomerates alternating with sandstones and minor sandy siltstones. The components originated from basement rocks of the Garzón Massif. The formation is only present in the east of the basin, where it covers the underlying Gigante Formation with an angular unconformity.

Quaternary alluvial fan deposits: poorly sorted coarse-grained conglomerates and sandstones with minor sandy siltstone intercalations. The components are mainly derived from rocks of the Garzón Massif. The deposits are not folded and cover the older formations unconformably. The deposits form westward thinning wedges in the east of the study area. To a minor degree, alluvial fan deposits are developed at the west side of the Río Magdalena. The majority of the alluvial fan deposits is fault-bounded.

Quaternary river terraces: several terrace levels are found along the main rivers within the basin. The terraces consist of intercalated fluvial and volcanoclastic deposits like (tuffaceous) sandstones, conglomerates, volcanic debris flow deposits and minor siltstones and mudstones.

Youngest Quaternary deposits: low terraces, recent alluvial sediments, young undissected alluvial fans, scree and infills of small, intramontane basins.

2. 2. La Cira Formation

A short description of this formation is given in chapter VI. Deposits, which probably belong to the formation are found in the section Quebrada Guandinosa (fig. 15). As the formation is only 35 m thick in the S. Neiva Basin, it will not be discussed any further.

2. 3. Honda Formation

Nomenclature

An elaborate description of the nomenclature of the Honda Formation is given by Wellman (1970). The Honda Stage was named by Hettner (1892) after the town of Honda, located in the very north of the Department of Tolima. As confusion arose as to what units Hettner had intended to include in the Honda Stage, the Honda was redefined and extended by Butler (1942). Butler distinguished two major units: a lower and an upper Honda. The lower Honda, which is about 1600 m thick in the type section east of the town of La Dorada, consists of redbrown mudstones and sandstones resting conformably on the "La Cira faunal zone" of the La Cira Formation. Conglomerate is rare. The lower boundary of the conformable upper Honda is an arbitrary horizon above which conglomerate is abundant and pebbles of dacite and andesite are present. The upper Honda becomes more volcanic towards the top. East of the town of Honda, in the type section, the upper Honda has an estimated thickness of 2400 m.

An elaborate stratigraphical/sedimentological/petrological study of the Honda Formation was performed by Wellman (1968, 1970) in the Neiva and Honda Basins. This author originally subdivided the Honda Formation into two members, a lower La Dorada Member and an upper Villavieja Member. In 1970 Wellman elevated the formation to the rank of group and the members to the rank of formation. This subdivision, however, proved to be untenable in the S. Neiva Basin because small, isolated outcrops cannot be determined on the formational level. For that reason the Honda Formation is considered here as a formation (table V).

In chapter VI the deposits of the Honda Formation are discussed in terms of four large-scale sedimentary sequences showing different sedimentological properties. From below to above, these sequences are named A to D.

Table V. Subdivision of the Honda Formation.

EPOCH	AGE (Ma)	subdivision of present article		subdivision of Honda Fm. by Wellman (1968)	ENVIRONMENT	OROGENESIS
		Formation	Mbr./Sequence			
MIOCENE	7.9 ± 0.1	Gigante Formation	Los Altares Mbr.		Fluvial / Volcanic	UPLIFT GARZÓN MASSIF (± 12 Ma)
			Neiva Mbr.			
	Honda Formation	Sequence D	Villavieja Mbr.	Fluvial	VOLCANISM INTERMITTENT UPLIFT C. Cordillera	
		Sequence C	Río Seco Congl.			
		Sequence B	La Dorada Member	Fluvial / Volcanic		
		Sequence A				
— ? —	La Cira Fm.		Fluvial			
OLIGOCENE		Gualanday Group		Fluvial		

Sequences A to C coincide with Wellman's La Dorada Member, while sequence D corresponds to the Villavieja Member (table V).

Indication on the geological map

Where possible, the lower La Dorada Member and the upper Villavieja Member (Wellman, 1968) have been indicated separately on the geological map. The La Dorada Member is indicated with the letters Th_d; the Villavieja Member with the letters Th_v. The "Río Seco conglomerate", within the upper part of the La Dorada Member, is indicated by small circles. Where subdivision of the Honda proved impossible, the formation is indicated simply as Th.

Type section and type locality

The type section of the Honda Formation is found in the Quebrada Guandinosita (section QGt, fig. 15). Along the middle course of the small river, the upper 1000 m of the formation are well exposed in the cliffs of the ravine. The lower 500 m of the formation are poorly exposed along the lower reaches of the river, but can be studied 2 km further to the SW, SSE of the confluence of the Río Magdalena and the Río Páez (see geological map and fig. 28, p. 90). The exact thickness of the Honda Formation in this section is 1520 m. The section is described below.

Development of the La Dorada Member in the Q. Guandinosita section

The lower 900 m of the member consists of alternations of thick mudstone intervals with pebbly sandstones and sandstones. The sandstones have a colour varying between grey-brown, reddish and dark grey after weathering. The colour of the unweathered rocks is light-grey, beige-grey or grey-brown. The mudstone intervals have a reddish colour. Mottling is scarce. The sandstone intercalations in the lower 450 m are massive or horizontally bedded; from 450 m onward planar cross-bedding and trough cross-bedding is common (photo 9, p. 99). At 310 and 315 m, two tuffs are present. The lower unworked tuff is made up entirely of fresh volcanic constituents dominated by green hornblende and fresh plagioclase. The upper tuff shows some evidence of reworking.

In the interval between 450-900 m fossil rests of turtles were encountered locally. Furthermore, silicified and otherwise fossilized wood was found throughout the lower 900 m of the formation.

The interval between 900-1260 m is dominated by sandstones, pebbly sandstones and orthoconglomerates (photos 10, 11, 12, p. 99). Planar and trough cross-bedding are frequent in the sandstones and pebbly sandstones; the orthoconglomerates are massive or horizontally bedded. No fining upward tendency was noted in the conglomerate beds. However, many of the sandstone banks fine upward. The sandy matrix of the conglomerates and the sandstones have a light-brown, red-brown, grey-brown or dark grey colour when weathered and when fresh.

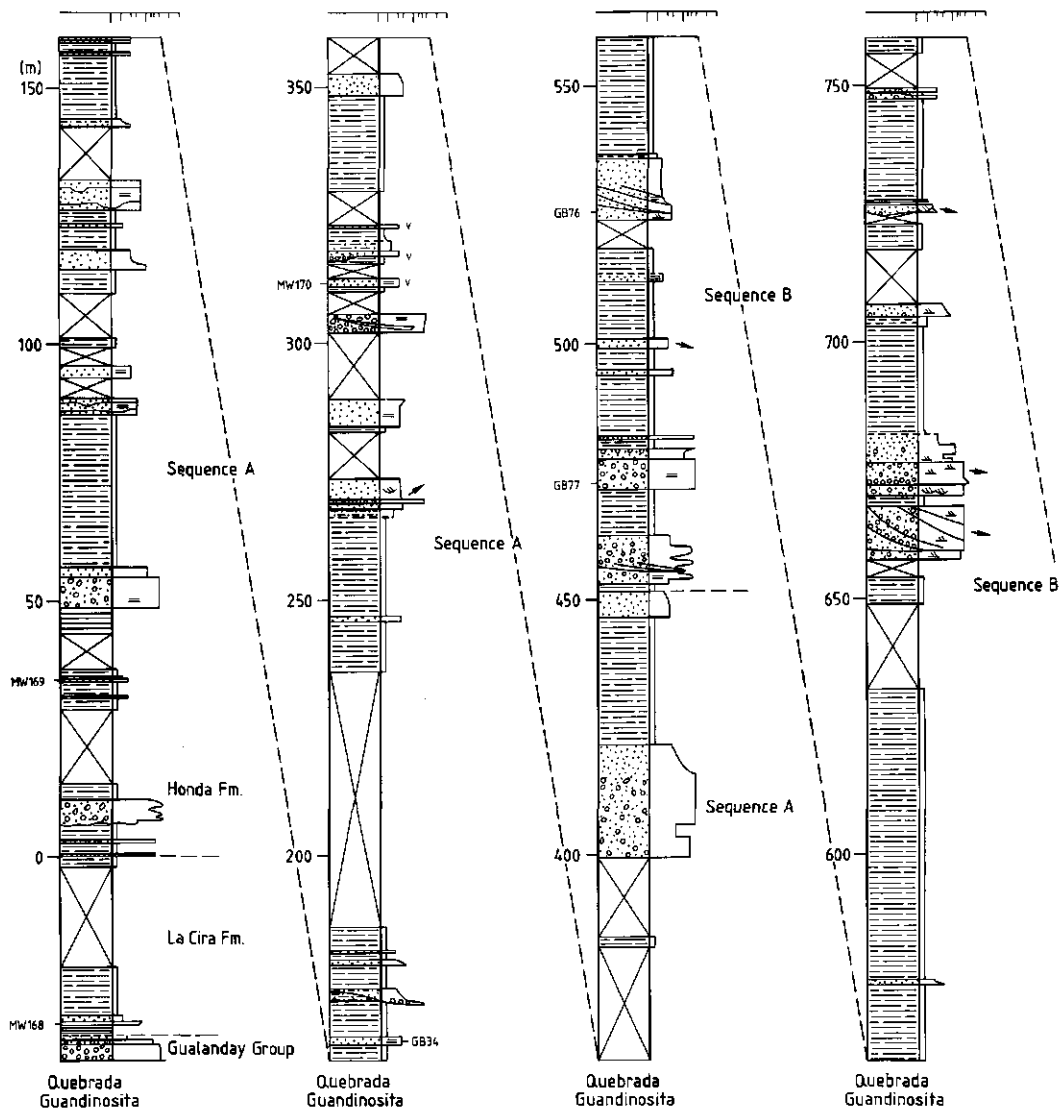
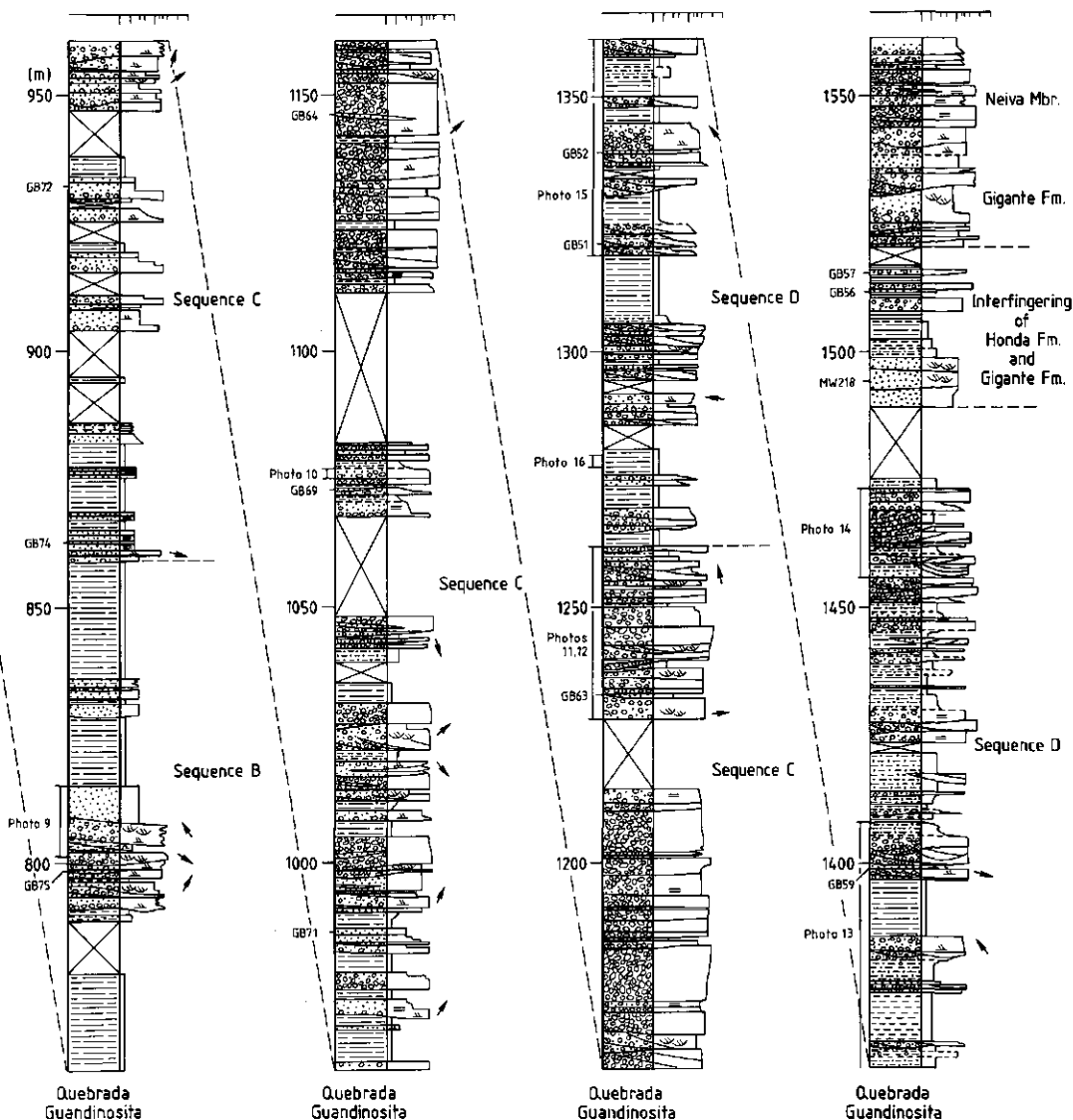


Fig. 15. Stratigraphy of the Honda Formation in the Quebrada Guandinosita section and other sections. For location of sections, see appendix 1 and figure 28. In the Q. Guandinosita section the paleocurrent directions are indicated by arrows at the right-hand side of the stratigraphical column. Sample numbers refer to

Mudstones intercalations are thinner and much scarcer. The mudstones have a red-brown colour and usually show grey mottling. The upper part of this interval, where orthoconglomerates predominate, was termed by Wellman (1968, 1970) the "Río Seco conglomerate" (photo 12, p. 99).

Development of the Villavieja Member in the Q. Guandinosita section

The interval between 1260-1490 m is characterized by approximately equal proportions of sandstones, pebbly



samples taken for point counting and/or radiometric or fission track age determinations. (Slightly reworked) air-fall tuffs are indicated by the letter v. Position of photos is also indicated. For legend, see fig. 16.

sandstones and conglomerates on the one hand and mudstones on the other hand (photo 13, p. 100). Orthoconglomerates are scarce, but pebbly sandstones abound (photos 14, 15, p. 100). The coarse-grained deposits exhibit strong channeling and the beds usually have scouring lower surfaces (photo 13, p. 100). Planar cross-bedding and trough cross-bedding are common. Many of the beds fine upward. The channel deposits have a light-brown, grey-brown or red-brown colour when weathered; fresh exposures have a grey-brown to light-grey colour. The mudstones are red-brown with grey mottles (photo 16, p. 100).

The transition to the overlying Gigante Formation is gradual: at 1490 m in the section a thick tuffaceous sandstone bed is found. This bed contains abundant fresh hypersthene grains and volcanic fragments, originating from contemporaneous volcanism. Above this bed, however, typical "Honda" sandstones are found up to a height of 1520 m in the stratigraphy. On the ground of the pebble and sandstone composition, the boundary between the Honda and the Gigante Formation is drawn at the base of a pebbly sandstone bed at 1520 m.

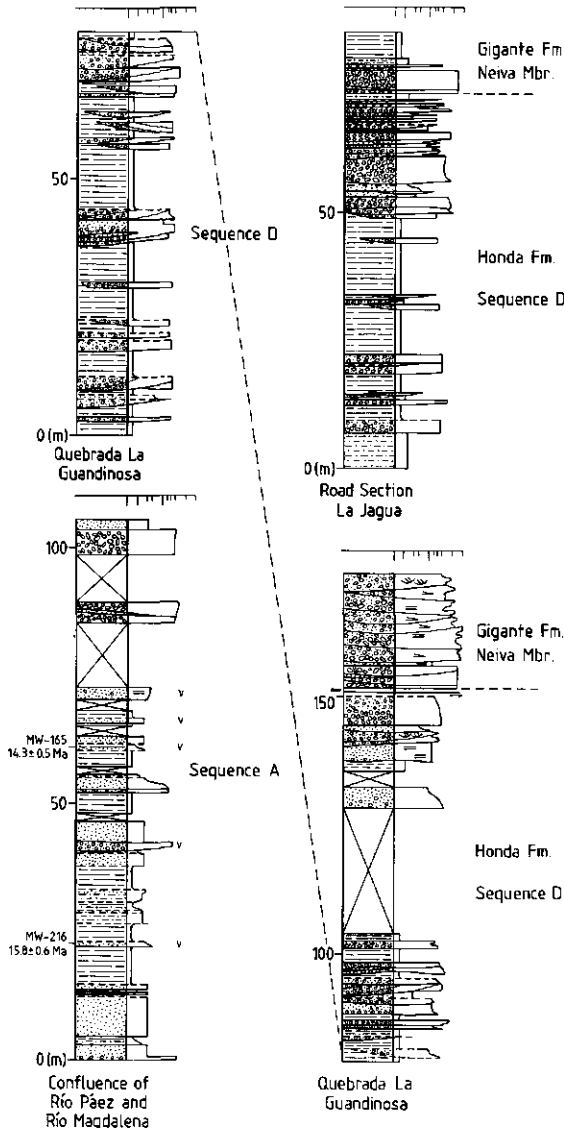


Fig. 15. Continued

Other sections

Other sections of the Honda Formation (fig. 15) are exposed at the west side of the confluence of the Río Magdalena and the Río Páez (section CPM), in the Quebrada La Guandinosita (section GGS) and along the main road from Garzón to La Jagua (section RSLJ; see geological map for exact locations). Although all these sections are much less complete than the Q. Guandinosita section - most of them show less than 150 m of the Honda stratigraphy - it can be concluded from both these sections and from outcrops of the formation that could be determined to the member level, that the upper part of the rock sequence of the Honda Formation is very constant throughout the basin (in the S of the basin the lower part of the formation is not exposed). Furthermore it is clear that at least in the northern part of the basin, the rock sequence of the whole formation shows little variation:

- In the section west of the confluence of the Río Páez and the Río Magdalena (indicated as CPM on the geological map), which exposes 100 m of the lower part of the La Dorada Member, three tuff beds are found that can be correlated with the tuffs in the Q. Guandinosita section. Similar tuffs were also encountered in a small outcrop along the lower reaches of the Quebrada Alonso Sánchez, N of the village of Ríoloro (see appendix 1).

- The "Río Seco conglomerate" was found in several outcrops in the northern half of the fieldwork area. Further to the south, the conglomerate is lacking as a result of reverse faulting within the formation (see geological map).

- The contact between the Honda Formation and the overlying Gigante Formation is well exposed in the section along the road to La Jagua (RSLJ on the map) and in the section taken on the Cuchilla del Tigre (section CdT).

In both cases interfingering of the formations is found. This interfingering is evident from the different compositions of the Honda and Gigante sandstones and conglomerates (chapter V, section 1).

- In the road section La Jagua and in the section taken in the Q. La Guandinosita, part of the Villavieja Member is disclosed. In both cases the rock sequence consists of approximately equal proportions of mudstones and channel deposits, as in the Q. Guandinosita. Also, the channels are strongly scouring and small, and the channel deposits are predominantly formed by pebbly sandstones while orthoconglomerates are virtually absent.

Thickness of the formation

In the Q. Guandinosita section the Honda Formation is 1520 m thick. In the very S of the fieldwork area the thickness of the formation could not be determined because the lower contact with the Gualanday Group is not exposed. In the center of the area only 800 m of the formation are exposed. This can partly be explained by the presence of a reverse fault in the upper part of the formation which cuts the "Río Seco conglomerate" (appendix 1). On the other hand it is clear from the geological map that the formation is thinner in this area. It is likely that thinning of the formation in the center of the basin is due to the presence of a very pronounced anticline in the Gualanday Group (Cerro de Matambo; see geological map, appendix 1). This structure was probably formed during deformation of the Chusma fault system (chapter I, section 3.3) and acted as a rigid block during deposition of the Honda Formation. This explanation is corroborated by the fact that directly south of the Cerro the Matambo, along the Quebrada Buenavista, the thickness of the formation increases again to at least 1200 m.

2. 4. Gigante Formation

Nomenclature

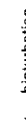
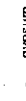
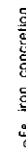
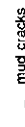
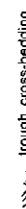
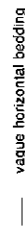
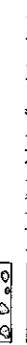
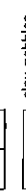
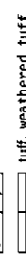
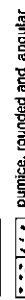
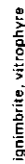
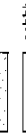
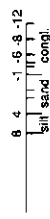
The Gigante Formation was originally described by Howe (1969) as one of the three rock units which together form the Mesa Group. The name Mesa (Weiske, 1938) was first applied to sedimentary rocks west of Honda (Department of Tolima). Butler (1942) designated a type locality northwest of Honda and described the formation more specifically as a predominantly volcaniclastic series overlying the Honda Formation in the Honda Basin. Similar volcaniclastic rocks in the Neiva Basin were correlated with the Mesa Formation on geological maps edited by the Servicio Geológico Nacional (1957, 1959). Van Houten and Travis (1968) divided the formation into three informal units: a lower and upper conglomeratic unit and a middle volcaniclastic unit.

Table VI. Subdivision of the Gigante Formation.

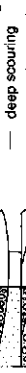
EPOCH / SUB-ERA	AGE (Ma)	subdivision used in present article		subdivision used by other authors	ENVIRONMENT	OROGENESIS
		Formation	Mbr. / Sequence			
QUATERNARY		younger volcanic deposits and terraces			Fluvial / Volcanic	↓
PLIOCENE		Las Vueltas formation			Fluvial	
MIocene	± 6.4	Gigante Formation	Garzón Mbr.	MESA GROUP Ceibas Congl. (Beltrán & Gallo 1968)	Fluvial / Volcanic	↑ VOLCANISM ↓
			Los Altares Member			
	± 8.0		Neiva Mbr.	Neiva Fm. (Howe, 1969, 1974)		
		Honda Formation	Sequence D		Fluvial	↑ INTERMITTENT UPLIFT C. Cordillera
			Sequence C			

LEGEND

COMPOSITION AND MAXIMUM GRAIN SIZE IN ϕ



BED BASE AND BED SURFACE STRUCTURES



OUTCROP DATA

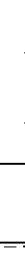
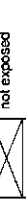
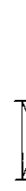


Fig. 16. Legend of all stratigraphical columns depicted in this thesis.

On the ground of the fact that all units are lithologically distinct throughout the Neiva Basin, Howe (1969) elevated the Mesa Formation to the rank of group and the lower two rock units to the rank of formations. These formations are the Neiva and Gigante Formation respectively (table VI). The upper conglomeratic unit, was not studied sufficiently by Howe to be proposed as a formal rock-stratigraphic unit.

Radiometric age determinations on Mesa deposits west of Honda gave ages between 4.3-3.5 Ma (Thouret, 1988), while K-Ar determinations on samples from the middle and upper part of the Gigante Formation in the Neiva Basin gave average ages between 8.0-6.4 Ma (Van Houten, 1976; Takemura and Danhara, 1983; this thesis, chapter IV).

Therefore, it is clear that the Mesa Formation in the Honda Basin cannot be correlated with the volcaniclastic deposits in the Neiva Basin. In order to prevent further confusion, it is proposed here to avoid the name "Mesa" for the volcanoclastics in the Neiva Basin.

The present study revealed that, in fact, the upper and lower conglomeratic units were deposited by the same fluvial system, *i.e.* a north-flowing paleo-Magdalena River (chapter VII). Only the clast composition of the two units is different (see below). Furthermore, according to Beltrán and Gallo (1968) the three different units of the formation were already defined together as the "Gigante Formation" by Richmond geologists in 1939, who chose the Quebrada Guandinosita as the type locality. The Name "Gigante Formation" has been used by several authors since that time (Beltrán and Gallo, 1968; Kroonenberg and Diederix, 1982). For these reasons it seems preferable to consider the three rock units as the three members of the Gigante Formation. It is proposed here that the members be called the Neiva Member (lower conglomeratic unit; formerly Neiva Formation), the Altares Member (middle volcanoclastic unit; formerly Gigante Formation) and the Garzón Member (upper conglomeratic unit) respectively (table VI). The Quebrada Guandinosita remains the type locality of the formation: here the whole rock sequence of the Neiva Member and Los Altares Member, as well as the contact between the Los Altares Member and the Garzón Member are exposed. Unfortunately only the lower 70 m of the Garzón Member are present in this section. No complete sections of the Garzón Member are found in the study area. The surroundings directly west and north of the town of Garzón give the most complete picture of the member: in the low hills directly W and N of Garzón thick conglomerate sequences are present, while the exposures north of Garzón along the main road to the town of Gigante show alternations of conglomerates and volcanoclastic deposits (fig. 17: Road Section Garzón).

Finally, it should be mentioned here that Howe (1969) considered the upper conglomeratic unit as a lateral equivalent of the "Ceibas conglomerate", which is exposed along the Río Ceibas E of the town of Neiva (Beltrán and Gallo, 1968). During the present investigation, however, it appeared that this "upper conglomeratic unit" could be further differentiated. In fact, the unit consist of two conglomeratic deposits with a very different composition and origin. The lower part of the upper conglomeratic unit overlies the Altares Member conformably and locally interfingers with it. Except for a higher percentage of clasts with a metamorphic origin, it is very similar in composition to the Neiva Member. The upper part of the upper conglomeratic unit, however, overlies the lower part with an angular unconformity of 10-13° and has a very different clast size and composition.

Only the lower part, which is described below as the Garzón Member of the Gigante Formation, is considered here to be the lateral equivalent of the "Ceibas conglomerate" in the sense of Beltrán and Gallo (1968). The upper part is described below as the lower unit of the Las Vueltas formation (table VI).

Indication on the geological map

On the map, the Neiva Member is indicated with the letters Tg_{1n}; the Los Altares Member with the letters Tg_{1a} and the Garzón Member with the letters Tg_{1g}.

Type section and type locality

The type section of the Gigante Formation is the Quebrada Guandinosita section, where the formation is 870 m thick. The lower 150 m of the section, belonging to the Neiva Member, are exposed in the quebrada while the rest of the section can be studied along the road from Gigante to El Hobo. This section, and other sections are described below. In order to facilitate direct comparison of the development of the members over the entire study area, however, parts of the same section, which belong to different members, will be described separately under the "member" headings.

Neiva Member

In the Q. Guandinosita (fig. 17), the Neiva Member is ±150 m thick and consists of 52 m of alternations of pebbly sandstones, sandstones and orthoconglomerates, followed by 45 m of mudstones and capped by another 52 m of massive orthoconglomerates with few sandy intercalations. The colour of the sandstones and sandy matrix of the conglomerates is light-brown to yellowish-brown after weathering; the colour of the unweathered sandstones and sandstone matrix is beige, light-brown or dark-brown. In the lower 52 m of the section, sandstones and pebbly sandstones predominate over orthoconglomerates (photo 17c, p. 113). The pebbly sandstones and sandstones often have conglomeratic channel lags. In these channel lags intraformational clasts may be present. Most beds are

horizontally bedded, but planar cross-stratification and trough-stratification also occur. The lower part of the mudstone interval is poorly exposed. The mudstones have a red-brown colour without mottles.

The multistoried conglomerate beds, which form the upper 52 m of the member, are clast supported and often show imbrication. They are massive or horizontally bedded. The basal contacts of the beds are scouring. The clasts are well rounded, moderately sorted and vary in size between 3-30 cm. The clast composition indicates that they are mainly derived from the Central Cordillera. Both clasts from the basement and the cover of the Central Cordillera and fresh volcanic clasts, originating from contemporaneous volcanism are present. Only some 3% of the clasts has an eastern provenance (chapter V, section 1.3). Intercalated sandstones lenses and beds are horizontally bedded or show low angle cross-stratification or tabular cross-stratification.

In the section, the contact between the Neiva Member and the overlying Los Altares Member is sharp: immediately above the last conglomeratic bank tuffaceous sandstones are found. As pumice-containing sandstones are found nowhere in the Neiva Member, the boundary between the members is placed at this contact.

In the center and the southern part of the basin good exposures of the Neiva Member are found in the sections in the Quebrada La Guandinosita (section QGs), on the Cuchilla del Tigre (section CdT) and in the Quebrada las Damas (sections QLD-A and QLD-B, fig. 17). The contact with the underlying Honda Formation on the Cuchilla del Tigre has already been discussed (section 2.3). In the other two sections the contact is a fault.

In all cases the rock sequence of the Neiva Member is different from the sequence observed in the Q. Guandinosita. Apparently, cyclicity is lacking and no fixed rock sequence is developed in the Neiva Member, as has already been mentioned by Howe (1974). Similarities between the development of the Neiva Member in the different sections, are the occurrence of thick sequences of multistoried conglomerate, the intercalations of sandstones and pebbly sandstones which sometimes contain intraformational mudstone clasts, the type of sedimentary structures present, the clast composition, the lack of tuffaceous sandstones and the colour of the deposits. In contrast to the other sections, the Neiva conglomerates and sandstones of the lower part of the Quebrada las Damas section exhibit lateral accretion surfaces.

In the south, the thickness of the Neiva Member is much greater than in the rest of the S. Neiva Basin. The lower 200 m of the section Quebrada las Damas (Q. las Damas-A, fig. 17) show alternations of Neiva conglomerates and sandstones. The following 200 m are not exposed. In the upper part of the section (Q. las Damas-B), Neiva conglomerates interfinger with tuffaceous sandstones of the Los Altares Member up to a height of ± 100 m. This means that in total, Neiva deposits predominate to a height of 500 m of the stratigraphy.

Toward the N, the great thickness of the Neiva deposits gradually declines. On the geological map it is visible that 4 km NNW of Garzón, at the point where the road from Garzón to Agrado crosses the Río Magdalena, the Neiva Member has a thickness of 150-200 m and does not interfinger extensively with the Los Altares Member anymore.

Los Altares Member

In the Q. Guandinosita section the 580 m thick Los Altares Member consists of alternations of tuffaceous sandstones, polymict orthoconglomerates, siltstones, volcanic debris flow deposits, hyperconcentrated flow deposits, ignimbrites and some reworked tuffs. The rock sequence is characterized by a lack of cyclicity. The sandstones and volcanoclastic rocks have a brown-grey to dark-grey colour when weathered; fresh exposures have a brown-grey, grey or light-grey colour. The grey mudstones do not show any mottling.

The lower 70 m are dominated by alternating mudstone intervals and sandy fluvial channel deposits; the next hundred meters by volcanic debris flow deposits. Above that interval, two series of superimposed volcanic debris flow deposits are found with thicknesses of individual deposits up to 17.5 m (photo 23a, p. 116). These deposits are separated from one another by 5-20 cm thick parallel laminated pebbly sandstones (Sh) that scour the underlying deposits and also have sharp contacts with the overlying flow deposits (Howe, 1969; see also photo 23b, p. 116).

The sandstones were either formed by reworking of the top of the underlying debris flow deposit by fluvial processes (Schmincke, 1967) or by shearing of the top of the lower debris-flow deposit by the next debris flow. Horizontally bedded tuffaceous sandstones predominate throughout the upper part of the sequence (photo 23c, p. 116). Conglomeratic intercalations become scarcer toward the top of the member, while the siltstone intervals become more abundant and thicker.

All deposits are massive or horizontally bedded or exhibit low angle cross-stratification; trough cross-bedding and planar cross-bedding are very scarce. Most beds have planar basal contacts with the underlying beds; only the conglomerates and some of the sandstones have scouring lower contacts.

The contact with the Garzón Member is abrupt: it is put at the base of the first of a series of orthoconglomeratic intercalations.

An almost complete section through the Los Altares Member is also found in the center of the S. Neiva Basin. In the Quebrada La Honda section (section QLH, fig. 17), which is located 9 km further to the SSW with respect to the Quebrada Guandinosita section, only the upper 2 m of the Neiva Member are exposed. The contact with the Los

Altares Member is probably abrupt: above the conglomeratic upper 2 m of the Neiva Member some thin pebbly sandstones are found, followed by a tuffaceous siltstone bed. The top of the conglomerate was taken as the boundary between the members.

In this section, the exact thickness of the member cannot be determined, because the interval between 552-670 m is not exposed. On the ground of the surrounding geology, it was decided to place the boundary with the Garzón Member at 670 m.

The rock sequence of the Los Altares Member is somewhat different from the sequence in the Quebrada Guandinosita section: the deposits are finer-grained and siltstones are much more common. Conglomerates are virtually absent and no thick volcanic debris flow deposits are found in the lower part of the member. Similarities with the Quebrada Guandinosita section are the flat basal contacts of the beds with the underlying deposits, the complete predominance of massive and horizontally bedded deposits and beds with low-angle cross-stratification, the lack of a consistent order of the bed sequence and the grey colour of the deposits.

In the center and the south of the study area, in the section La Laguna (section LL), the section along the road from Garzón to Agrado (section RSGA) and the section in the Quebrada Jagualito (section QJto) (fig. 17; see appendix 1 for locations), only part of the Los Altares Member is exposed. The development of the member is very similar to its development in the Quebrada La Honda: fine-grained tuffaceous sandstones predominate. Only the lower part of the Quebrada Jagualito section is different. This part of the section consists almost entirely of multistorey polymict conglomerate beds with minor sandstone intercalations. The composition of the conglomerate is very similar to that of the conglomerates of the Neiva and Garzón Members; the maximum size of the clasts is 30 cm.

In the very south of the basin, around the town of Garzón, the Los Altares Member is poorly exposed. Estimates of the thickness of the member on the geological map (appendix 1) suggest a total thickness of 250-300 m. It has already been pointed out above that in this part of the area, the Los Altares and Neiva Members show extensive interfingering. The sum of the thicknesses of both members amounts to 750-800 m, which agrees with the total thickness of both members in other places.

Garzón Member

In the Q. Guandinosita section (fig. 17), only 70 m of the Garzón Member are preserved. It is likely that the member was originally much thicker at this locality, but that the top was eroded during regional folding and faulting. The member consists mainly of polymict orthoconglomerates with intercalations of blue-grey coloured sand. A similar hue, found in some of the sandstones occurring in the Honda Formation and at the transition from the Neiva Member to the Los Altares Member, was attributed by Van Houten and Travis (1968), Wellman (1970) and Howe (1974) to montmorillonite coatings on the grains. In thin section, however, no clay coatings are visible on the majority of the sandstone grains of the Gigante Formation. It seems more likely that, at least in this formation, the blue color is the original color of the andesitic clasts which make up the greater part of these sandstones.

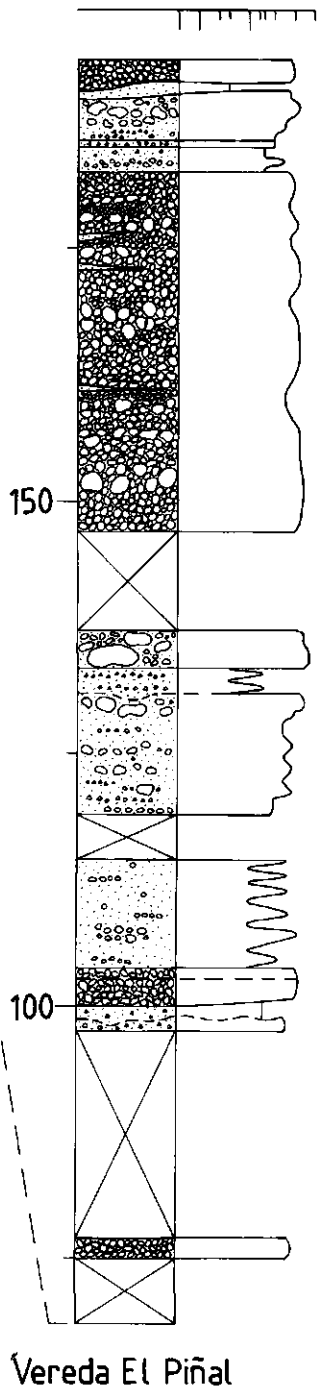
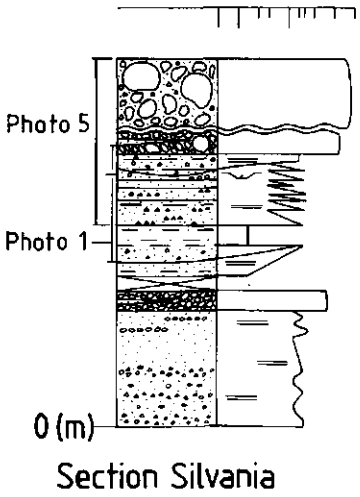
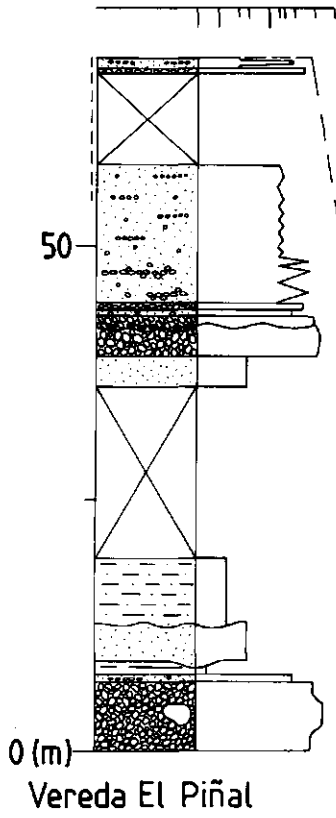
The sandstones are massive or horizontally bedded, or show low-angle cross-bedding. The orthoconglomerates are well rounded, moderately to poorly sorted and often exhibit pebble imbrication. Individual beds form multistorey sequences of up to 20 m thickness. The composition of the conglomerates indicates that at least 18% of the clasts is derived from erosion of the Garzón Massif to the east (chapter V, section 1.3). The sandy matrix of the conglomerates has a brown-grey, grey or dark-grey colour after weathering; the fresh rock has a yellow-grey, blue-grey or grey colour.

The development of the Garzón Member in the Quebrada La Honda, of which only the lower 50 m are present, is comparable to the development of the member in the Quebrada Guandinosita. Multistorey polymict orthoconglomerates predominate and alternate with intercalations of blue-grey sandstones. In the middle of the member an ignimbrite is found.

In the center of the basin the sediments of the Garzón Member are strongly disturbed by the La Jagua Fault. Only a small portion of the Garzón Member is exposed in a section at the NNW termination of the Zanjón de la Barrialosa (section ZdB, fig. 17). Here, 50 m of alternating multistorey conglomerates, blue-grey sandstones and some white siltstones are present. The maximum clast size of the conglomerates is 25 cm. The sandy matrix of the conglomerates has a brown to blue-grey colour when fresh and when weathered.

Further south, the approximate thickness of the member is about 250 m, as can be estimated from profile B-B' (appendix 1). In this area, the maximum clast size of the conglomerates appears to be much coarser than in the N. In one outcrop even an andesite boulder with a diameter of 2.5 m was found (photo 18, p. 113). In most outcrops, however, the maximum clast size lies between 30-130 cm.

Further to the S, along the road Garzón-Gigante, several small outcrops of the Garzón Member are present. In the southernmost part of the area, the upper 70 m of the Garzón Member are well exposed in the section along the road from Garzón to Gigante, just N of Garzón (section RSG, fig. 17). The sequence consists again of coarse, well rounded and poorly to moderately sorted conglomerates which alternate with, partly tuffaceous, sandstones. The



maximum clast size of the conglomerates is 60 cm. A layer of weathered ash situated some 15 m below the top of the section was used for fission-track dating (sample MW 537). Measurements on the geological map indicate that the thickness of the member at this location is ± 130 m. An identical ash layer was found in the N of the study area where the estimated thickness of the member is ± 250 m (see above). At that location the ash is positioned some 75-100 m below the top of the member. As it seems to be very probable that the weathered ash layer in the N represents the same layer found in the S of the basin, it is likely that the member is incomplete in the S. Assuming that the ash layer in the S of the study area was also located some 75-100 m below the top of the Garzón Member, this means that at least 60-85 m of sediment have been eroded away as a result of folding and faulting of the area.

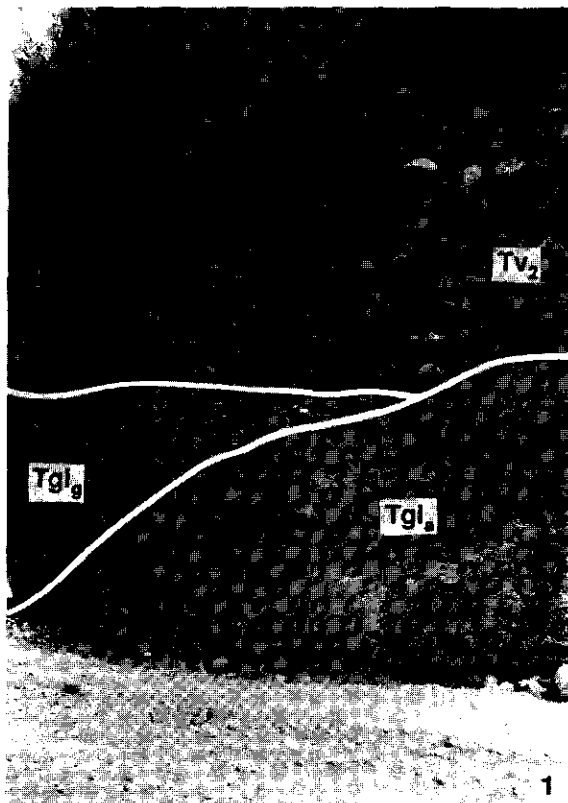
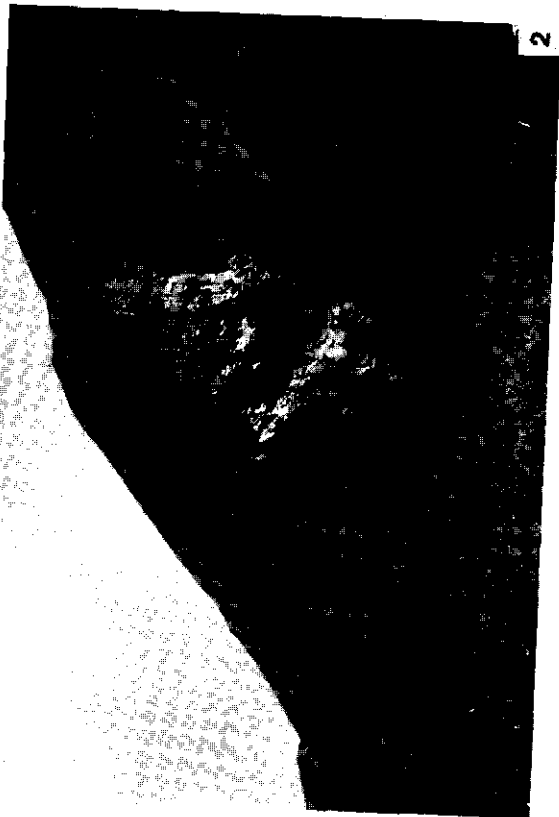


Photo 1. Contact between the Los Altares Member (Tgi_a) and the Garzón Member (Tgi_g) in the Section Sylvania. The Gigante Formation is unconformably overlain by a debris flow deposit, belonging to the upper unit of the Las Vueltas formation (Tv_2). View of the photo is toward the SE. Length of hammer is ± 30 cm.

Sections in the east of the basin

From the above it is clear that, apart from the greater thickness of the Neiva Member in the S of the basin and apart from variations in grain size and rock sequence, the thickness and composition of the different members of the Gigante Formation are very consistent throughout the basin. In the very east of the study area, however, just west of the Garzón-Algeciras Fault, the situation is different. In this area the Los Altares Member is only 310 m thick, as can be estimated on the geological map. Two sections from this region are shown in fig. 18. In the section Sylvania (section SS on the geological map) only 27 m of the Altares Member are exposed. The sediments are overlain conformably by a conglomerate of the Garzón Member. This conglomerate is covered unconformably by the upper unit of the Las Vueltas formation (photo 1).

Fig. 18. Stratigraphy of the Gigante Formation in the eastern part of the S. Neiva Basin. For location of sections see geological map and figure 32. Position of photos is also indicated. For legend see fig. 16.



The Los Altares Member consists predominantly of horizontally bedded pebbly sandstones with some intercalations of sandy silt and a conglomerate bed. In contrast to exposures of the member further to the W which have a grey colour, the sediments in the Sylvania section have a brown to red-brown colour, both after weathering and when fresh. This colour is due to the presence of Fe-oxides. Furthermore, the composition of the conglomerates and the pebbles within the pebbly sandstones is different, the portion of east-derived components being much higher than further to the west (chapter V, section 1.3). The Garzón Member conglomerate lacks west-derived components, and also has a brown colour. A paleocurrent measurement in this conglomerate indicates paleoflow toward the west.

The same is valid for the section Vereda el Piñal (section VeP). In this section the upper part of the Los Altares Member and the Garzón Member interfinger: east-derived coarse conglomerates with a brown sandy matrix and poorly rounded and sorted brown sandstones alternate with conglomerates with a high share of fresh volcanic clasts and blue-grey sandstones containing heavy minerals. The maximum clast size of the conglomerates varies between 20 cm and 2 m.

2. 5. *Las Vueltas formation*

Nomenclature

The Las Vueltas formation is named after the Quebrada Las Vueltas, where the formation is well exposed 1.5 km NNW of the village of Potrerillos. Here, the formation crops out in the cliffs along the E side of the small river. No sections could be taken in the formation, because outcrops were too small or could not be reached. The formation is present only on the east side of the S. Neiva Basin. To the south, it gradually disappears. The contact with the underlying Gigante Formation is formed by an angular unconformity. The formation may be subdivided informally into two units. Lithologically, these units are indistinguishable, but their distribution and angular unconformity with the underlying sediments vary.

Indication on the geological map

On the map the older unit of the Las Vueltas formation is indicated as Tv₁ and the younger unit of the formation as Tv₂. The names "lower" and "upper" unit have been avoided deliberately, because the deposits are separated by an angular unconformity and because they have a different distribution: the younger unit only partly covers the older one.

Type locality and type section

The type locality of the formation is the Quebrada Las Vueltas, located directly N of the village of Potrerillos. Here, the lower unit of the formation crops out in the cliffs along the E-side of the small river. No type section could be taken, because the cliffs are too steep to allow stratigraphical measurements. The description of the older unit, given below has been pieced together from the development of the unit in isolated outcrops as well as from a generalized description of the outcrops in the cliffs.

No type section could be taken in the younger unit either, because it is very poorly exposed. The description of the unit is based on several isolated outcrops.

The older unit

The older unit of the Las Vueltas formation is found in the NE of the study area in the Gigante Syncline and the N part of the Zuluaga Anticline. Although the unit covers the underlying Garzón Member of the Gigante Formation with an angular unconformity of 10-13°, it has been folded along with the underlying formations. The unit disappears S of the Quebrada Alonso Sánchez. It consists of at least 300 m of poorly sorted and poorly to

Photo 2. Lower unit of the Las Vueltas formation. Bank thickness of the conglomerates and sandstones is 2 to 5 m. Q. Las Vueltas. View of the photo is toward the NNW.

Photo 3. Very poorly sorted and rounded conglomerate in the lower unit of the Las Vueltas formation. Q. Las Vueltas. View of the photo is toward the NNW.

Photo 4. Lower unit of the Las Vueltas formation. Irregular conglomerate and sandstone beds, varying in thickness between 0.5-2 m. W-limb of the Gigante Syncline ±3.5 km NNE of Gigante. View of the photo is toward the WNW. Length of hammer is ±30 cm.

Photo 5. Upper unit of the Las Vueltas Formation, consisting of a debris flow deposit which unconformably overlies deposits of the Los Altares Member of the Gigante Formation. Section Sylvania. View of the photo is toward the SE.

moderately rounded pebble to boulder conglomerate, with intercalations of coarse-grained, poorly sorted sandstones and minor sandy siltstones and mudstones. The conglomerates may be either clast supported channel conglomerates with a sandy matrix, or matrix supported non-volcanic debris flow deposits.

In the very NE of the basin, clast-supported conglomerates are found in layers of 2-5 m thickness, separated by very thin sandstone intercalations (photo 2). The layers cannot be followed over large distances but rapidly pinch out laterally. The basal contacts of the beds are often strongly scouring (photo 2). Locally, the beds are separated by a crust of Fe-oxides of a few cm thickness. The matrix of the conglomerates is very poorly sorted and consists of material, varying in grain size between silt and coarse sand. The major fraction of the conglomerates in this area is formed by clasts of Jurassic intrusives. The clasts are subrounded to angular; the maximum clast size is 3 m (photo 3). Locally, they show imbrication. Imbrication measurements on 20 pebbles of one of the conglomerate beds revealed a paleocurrent direction towards the NNW. No other measurements could be taken. The sandstones and the sandy matrix of the conglomerates have a light-brown to pink-brown colour. Intercalated sandy and pebbly mudstones have a green to bluish-grey colour.

Debris-flow deposits which are exposed somewhat further to the south are extremely poorly sorted. The clasts are angular to subangular. The debris flow beds have strongly scouring bases.

On the W-side of the axis of the Gigante Syncline, the deposits of the older unit of the Las Vueltas formation are generally finer-grained and better rounded. No debris-flow deposits are found in this area; the conglomerates are clast-supported. The conglomerates and sandstones occur in irregular beds varying in thickness between 50 cm and 2 m (photo 4). The clasts are rounded to subrounded in some beds and subrounded to subangular in others. The maximum observed clast size is 2 m, but a clast size of 30-100 cm is more common. The sandy matrix of the conglomerates is very poorly sorted and varies in grain size between silt and coarse sand. Silty sandstone intercalations sometimes show paleosol development and mottling. The colour of the deposits is variable: siltstones and fine-grained sandstones are generally white; the colour of the coarser sandstones and sandy matrix of the conglomerates may be white, beige or pink-beige. In the western limb of the syncline the original geomorphic form of the deposits has been conserved, clearly showing that the deposits were laid down on alluvial fans.

The younger unit

The younger unit of the Las Vueltas formation has not been folded, but covers the underlying folded sediments horizontally. Locally, the unit has been slightly disturbed tectonically.

Like the older unit, the younger unit is found only in the east of the basin. The unit is found east of Gigante, to the E and NE of the Zuluaga Anticline, and extends to the Quebrada de Mayo, 20 km further to the SSW. Deposits of this unit are found both east and west of the Garzón-Algeciras Fault, although the greater part of the deposits ends against the fault. The deposits that occur east of the Garzón-Algeciras Fault are also fault-bounded and end against a fault directly SE of the Garzón-Algeciras Fault.

Geomorphologically, the deposits have a very irregular hummocky surface. On the aerial photographs it is visible that the northern part of the unit consists of superimposed fans with a different extent and distribution.

Exposures in the younger unit are scarce. East of Gigante, some exposures in the fan deposits show alternating layers of very poorly rounded and sorted coarse sand with clast-supported conglomeratic layers. The maximum clast size of the conglomerates amounts to some 90 cm. The conglomerates mainly consist of Jurassic intrusives. The sandy matrix of the conglomerates and the sand intercalations may have a white, orange-red, red or brown colour, both after weathering and in fresh exposures.

East of the Zuluaga Anticline a single exposure is found in a very poorly sorted massive debris flow deposit of at least 6 m thick, with a high content of clasts of gneisses and intrusives (photo 5). The maximum diameter of the angular to subrounded clasts is 2 m. The colour after weathering and the fresh colour of the deposit are brown.

2. 6. *Quaternary alluvial fan deposits*

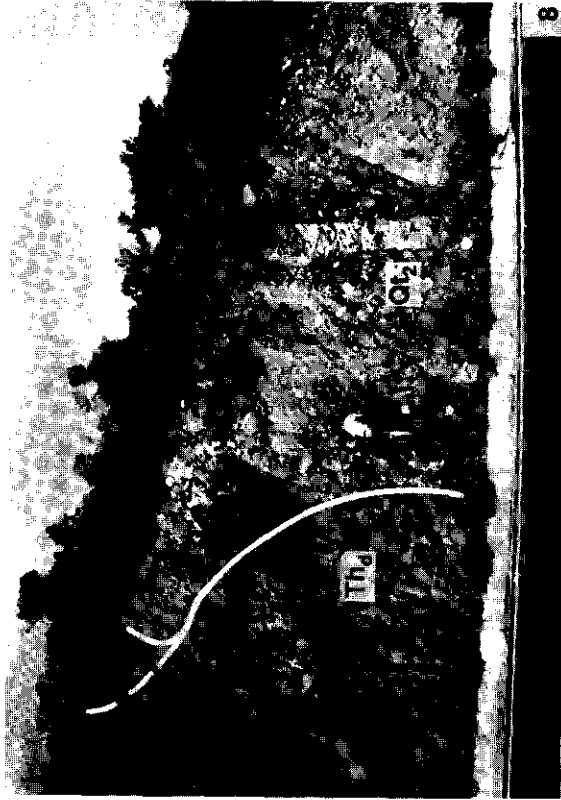
Indication on the geological map

On the map, two kinds of Quaternary alluvial fan deposits have been distinguished: older, dissected alluvial fan deposits are indicated as Qaf₁, while younger, only slightly dissected deposits are indicated as Qaf₂.

Photo 6. Little dissected alluvial fan S of Gigante along the Q. La Honda, belonging to the "younger, slightly dissected alluvial fan deposits". View of the photo is toward the NNE.

Photo 7. Alluvial fan deposit containing tuffaceous sandstone blocks from the underlying Gigante Formation. Zanjón de la Barrialosa. View of the photo is to the NW. Man is 1.85 m tall.

Photo 8. High terrace along the Q. Guandinosita (Qt₂). At the site of the photograph, the terrace is traversed by a reverse fault and juxtaposed against overturned sediments of the lower member of the Honda Formation (Th_d). Photo was taken along the road from El Hobo to Gigante. View of the photo is toward the E. Man is ± 2 m tall.



Older, dissected alluvial fan deposits

Older, dissected alluvial fan deposits are found both on the west and the east side of the Río Magdalena. Deposits to the NW of the Cuchilla del Tigre, on the west side of the river, appear to be related to a small fault within the Upper Gualanday conglomerate. This fault is not indicated on the map. The alluvial fans consist entirely of Gualanday conglomerate.

On the east side of the Río Magdalena deposits belonging to this mapping unit are found east of the confluence of the Magdalena and Suaza Rivers and in the central part of the basin along the axis of the Garzón Syncline. Although the fans in the center of the study area consist mainly of material provening from the Garzón Massif, above all Jurassic intrusive rocks, the fans are clearly younger than the deposits of the Las Vueltas formation.

East of the confluence of the Río Magdalena and the Río Suaza, some strongly dissected and eroded alluvial fans are found. The fans have a clast composition which is different from that of the other fans. Apart from a high percentage of clasts originating from Jurassic intrusives, clasts from volcanoclastic rocks belonging to the Saldaña Formation, Precambrian metamorphic clasts, chert from Cretaceous deposits, Paleozoic quartzite and shale and reworked volcanics from the Gigante Formation are present. Furthermore, the material is very angular. As the fans are found just W of some thrusts consisting of Paleozoic and Jurassic material (appendix 1), it is likely that they originated from erosion of these small thrust sheets.

Younger, slightly dissected alluvial fan deposits

Younger, slightly dissected alluvial fan deposits are present only at the east side of the Magdalena River (photo 6). Although the apex of some of the fans has been eroded away, the majority appears to have originated along faults within the massif. The smaller fans E and S of Gigante, however, seem to have originated along faults within the Las Vueltas formation.

The fans consist for the greater part of erosional material from the Garzón Massif. In the fans that do not have their origin in the Garzón Massif some admixture of erosional material from the Honda and Gigante Formations may be present. An example is the young alluvial fan along the Quebrada La Honda, just S of Gigante, which contains up to 3 m large blocks of tuffaceous Gigante sandstone and ignimbrites (photo 7).

2. 7. Quaternary terraces

Indication on the geological map

Four main terrace levels are present. The highest level, indicated on the map as Qt₁ lies 500 m above above the streambed of the present Magdalena River, the high terrace (Qt₂) 90-50 m, the middle terrace (Qt₃) 50-20 m and the low terrace, which has been included in the Qal deposits on the map, 0-10 m

Although it is possible to make a finer subdivision within the terrace levels, this has not been done, because a very elaborate study of the Quaternary deposits is outside the scope of the present investigation.

The highest terrace

The highest terrace is found at an elevation of 500 m above the present-day base level of the Magdalena River, is only present at two locations in the study area. Both times it is found unconformably on deposits in the eastern limb of the Zuluaga Anticline in the E of the basin. The location of these terrace remnants in the very E of the basin suggests that either the Magdalena River flowed much further to the east at the time of their formation or that the terraces were not deposited by the Magdalena River, but by two of its tributaries, *i.e.* the Río Loro and the Q. de Garzón.

In the southernmost of the two remnants 15 m of conglomerate deposits are disclosed. The conglomerate consists of well rounded and moderately sorted pebbles and boulders with a maximum diameter of 50 cm. The average clast size is 15 cm. The conglomerate is formed by clasts originating from Precambrian gneisses and granulites, Jurassic intrusives, volcanics from the Saldaña Formation and from contemporaneous volcanism and sandstone pebbles from Cretaceous formations.

The high terrace

The high terrace is found along the present course of the Magdalena River. The terrace sediments consist of alternations of fluvial conglomerates, volcanoclastic and fluvial sandstones, minor siltstone and volcanic debris flow deposits. In the N of the study area the terrace is found at an elevation of some 70-90 m above the streambed of the Magdalena River. One of these terraces, however, which unconformably covers the Honda Formation along the Quebrada Guandinosita, is faulted and partly uplifted to an elevation of 250 m above the Magdalena River streambed. The faulted terrace is turned to a near-vertical position and rests unconformably against overturned Honda deposits (photo 8). A section through the terrace is given in fig. 19.

(ROAD SECTION EL HOBO - GIGANTE)
Terrace Qt₂ on Honda Fm.; Quebrada Guandinosita

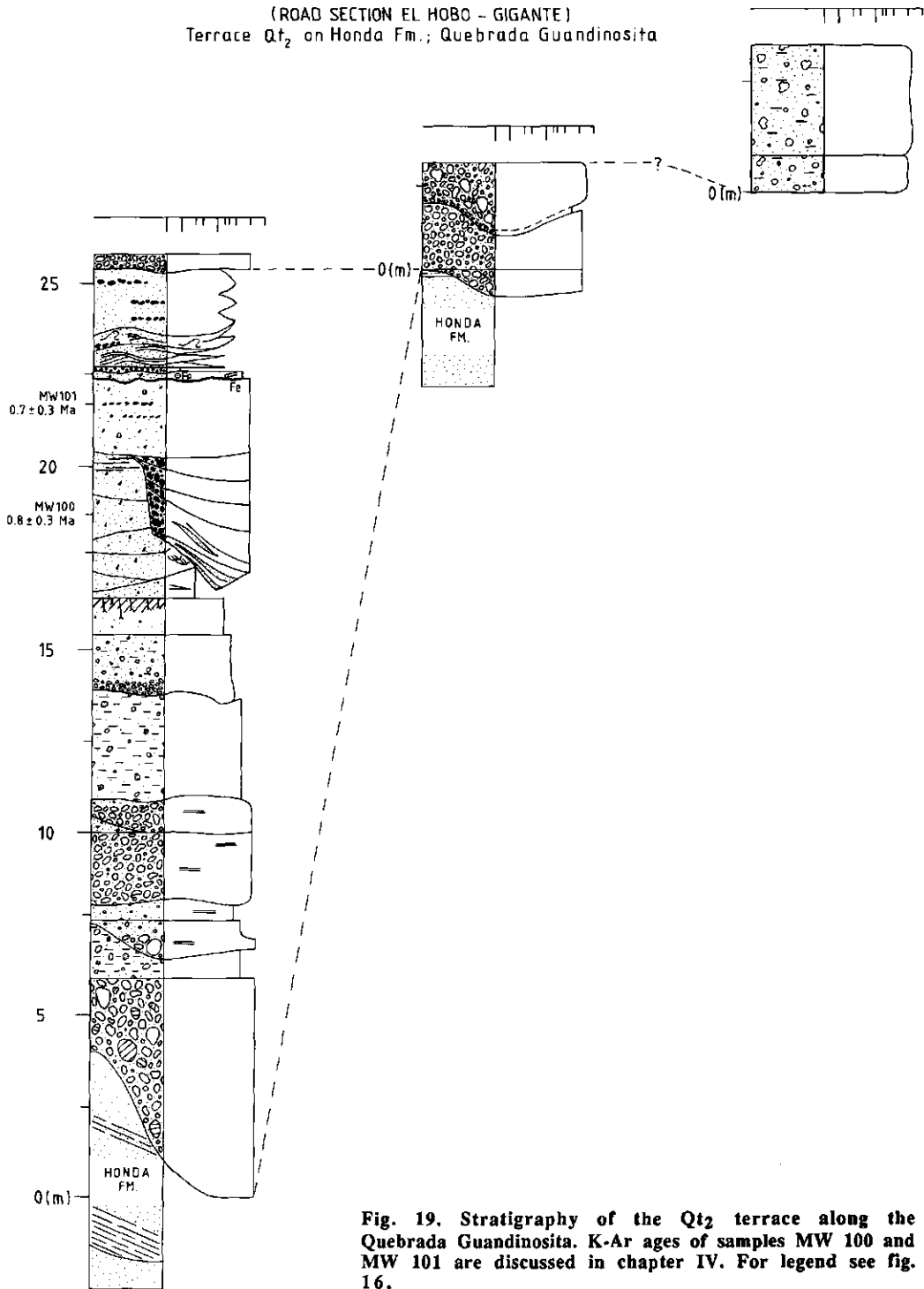


Fig. 19. Stratigraphy of the Qt₂ terrace along the Quebrada Guandinosita. K-Ar ages of samples MW 100 and MW 101 are discussed in chapter IV. For legend see fig. 16.

In the S of the study area, the same terrace level is developed in deposits of the "Altamira Lahar". The "Altamira Lahar" has been described originally by Van Houten (1976). In fact, the name is incorrect because the "Altamira Lahar" consists of a sequence of volcanic debris flow deposits and intercalated fluvial deposits. For this reason the name is given in quotes here.

The maximum thickness of the "Altamira Lahar" amounts to some 30-40 m. The 2-7 m thick volcanic debris flow deposits consist of up to 1.30 m big angular lava blocks of predominantly andesitic composition in a sandy matrix of fine volcanic fragments. In the uppermost and lowermost parts of the sequence fluvial imbricated conglomerates, sandstones and siltstones are found intercalated with much thinner (≤ 70 cm) volcanic debris flow deposits. The imbrication of the conglomerates indicates paleoflow towards 34° . The conglomerates are well rounded and moderately to poorly sorted and consist of chert, Saldaña Formation volcanics, Jurassic intrusives, Precambrian metamorphic rocks, and pumice and andesite clasts originating from contemporaneous volcanism. The sandstones are horizontally laminated and consist mainly of poorly rounded andesite fragments. The sandy siltstone intercalations are maximally 80 cm thick and may exhibit paleosol development. The "Altamira Lahar" terrace (Qt_{2a}) lies ± 50 m above the present-day streambed of the Río Magdalena. It is probable that the terrace is an erosional terrace that formed after deposition of the fluvio-volcanic sequence.

The middle terrace

The middle terrace is found at an elevation of 50-20 m above the river bottom of the present-day Magdalena River. Terraces at this level consist of fluvial deposits like fluvial sandstones and conglomerates. The fluvial sediments are usually topped by one or more volcanic debris flow deposits or by a pumice-rich sandstone layer.

The intercalated debris flow deposits are finer-grained than the deposits of the "Altamira Lahar" and have a maximum clast size of 20-30 cm. Furthermore, the composition of the debris flow deposits is more heterogenous than that of the "Altamira Lahar": apart from some 60-70% of andesite blocks, dacite, granite and schist may be present. Well-rounded andesite cobbles indicate that reworked older material may be present. In spite of these differences, it is quite possible that the middle terrace found at the north- and east-side of the "Altamira Lahar" terrace represents a younger erosional terrace, formed in the "Altamira Lahar" deposits.

2. 8. Youngest Quaternary alluvial deposits

Indication on the geological map

On the map, all deposits belonging to this group are indicated as Qal.

Description

This group comprises the youngest, undissected alluvial fans, recent alluvial sediments in the main rivers and main tributaries, low river terraces, located at an elevation of 0-10 m above the present-day streambed of the three main rivers, scree and sedimentary fills of small intramontane basins. The latter sediments consist mainly of coalescing alluvial fan deposits but may include thin sequences of fluvio-lacustrine sediments.

The low terraces consist of fluvial deposits like sandstones, pebbly sandstones and conglomerates. Imbrication in the conglomerates is common. The conglomerates are polymict and include reworked rocks from many of the older formations as well as pebbles originating from contemporaneous volcanism. Debris flow deposits are generally absent.

Chapter IV

Geochronology of the Neogene deposits of the S. Neiva Basin

A.M. van der Wiel, E.H. Hebeda¹ and P.A.M. Andriessen²

1. Methods

To date the Honda and Gigante Formations and the younger deposits, 5 kilo samples of volcanic and volcanoclastic rocks with a well-known stratigraphical position within the study area were collected for K-Ar mineral age determinations at different locations.

Zircon fission track age determinations were performed on rocks which could not be dated by the K-Ar method due to a lack of suitable minerals (hornblende or biotite). From the samples MW 105 and MW 202 both zircon (fission track method) and biotite (K-Ar method) were dated.

Biotite and hornblende were separated from those rocks which exhibited minimal effects of weathering and no signs of reworking. Only the separates with grain diameters between 100-250 μm were used. Mineral separation of hornblende and biotite was executed according to standard methods described by Andriessen (1978). In order to dissolve the volcanic glass adhering to some of the hornblende crystals, the grains were treated 4 min. with a 16% solution of HF. Subsequently, they were rinsed 8 times with aquadest and twice with pure ethanol. Finally, they were dried at 50°C for two hours.

K determinations were done on aliquots of 100 mg biotite and 100-125 mg hornblende. The potassium content of the samples was determined by flame photometry with a lithium internal standard and caesium chloride-aluminium nitrate buffer. Argon was extracted in a glass vacuum apparatus and determined by isotope dilution under static conditions in a Varian GD-150 mass-spectrometer. Aliquots of 200-300 mg biotite and 500-650 mg hornblende were used.

The analytical accuracy is believed to be within 1.0% for K and 2% for radiogenic Ar. These estimated overall limits of relative error are the sum of the known sources of possible systematic error and the precision of the total analytical procedures.

The analytical procedures used for the fission track age determinations are described in chapter II.

2. Results and discussion

The results of the K-Ar analyses are given in table VII; the results of the fission track age determinations in table VIII. The mineralogical composition of the dated rocks are given in appendix 2.

Honda Formation

Hornblende samples from two tuffs from the Honda section, situated at the west side of the confluence of the Río Magdalena and the Río Páez (fig. 15) gave K-Ar ages of 15.8 ± 0.6 Ma and 14.3 ± 0.5 Ma, respectively.

The tuffs levels can be traced laterally over a great part of the northern part of the study area: in some places two tuff beds and in other places three beds are present. In an outcrop along the

¹ Former address: Laboratory for Isotope Geology, Institute for Earth Sciences, Free University, De Boelelaan 1085, 1081 HV Amsterdam. Present address: Ringstrasse 10, Parsberg D 8433, Germany.

² Laboratory for Isotope Geology, Institute for Earth Sciences, Free University, De Boelelaan 1085, 1081 HV Amsterdam.

Table VII. K-Ar mineral data of the Honda and Gigante Formations and the high terrace along the Q. Guandinosita.

Sample no.	Name of section Formation/Mbr.	Mineral	K (ppm wt.)	Radiogenic ⁴⁰ Ar (ppb wt.)	Atmospheric ⁴⁰ Ar (% total ⁴⁰ Ar)	Calculated age ±σ (Ma)
Honda Formation						
MW 216	Confl. Páez/Magd.	Hbl	0.33	0.37	87	15.8±0.6
	Th (d)		0.33	0.36	87	
MW 165	Confl. Páez/Magd.	Hbl	0.38	0.39	87	14.3±0.5
	Th(d)		0.39	0.38	88	
Gigante Formation						
MW 104	Q. Guandinosita	Biot	7.01	3.83	49	7.9±0.1
	Tgi(a)		7.01	3.88	51	
MW 105	Q. Guandinosita	Biot	6.30	3.25	88	7.7±0.3
	Tgi(a)		6.24	3.44	88	
MW 110	Q. Guandinosita	Biot	6.70	3.27	70	7.0±0.1
	Tgi(a)		6.70	3.23	73	
MW 126	Q. Guandinosita	Hbl	0.58	0.25	91	6.2±0.4
	Tgi(g)		0.58	0.24	95	
MW 146	Q. la Honda	Biot	7.12	4.24	44	8.3±0.8
	Tgi(a)		7.11	3.96	42	
MW 154	Q. la Honda	Biot	6.73	3.42	63	7.2±0.2
	Tgi(a)		6.67	3.33	72	
MW 157	Q. la Honda	Biot	6.59	3.14	50	6.6±0.4
	Tgi(g)		6.61	2.92	46	
MW 202	La Laguna	Biot	6.58	3.46	71	7.5±0.2
	Tgi(a)		6.58	3.37	76	
MW 179	Q. Jagualito	Biot	6.71	3.32	74	7.2±0.2
	Tgi(a)		6.71	3.42	76	
MW 195	Q. las Damas	Biot	6.53	3.45	71	7.6±0.1
	Tgi(a)		6.57	3.42	70	
MW 206	Exposure 280	Biot	7.04	3.89	37	8.0±0.1
	Tgi(a)		7.07	3.98	42	
High terrace						
MW 100	Q. Guandinosita	Hbl	0.43	0.02	99	0.8±0.3
	Qt(2)		0.43			
MW 101	Q. Guandinosita	Hbl	0.43	0.21	99	0.7±0.3
	Qt(2)		0.44			

lower reaches of the Quebrada Alonso Sánchez on the east side of the Río Magdalena (see geological map, appendix 1) one of these tuff beds gave a zircon fission track age of 12.7 ± 5.3 Ma (table VIII, sample MW 212), which falls within the error of the K-Ar ages. In the Quebrada Guandinosita section two similarly developed tuffs are found at a height of ± 310 m above the base of the Honda Formation. Therefore, it is clear that the base of the Honda Formation has a minimum age of 16 Ma.

Zircons from three tuffs found in the Honda Formation in the N.Neiva Basin (La Venta Badlands) gave ages of 16.1 ± 0.9 , 14.6 ± 1.1 and 15.7 ± 1.1 Ma, respectively (Setoguchi and Rosenberger, 1985). Although these ages agree with the ages obtained during the present study, they appear to come from a different stratigraphic level. The ages obtained during the present study come from the lower part of the La Dorada Member as defined by Wellman (1968), while the ages published by Setoguchi and Rosenberger are from the lower, fossil-bearing part of the Villavieja Member, *i.e.* from the interval between the Monkey Unit and the Lower Red Bed

Table VIII. Zircon fission track analytical data of some samples from the Honda and Gigante Formations.

Sample	ρ_s^1 ($\times 10^6$ ν/cm^2)	ρ_i^2 ($\times 10^6$ ν/cm^2)	t^3 ($\times 10^6$ yr)	1σ ($\times 10^6$ yr)	Number of grains	ρ_{glass}^4 ($\times 10^5$ ν/cm^2)	Uranium (ppm)	$P(\chi^2)$ %
Honda Formation								
MW 212	1.2 (391)	5.7 (919)	12.7	5.3	15	198811.8 (4361)	175	<1
Gigante Formation								
MW 105	1.3 (324)	11.4 (1389)	6.7	0.9	10	186782.9 (2883)	375	10
MW 202	0.8 (255)	8.7 (1445)	5.1	1.8	10	186782.9 (2883)	287	<1
MW 537	0.4 (162)	4.3 (801)	6.4	2.4	10	198811.8 (4361)	133	<1

1) ρ_s : density of spontaneous fission tracks; the number of actually counted tracks is given in parenthesis

2) ρ_i : density of induced fission tracks; the number of actually counted tracks is given in parenthesis

3) age calculated according to the Zeta approach with a Zeta value of 308.1; zircon standard used: Fish Canyon with a calculated age of 27.2 ± 3.5 Ma

4) ρ_{glass} : density of fission tracks in standard glass NBS 962; the number of actually counted tracks is given in parenthesis

(see fig. 20). The cause of this discrepancy is unclear. The possibility cannot be excluded that the Honda Formation is diachronous in time. More research, both in the southern and northern parts of the Neiva Basin, is needed to acclarate this point.

Gigante Formation

No radiometric age determinations could be performed on the lower member of the Gigante Formation, the Neiva Member, because of a lack of suitable material.

The age of the base of the Los Altares Member can be deduced from the ages of samples MW 104 and MW 206. Sample MW 104 comes from the base of the member in the Quebrada Guandinosita section. Sample MW 206 was taken in the SW of the study area, W of the confluence of the Magdalena and Suaza Rivers (appendix 1). The sample comes from a tuffaceous sandstone containing up to 12 cm large clasts of pumice, situated just above the transition from the Neiva Member to the Los Altares Member. The average of the ages of the two samples is 8 Ma. The age of sample MW 146 was left out of consideration because its relatively large error, which is caused by a high variation in radiogenic ^{40}Ar (see table VII). Furthermore, the sample consists of a 40 cm large ignimbrite clast which may have been reworked from the base of the member.

The calculated age of 8 Ma corresponds well with a zircon fission-track age of 7.8 ± 0.5 Ma for the base of the Los Altares Member given by Takemura and Danhara (1983) and a biotite K-Ar age of 8.5 ± 0.4 Ma given by Van Houten (1976).

The age of the top of the Los Altares Member can be deduced from the ages of samples MW 126 and MW 157. Sample MW 126, giving a K-Ar biotite age of 6.2 ± 0.4 Ma was taken 47 m below the transition from the Los Altares Member to the Garzón Member in the Quebrada Guandinosita section. Sample MW 157, which gave a K-Ar biotite age of 6.6 ± 0.4 Ma comes from the Quebrada La Honda section. The sample was taken within the Garzón Member, 27 m above the contact with the Los Altares Member (fig. 17). When the average of the ages of the two samples is taken as the age of the contact, the transition from the Los Altares Member to the Garzón Member has an age of 6.4 ± 0.4 Ma.

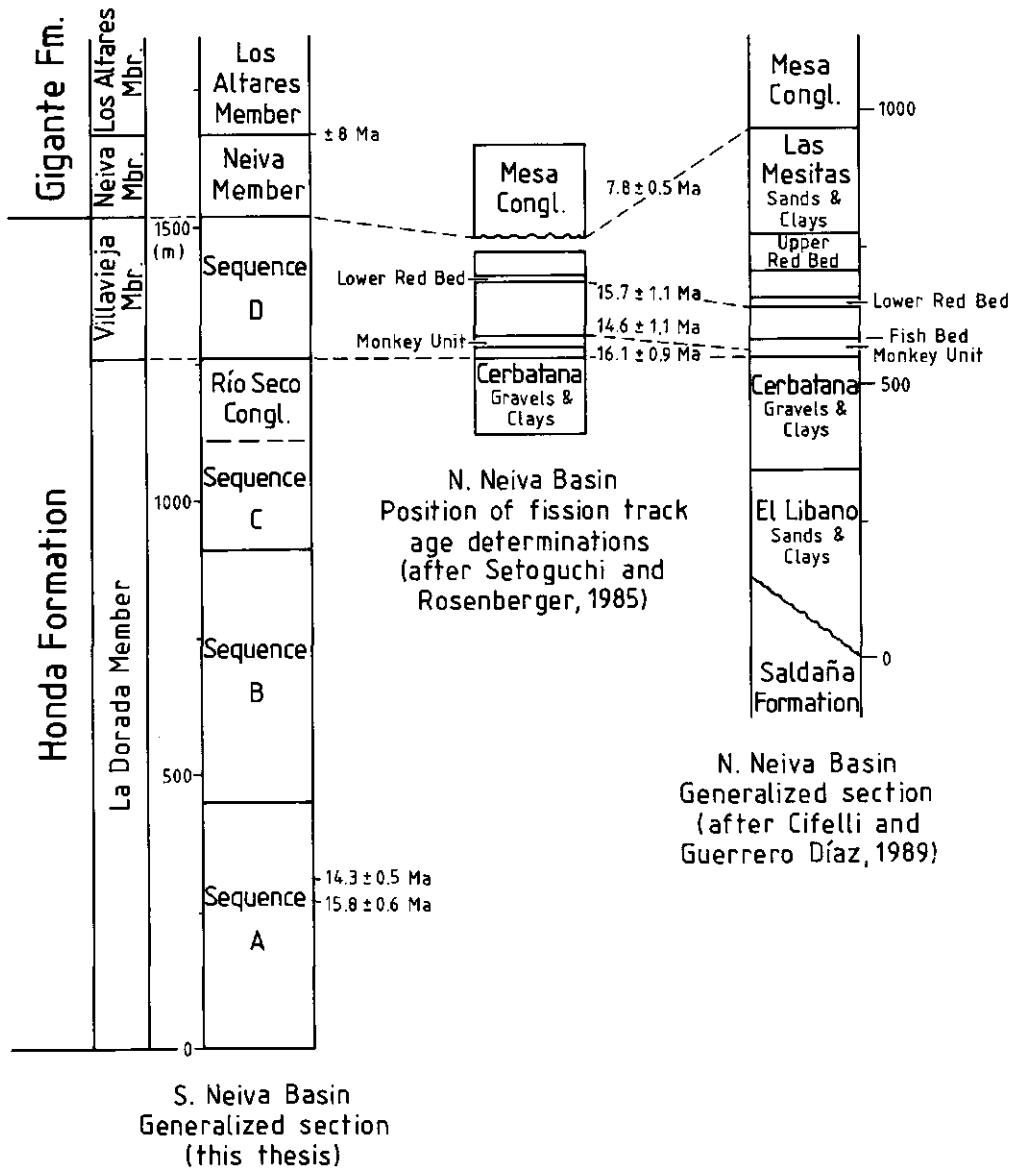


Fig. 20. Comparison of the K-Ar and zircon fission track ages of the deposits of the Honda Formation in the N and S part of the Neiva Basin.

The top of the Garzón Member could not be dated. In many places the upper part of the member has been eroded and its precise thickness is unknown. In the center of the basin the member reaches its greatest thickness of ± 250 m. Although it is possible that the member is complete here, no suitable samples for radiometric age determinations were encountered. A fission track age determination on zircon from a weathered ash layer in the upper part of the

section along the road from Garzón to Gigante (section RSG) gave an age of 6.4 ± 2.4 Ma (sample MW 537). According to estimates of the thickness of the member on the geological map, this sample is situated some 130 m above the contact with the Los Altares Member. It has already been suggested elsewhere (chapter III, section 2.4) that the ash layer is located some 75-100 m below the top of the Garzón Member. Therefore, it is likely that the age of the top of the member is younger than 6 Ma.

The remaining samples, which were all taken in the Los Altares Member, give ages that are intermediate between 8.0 and 6.4 Ma, agreeing well with the age of the member calculated above. When more than one dated sample is present in the same section, the ages of the samples get progressively younger from the base to the top of the section. According to Dalrymple and Lanphere (1969, p. 197) the probability is good that radiometric ages are reliable when the potassium-argon ages of a group of rocks agree with the stratigraphic sequence determined on the basis of physical relationships.

It has been mentioned above that two samples were dated by both the K-Ar and the fission track method. Within errors, the zircon fission track age (6.7 ± 0.9 Ma) and the K-Ar age (7.7 ± 0.3) of sample MW 105 overlap. This is not the case for sample MW 202: even within errors, the zircon fission track age of this sample is still somewhat younger (5.1 ± 1.8 Ma) than its K-Ar age of 7.5 ± 0.2 Ma. Because the K-Ar age of the sample falls within the range of Los Altares ages, while the individual zircon grains gave a wide range of fission track ages, it seems probable that the K-Ar age is correct and the fission track age somewhat too young. As the pooled zircon FT data failed the Chi square test, the fission track age of the sample was calculated from the mean crystal age.

The high terrace

Because the Las Vueltas formation consists entirely of erosional material of the Garzón Massif and does not contain any volcanic material, no radiometric age determinations could be carried out on samples from this formation.

Two samples taken in pumice-containing deposits from the Qt_2 terrace along the Quebrada Guandinosita (fig. 19) were dated by the K-Ar method. Hornblende from the pumice samples MW 100 and MW 101 gave ages of 0.8 ± 0.3 Ma and 0.7 ± 0.3 Ma, respectively. Because the samples were taken in two tuffaceous sandstones directly overlying each other, it can be stated safely that they have, in fact, the same age. For this reason only one age determination was performed on each sample.

Radiometric age determinations were performed on deposits of this terrace for several reasons:

1) In order to constrain the age of the Neogene uplift of the Garzón Massif as well as possible, both pre- and post-uplift deposits within the S. Neiva Basin were dated. The deposits of the Qt_2 terrace represent the oldest post-uplift sediments that could be dated, because they contain volcanic material.

2) At the sampling site, the Qt_2 terrace has undergone considerable faulting since its deposition. The real elevation of the terrace above the present-day level of the Río Magdalena has been conserved at the W-side of the fault (± 90 m). The E-side has been uplifted some 160 m relative to the W-side by reverse faulting along the Puerto Seco Fault and is nowadays located at an elevation of ± 250 m (appendix 1). It was hoped that the radiometric age determination of the terrace deposits in conjunction with the faulting history of the terrace would give information on the youngest uplift history of the Garzón Massif.

According to Diederix (pers. comm.), geological evidence like the orientation of the slickensides on the fault plane and the displacement of part of the Gualanday Formation along the fault suggest that, beside reverse faulting, right lateral strike slip movements took place. From the fact that the terrace has not been displaced horizontally, it may be concluded that wrench faulting took place before vertical movements along the fault occurred. It is shown in chapter XII that wrench-faulting probably started in the Pliocene, when uplift of the massif had ended, and continued intermittently up to the present day. Thus it is clear that, although reverse

faulting on the Puerto Seco Fault must be caused by continuing E-W compression, the faulting cannot be related to uplift of the massif.

3) To determine whether the terrace might be the distal continuation of the "Paicol terrace" along the Río Páez, as has been suggested by Van Houten (1976). If this supposition is correct, a direct correlation would be obtained between the deposits in the S. Neiva Basin with deposits further to the west. This is of interest, because it would then be possible to compare the geological histories of both regions.

Two radiometric age determinations on biotite from pumice samples in the "Paicol terrace" indicate that the ages of the Qt_2 terrace and the Paicol terrace indeed overlap. Also, the stratigraphy of the two terraces is very similar. The consequences of these results are discussed in chapter XI.

Although the ages with their standard errors also overlap with the age of 0.6 ± 0.1 Ma of the tuffaceous Tarqui Valley Fill which forms part of the Río Magdalena terraces further upstream in the immediate surrounding of Tarqui (Van Houten, 1976), it is unlikely that the Qt_2 terrace is the downstream continuation of the Tarqui Valley Fill, because the Tarqui Valley Fill is found at an elevation above the river which rather agrees with the middle terrace, and because tuffaceous terrace deposits are lacking in the interjacent area.

Chapter V

Petrology of the Honda, Gigante and Las Vueltas formations

This chapter concerns the petrology of the Honda, Gigante and Las Vueltas formations. The chapter is subdivided into two parts. In section 1, the conglomerate and sandstone composition of the three formations will be discussed. In section 2, attention will be given to the petrography and chemical classification of the volcanic rocks of the Los Altares Member and -to a lesser degree- of the Garzón Member of the Gigante Formation.

1. Petrology of the conglomerates and sandstones

1. 1. Introduction

The sedimentary rocks of the Honda, Gigante and Las Vueltas formations consist of clastic material which comes from two source areas, *i.e.* the southernmost part of the Eastern Cordillera, the Garzón Massif, and the Cordillera Central. Sediments originating in these two areas may be distinguished from one another by differences in composition.

The Garzón Massif consists of Precambrian rocks like augengneisses, granulites, gneisses, amphibolites and minor ultramafic and calcsilicate rocks (Kroonenberg, 1982a; b), which were intruded by granodiorites, monzonites, and granites in Jurassic time (Kroonenberg and Diederix, 1982; Irving, 1975; Aspden *et al.*, 1987). Minor amounts of Upper Paleozoic sandstones and shales, as well as volcanoclastics belonging to the Late Triassic/Jurassic Saldaña Formation and Cretaceous sedimentary rocks mantle the basement rocks.

The southern part of the Central Cordillera, alongside the S. Neiva Basin, mainly comprises Jurassic intrusives, rocks of the Saldaña Formation and Cretaceous sedimentary rocks. Furthermore, the Central Cordillera is the sole source of the contemporaneous volcanic and volcanoclastic rocks encountered in the Neogene basin fill. Paleozoic schists, which form the core of the Central Cordillera further to the north, are scarce in the southern part of the chain. Precambrian rocks are virtually absent. A small outcrop is found 20 km to the W of la Jagua. (Kroonenberg and Diederix, 1982; geological map).

Uplift of the Garzón Massif should thus lead to an increased input of erosional material of Precambrian metamorphic rocks into the basinal sediments, while uplift of the Central Cordillera should lead to a greater share of the Late Triassic/Jurassic Saldaña Formation and Cretaceous sediments. Activity of the Central Cordillera volcanic arc would lead to the incorporation of contemporaneous volcanics into the basin fill.

In order to acquire information on the uplift history of the surrounding mountain chains, both pebble counts on conglomerates and point counts on sandstones of the Honda, Gigante and Las Vueltas formations were performed.

1. 2. The pebble counts: method

The most complete section through the Honda and Gigante Formations was obtained in the Quebrada Guandinosita. During the stratigraphical description of this section, pebble counts of 100 pebbles were done at intervals of 50-100 m in the Gigante Formation and upper part of the Honda Formation (fig. 21, to the left). The spacing of the pebble

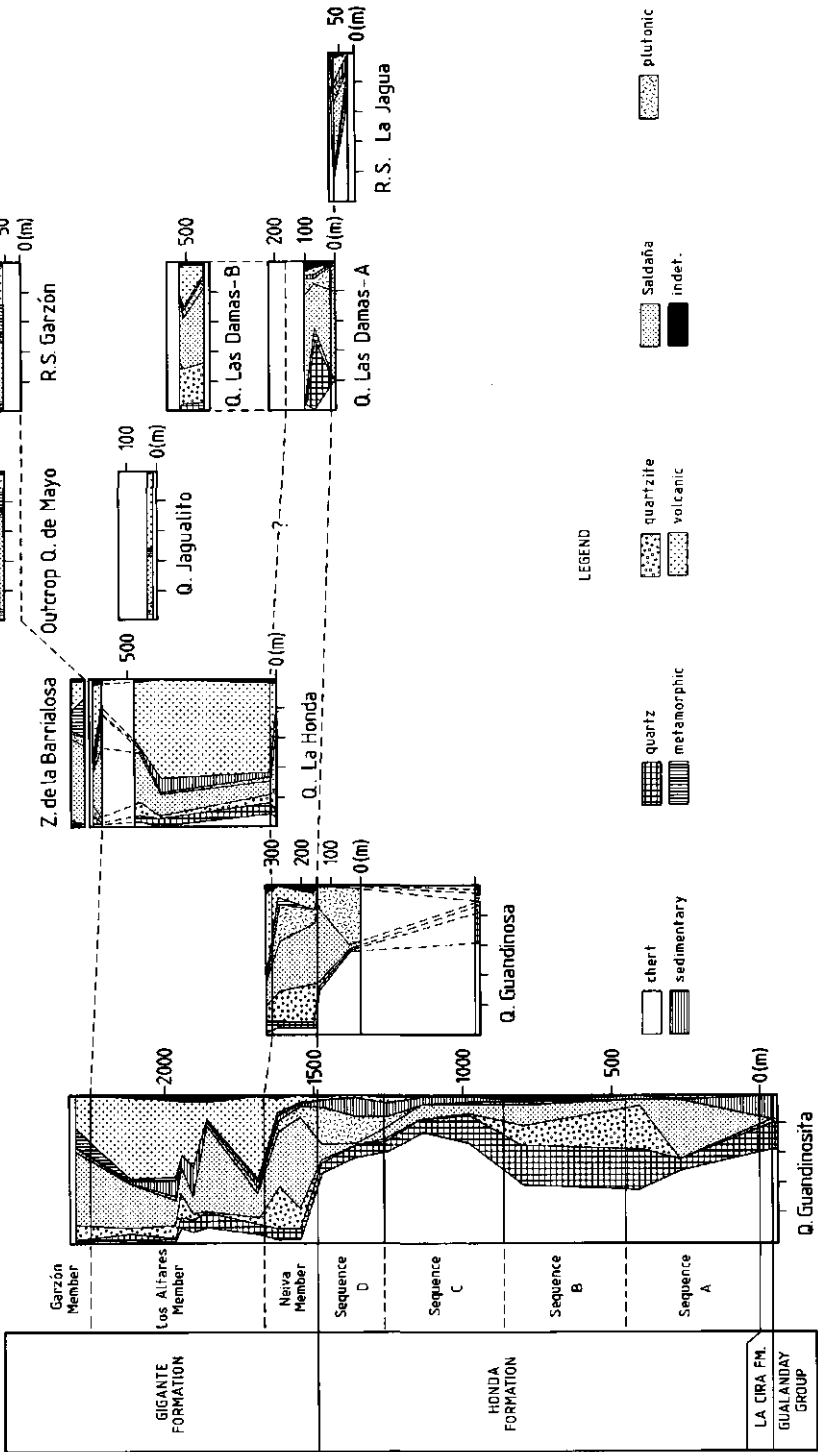


Fig. 21. Results of the pebble counts on the Honda and Gigante Formations from the central part of the S. Neiva Basin.

counts in the lower part of the Honda Formation is more irregular and varies between 200-400 m. Furthermore, pebble counts were performed at various intervals on several other stratigraphical sections as well as on a number of isolated outcrops in the Honda, Gigante and las Vueltas formations. The results of the most important sections and outcrops are given in figs. 21 and 22.

For the counts, pebbles were selected with a minimum length of the c-axis of 1 cm and a maximum length of the a-axis of 18 cm. The finer fraction was left out of consideration, although Howe (1974) showed that the finer fraction of the Neiva Member (the fraction with a c-axis < 5 cm) has a different composition from the coarse fraction, chert, quartz and sedimentary clasts predominating in the finer one. This was, however, unimportant to our purpose of distinguishing between east-derived and west-derived components, Precambrian metamorphic rocks and contemporaneous volcanics being the main parameters for differentiating between the two. Nine rock groups are distinguished, which will be described first.

Quartz is a milky-white vein variety that might have come from any of the older formations. Black micaceous and white quartzite clasts are reworked from Paleozoic metamorphic rocks and have a western provenance. White and pink plutonic clasts are derived from the Jurassic intrusions which are found both in the Central Cordillera and the Garzón Massif. The metamorphic clasts derived from the Garzón Massif consist of gneisses, augengneisses, amphibolites and ultramafic and mafic granulites. A subordinate proportion of the metamorphics is formed by Late Palaeozoic schists, reworked from the Paleozoic core of the Central Cordillera.

Chert is originally derived from Cretaceous porcelanites, although some reworking from older Tertiary formations (*i.e.* the Gualanday Group) may have played a minor role. The remaining sedimentary clasts, *i.e.* sandstones, shales, mudstones and siltstones, form a minor component and are derived from Middle and Upper Paleozoic marine sedimentary rocks, Cretaceous sandstones and shales, rocks belonging to the Guaduas Formation and reworked Tertiary deposits.

The "Saldaña" clasts, provening from the Late Triassic/Jurassic Saldaña Formation, consist of purple and reddish-brown to brown, strongly altered volcanoclastic rocks like rhyolitic-rhyodacitic ignimbrites, volcanic agglomerates, tuffaceous sandstones etc. The most conspicuous feature of the rocks is the lack of primary mafic minerals (biotite, opaques) and the predominance of quartz and plagioclase. The few hornblende crystals present are heavily altered and often have thick opacite rims. Rocks belonging to this formation occur on both sides of the S. Neiva Basin. Recent volcanic andesite and dacite clasts may be readily distinguished from the older Saldaña clasts by the difference in colour (the recent clasts are white, light grey, bluish grey and pink grey) and by the presence of fresh biotite, hornblende and opaques.

Finally, in the category "indet." strongly weathered clasts were grouped, which could not be determined with any degree of certainty.

1. 3. Results of the pebble counts

Honda Formation

The Honda conglomerates are dominated by chert pebbles. On the average, chert makes up 40-60% of the total. In addition, quartz, quartzite and older volcanic pebbles, derived from the Saldaña Formation, constitute an important fraction. In the upper part of the formation (the Villavieja Member) pink granite, reworked siltstones and quartz sandstones become increasingly abundant (fig. 21, to the left).

Volcanic clasts derived from contemporaneous volcanism are very rare. Dacitic pumice clasts were encountered in an otherwise typical Honda conglomerate, some 300 m above the base of the formation, just above the two tuffs described in chapter III, section 2.3. Towards the top of the formation some isolated andesitic and dacitic pebbles were found.

An abrupt change in pebble composition occurs at the transition from the Honda Formation to the lower conglomeratic Neiva Member of the Gigante Formation. The contribution of chert drops dramatically, while the share of Saldaña volcanics increases accordingly. At the same time the amount of pebbles and cobbles originating from contemporaneous volcanism becomes larger. These changes are recorded both in the Q. Guandinosita section and the Q. La Guandinosita section (fig. 21). In the Road Section La Jagua (fig. 21, to the right), interfingering of the Honda Formation and the Neiva Member of the Gigante Formation is characterized by rapid alternations of conglomerates dominated by Saldaña pebbles and conglomerates dominated by chert pebbles.

Beside the composition, the pebble size changes also. Apart from the Río Seco conglomerate, the maximum pebble size of the different La Dorada conglomerates lies between 1-4 cm. In the lower part of the "Río Seco conglomerate" the maximum pebble size is 5-10 cm, but in the upper part, which is dominated by orthoconglomerates, the maximum size increases to 16 cm.

In the Villavieja Member, the conglomerates are somewhat coarser than in the lower part of the La Dorada member and the maximum pebble size of the different banks lies between 5-13 cm. The maximum size of the different Neiva conglomerates, however, lies between 5-40 cm.

Gigante Formation

The composition of the conglomerates of the lower two members of the Gigante Formation is very constant throughout the basin (compare the different sections of fig. 21). Saldaña pebbles and Paleozoic quartzite predominate in the Neiva Member, while andesite clasts from contemporaneous volcanism reach percentages of 5-10%. In the Los Altares Member volcanic clasts from contemporaneous volcanism form \pm 40-60% of the total. In most sections chert, quartz, quartzite and plutonic and sedimentary clasts are present in subordinate amounts. In both members the share of Precambrian metamorphics is negligible.

In the Garzón Member the proportion of metamorphic clasts provening from the Garzón Massif increases drastically: in most measured sections up to 13-18%. This proportion, however, may locally be even higher. In the center of the basin, conglomerates in the Zanjón de la Barrialosa section contain as much as 27% of Precambrian metamorphic clasts.

The composition of the Garzón Member conglomerates is more variable than the composition of the lower two members of the Gigante Formation. This is due to the input of both west-derived and east-derived components. In conglomerates, dominated by west-derived components, the majority of the clasts are andesite clasts originating from contemporaneous volcanism. In conglomerates, consisting mainly of east-derived components, clasts of Jurassic intrusives and Precambrian metamorphics predominate.

In all outcrops of the member both west-derived and east-derived components are present. Sometimes these components are not completely mixed: in one of the outcrops in the south central part of the basin separate layers with andesitic material from the Central Cordillera volcanic arc and metamorphic material from the Garzón Massif were found. In some sections the contribution of Saldaña Formation volcanics is very high.

Las Vueltas formation

The deposits of the Las Vueltas formation consist entirely of erosional material from the Garzón Massif. The colour of the deposits and the content of the conglomerates are very variable. At some localities the conglomerates originated from erosion of the Jurassic intrusives found in the massif, in other places the content of the conglomerates is dominated by metamorphic clasts, formed by erosion of the Precambrian basement. Thus, the components of the conglomerates consist of white to pink granites and monzonites, dark-coloured granodiorites, white to dark-coloured gneisses, augen gneisses, amphibolites and granulites, dark-coloured ultramafics, white and black Paleozoic quartzites and dirty-brown Paleozoic sandstones. Pink, reddish and purple clasts from the Jurassic volcanoclastic Saldaña Formation as well as fragments from Jurassic lamprophyres may be present in minor quantities.

In the N of the basin, along the Q. de las Vueltas (the type locality of the Las Vueltas formation) a single pebble count was performed on a deposit of the Las Vueltas formation. For comparison with the pebble composition of the Garzón Member, the result of the pebble count is given in fig. 22 (to the left), above the Q. Guandinosita section.

A second pebble count on a conglomerate from the Las Vueltas formation was performed in the Q. Guandinosita on a conglomerate directly overlying the Garzón Member (see fig. 17: top of the Q. Guandinosita section: Quaternary alluvium). Because this conglomerate appears to have undergone later reworking (it forms part of a small secondary alluvial fan), the results are not indicated in figs. 21 and 22. On the other hand, this reworking seems to have had little effect on its original composition. For this reason the results of the count are given below (table IX).

Table IX. Pebble composition of a conglomerate of the Las Vueltas formation (Q. Guandinosita).

Chert	1%	Plutonic	21%
Saldaña	10%	Metamorphic	68%

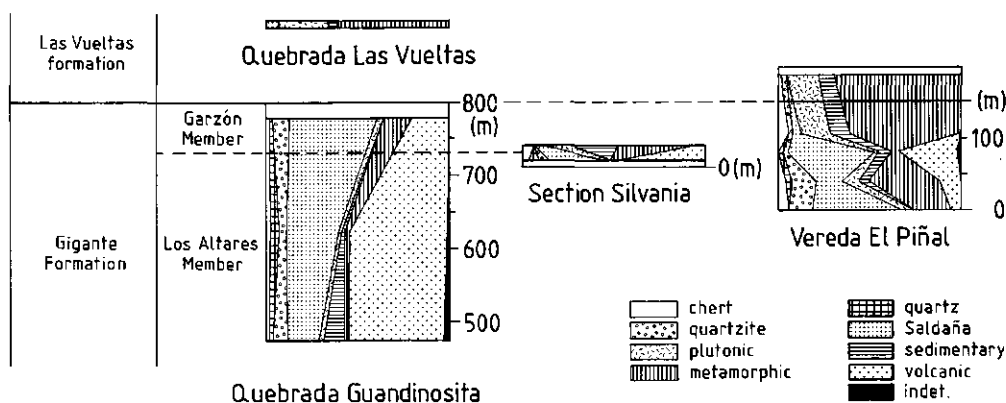


Fig. 22. Results of the pebble counts on the Gigante and Las Vueltas formations. Data from the Q. Guandinosita section (central part of the basin) are compared with data from the sections Sylvania and Vereda El Piñal in the eastern part of the basin.

Deposits in the east of the basin

It has already been mentioned in chapter III, section 2.4, that in the E of the S. Neiva Basin, the conglomerate composition of the Los Altares and Garzón Members is different from the composition in the center. The results of the pebble counts performed in the Sylvania and Vereda el Piñal sections are given in fig. 22. A direct comparison with the upper part of the Quebrada Guandinosita section (fig. 22, to the left) clearly indicates the differences. In the east of the study area, the conglomerates of the Los Altares Member contain east-derived components like Precambrian gneiss and granulite clasts and the Garzón Member conglomerates are dominated by this material. In the Sylvania section, for example, the Garzón Member contains 50% of Precambrian gneisses and 26% of Cretaceous sandstone and shale. West-derived components like fresh andesite clasts are much scarcer than in the center of the basin, making up only 0-5% of the total.

In the section Vereda el Piñal, strong interfingering of the Los Altares and Garzón Members is reflected in the variable proportions of fresh volcanics and metamorphics. In the same section the transition from the Garzón Member to the Las Vueltas formation is gradual: towards the top of the section the percentage of east-derived clasts and the pebble size increase. At the same time the conglomerates become very poorly sorted, the pebbles are less well rounded and the bank thickness increases. Furthermore, the transition between different banks becomes diffuse; while the lower part of the section is characterized by alternations of well-banked conglomerates and sandstone layers, the upper part of the section consists entirely of pebbly sandstones.

1. 4. The point counts: method

In order to compare the composition of the sandstones of the Honda Formation and the different members of the Gigante Formation, 46 point counts, each based on 300 counts of framework constituents, matrix and cement, were carried out on sandstones exposed in the Quebrada Guandinosita and Quebrada La Honda sections. Their position is indicated in figs. 15 and 17. No point counts were done on sandstones from the Las Vueltas formation.

In the Quebrada Guandinosita, 15 point counts were performed on Honda sandstones, 3 point counts on sandstones taken in that part of the section where the Honda and Gigante Formations interfinger and 21 on Gigante sandstones. A single point count was performed on a sandstone from the La Cira Formation. The other 6 point counts were done on Gigante sandstones in the Q. La Honda.

The sandstones that were used for point counting had an average grain size ranging between 150-400 μm (fine to medium sand). The results of these point counts are given in tables X and XI.

Table X. Point counts of some sandstones, belonging to the Honda and La Cira Formations.

Formation Member/ (Sequence)	Sample no.	Volc. glass	Clay Matrix/ Cement	CaCO ₃	Fe oxides	Zenite Cement + Matrix grains	Qtz. work	Plag./ K-Fsp.	Biot. basalitic hbl.	Aug. hbl.	Hyp. min.	Opaque Pumice	Fresh volc.	Sald./ fresh volc.	Sald./ quartz	Poly- plut.	Met/ plut.	Sed.	Alt.				
Interf. of Honda and Gigantic Fms.	GB 57	0	14/0	0	1	0	15	85	26	1/0	0	0/0	0	0	0	13	26	8	26	0			
	GB 56	1	11/0	0	1	1	15	85	40	5/2	0	0/0	0	0	0	13	8	7	21	2			
	MW 218	0	0/12	0	0	9	21	79	11	0/2	0	0/0	0	62	0	1	6	0	0	9			
Villavieja Mbr. (D)	GB 59	0	11/0	0	0	0	11	89	32	2/2	0	0/0	0	0	2	0	8	13	6	29	5		
	GB 52	0	1/0	0	9	0	10	90	27	3/12	0	0/0	0	0	0	0	2	9	18	24	4		
	GB 51	0	21/0	0	0	0	21	79	33	3/2	0	0/0	0	0	0	10	15	7	25	2			
La Dorada Mbr. (C)	GB 63	0	21/0	0	0	0	21	79	36	6/2	1	0/0	0	0	4	0	7	9	6	5	15	9	
	GB 64	0	26/0	0	0	0	26	74	28	3/1	0	0/0	0	0	1	0	0	17	14	5	26	5	
	GB 69	0	4/0	15	0	0	19	81	23	3/7	0	0/0	0	0	0	0	20	9	11	27	0		
	GB 71	0	1/0	18	0	0	19	81	27	2/4	0	0/0	0	1	0	3	0	18	9	9	24	3	
	GB 72	0	1/0	23	0	0	24	76	37	4/1	0	0/0	0	0	0	2	15	8	9	24	0		
GB 74	0	4/0	0	0	0	4	96	23	3/3	0	0/0	0	0	4	0	10	6	10	7	5	18	11	
La Dor. Mbr. (B)	GB 75	0	11/0	0	0	0	11	89	22	10/2	1	5/0	2	0	5	1	12	1	3	12	11	5	8
	GB 76	0	0/0	32	0	0	32	68	9	18/2	2	1/0	0	0	0	27	2	9	11	10	1	8	
	GB 77	0	0/0	15	0	0	15	85	18	13/3	0	5/0	1	0	5	2	10	3	4	16	11	4	5
La Dor. Mbr. (A)	MW 170	0	10/0	0	0	0	10	90	2	42/0	1	29/3	0	1	6	0	12	2	0	0	0	0	2
	GB 34	0	7/0	0	0	0	7	93	13	17/0	0	9/0	0	2	0	36	5	0	9	1	5	8	
	MW 169	0	6/0	0	0	0	6	94	17	19/3	0	6/0	0	2	1	11	6	5	4	5	8	9	
La Cira Fm.	MW 168	0	8/0	0	9	0	17	83	28	11/4	0	0/0	0	1	0	0	0	9	2	11	7	15	13

Table XI. Point counts of some sandstones, belonging to the Gigante Formation.

Section	Formation Member	Sample no.	Volc. glass	Clay	CaCO ₃	Fe-oxides	Zeolite + matrix	Cement	Frame work grains	Qtz	Plag./K-fsp	Biot.	Hbl./basaltic hbl.	Aug.	Hyp.	Opaque min.	Pumice + shards	Fresh volc.	Sald./fresh volc.	Sald./plut.	Sed.	Alt.			
QLH	Gigante Fm. Garzón Mbr. MW 158		0	0	0	0	0	0	100	0	12/0	0	2/0	1	0	1	0	81	0	2	1	0	1		
	Altares Mbr. GB 24		11	0	0	0	11	89	9	33/0	1	1/0	0	0	0	0	0	0	44	6	2	4	0	0	
	GB 23		0	0	0	1	1	99	1	10/1	0	1/0	0	5	1	0	0	0	78	0	0	3	0	0	
	GB 26		0	0	21	4	25	75	3	20/0	0	1/0	0	4	0	1	0	0	59	1	3	4	0	4	
	GB 22		0	4	14	0	18	82	2	14/1	0	1/0	0	0	0	0	0	0	79	1	0	2	0	0	
GB 21		1	4	0	0	5	95	0	23/0	2	8/0	2	8/0	0	0	2	0	61	2	0	2	0	0		
QQt	Gigante Fm. Garzón Mbr. MW 129		0	0	0	0	2	98	0	27/0	0	1/3	2	2	0	0	0	0	63	0	0	2	0	0	
	MW 128		0	0	0	0	0	100	0	11/0	0	3/1	3	3	1	0	0	0	74	0	3	1	0	0	
	Altares Mbr. GB 16		7	0	0	0	7	93	1	26/0	0	3/0	0	0	0	0	0	0	6	2	0	3	0	0	
	MW 124		1	5	0	0	6	94	0	17/0	1	5/0	1	0	1	0	0	0	0	65	4	0	4	0	2
	GB 13		16	5	0	0	21	79	9	48/0	5	20/0	0	0	0	0	0	0	2	8	0	0	3	0	5
	GB 12		20	2	0	0	4	26	74	7	44/1	7	13/0	0	0	0	1	14	5	1	1	1	0	0	
	GB 11		25	4	0	0	29	71	11	45/0	7	14/0	0	0	0	0	3	0	4	2	3	7	0	4	
	GB 10		0	0	19	0	19	81	14	53/0	3	4/0	0	0	0	0	1	0	16	0	1	6	0	2	
	MW 107		16	0	0	0	16	84	20	55/0	5	11/0	0	0	0	0	0	0	2	0	0	6	0	1	
	MW 106		13	3	0	1	17	83	10	63/0	2	6/0	0	0	0	0	3	0	13	0	0	5	0	1	
	GB 8		9	8	0	1	20	80	9	58/0	4	8/0	0	0	0	0	0	0	4	0	0	5	0	9	
	GB 5		0	16	0	0	17	83	2	53/0	6	5/0	6	5/0	0	0	0	1	6	1	0	6	0	20	
	GB 3		0	10	2	0	4	16	94	2	4/1	1	0/0	6	0	0	2	0	77	0	0	5	0	2	
	GB 2		0	3	0	0	3	6	94	2	11/0	0	1/0	0	0	0	0	0	78	2	0	4	0	2	
	MW 131		2	4	0	0	2	8	92	1	20/0	2	4/0	0	0	1	0	0	52	1	7	9	0	3	
GB 1		1	8	0	0	9	91	4	55/0	0	9/0	0	0	0	2	0	0	19	0	1	9	0	1		
GB 29		2	4	0	0	6	94	8	19/0	2	13/0	2	13/0	0	0	2	0	33	0	0	23	0	0		
GB 62		0	0	18	0	20	80	10	25/1	1	9/0	1	9/0	0	0	0	0	29	4	6	11	0	4		
GB 61		11	2	0	0	13	87	5	16/1	2	13/0	2	13/0	0	0	1	0	47	0	1	13	0	1		
Neiva Mbr. GB 60		0	5	0	0	14	86	19	4/3	1	6/0	1	6/0	1	2	2	0	19	4	11	21	0	7		
GB 58		0	0	23	0	23	77	16	2/2	0	0/0	0	0/0	1	4	2	0	2	0	25	38	8	0		

At the left-hand side of these tables the different types of matrix (volcanic glass and clay) and cement (in situ formed clay, carbonate, Fe-oxides and zeolites) are quantified. Also, the ratio of total cement+matrix versus framework grains is given. The framework grains comprise mineral grains (excluding secondarily formed minerals) and rock fragments.

The rock fragment categories include the following rock types: recent **pumice and glass shards**, derived from reworking of ignimbrites and tuffaceous sandstones were counted as a separate category. In the category of the **volcanic rock fragments**, fragments of recent dacites, andesites and basalts were grouped, as well as glass fragments and devitrified glass fragments containing small feldspar laths.

The next group comprises the fragments derived from the Saldaña Formation (see section 1.2). It proved to be more difficult to discriminate between fresh andesite and dacite grains and reworked older Saldaña grains at the sand scale than at the pebble scale, because both rock types show strong devitrification of the ground mass. When no phenocrysts of biotite or hornblende are present, as is often the case in the smaller fragments, it is impossible to determine the rock type. Therefore, a separate category Saldaña/recent was created, consisting of grains that could not be classified with certainty.

The **metamorphic/plutonic** group comprises quartzite grains, schist fragments, fragments of Jurassic intrusives and of Precambrian rocks (gneisses, amphibolites and granulites) and some muscovite grains, because this latter group was too small to count separately and muscovite is mainly derived from metamorphic and plutonic rocks. Furthermore, the group includes perthite and antiperthite grains. These were grouped in this category because of their metamorphic origin. In table XI (pointcounts of the Gigante Formation sandstones) fragments of polycrystalline quartz were also included in this category. Because of their greater share in the Honda sandstones, they are indicated as a separate group in table X.

The category **sedimentary** consists of Cretaceous chert and mudstone fragments from the Maastrichtian-Paleocene Guaduas Formation. No other sedimentary grains were encountered.

The category **altered rock fragments** contains fragments that have undergone such strong weathering and in situ formation of clay minerals that they could not be classified with certainty.

1.5. Results of the point counts

Honda Formation

The composition of the sandstones of the Honda Formation generally corresponds with the data given by Wellman (1968, 1970), although this author did not differentiate between contemporaneous volcanic grains and grains derived from the Jurassic Saldaña Formation (Kroonenberg and Diederix, 1982).

In the majority of the sandstones, the percentage of clay matrix lies between 0-11%. Only some samples in the upper part of the "Río Seco conglomerate" and the lower part of the Villavieja Member contain 21-26% clay matrix and should thus be classified as graywackes (classification according to Dott, 1964).

Some of the sandstones are cemented by secondary carbonate. In the field, the carbonate forms concretions along the bedding planes of the sandstones with diameters up to 40 cm. Identical carbonate concretions are found in sandstones of the Gigante Formation. Both in the Honda and the Gigante Formations the carbonate replaces all other cements, indicating that this is the youngest diagenetic material. It is very aggressive and has locally even replaced the clasts and crystal grains. Similar concretions are described by Schmincke (1964) as occurring in arkosic sandstones from the volcanoclastic Ellensburg Formation in southcentral Washington.

According to the classification of Folk (1968) a single sample taken in the La Cira Formation (MW 168) should be classified as a feldspathic litharenite (fig. 23). The sandstones from the upper part of the La Dorada Member (860-1260 m) and the Villavieja Member are litharenites and feldspathic litharenites (fig. 23), dominated by sedimentary fragments (especially chert) and fragments derived from the Saldaña Formation, with minor amounts of plutonic and metamorphic rock fragments. The sandstones from the lower 860 m of the La Dorada Member are feldspathic litharenites to lithic arkoses, due to the presence of contemporaneous volcanic fragments. In this part of the formation, volcanic plagioclase is more abundant than various types of K-feldspar of plutonic and metamorphic origin. A thin section from a slightly reworked tuff bed, located 310 m above the base of the formation (sample MW 170), shows that green hornblende and fresh plagioclase crystals form the major constituents. Above 860 m, fresh volcanic plagioclase grains become rarer and the grains are increasingly sericitized and weathered, while other volcanic minerals like biotite, hornblendes and pyroxenes are absent.

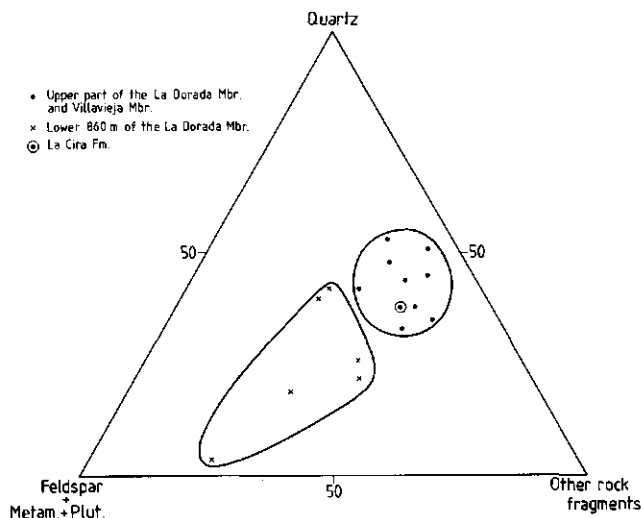


Fig. 23. Classification of the La Cira and Honda sandstones in a feldspar-quartz-rock fragments diagram, as developed by Folk (1968).

The quartz grains, encountered in the Honda sandstones are for the greater part stretched or undulatory grains, which may have originated both from plutonic and deformed metamorphic or sedimentary rocks. Only a very minor percentage of the grains are fresh volcanic HT quartz grains, restricted to the lower part of the formation.

The rock fragments found in the Honda Formation are generally well rounded and have suffered a certain amount of weathering. They are mainly derived from Cretaceous to Paleocene sedimentary rocks, volcanics of the Saldaña Formation and metamorphic/plutonic rocks. About 50% of the latter category consists of fragments of polycrystalline quartz which may have been derived from Jurassic plutons or quartzites. The category also comprises many fragments consisting of quartz crystals and chlorite, derived from quartz veins. Thus, most of the metamorphic/plutonic rock fragments appear to be derived from Jurassic intrusives and quartzites.

Gigante Formation

The sandstones of the Gigante Formation can be classified mainly as volcanic arenites with the exception of the Neiva Member, where subarkoses dominate (classification according to Folk, 1968). The volcanic arenites are texturally immature to mature and mineralogically immature. The grains are poorly to moderately sorted and rounded, while the concentration of instable lithic fragments is high. The matrix of the sandstones consists of some volcanic glass and clay. The clay content varies between 0-15%. Clay is present both as a constituent of the matrix and as a cement. Beside clay cement, minor percentages of zeolites and Fe-oxides are found. Some of the sandstones are cemented by secondary carbonate (see above).

In the Los Altares and Garzón Members only a few grains of perthitic and antiperthitic K-feldspar are present, but plagioclase forms a major constituent of the sandstones. This plagioclase (An_{30-50}) is clearly fresh volcanic plagioclase, often with strong magmatic zoning and corrosive embayments. Other primary volcanic minerals are green hornblende, biotite and minor amounts of augite, hypersthene, apatite and opaques. Redbrown basaltic hornblende is sometimes present, but is always found as a component of andesitic rock fragments. Quartz occurs in the majority of the samples as a minor constituent. In the Los Altares Member the majority of the quartz grains is of the volcanic HT modification, but in the Neiva Member undulatory quartz predominates. In the latter member perthitic and antiperthitic K-feldspar

grains are much more frequent than in the Los Altares Member, while fresh volcanic plagioclase grains form at most 10% of the total. Zeolites and Fe-oxides are present in somewhat greater quantities in these subarkoses than in the volcanic arenites. A glassy matrix is virtually absent.

Cretaceous chert and mudstone fragments from the Guaduas Formation occur in the Neiva Member, but are absent from the middle and upper members of the Gigante Formation. Pumice, glass shards and fragments of dacite and andesite, resulting from contemporaneous volcanism, are mostly restricted to the Los Altares and Garzón Members. Metamorphic/plutonic components and grains from the Saldaña Formation are much more abundant in the Neiva Member than in the upper two members of the formation. More than half of the metamorphic/plutonic fragments are composed of polycrystalline quartz, while fragments of quartzite and phenocrysts of perthite are responsible for the greater part of the remaining percentage.

1. 6. Discussion and conclusions

Both from the pebble counts and the point counts it may be concluded that the sedimentary rocks of the Honda Formation have a western origin, which is in accordance with measured paleocurrent directions (chapter VI, section 3.2).

Uplift of the Garzón Massif ≥ 12 Ma ago (chapter II), which coincided with deposition of the "Río Seco conglomerate" (chapter VI) appears to have had little influence on the pebble composition of this conglomerate. No indications are found that much material came from eastern sources. In the N of the S. Neiva Basin, where most of the pebble counts on Honda conglomerates are concentrated, the main source of Jurassic intrusives within the Garzón Massif is the plutonic terrain N and NE of the town of Gigante. On the geological map (appendix 1), however, the stratigraphic and tectonic relations between the Miocene formations and this terrain clearly show that the Jurassic intrusives were thrust over the Miocene deposits after sedimentation of the Gigante Formation had ended. Therefore, it is unlikely that much of the Jurassic plutonic material found in the Honda Formation has an eastern provenance.

In the conglomerates of the La Dorada Member, the bulk of the material is formed by chert and quartz pebbles, while the remaining portion consists mainly of pebbles of quartzite and Saldaña volcanics. Anderson (1972) suggested that the quartz pebbles may also have been derived from Cretaceous rocks. If this suggestion is correct, 60-80% of the La Dorada conglomerates comes from Cretaceous rocks and a great part of the remaining 20-40 % is derived from Late Triassic/Jurassic volcanics.

The increase in Jurassic intrusives in the Villavieja Member, followed by an increase in Saldaña volcanics and a simultaneous sharp decrease in Cretaceous clasts at the transition to the Gigante Formation may well point to stripping of the Cretaceous sedimentary cover and the gradual unroofing of Triassic/Jurassic volcanic and plutonic rocks of the Central Cordillera.

The sedimentary rocks of the Gigante Formation have a much more variable origin than those of the Honda Formation.

In the conglomerates of the Neiva Member only some 3% of Precambrian metamorphic pebbles from the Garzón Massif is encountered. The sandstones contain between 20-40% of grains of plutonic/metamorphic origin. The composition of these grains suggests that they resulted mainly from erosion of Jurassic plutonic rocks.

Both the sandstones and the conglomerates comprise much material of the Saldaña Formation and contain increasing quantities of fragments and pebbles with a contemporaneous volcanic origin. Thus, the major part of the sediments of the Neiva Member seems to have originated in the Central Cordillera.

The sudden increase in pebble size as compared to the Honda Formation suggests that deposition of the Neiva Member coincided with uplift of the Central Cordillera. This possibility will be further discussed in chapter VII.

The rocks of the Los Altares Member are composed mainly of contemporaneous volcanic clasts, provingen from the Central Cordillera volcanic arc, in accordance with the eastwardly fanning

paleocurrent directions (chapter VII, section 3.1). The composition of the sandstones of this member indicates that they are first-cycle sandstones resulting directly from volcanic eruptions, or from mobilization of loose volcanic debris on the slopes of the volcanoes as a result of heavy rainfall.

The very high percentages of volcanic material, both in the pebble counts and the point counts, somewhat obscure the trends of the other rocks. From the diagrams of the pebble counts, however, it is clear that most of the material has a western provenance, rocks from the Saldaña Formation still playing an important role. The presence of very low, but persistent percentages of Precambrian metamorphic rocks shows that some material originated from erosion of the Garzón Massif. In the very east of the basin, the influence of the massif was greater, as is shown by pebble composition of the sections Silvania and Vereda el Piñal. It is likely that the input of volcanic material from the west was so great that erosional material from the Garzón Massif could not extend far west into the S. Neiva Basin, restricting deposition of this material to the eastern border of the basin.

In the Garzón Member and the overlying Las Vueltas Formation, finally, the influence of the Garzón Massif becomes much greater. The increasing coarseness of the clasts of Precambrian metamorphic origin suggests uplift of the massif and westward extension of alluvial fans into the S. Neiva Basin.

The mixed origin of the deposits of the Garzón Member, which contains both east-derived and west-derived products, is corroborated by the northward paleocurrent directions measured in the member (chapter VII). Apparently, an ancestral Magdalena River was present that was fed with erosional material from the west and from the east.

The sediments of the las Vueltas formation consist entirely of erosional material of the Garzón Massif. Although only one paleocurrent direction could be measured (chapter III, section 2.5) the diminution of the pebble size in an westward direction and the sedimentology of the deposits indicates that the material was laid down on alluvial fans that extended basinward from the massif.

2. Petrology of the volcanic deposits of the Gigante Formation

2. 1. Microscopical description of the volcanic deposits

Volcanic deposits of the Gigante Formation comprise ignimbrites, volcanic debris flow deposits and air-fall tuffs. Hyperconcentrated flow deposits, which are formed by downstream dilution of volcanic debris flows by a decrease in sediment concentration (Pierson and Scott, 1985), are intermediate between volcanic and fluvial deposits. These deposits will not be dealt with in this section, because the petrology of the hyperconcentrated flow deposits are roughly identical to that of the volcanic debris flow deposits, if the flows have not incorporated much fluvial material.

Field descriptions of the volcanic deposits are given in chapter VII, section 2; in the present section only the microscopical aspects of the deposits will be dealt with. Because only the blocks within the volcanic debris flows were used for XRFS analyses and because it is impossible to make thin sections of the debris flow material, the microscopical description of those deposits will be delimited to a description of the blocks.

The volcanic debris flows blocks

In thin section, the blocks of the volcanic debris flows consist either of compact andesite fragments, or of amalgamated small fragments and isolated phenocrysts in a clayey matrix. Plagioclase, quartz, biotite and hornblende are present as phenocrysts, both in the fragments and as isolated crystals. Opaques, zircon and apatite are accessories.

The plagioclase crystals are euhedral laths up to about 4 mm in length. Many of the crystals are fragmented. As both isolated plagioclase crystals and crystals within the fragments are broken, fragmentation must have taken place during eruption. Beside corrosive embayments, the phenocrysts show features of dissolution and recrystallisation. Many of the phenocrysts exhibit a fine-scale oscillatory optical zoning. The oscillatory zoning in any crystal represents a compositional variation of only a few percent from the average composition, from An₂₀ to

An₄₄ (oligoclase-andesine). The larger plagioclase crystals form subophitic intergrowths with hornblende, biotite, apatite and/or opaques. The grains are twinned according to the albite and Karlsbad laws. Polysynthetic twins are also present.

Two types of hornblende may be present: common hornblende and basaltic hornblende. Euhedral prismatic crystals of common green hornblende, 1.5 to 2 mm in length, are distributed throughout the samples. The dark green to yellow-green pleochroitic crystals are often broken.

The basaltic hornblende crystals are also 1.5-2 mm long and darkbrown-brown-greenbrown pleochroitic. These phenocrysts only form a component of the andesite fragments and are not found as isolated crystals. Both basaltic hornblende and common hornblende may have thick coronas of opaques.

Biotite occurs as brown to reddbrown pleochroitic euhedral laths up to 2 mm in length. The crystals are often kinked. Most of the crystals are partly or completely altered to opacite. This texture could be interpreted as due to reaction with the magma under conditions of lower pressure than primary phenocryst growth or, alternatively, as a post-depositional phenomenon. The phenocrysts may contain smaller crystals of plagioclase and opaques.

The 1-2.5 mm large HT bipyramidal quartz crystals are euhedral to anhedral and show extensive corrosive embayments. Many of the crystals are broken.

In one of the volcanic debris flow deposits a few euhedral to subhedral phenocrysts of augite were encountered as free crystals in the matrix.

The volcanic debris flow blocks which consist of amalgamated lithic fragments may also contain a few non-cognate xenoliths, e.g. fragments of Paleozoic schist and quartzite, Saldaña volcanics and Jurassic intrusives.

The ignimbrites

In thin section the ignimbrites are vitric crystal tuffs with a vitrophyric structure. The matrix of the tuffs consists of very compact, small pumice fragments. No X and Y-shaped glass shards are present. The pumice fragments include unwelded and white fragments with rod-shaped vesicules and fragments with circular vesicules. Generally, the fragments show little devitrification, although in a few thin sections spherulites, of fibrous crystals of quartz and alkali feldspar, are found. In several samples the pumice fragments have partly undergone secondary alteration to clay minerals. Beside matrix-sized fragments, variable amounts of larger pumice fragments are present.

Phenocrysts form 40-60% of the total volume. Phenocrysts of plagioclase (20-40%), biotite (5-7%), hornblende (6-12%) and quartz (2-5%) are present. Opaques, apatite and zircon are accessories. Some of the phenocrysts have irregular rims of adhering volcanic glass.

The euhedral to subhedral plagioclase crystals (An₃₀₋₄₅) generally show an oscillatory optical zoning which represents a compositional variation of only a few percent from the average composition. The phenocrysts vary between 2 to 3.5 mm in length and may be strongly fragmented. The fact that the fragments lie together indicates that fragmentation took place during cooling and compaction, and not during eruption of the ignimbrites. Beside corrosive embayments, the phenocrysts show dissolution and recrystallisation features. Synneis structures are frequent. The larger plagioclase crystals are poikilitic and have inclusions of small phenocrysts of hornblende, biotite, apatite and/or opaques. The grains are twinned according to the albite and Karlsbad laws. Polysynthetic twins are also present.

The red to red-brown pleochroitic biotite crystals are generally euhedral and have a length varying between 1 and 2 mm. Some of the phenocrysts are kinked. The rims of the crystals are often oxidized, forming thick opacite coronas. Many of the phenocrysts contain small crystals of zircon and/or opaques.

Hornblende forms darkgreen-green-greenbrown pleochroitic euhedral crystals of 1 to 2.5 mm in length. The phenocrysts may contain inclusions of small crystals of opaques and plagioclase or biotite.

The high temperature bipyramidal quartz crystals have a size varying from 1-3 mm. The phenocrysts are euhedral but often show corrosive embayments and/or breakage. Cavities and cracks are filled with glass.

Variable amounts of xenoliths are present. In some ignimbrites the percentage of xenoliths is very high and the deposits may be classified as lithic tuffs. Other tuffs contain less than 1% of lithics. Both cognate and non-cognate xenoliths are found. The cognate xenoliths comprise devitrified and non-devitrified glass fragments with phenocrysts of plagioclase, biotite, hornblende and quartz. The non-cognate xenoliths include fragments of fresh andesite, Paleozoic schist, Jurassic intrusives, volcaniclastic rock fragments of the Late Triassic/Jurassic Saldaña Formation, and various metamorphic clasts.

The air-fall tuffs

Relatively few unworked air-fall tuffs are present in the Gigante Formation. In thin section, the air-fall tuffs consist of coarse- and fine-grained layers of angular to subangular pumice fragments, locally intercalated with layers of X and Y-shaped glass shards. The pumice clasts contain euhedral or anhedral, broken phenocrysts of plagioclase, biotite, hornblende, basaltic hornblende and opaques. These phenocrysts may also be present in separate layers, where they show a preferential horizontal orientation. No lithic fragments are found. The coarse-grained layers comprise clasts or crystals with a maximum grain size of 1.5 mm; the fine-grained layers consist of clasts and crystals with a maximum grain size of 0.6 mm.

2. 2. Chemical composition and classification of the volcanic deposits

2.2.1. Methods

Rock samples were sawn to small pieces (1-2 cm³). Only homogeneous pieces without weathered surfaces and without inclusions of lithic fragments were selected for further reduction. Splits of 50 to 100 g were ground in an agate-mill for 5 minutes to a size of <60 μm.

Samples of 1 g were dried in an oven at 105°C during one hour before being ignited at 900 °C for another hour. In order to determine the loss on ignition between 105-900°C (L.I.) the samples were weighted before and after ignition.

XRFS was performed using a Philips PW 1404 spectrometer with a Rh-anode X-ray tube operated at 25-60 kV and 25-60 mA for 11 major elements. For this purpose, 0.6 g of pulverized rock was fused with 2.4 g of Li-tetraborate to a homogeneous glass disk. The system was calibrated using USGS geochemical standards as listed by Abbey (1980, p. 16); correction for residual matrix effects was based on theoretical interelement influence coefficients provided by Philips. The concentrations were recalculated to oxide weight percentages. All samples were prepared and measured at the Department of Soil Science and Geology of the Agricultural University of Wageningen.

2.2.2. Results and discussion

Major element XRFS analyses were performed on 27 samples collected in volcanic deposits of the Gigante Formation. The location of the samples is indicated in figs. 17 and 32. Twentyfive samples were taken in rocks belonging to the Los Altares Member, one sample in a volcanic rock from the Garzón Member, and one sample was taken in the dated ignimbrite from the Suaza Valley section ("Picuma conglomerate"). No samples were taken in volcanic pebbles encountered in the Neiva Member, because these pebbles represent reworked volcanic deposits. Thin sections of these pebbles, however, revealed that they are rich in augite phenocrysts and have an andesitic to basaltic composition. This is corroborated by the observations of Van Houten (1976).

Chemical analyses of all samples are given in appendix 3, together with calculated CIPW norms and ANKC-values (Chappell and White, 1974, 1984).

Weathering and secondary clay formation

The ignimbrites and pumice clasts of the Gigante Formation range in SiO₂ from 59 to 64%; the debris flow blocks range from 61 to 66%. This difference is probably caused by differences in water content: both the ignimbrite and pumice samples show relatively high values for the loss on ignition (L.I.), which comprises crystal water and CO₂. From the microscopical description of the ignimbrites it is clear that they contain some 11-19% of biotite and hornblende phenocrysts. The same is true of the pumice clasts. Therefore, only a small percentage of the L.I. may be attributed to water loss of hydrous minerals during heating of the samples. In thin section, the matrices of *e.g.* samples MW 104 and MW 105, which have lost 8.93% and 6.65% respectively, of their total weight as a result of heating to 900°C, are found to contain secondary clay minerals. Thus, it is likely that very high values of L.I. observed in several of the ignimbrite and pumice samples are due to weathering and in situ formation of clay minerals. This process appears to be more restricted in the debris flow blocks, probably because the material is much less porous.

When it is estimated that ±0.65 weight% of the L.I. in the ignimbrite and pumice samples may be attributed to the presence of biotite and hornblende phenocrysts (calculated for samples containing 12 volume% of hornblende and 7 volume% of biotite) and the rest of the L.I. is due to secondary processes, the original percentages of SiO₂ in these rocks would have ranged from 60-65%, which agrees with the values found for the debris flow blocks.

Because the samples with a L.I.>5% are thought to give an unreliable representation of the chemistry of the volcanics of the Gigante Formation, they are not plotted in the classification and variation diagrams given below.

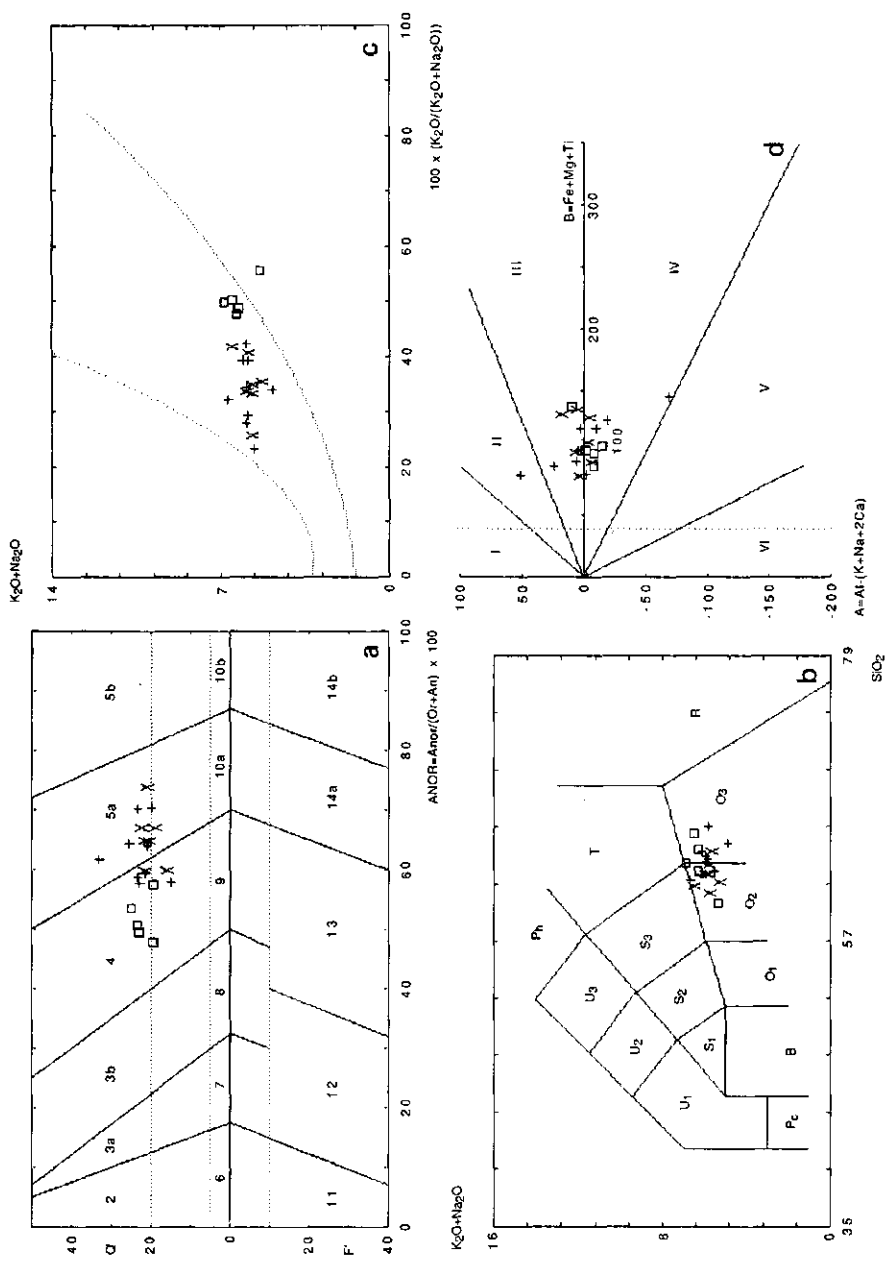


Fig. 24a. Classification of the volcanic rocks of the Gigante Formation in a Q'-ANOR diagram (Streckeisen and Le Maitre, 1979). Fig. 24b. Idem, in a diagram of total alkalis vs. silica (Le Bas *et al.*, 1986). Fig. 24c. "Igneous Spectrum" (Hughes, 1973). Samples outside the funnel-shaped area are alkali-altered. Fig. 24d. BA diagram (Debon and Le Fort, 1983). Field labels are from the original publications. Symbols are as follows: open squares: pumice clasts; plus-signs: debris flow blocks; crosses: ignimbrites.

Table XII. Average major element compositions and ANKC values of the three sample groups of the Gigante Formation.

	Ignimbrites		Pumice clasts		Debris flow blocks	
	x (n=7)	σ	x (n=5)	σ	x (n=9)	σ
SiO ₂	62.08	1.06	62.94	1.99	63.40	1.27
TiO ₂	0.55	0.08	0.54	0.08	0.56	0.11
Al ₂ O ₃	17.29	0.77	16.29	0.78	16.42	0.68
Fe ₂ O ₃	4.14	0.07	4.02	0.58	4.19	0.82
MnO	0.07	0.01	0.08	0.02	0.07	0.02
MgO	2.10	0.49	2.00	0.43	1.90	0.50
CaO	4.79	0.22	4.37	0.42	4.36	0.63
Na ₂ O	3.76	0.26	3.11	0.43	3.89	0.45
K ₂ O	2.05	0.40	3.15	0.20	1.97	0.41
P ₂ O ₅	0.18	0.03	0.22	0.05	0.19	0.06
SiO ₂ /Al ₂ O ₃	3.60	0.18	3.87	0.21	3.86	0.21
ANKC	1.01	0.02	0.99	0.03	1.02	0.11

Classification of the samples

The composition of the samples was calculated according to the method of Streckeisen and Le Maitre (1979) and plotted in a Q'-ANOR diagram (fig. 24a). From this figure it is clear that the majority of the samples are dacites and quartz-andesites, with minor trachyandesites and a single andesite. In a diagram of total alkalis vs. silica (Le Bas *et al.*, 1986) the rocks plot in the dacite and andesite fields (fig. 24b).

Comparison of the chemical characteristics of the three sample groups

For a comparison of the chemical composition of the ignimbrites, the pumice clasts and the debris flow blocks, variation diagrams were drawn and average weight percentages of all oxides were calculated for the three groups.

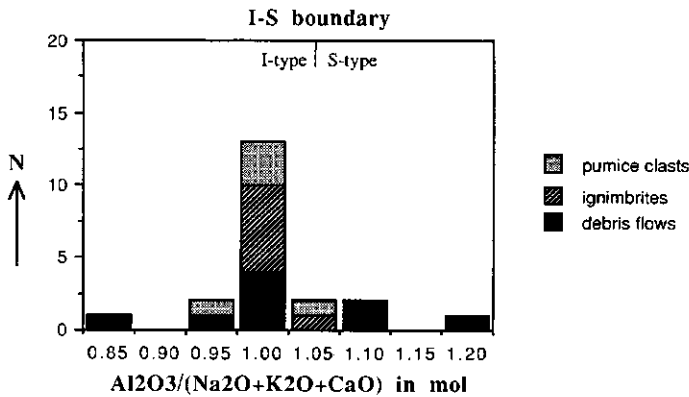
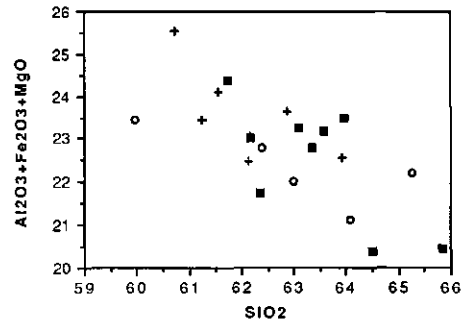
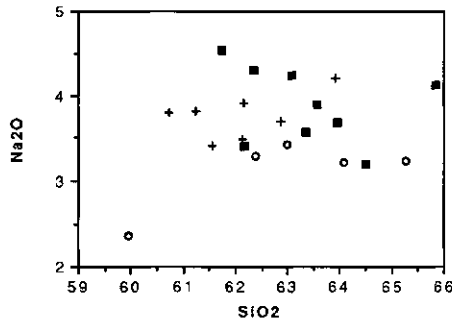
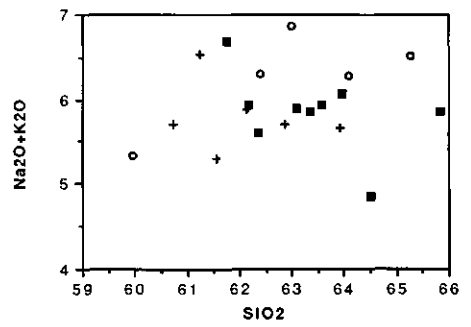
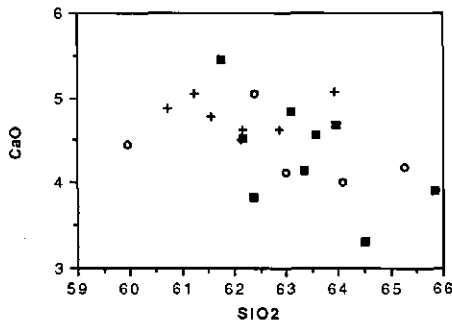
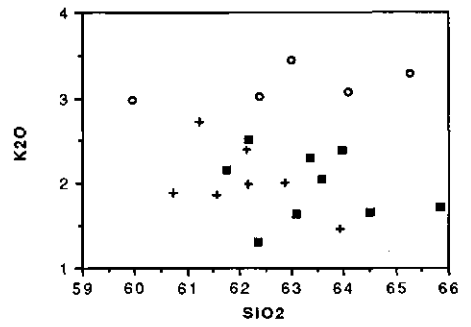
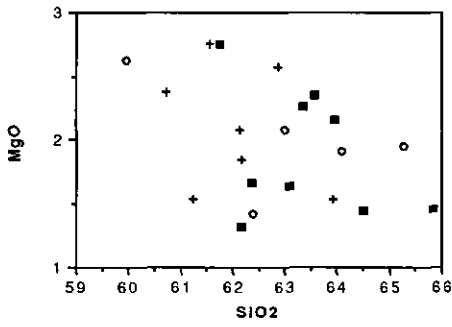
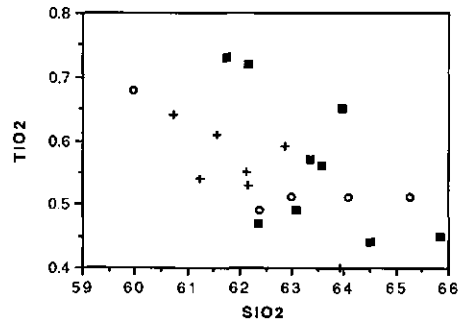
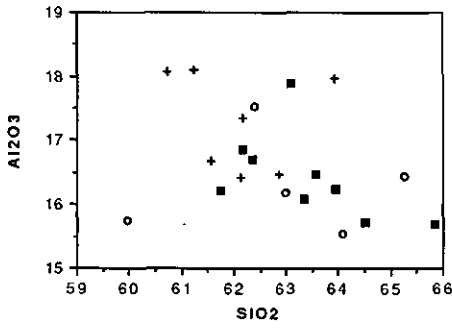


Fig. 25. Histogram of ANKC ratios for the three sample groups. I-S boundary is located at an ANKC-value of 1.05 mol (Chappell and White, 1974, 1984).



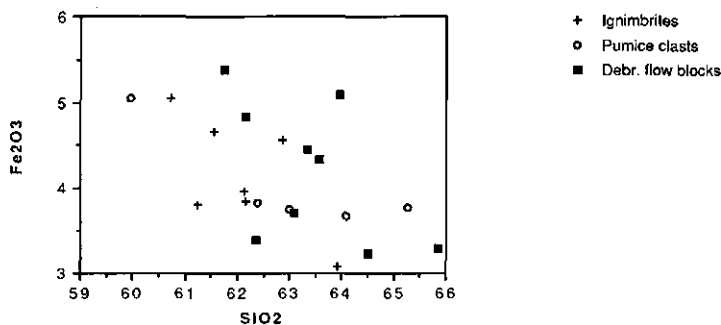


Fig. 26. Variation diagrams for the different oxides, showing comparable chemical trends in the three sample groups.

The average weight percentages of all oxides (table XII) indicate that, within errors, the major element chemistry of all three groups is identical. Only the percentage of K_2O of the pumice samples is higher than that of the ignimbrites and debris flow blocks. When the samples are plotted in the alkali ratio diagram by Hughes (1973), it is clear that the differences cannot be caused by K-alteration (fig. 24c). All samples lie more or less on a horizontal line within the igneous spectrum, indicating that variations in the K-content are compensated by variations in the Na-content. Only one sample plots outside the igneous spectrum. Although this is a pumice sample, the alteration has resulted in lower values of both alkalis. Compared with the other pumice samples, the sample has the lowest potassium content.

At the bottom of table XII calculated average ANKC values for the three groups of samples are shown. The average ANKC values of all groups plot exactly at the I-S boundary (Chappell and White, 1984). Fig. 25 gives a histogram of the ANKC values of all samples. The samples plot on both sides of the I-S boundary, suggesting that they originated from melting of both I-type and S-type granites. In the diagram developed by Debon and Le Fort (1983), which discriminates between peraluminous and metaluminous rocks, the samples of the Gigante Formation plot in both domains (fig. 24d), supporting the results of the ANKC histogram.

When the samples are plotted in an AFM-diagram (fig. 27), they plot within a very small area in the calcalkaline field.

Although the variation diagrams (fig. 26) generally show a relatively high degree of scatter, the oxides of the three different sample groups exhibit comparable chemical trends. With the exception of the alkalis, all oxides show decreasing weight percentages with increasing SiO_2 -content. This trend is not very well developed in Al_2O_3 , but clearly present in the other oxides. The percentages of Na_2O and K_2O , on the other hand, appear to be independent of SiO_2 .

With the exception of sample MW 157 (see appendix 3) all samples come from the Los Altares Member. It was shown in chapter IV that this member was deposited over a time interval of ± 1.6 Ma (*i.e.* between 8 Ma and 6.4 Ma ago). It is likely that in this period several volcanoes were active at distinctive times, erupting different products of a comparable magma source. This would explain the scatter of the data points on the one hand and the similarities in chemical characteristics of the sample groups on the other hand.

Distribution of the dacites and andesites in time and space

When all samples, taken in the Q.Guandinosita section, are put in order from old to young and their major element chemistry is compared, no systematical variations in the chemical trends are observed. The same observation is made when the samples from the different groups are compared in a N-S sense: samples of dacitic and andesitic composition appear to be spread in a random manner over the basin. These observations strengthen the hypothesis that the volcanics of the Gigante Formation were erupted by different volcanoes at distinctive times.

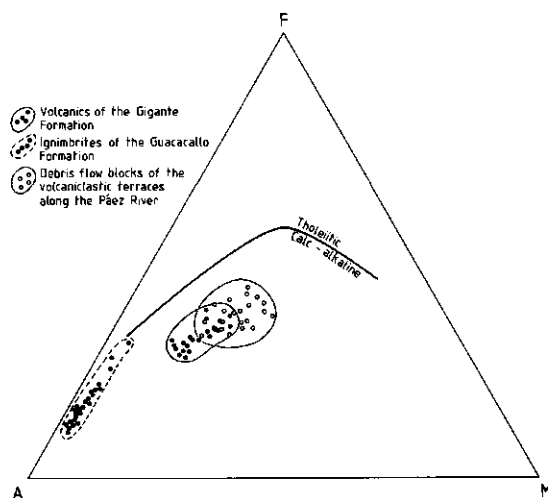


Fig. 27. AFM-diagram showing limit between calc-alkaline and tholeiitic rocks. In the diagram, total alkalis ($\text{Na}_2\text{O}+\text{K}_2\text{O}$) is plotted against $(\text{FeO}+0.8984 \text{ Fe}_2\text{O}_3)$ and MgO . Beside the volcanics of the Gigante Formation, the ignimbrites of the Guacacallo Formation (chapter X) and the debris flow blocks of the volcanoclastic terraces along the Páez River (chapter XI) are plotted in the diagram.

2. 3. Conclusions

1. While the contemporaneous volcanic pebbles in the conglomerates of the Neiva Member have an andesitic to basaltic composition, volcanics from the Los Altares have a dacitic to andesitic composition. Thus, volcanism became more acidic in time.
2. The volcanics and volcanoclastics of the Los Altares Member probably resulted from several volcanoes, erupting magmas of both dacitic and andesitic composition.
3. Volcanic debris flow deposits, ignimbrites and pumice clasts of the Los Altares Member have comparable chemical compositions, suggesting that the material was derived from related magma sources. The position of the samples in the calc-alkaline field of the AFM diagram and the fact that the magma producing the volcanics has characteristics of both I-type and S-type granites, suggest that the volcanics originated in a continental margin setting by partial melting of subducted oceanic crust under wet conditions.
4. Field observations and chemical analyses of samples MW 157 and MW 178 suggest that the volcanics of the Garzón Member and the volcanics from the Suaza Valley have similar compositions as the volcanics of the Los Altares Member.

Chapter VI

Sedimentation patterns of the Miocene Honda Formation: influence of uplift and basin subsidence on fluvial deposition¹

A.M. van der Wiel and G.D. van den Bergh²

1. Introduction

The last fifteen years, one of the major interests in fluvial sedimentology has been on the interpretation of the autocyclic and allocyclic mechanisms (Beerbower, 1964) that influence the development of sedimentological successions.

Autocyclic mechanisms are controls that are inherent to the fluvial regime, such as avulsion, lateral migration of channels, crevassing etc. Allocyclic controls are those which result from changes in supply of energy or material to the fluvial system and may include tectonic factors such as uplift and subsidence (Heward, 1978; McLean and Jerzykiewicz, 1978; Miall, 1978a; Steel, 1976; Steel and Aasheim, 1978; Bridge and Leeder, 1979) and/or climatic factors such as vegetation and rainfall (Schumm, 1968; Baker, 1978) as well as volcanism (Davies *et al.*, 1978; Vessell and Davies, 1981; Mathisen and Vondra, 1983; Smith, 1987a, b).

This chapter addresses the different allocyclic influences that played a role during deposition of the Honda Formation.

Wellman (1968, 1970) did a great amount of sedimentological, stratigraphical and petrological work on the formation, but his work does not go into great detail with regard to the processes responsible for the deposition of the formation.

2. Facies types and facies associations of the Honda Formation

2.1. Introduction

The interpretation of the stratigraphy and facies of the Honda Formation is based on 5 sections measured throughout the region, and on detailed stratigraphical and structural mapping of the whole study area. The stratigraphy of the Honda Formation is described in chapter III. The stratigraphical sections are given in fig. 15, p. 44-46). The interpretation of the Honda Formation in terms of facies associations is based especially on the Q. Guandinosita section, because this section is the most complete. The locations of the different sections are indicated in fig. 28 and on the geological map (appendix 1).

2.2. Lithofacies types of the Honda Formation

The deposits were described in terms of lithofacies codes that are mainly based on the lithofacies codes for braided river systems, introduced by Miall (1977, 1978b) and Rust (1978).

¹ Submitted in more elaborate form to the Journal of South American Earth Sciences

² Institute for Earth Sciences, University of Utrecht, Budapestlaan 4, 3508 TA Utrecht

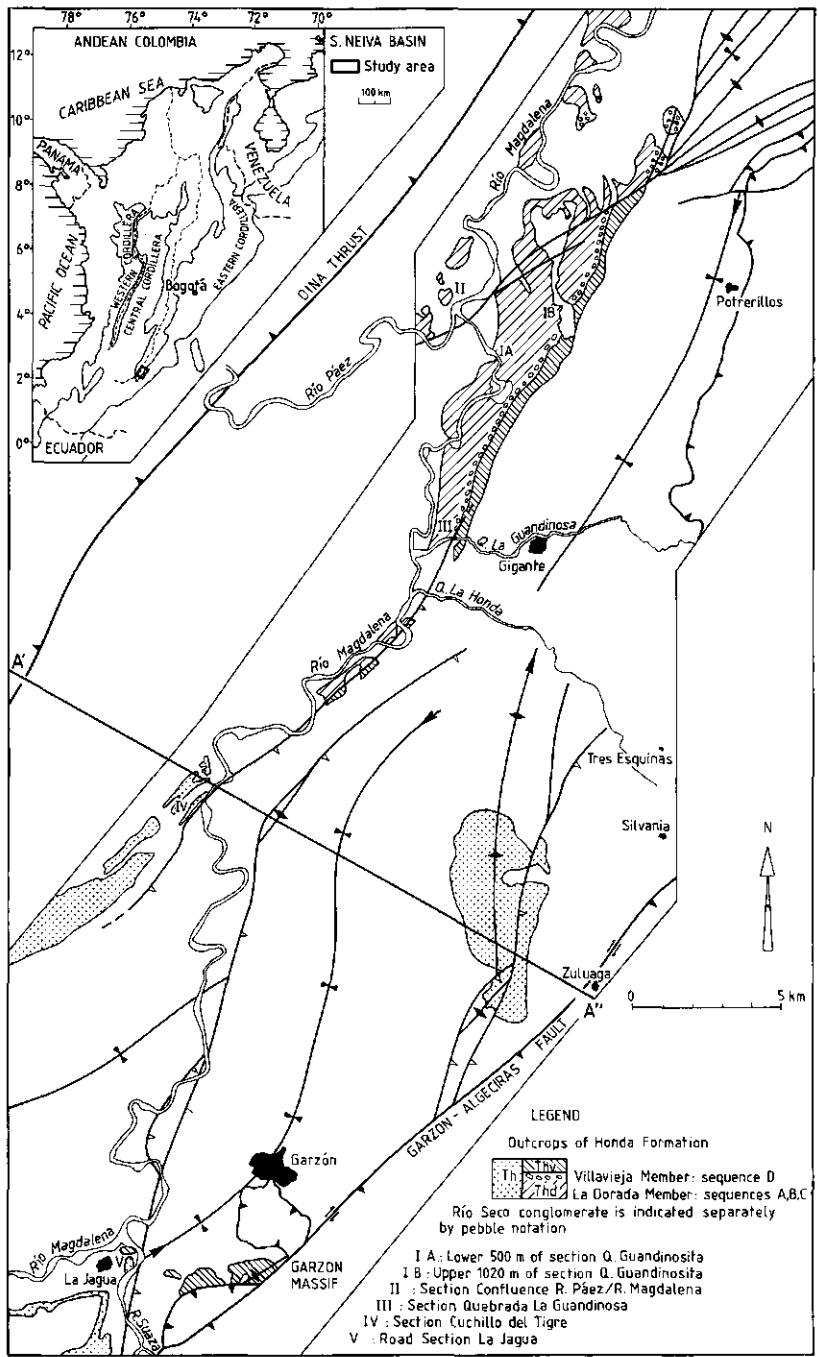


Fig. 28. Geology of the Honda Formation and position of stratigraphical sections. A'-A'' corresponds with part of the profile given in fig. 5 (p. 15).

A few facies types have been added: facies Gp of Miall has been split up into two types, Gp(b) and Gp(p). Gp(b) corresponds with facies type Gp used by Miall, whereas Gp(p) is used here for large-scale inclined heterolithic bedding in the sense of Thomas *et al.* (1987). It is distinguished from lithofacies Sp by the much higher percentage of pebbles. The lithofacies codes used here are given in table XIII.

2. 3. Interpretation of the data in terms of facies associations

The sediments of the Honda Formation may be divided into five major lithofacies associations using the lithofacies codes given above. The associations comprise a non-channelized sandy facies association (I), three fluvial channel facies associations (II, III, IV) and an overbank facies association (V). The sandy and gravelly facies associations are depicted in fig. 29.

I. A non-channelized sandy facies association dominated by Sh and Sl

Facies Sh and Sl are dominant, while facies Sp, St, Sr and Gm form minor facies. The sandbodies generally have non-erosional basal contacts. Individual beds are between 1-6 m thick. The sand is poorly rounded and poorly to moderately sorted. The grain size varies from very coarse to coarse. Pebbles are present as channel lags (Gm), as thin pebble stringers or scattered throughout the sand. Pebbly sandstones are also common (fig. 29).

II. A fluvial channel facies association dominated by Sp

The major facies type of this association is Sp; minor facies are St, Sh, Sl and Fl. Channel fills consist of pebbly sandstone and sandstone. The association is characterized by large-scale channel fills (≤ 8 m). The sandstones and pebbly sandstones may occur in single-storied or multi-storied units. Especially in some of the thicker sandstone beds in the multi-story sequences, large-scale inclined heterolithic stratification as defined by Thomas *et al.* (1987) and called epsilon-cross-stratification by Allen (1963), is developed, with set heights up to 8 m (facies Sp).

III. A fluvial channel facies association dominated by Gp(p)

The major facies type of this association is Gp(p); minor facies types are Gp(b), Gt and St. The channel fills consist of highly conglomeratic sandstones and sandy conglomerates. The association is dominated by single-storied small-scale channel fills (≤ 4 m). The set height of facies Gp(p) is usually equal to or slightly less than the total bed thickness. Most of the beds have an erosive base with the coarsest sand and pebbles occurring in the lower two-third of the bed and fining upward to fine sand and silty sand. The beds frequently pinch out laterally over distances of only several meters (fig. 29).

When facies Gt or St are found at the lateral termination of a bed, the trough cross-bedding should be interpreted as a channel-fill that was formed along the cut bank of the river during abandonment of the channel. In those cases that the inclined stratification of facies Gp(p) is developed at the lateral termination of a bed, the dip of the stratification is oriented perpendicularly away from these lateral boundaries, suggesting that the inclined strata were formed as a result of lateral accretion. Facies Gp(b) is thought to have formed by avalanching on the lee side of transverse bars.

IV. A fluvial channel facies association dominated by Gm

This association is almost exclusively represented by facies Gm, with only very minor Gt, Gi, Gp(b) and Gp(p). Intercalated sandstone lenses and beds exhibit facies Sh and St (figs. 15, 29). The conglomerates of this facies association are crudely horizontally stratified, or massive and clast-supported. Clasts are generally well rounded and moderately sorted. The maximum clast size is 16 cm.

The massive conglomerates occur in thick multi-storied sequences of up to 37 m. The individual conglomerate layers, with maximum thicknesses of 14 m, are separated by sandstone lenses and beds of less than 1 m thick. Imbrication is absent because few pebbles have a flat shape.

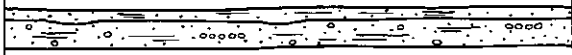
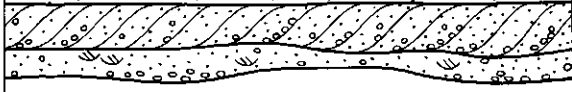
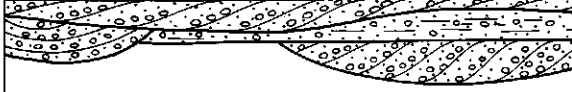
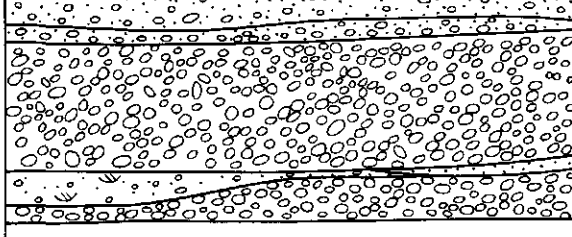
Facies association	Morphology and internal structures of lithosomes	Thickness of individual beds	Channel characteristics
I		1-6 m	narrow to broad simple sheets
II		≤ 8 m	broad multistory sheets
III		1-4 m	narrow multistory sheets and ribbons
IV		≤ 14 m	broad multistory sheets

Fig. 29. Morphology and internal structures of the sandy and gravelly lithosomes of the different facies associations of the Honda Formation.

V. An overbank facies association

Facies of this association are Fm and Fl with minor Sh, Sl and Sp. The association is dominated by silty mudstones and siltstones that may be intercalated with thin beds of less than 2 m, consisting of fine to medium grained sandstone. These beds show parallel lamination and occasionally low-angle cross-bedding or planar through cross-bedding. The facies association consist both of massive mud- and siltstone intervals and of thin interbedded mud, silt and sand deposits. Pieces of fossilized wood, plant roots, and evidence of burrowing are typical for the overbank deposits. The mud- and siltstones have a purplish-brown to red-brown colour and often show grey mottling reflecting paleosol development.

3. Depositional environments

3. 1. Distinction of four large-scale sequences in the Honda Formation

Fig. 30 (middle) shows the fluvial channel/overbank deposits ratio as a function of the depth in the stratigraphy, and fig. 30 (left) shows the relation between the average thicknesses of the overbank intervals and fluvial channel intervals and the position in the stratigraphy. In fig. 30

Table XIII. Lithofacies of the Honda Formation.

Facies code	Lithofacies	Sedimentary structures	Interpretation
Gm	Gravel, massive or crudely bedded, clast supported	Horizontal bedding, gravel imbricated predominantly on b-axis (<i>i.e.</i> a-axis transverse to flow direction)	Channel lag, longitudinal bars
Gt	Gravel, stratified	Large-scale trough cross-beds	Channel fill
Gp(b)	Gravel, stratified	Planar tabular cross-beds, single or grouped	Straight-crested transverse bars
Gp(p)	Gravel, stratified	Low-angle (5-20°) planar tabular cross-beds; sets to 4 m thick, azimuth perpendicular to lateral channel scour	Lateral accretion surfaces of pointbars
St	Sand, medium to very coarse, may be pebbly	Trough cross-beds, single or grouped	Dunes (lower flow regime)
Sp	Sand, medium to very coarse, may be pebbly	Planar tabular cross-beds, single or grouped; sets to 8 m thick, often azimuth perpendicular to lateral channel scour	Transverse bars, sand waves (lower flow regime), lateral accretion surfaces of point bars
Sl	Sand, fine to coarse	Low-angle (<10°) cross-beds	Scour fills, antidunes
Sr	Sand, very fine- to medium-grained	Ripple marks and ripple cross-lamination of all types	Ripples: bar-top, secondary channel, flood plain (lower flow regime)
Ss	Sand, fine to coarse, may be pebbly, may contain intraclasts	Broad, shallow scours, including eta cross-stratification	Scour fills
Sh	Sand, medium to very coarse, may be pebbly	Parallel lamination, plane bedding	Planar bed flow (lower and upper flow regime)
Fl	Sand (very fine to fine), silt, mud	Ripple marks, plane lamination, convolute bedding, burrows, plant rootlets, leaf impressions	Deposit of waning floods, overbank deposits
Fm	Silt, clay	Massive	Overbank or drape deposits

(right) the maximum clast size of the conglomeratic deposits is plotted as a function of the stratigraphical position.

In the figure, four large-scale sequences are clearly visible, each one of these representing 400-450 m of the stratigraphy, excepting the uppermost sequence which is only 260 m thick. In order to facilitate comparison between these informal units, the Honda Formation will be further described in terms of these four sequences, named from below to above A, B, C and D. The lower two sequences A and B are represented by thickening upward sequences of the fluvial channel sequences, thinning upward of the overbank sequences and increasing ratios of the

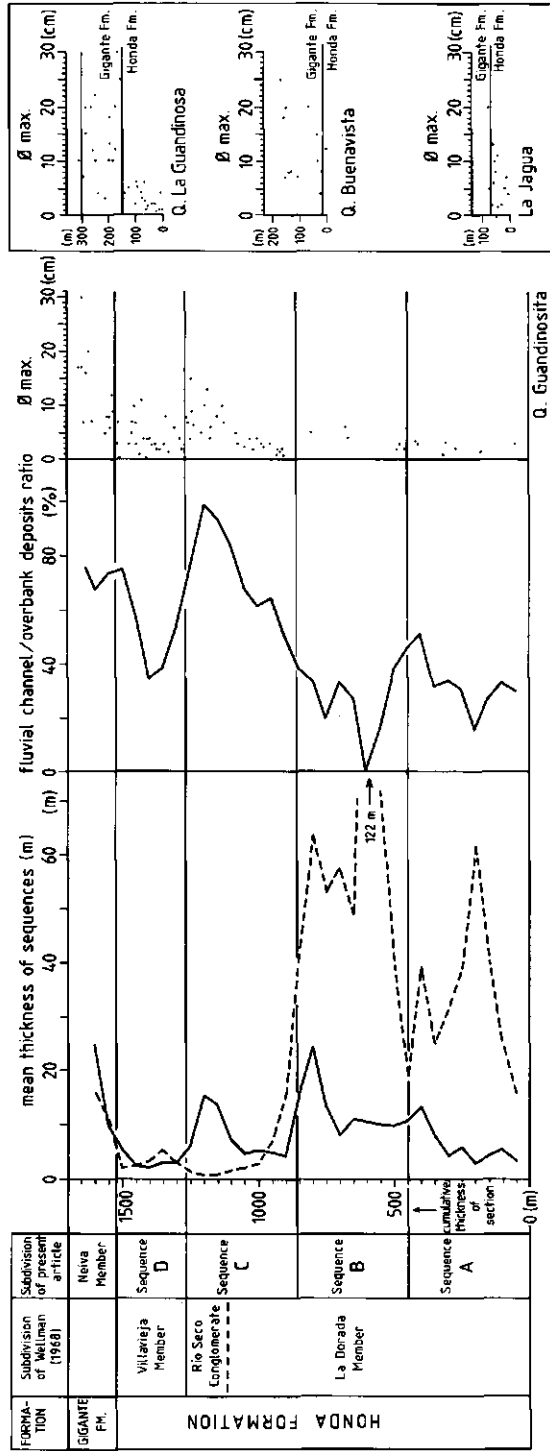


Fig. 30. Distinction of four large-scale sequences in the Honda Formation on the basis of the relation between the position in the stratigraphy and the average thicknesses of the overbank deposit sequences and fluvial channel intervals (left), the position in the stratigraphy and the changes of the fluvial channel/overbank deposits ratio (middle), and the position in the stratigraphy and the maximum clast size of the conglomeratic deposits (right).

fluvial channel/overbank deposits, as well as sandstones with high percentages of fresh volcanic components. The maximum clast size of the conglomerates shows a single coarsening upward trend from the base of sequence A to the top of sequence B. Sequence C corresponds to increasing ratios of the fluvial channel/overbank deposits, a thickening upward trend in the fluvial channel sequences and a coarsening upward trend of the conglomerates. Sequence D shows coarsening upward of the conglomerates and variable ratios of fluvial channel/overbank deposits. The sequences of channel deposits do not thicken upward.

The boundaries between the sequences generally coincide with changes in lithology and in the variance of the paleocurrent directions (see below), and the deposits of each sequence belong to different facies associations (table XIV). The lower three sequences correspond to the La Dorada Member of Wellman (1968), while sequence D coincides with the Villavicija Member.

3. 2. *Paleocurrent directions*

The total number of 22 paleocurrent measurements, made in the present investigation is rather low due to the lack of suitable outcrops. Measurements on planar and trough cross-bedding were performed in the Quebrada Guandinosita (fig. 15: p. 44-45). The results of these measurements are as follows: in sequence A only one direction (towards 57°) could be measured, because the sandstones are massive and lack paleocurrent indicators. Paleocurrent directions of sequence B are to the ENE (the average of measurements taken in 7 sandstone beds is towards 73°); the variance between different beds and within the same bed is low at first, but increases towards the top of the sequence (fig. 15).

In sequence C the variance between different measurements within the same bed is low, but the variance between different beds is rather high. Paleocurrent directions are towards the ENE (the average of measurements in 10 beds is towards 60°). In sequence D measurements could only be taken in four beds; directions vary between 279° and 107°.

According to Wellman (1968, 1970) paleocurrent directions in the Honda Formation, both from the S. Neiva Basin and from the more northerly basins, are to the east. This is in approximate accordance with the paleocurrent directions measured in the present study.

3. 3. *Depositional environments of sequences A and B*

Description

Both sequences are characterized by extremely thick floodplain units (fig. 30, left). Other characteristics of these sequences are the very low fluvial channel/overbank deposits ratio (fig. 30, middle) and the ENE paleocurrent directions. The sequences consist of alternations of red-brown to purplish-brown mudstones (fig. 15) with grey to beige sandstones.

Sequence A is distinguished from B on the basis of the dominant sandy facies association (table XIV). The sandy deposits of sequence A correspond mainly to facies association I dominated by facies types Sh and Sl (fig. 15). The maximum thickness of the sandstone bodies amounts to 5 m. The sandstones have non-erosional lower contacts and often fine upward. Conglomeratic deposits are scarce. The sandbodies form narrow to broad simple sheets (terminology after Blakey and Gubitosa, 1984) that extend laterally over hundreds of meters. Thin sections of the sandstones show that they contain large quantities of unweathered volcanic fragments derived from contemporaneous volcanism (chapter V, section 1.5). The two dated tuffs mentioned in chapter IV are found in this sequence. Some conglomerate bodies above and below these tuffs contain well rounded clasts of fresh dacitic pumice.

The sandy and gravelly deposits of sequence B belong to facies association II dominated by facies type Sp (fig. 29). Individual sandstone layers are between 0.5 and 20 m thick; the average thickness is 5 m. Many of the sandstone beds show a fining-upward trend (photo 9, p. 99). Towards the middle of the sequence the sandbodies become multi-storied. The maximum thickness of these multi-storied units amounts to 24 m at the top of sequence B. Large-scale inclined heterolithic stratification is developed especially in the thicker sandstone beds of the multi-storied sequences. Channel depths are 8 m or less, as may be deduced from the thickness of the lateral accretion deposits. In one of these lateral accretion units intercalated silt layers are slumped (fig. 15, Q. Guandinosita section: 800 m above the base of the formation). Conglomeratic deposits other than lag-deposits are absent. The sandbodies at the top of the sequence form broad multistory sheets with a very great lateral extent, that may be followed over various hundreds of meters up to distances of 5 kilometers. In the overbank facies association thin sandstone beds displaying facies type Sh are frequent.

Interpretation

The sedimentation characteristics of the lower two sequences A and B show a gradual transition from sedimentation by a non-channelized fluvial system to a sedimentation type determined by a channelized fluvial system:

- sequence A is characterized by a predominance of facies Sh and Sl. The predominance of facies Sh and Sl and the lack of clearly channelized sandstone bodies suggest that the sediments were deposited by sheetfloods under high energy flow conditions (McKee *et al.*, 1967; Miall, 1978b, 1985; Rust, 1978).

- in sequence B, deposits of facies types Sh and Sl become progressively scarcer and large-scale heterolithic stratification increases in abundance, indicating that a channelized river system with lateral accretion developed. The lack of conglomeratic deposits other than lag-deposits, slumping of the silt layers, indicative of the instable conditions on the sloping part of the lateral accretion surfaces, and the fining-upward trend of many of the fluvial channel deposits of sequence B point to pointbar deposition. The thin sandstones of the overbank facies association, displaying facies Sh, could represent crevasse splay deposits. An interpretation in terms of pointbar deposition is also supported by the fact that in the upper part of the sequence paleocurrent measurements within the same bed and between beds show a high variance.

The composition of the sandstones shows that volcanic activity culminated during deposition of sequence A and gradually diminished towards the top of sequence B (chapter V, section 1.5). Thus, the transition from the sheetflood dominated fluvial system of sequence A to the meandering river system of sequence B may well reflect the waning activity of the Central Cordillera volcanic arc. A similar mechanism is described by Vesell and Davies (1981) in the forearc basin of Guatemala, where sedimentation is dominated by large, active stratovolcanoes. The authors are of the opinion that the observed change from a braided to a meandering system is a function of the amount of sediment introduced into the system rather than a change in slope or rainfall.

3. 4. Depositional environment of sequence C

Description

This sequence is characterized by a coarsening upward trend of the conglomerates, a strong upward decrease in the thickness of the overbank deposits, a thickening upward trend in the fluvial channel sequences and corresponding increasing ratios of the fluvial channel/overbank deposits (fig. 30). The paleocurrent directions have a high variance and are towards the ENE (fig. 15, Q. Guandinosita section).

In sequence C, three facies associations may be distinguished that gradually replace each other (table XIV): the fluvial channel deposits of the lower part of the sequence belong to facies association II; the deposits of the middle part of the sequence belong to facies association III (photos 10, 11, p. 99) and grade upward into facies association IV (photo 12).

At the base of sequence C, the large-scale channel deposits typical of sequence B are replaced by small-scale channels, less than 4 m deep, as may be deduced from the thickness of the beds (fig. 15, Q. Guandinosita section). Most of these sandy channel deposits fine upward. The channels display planar tabular cross-stratification and, to a much lesser extent, trough cross-bedding. The sandstones are only slightly conglomeratic and single-storied. Both

Table XIV. Abundances of facies associations found in the different sequences of the Honda Formation.

Sequence	Dominant facies associations	Minor facies associations
A	I, V	
B	II, V	
C	From below to above: II, III, IV	I
D	III, V	V

the sandstones and the intercalated mudstones have a redbrown colour. The mudstones exhibit grey mottling. Gradually the sandbodies are replaced by multi-storied conglomerates and pebbly sandstones exhibiting planar tabular cross-stratification, belonging mainly to facies types Gp(p) and Gp(b). Towards the top of the sequence, multi-storied, up to 37 m thick redbrown orthoconglomeratic units consisting of facies type G(m) predominate (fig. 15, photo 12, p. 99). The contacts of these units with underlying overbank deposits are planar non-scouring or erosional. Internally, the contacts are strongly scouring. Individual conglomerate beds have thicknesses up to 14 m. The broad multistory sheets extent over great distances of at least several km.

Interpretation

It is clear that during deposition of sequence C the fluvial system was carrying progressively more bed-load and less suspension-load (terminology after Schumm, 1968), which is in accordance with the increasing ratio between fluvial channel and overbank deposits, the thinning of the mudstone intervals and the increase in multi-storied channel deposits culminating in massive conglomerates.

Fluvial facies dominated by conglomeratic planar cross-bedding, as found in the middle of sequence C, may be formed both on the lower parts of coarse-grained point-bars (Gustavson, 1978) and on chute-bars in meandering river systems (McGowen and Garner, 1970). Alternatively, lateral accretion may occur as a result of lateral growth of longitudinal bars in braided streams on alluvial fans, as has been shown by Ramos and Sopena (1983) in the Buntsandstein of the Iberian Ranges. Both cases indicate relatively high-energy streams, with prevalent bedload transport.

The horizontally bedded or massive conglomerates of facies Gm at the top of sequence C may be interpreted as superimposed longitudinal bars, which are separated by reactivation surfaces and originated during high stage flow (Boothroyd and Ashley, 1975; Rust, 1975, 1978), while the intercalated horizontally bedded thin sandstones (Sh) represent deposition during waning flow conditions. The facies association is very similar to the "sheets of massive conglomerates" described by Ramos and Sopena (1983), which are interpreted as stacked longitudinal bars deposited by alluvial fans.

In sequence C, paleocurrent measurements from the same bed exhibit a low variance, but measurements between beds show a high variance. In combination with the fact that both the middle and upper part of the sequence show very strong resemblances to the conglomeratic deposits of the basal Buntsandstein in the Iberian Ranges (Ramos and Sopena, 1983), this suggests that the conglomerates and pebbly sandstones of sequence C were deposited on longitudinal bars in braided channels on alluvial fans.

3.5. Depositional environment of sequence D

Description

Although sequence D also coarsens upward, the fluvial channel and overbank sequences do not show any thickening upward, and the ratio between the two types of deposits is variable throughout the sequence (fig. 30). The fluvial channel deposits of this sequence belong to facies association III, dominated by Gp(p). Multi-storied sequences of up to 18 m of redbrown pebbly sandstones and sandstones are most common (fig. 15, p. 44-46). These sequences can have either convex downward, strongly erosive lower contacts or planar basal contacts. Internal contacts are strongly erosive (photo 13, p. 100). Individual layers have thicknesses between 1-10 m, but most beds have thicknesses of some 2.5 m (photo 13). Pebbly sandstones are much more abundant than orthoconglomerates (photo 14). Many beds have a simple internal bedding consisting of facies Gp(p), with a relative low inclination (<15°) of the planar cross-bedded sets (photo 15, p. 100), or exhibit channel-fill cross-bedding. Channel depths averaged 2.5 m, as may be deduced from the height of the lateral accretion sets; the lateral extent of the sandbodies is usually in the order of some tens of meters. The sandstones form narrow multistory sheets and multistory ribbons. Many of the beds fine upward. The colour of the unweathered sandstones is grey-brown to light-grey. Intercalated mudstones, making up approximately 50% of the sequence, are redbrown with grey mottles (photo 16).

Interpretation

The erosive base of the beds in combination with the lateral accretion deposits, suggests that during the formation of the lithosomes each time an erosive phase took place first, resulting in the incision of channels. This incision phase was followed by a period of diminished discharge, leading to lateral sediment accretion. The limited lateral extent of the lithosomes indicates that

the channels underwent relatively little lateral migration before the channel system was abandoned. In some cases no lateral migration took place at all, but the channels were filled with deposits belonging to facies types Gt and Ss when discharge and current velocity diminished. Locally, separate cycles of channel erosion, migration and infill succeeded each other rapidly, causing the development of multi-storied lithosomes. Muddy reddish-brown siltstone and silty sandstone intercalations are often conserved in these sequences, because younger channels have incised preferentially into the older ones.

The planar tabular cross-stratification could be interpreted either as pointbar lateral accretion surfaces of meandering streams, or as formed by lateral growth of longitudinal bars in braided streams. The high variance between paleocurrent measurements of different beds and the low variance of measurements from the same bed, as well as the small scale and the relatively simple build of the lithosomes and the limited lateral migration of the channels, are uncharacteristic of coarse-grained pointbar deposition by meandering rivers and rather point to deposition by small braided streams on an alluvial fan.

4. Discussion

It has been shown above that the river systems of the Honda Formation show important deviations from either typically braided or meandering river facies models:

- Sequence A seems to have been deposited by sheetfloods, but is characterized by very thick overbank deposits.

- In the literature coarse-grained lateral accretion deposits are usually interpreted as resulting from deposition by a bed-load dominated meandering river system. It has been shown, however, that the lateral accretion deposits of sequences C and D should rather be interpreted as being caused by lateral growth of longitudinal bars in braided streams on alluvial fans.

Jackson (1978) and Galloway (1981) noted that a variety of fluvial sequences exists that are intergradational between meandering and braided sequences. Miall (1980) pointed out that the existing facies models for braided and meandering river systems do not incorporate the effects of allocyclic sedimentary controls and are therefore too generalized. This is certainly also valid for tropical river systems: Baker (1978) has shown that present day river systems from the tropical and subtropical environments of the Amazon Basin show pronounced deviations from the sediment size-sinuosity relationships that were developed by studies of rivers in temperate semi-arid and humid environments.

From the above it is clear that a correct interpretation of stratigraphical sections in terms of ancient river systems is only possible when the allocyclic factors that controlled the sedimentary processes are known. Therefore, it will be tempting first to define the controls which played a role during deposition of the sequences A to D. Secondly, a reconstruction of the sedimentary environment and the former river systems will be made.

4.1. Uplift, basin subsidence and volcanism

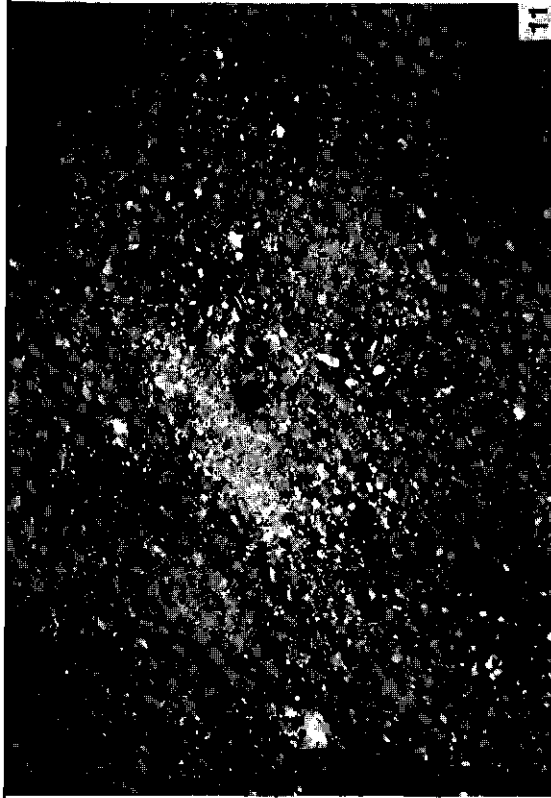
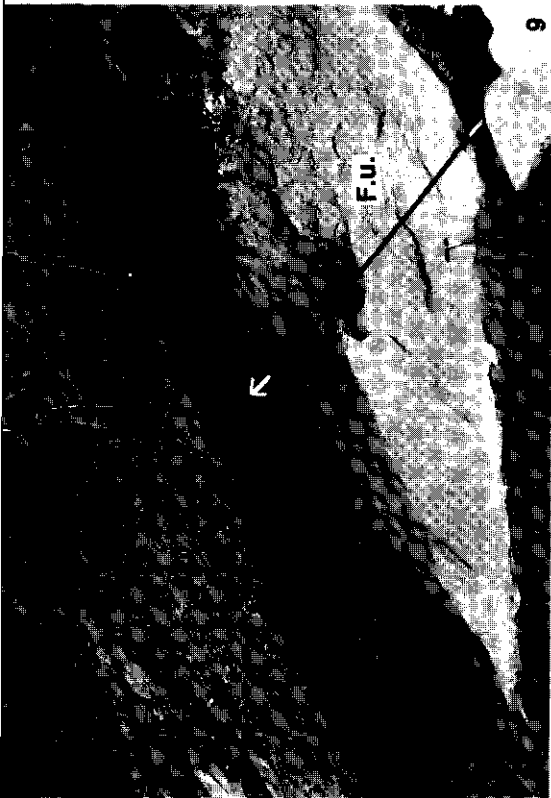
In contrast to the former supposition that floodplain deposits are largely restricted to high sinuosity river systems, the ratio between fluvial channel and overbank deposits appears to be

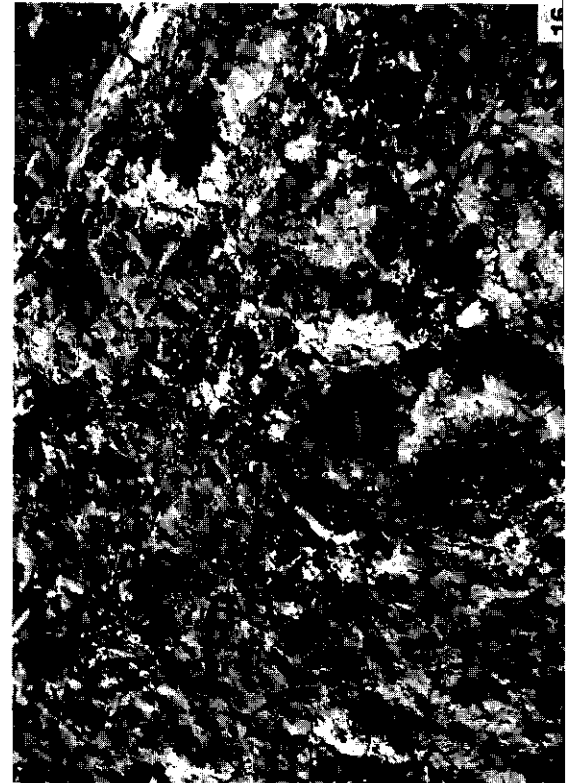
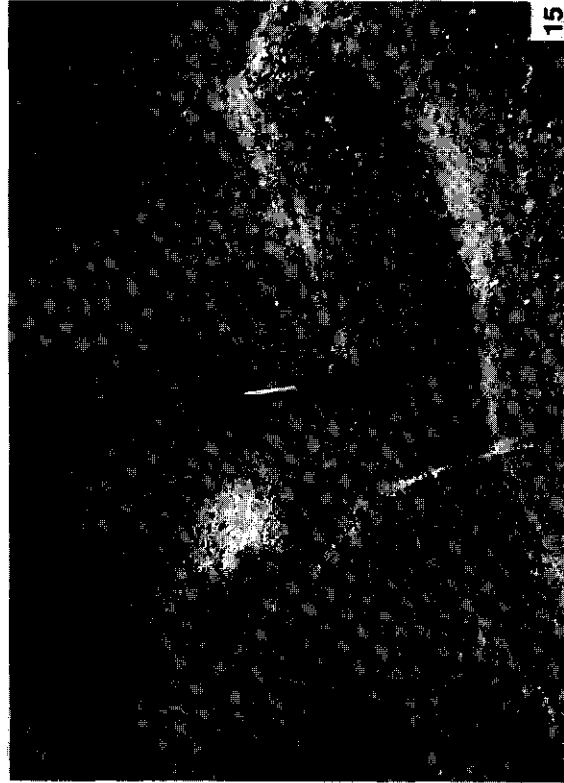
Photo 9. Part of the point-bar deposit in the upper part of sequence B at ± 800 m above the base of the Q. Guandinosa section (see fig. 15). Note fining upward (F.u.) of pebbly sandstone to sandy siltstone and slumping of the sandy siltstone bed. View of the photo is toward the S. Length of hammer is ± 30 cm.

Photo 10. Pebbly sandstones and intercalated sandstones in fluvial channel deposits of the middle part of sequence C. The photograph was taken in a deposit just below the "Río Seco conglomerate" in the Q. Guandinosa section. View of the photo is toward the S.

Photo 11. Detail of a pebbly sandstone bed, depicted in photo 10. Note the fact that most pebbles are well rounded, but have a low sphericity. This is due to the fact that the majority of the pebbles are chert pebbles, which originated from thin layers of porcelanite. View of the photo is toward the S.

Photo 12. "Río Seco conglomerate" in the Q. Guandinosa section. Individual beds show strongly scouring bases. View of the photo is toward the NNE. Woman is ± 1.60 m tall.





dependent on a number of different, partly interrelated allocyclic and autocyclic factors, *i.e.* the climate and thus the vegetation cover (Schumm, 1968), the type of sediment which is available as a result of tectonism and the climate (Schumm, 1968; Baker, 1978), the relation between tectonic movements in the source area and the combined effects of subsidence and compaction of the sediments in the depositional area (McLean and Jerzykiewicz, 1978), as well as the lateral energy gradient efficiency in homogenizing a flood plain, which depends on the frequency of channel avulsion and on the width of the flood-plain and thus on the restriction of the lateral movements of the channel area (Allen, 1978; Friend, 1978; Bridge and Leeder, 1979). The sedimentological differences between the four sequences in the Honda Formation seem to be determined largely by different combinations and different intensities of these factors.

Sequences A and B

It has already been stated that sequences A and B contain very large amounts of floodplain deposits and that these deposits thin upward (fig. 30, p. 94), while the conglomerates of sequences A and B together form a single coarsening upward sequence. It has been mentioned above that deposition of the Honda Formation started when foreland folding and thrusting of the Chusma fault system had ended. It is therefore clear, that the thick floodplain accumulations coincided with relatively quiet tectonic conditions in the source area (the Central Cordillera) and thus, probably, with a predominance of suspension-load transport. On the other hand, the absence of tectonism in the Central Cordillera does not explain the coarsening upward of the conglomerates, nor the fact that the floodplain deposits are not reworked. Miall (1980) argued that in a basin where lateral accretion deposits and floodplain deposits are formed, as is the case in sequence B, the overbank deposits will only be buried rapidly below the level of erosion and preserved intact during periods of rapid subsidence. When basin subsidence is low only the stacked coarser portions of the lateral accretion deposits will be preserved, because the finer units are planed off. Furthermore, Steel (1976) and Steel and Aasheim (1978) showed that in several Devonian basins in Norway coarsening-upward was the direct sedimentary response of the fluvial system to basin-floor subsidence. Therefore, it is likely that during deposition of sequences A and B, the S. Neiva Basin was subsiding. This subsidence could well be a response to sediment-loading, following the last phase of thrusting on the Chusma fault system. Similar sediment loading mechanisms are described by McLean and Jerzykiewicz (1978), by Beaumont (1981) and by Jordan (1981).

It is probable that subsidence of the S. Neiva Basin during deposition of sequence A and B was not very fast. In the first place, the observed coarsening upward tendency of these sequences is not very pronounced. In the second place, only 50 m of sediment were deposited between the two tuffs, found at the base of the Honda Formation. As the time interval between deposition of the tuffs averages 1.5 Ma (the minimum is 0.4 Ma), the sedimentation rate at that time was very low, the more so as few indications of reworking are found. Even allowing for variations in the sedimentation rate, it is clear that basin subsidence cannot have been very fast (table XV).

The role of volcanic activity of the Central Cordillera volcanic arc has already been mentioned above. Although volcanic deposits are found in the lower part of the Honda Formation, these deposits are much finer-grained and thinner than the volcanoclastic deposits found in the overlying Gigante Formation (chapter VII). The influence of volcanism on fluvial sedimentation was thus restricted during deposition of the Honda Formation, either because the volcanic centres were located at a very great distance from the S. Neiva Basin, or because volcanic activity was not very intense.

Photo 13. Multistory and single story channel sequences of sequence D, Q. Guandinosita section. The sandstone-mudstone ratio approximately equals 1. View of the photo is toward the N.

Photo 14. Multistoried sandstones and pebbly sandstones of sequence D, Q. Guandinosita. View of the photo is toward the S. Length of hammer is ± 30 cm.

Photo 15. Planar tabular sets in pebbly sandstones of sequence D in the Q. Guandinosita section.

Photo 16. Mottled mudstones of sequence D; Q. Guandinosita section.

Sequence C

In sequence C an upward change is recorded from small-scale fining-upward sandy channels, via a phase with pebbly lateral accretion deposits, to multistoried conglomerates showing a strong resemblance to alluvial fan deposits, described by Ramos and Sopeña (1983). These changes, reflecting increasing bed-load transport, are accompanied by a consistent increase of the fluvial channel/overbank deposit ratio. McLean and Jerzykiewicz (1978) pointed out that in the case of large-scale allocyclically controlled alternations of different facies associations, the ratio of fluvial channel to floodplain deposits may be attributed to the rate of subsidence of the depositional basin in relation to the rate of infilling. Coarsening upward sequences develop when the energy and sediment input into the system do not diminish in time, introducing coarse clastics progressively farther into the basin.

Probably, the consistent increase in the ratio of the fluvial channel/overbank deposits, the overall coarsening upward trend of the conglomerates and the predominance of very coarse orthoconglomerates in the upper part of the sequence signify major tectonic activity in the source area, *i.e.* the Central Cordillera, in combination with rapid basin subsidence. A similar situation is found in the Hornelen Basin in Norway (Steel, 1976; Steel and Aasheim, 1978) where coarsening upward of the conglomerate in conjunction with an overall increase of the amount of interbedded sandstone at the expense of the amount of mudstone resulted from simultaneous uplift of the source area and rapid basin subsidence.

The following arguments plead for uplift of the C. Cordillera and simultaneous basin subsidence during deposition of sequence C:

1. A single sample from the Manizales Pluton in the Central Cordillera (Jaramillo, 1978) gave an apatite fission track age of 10 Ma, which is much younger than the 56 Ma intrusion age of the pluton (Aspden *et al.*, 1987). It is likely that this fission track age records cooling of the apatites following uplift of the C. Cordillera.
2. The apatite fission track age of 10 Ma falls within the range of apparent apatite fission track ages of the Garzón Massif recorded in chapter II, which are interpreted as cooling ages, resulting from uplift of the massif ≥ 12 Ma ago. For this reason it is probable that uplift of the Central Cordillera also occurred 12 Ma ago.
3. The age of sequence C can be inferred from linear interpolation of the sedimentation rate, based on the age of 14.3 Ma of the upper tuff and the age of ± 8 Ma of the base of the Los Altares Member of the Gigante Formation, 150 m above the top of the Honda Formation (chapter IV, section 2). From this calculation it follows that the age of sequence C probably lies around 12 Ma.
4. On the base of cumulative subsidence curves for the Neiva Basin, Butler (1983) concluded that uplift of the Garzón Massif coincided with rapid subsidence of the basin.

Table XV. Overview of the main allocyclic controls, responsible for the sedimentological differences between the sequences A, B, C and D.

	Basin Subsidence	Uplift Central Cordillera	Uplift Garzón Massif	Volcanism
Sequence D	-	-	-	-
Sequence C	++	++	++	-
Sequence B	±	-	-	+
Sequence A	±	-	-	++

Sequence D

Sequence D, finally, is characterized by much smaller-sized channels showing little lateral migration and filled with lateral accretion deposits consisting predominantly of coarse bed-load material. It seems likely that sequence D was deposited during waning tectonic activity of the Central Cordillera. Besides, the uplifted Garzón Massif formed a barrier for the originally eastward flowing rivers and the rivers were partly deviated to a more northerly course. The low tectonic activity of the Central Cordillera resulted in less lateral migration of the channels, smaller channels and intermediate amounts of overbank deposits. Basin subsidence probably continued, as may be concluded from the coarsening upward of the conglomerates, but at a much lower pace.

The fact that sequence D of the Honda Formation is found to interfinger with the basal member of the Gigante Formation, the Neiva Member (fig. 15), which displays consistent paleocurrent directions to the N-NE and has a very different conglomerate composition, suggests that, when deposition of the Neiva Member commenced, a northward-flowing trunk river had developed due to the uplift of the Garzón Massif. Late Honda rivers joined this major river under a low angle, dumping their sediments into the main system. This is in accordance with the paleocurrent directions of sequence D, which vary between 279° and 107°.

4. 2. Climate

The deposits of the Honda Formation in the S. Neiva Basin are characterized by an abundance of mottled paleosols, the presence of fossil, sometimes silicified wood and the occurrence of fossil remains of land tortoises.

Wellman (1970) gives a summary of the literature, describing the tropical fauna and flora. Faunal and floral remains indicate that the climate during deposition of the Honda Formation was tropical wet and dry, with savanna interfluves separated by streams bordered by forests. Additional results on the N. Neiva Basin (Setoguchi and Rosenberger, 1985; Lundberg *et al.*, 1986; Cifelli and Guerrero Díaz, 1989) also give evidence of a neotropical climate with animal communities, dominated by forest to woodland-savanna forms.

On the ground of the occurrence of fresh iron-bearing minerals in the sandstones of sequence A, while the mudstones show strong altering of these minerals, Wellman (1970) is of the opinion that in the S. Neiva Basin the floodplain and the source area were subjected to intense weathering during deposition of this sequence. A tropical wet climate, however, seems to be contradicted by the presence of gypsum crystals and veins in the mudstone intervals and by the occurrence of layers of caliche. Therefore, it seems more likely that the climate of the basin itself was rather dry, while the climate of the source area, which was situated at a higher elevation, was wet. The precise influence of the climate on the sedimentation of the Honda Formation, however, remains unclear and more specific research is needed to acclarate this point.

4. 3. Paleogeographic reconstruction and interpretation of river systems

After the reconstruction of the allocyclic mechanisms that were responsible for the different modes of deposition found in the basin is made (table XV), the observed sequence of facies associations of the Honda Formation may be interpreted in terms of river systems. From the data presented above, it is clear that the Honda deposits were laid down by different alluvial fan systems which developed during periods of active volcanism or uplift, and a "high-sinuosity" river system which developed during a period of volcanic and tectonic quiescence.

It is difficult to reconstruct the former western basin boundary. According to the geological map presented by Kroonenberg and Diederix (1982), no Honda deposits are found west of the Dina Thrust, the easternmost fault of the Chusma Fault system (fig. 5). Deposits which probably belong to the underlying La Cira Formation are found solely in the center of the Tesalia Syncline, some 20 km to the WNW to the town of Gigante. Furthermore, the geological map of Butler (1983, plates A and B) indicates that only much further to the N, in the N. Neiva Basin,

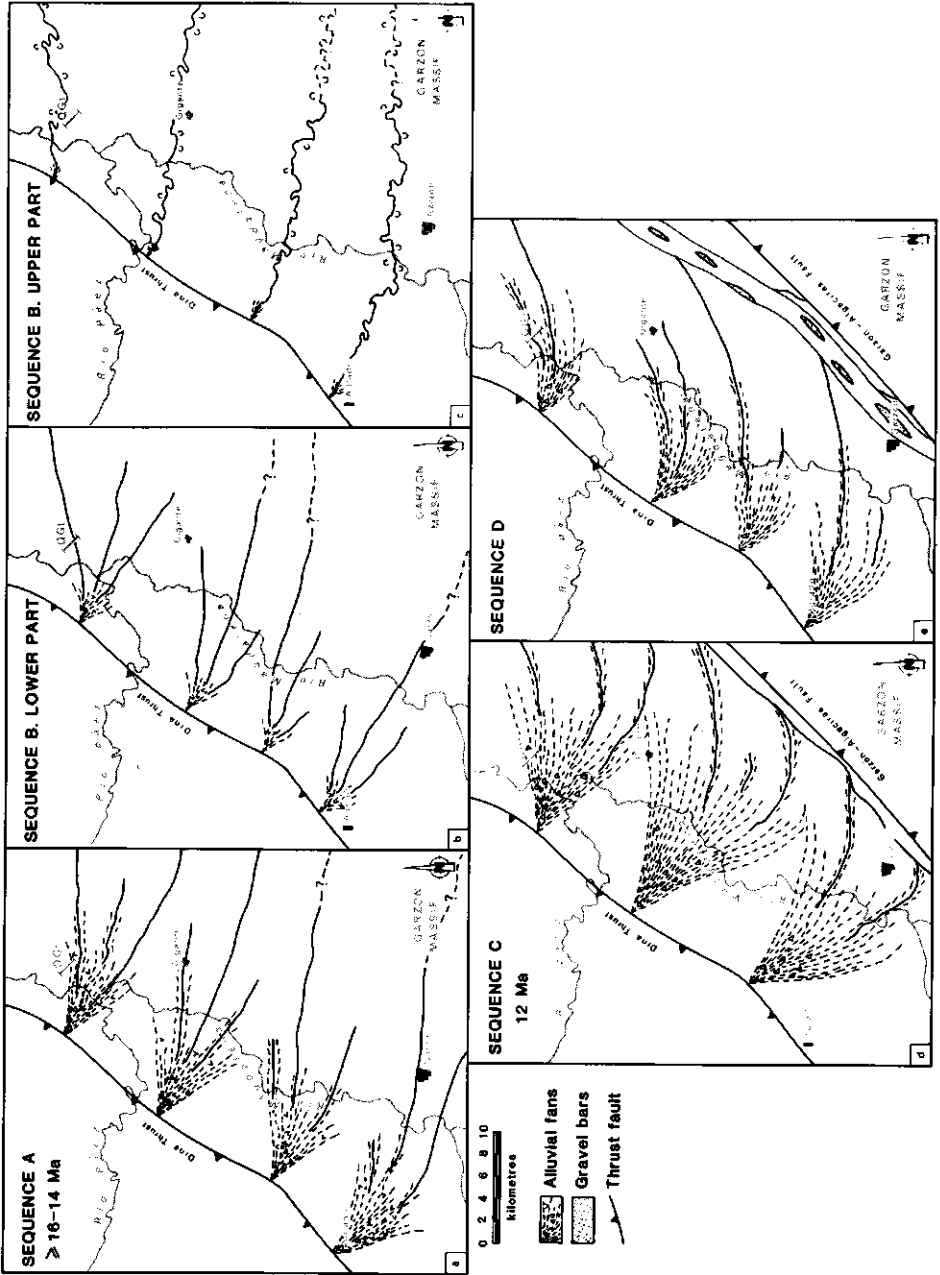


Fig. 31. Paleoenvironmental reconstruction of the Honda Formation. The Garzón-Algeciras Fault is only indicated from 12 Ma onward, when it was reactivated during Neogene uplift.

Honda deposits cover part of the Chusma Fault system unconformably. Therefore, it is assumed here that, at the latitude of the S. Neiva Basin, the former fold-and-thrust belt area, which for a great part consists of pre-Cretaceous basement rocks, formed a high at the time of the deposition of the Honda Formation. Rivers which transected this high from west to east, entered the S. Neiva Basin along the Dina Thrust.

During deposition of sequence A, tectonism played a minor role and supply of coarse clastic material was minimal. It is likely that proximally, at the western limit of the S. Neiva Basin, a small volcanic apron was present. Further basinward this volcanic apron graded into the alluvial plain (fig. 31). At the time of deposition, the Q. Guandinosita section was probably located proximally on the alluvial plain and underwent relatively little volcanic influence. Only the greatest eruptions resulted in sheetflood deposition beyond the volcanic apron s.s. and these sheetflood deposits were intercalated with alluvial plain deposits. Due to basin subsidence, the deposits were buried before they could undergo reworking.

During deposition of sequence B, volcanic activity gradually decreased and successive volcanic apron deposits did not extend very far eastward into the basin. Fluvial sedimentation in the basin was now determined by eastward flowing rivers. Braided unidirectional rivers - the distal continuation of the channels on the volcanic apron - were gradually replaced by high sinuosity rivers with pointbar deposition when volcanic activity ceased altogether.

Uplift of the Central Cordillera during deposition of sequence C led to basinward progradation of alluvial fans. Simultaneous uplift of the Garzón Massif caused rapid basin subsidence. Progressively coarser material extended ever further basinward, resulting in a coarsening upward sequence. At the site of the Q. Guandinosita section this led first to distal, and gradually to more proximal alluvial fan deposition (fig. 31). The lowest deposits of sequence C represent small low sinuosity channels on the distal fan, while the deposits in the middle of the sequence probably represent greater channels on the midfan. The highest deposits of sequence C may well represent very great channels on the upper part of the midfan or lower part of the upper fan.

During deposition of the middle part of sequence C, lateral accretion occurred as a result of lateral growth of longitudinal bars in these braided streams. Fast migration and fill of channels may have been due to frequent fluctuations in the discharge and sediment supply, resulting in strong scouring, small channels and the formation of narrow sheets and ribbons. Deposition of the upper part of sequence C resulted from rapid vertical stacking of longitudinal bars.

Sequence D, finally, was deposited during waning tectonic activity of the Central Cordillera and the Garzón Massif. Smaller fans were formed on top of the older fans. Streams on the fans still supplied large quantities of bedload material, due to erosion of the uplifted Central Cordillera. Finer material, however, must also have been transported, because renewed deposition of mudstones occurred. It is likely that the Q. Guandinosita section was located on the distal alluvial fan during deposition of sequence D, considering the fact that fine-grained and coarse-grained sediments are found in approximately equal proportions. Deposition on the distal fan took place in small stable channels which showed little lateral migration. Further to the east the alluvial plain was now bordered by the uplifted Garzón Massif. During latest Honda deposition eastward flowing Honda channels merged with the northward flowing trunk river of the Gigante Formation in the eastern part of the basin.

5. Conclusions

1. Although a small-scale cyclicity on the scale of the outcrops is found in the majority of the deposits of the Honda Formation, *i.e.* a fining upward tendency of the channel deposits resulting from autocyclic controls like lateral channel migration, migrating pointbars, avulsion etc., a large-scale first order cyclicity in the strict sense is lacking. It is true that the Honda Formation can be subdivided into several sequences on the basis of the coarsening upward trend of the conglomerates, but otherwise these sequences show different sedimentological properties like the fluvial channel/overbank deposits ratio, facies associations etc. This may be explained by different combinations and different intensities of the allocyclic controls, which were responsible for the deposition of the four sequences.

2. Two different modes of origin are distinguished for the sandstones and conglomerates of the Honda Formation. During periods of active uplift or volcanism, these sediments were deposited by different alluvial fan systems and volcanic aprons, prograding on a broad alluvial plain. During intervening periods of greater volcanic and tectonic quiescence, the alluvial fans or volcanic aprons became much reduced in size, and channel sediments were laid down by braided and meandering river systems, flowing toward the east on the alluvial plain.

Chapter VII

Sedimentation patterns of the Miocene Gigante Formation: influence of volcanism and uplift of the Garzón Massif on fluvial deposition¹

A.M. van der Wiel and G.D. van den Bergh²

1. Introduction

This chapter addresses the different allocyclic influences that played a role during deposition of the Gigante Formation. On the one hand, the influence of uplift of the Garzón Massif is assessed, on the other hand, the role of volcanic activity of the Central Cordillera volcanic arc is explored.

In recent years geologists have come to realise that very little is known of the influence of volcanism on distal sedimentation processes in fluvial basins. Although a number of publications on the subject have appeared (Mathisen and Vondra, 1983; Smith, 1987a, b) this field is still relatively unexplored. The southern Neiva Basin is well suited for such a study, because a period of low volcanic activity, resulting in the mainly fluvial deposits of the Honda Formation and the lower member (Neiva Member) of the Gigante Formation, was followed by a period of intense volcanism during which 800-950 m of distal volcanoclastics were dumped into the basin (deposition of the Los Altares Member). Comparison of the fluvial deposits and the volcanoclastic deposits of the Gigante Formation on the one hand and of the lateral variations between the volcanoclastics on the other hand leads to some new insights with respect to the depositional processes that play a role in distal settings during periods of intense volcanism and the way in which fluvial processes are disturbed by this volcanic activity.

2. Facies types and facies associations of the Gigante Formation

2. 1. Introduction

The interpretation of the stratigraphy and facies of the Gigante Formation is based on 13 sections measured throughout the region, on detailed stratigraphical and structural mapping of the study area and on a great number of paleocurrent direction measurements. The most important sections are given in figs. 17 (p. 49-52) and 18 (p. 56). The location of the sections is indicated in fig. 32 and on the geological map (appendix 1).

2. 2. Lithofacies types of the Gigante Formation

The deposits may be described in terms of lithofacies codes that are mainly based on the codes for braided river systems introduced by Miall (1977, 1978b) and Rust (1978) and partly on the codes used by Mathisen and Vondra (1983) and Smith (1987a) for volcanoclastic and volcanic

¹ Submitted in more elaborate form to the Journal of South American Earth Sciences

² Institute for Earth Sciences, University of Utrecht, Budapestlaan 4, 3508 TA Utrecht

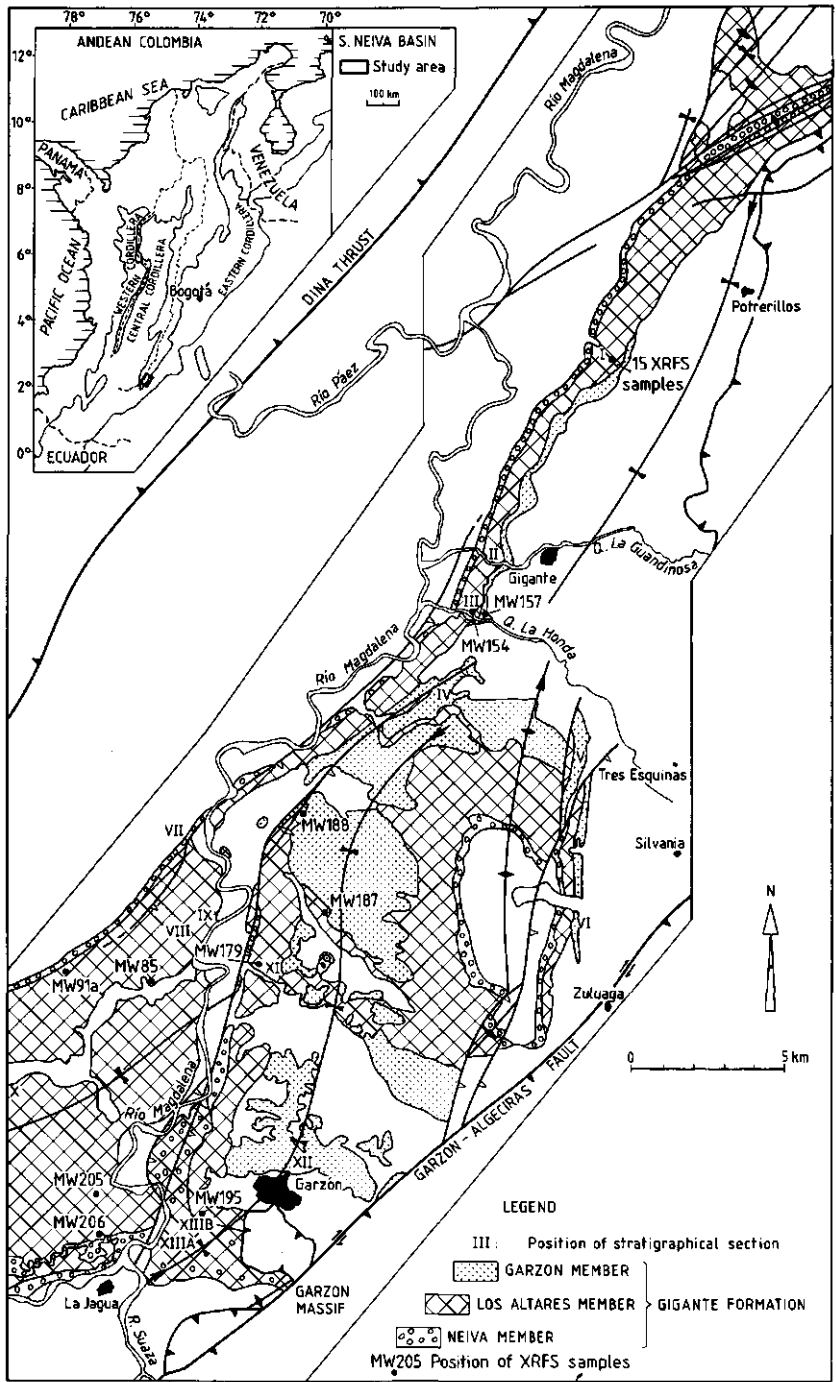


Fig. 32. Geology of the Gigante Formation, and position of stratigraphical sections and XRF samples.

deposits. The classification of the latter two kinds of deposits was slightly modified. The lithofacies codes used in the present article are given in table XVI.

2. 3. Interpretation of the data in terms of facies associations

The sediments of the three members of the Gigante Formation may be divided into six major lithofacies associations, using the lithofacies codes given above. The associations are listed in table XVII.

I. The overbank facies association

Facies of this association are Fm and Fl with minor Sh, Sl, Sr and Pp. The association is formed by mudstones, silty mudstones and siltstones. They are occasionally intercalated with usually less than 2 m thick beds of fine to medium-grained sandstones, showing climbing ripple and other types of ripple lamination, parallel lamination, trough cross-bedding and low-angle trough crossbedding. The facies association consist both of massive mud- and siltstone intervals and of thin interbedded mud, silt and sand deposits. Pieces of wood, leaf impressions, plant roots, evidence of burrowing, convolute bedding, and the presence of gypsum crystals or gypsum layers are all typical for the overbank deposits.

II. The conglomeratic fluvial channel facies association

This association is dominated by facies Gm(b) with minor Gt, Gi and Gp. Intercalated sandstone lenses and beds exhibit facies Sh, Sl, Sp and Ss. The conglomerates of this facies association are crudely horizontally stratified, or massive and clast-supported.

The conglomerates are often imbricated and occur in banks of 1-15 m separated by thin lenses of horizontally bedded or low-angle cross-bedded sand (photos 17a, b, c, p. 113). In some places the sand intercalations show solitary or grouped planar cross-beds. Clasts are generally well rounded and moderately sorted. Maximum clast size varies from medium gravel to boulders (photo 18, p. 113).

The conglomerates mostly occur in multi-storied sequences up to 40 m thick. These sequences usually have sharp, flat basal contacts with the underlying sediments, but internally the contacts are scouring. Channel depths vary between 1 and 15 m (photo 17b); channel widths are maximally one hundred meters for the greatest conglomeratic channels.

The horizontally bedded or massive, often imbricated conglomerates (facies Gm(b)) may be interpreted as superimposed longitudinal bars which are separated by reactivation surfaces and originated during high stage flow (Rust, 1975, 1978; Boothroyd and Ashley, 1975; Miall 1977, 1978b), while the intercalated horizontally bedded thin sandstones (Sh) represent deposition during waning flow conditions.

III. The sandy channel facies association

This facies association may be subdivided into two subassociations, which will be described separately.

IIIa. A subassociation dominated by Sp and St

Facies Sp and St are dominant in this subassociation, while facies Sh, Sl, Ss and Gm(b) occur less frequently. Facies Gm(b) is found as channel lag at the base of the pebbly sandstone bodies. These pebbly sandstones often fine upward to medium sand, exhibiting planar cross-bedding, trough cross-bedding or horizontal lamination (photo 19). The conglomeratic base of the sandbodies may contain silt or clay intraclasts. The beds usually have scouring basal contacts with underlying deposits. They vary in thickness from 0.5-7.5 m.

Facies Sp is formed by migration of transverse or linguoid bars in shallow water under lower-flow conditions (Smith, 1970), while facies St is formed by sinuous-crested dunes under lower-flow conditions (Harms and Fahnestock, 1965).

IIIb. A subassociation dominated by Sh and Sl

In this subassociation facies Sh and Sl are dominant, while facies Sp, St, Sr and Gm(b) form

Table XVI. Lithofacies of the Gigante Formation.

Faciescode	Lithofacies	Sedimentary structures	Interpretation
Gms ^a	Gravel, massive, matrix supported, very poorly sorted; clasts may be angular to rounded	None, normal or reverse grading (often coarse-tail grading)	Debris flows and mudflows
Gm(b) ^c	Gravel, massive or crudely bedded, clast supported	Horizontal bedding, gravel imbrication	Channel lag, longitudinal bars
Gm(a) ^c	Gravel, massive, abundant sand matrix, largely clast support, poorly sorted, subangular to rounded clasts	No imbrication	Coarse grained hyper-concentrated flow deposits; rapid deposition both from suspension and by traction
Gi ^a	Gravel, stratified	Large-scale trough cross-beds	Channel fill
Gi ^c	Gravel, stratified	Low-angle (5-20°) inclined stratification; sets to 6 m thick	Lateral accretion surfaces
Si ^a	Sand, medium to very coarse, may be pebbly	Trough cross-beds, single or grouped	Dunes (lower flow regime)
Sp ^a	Sand, medium to very coarse, may be pebbly	Planar tabular cross-beds, single or grouped	Transverse bars, sand waves (lower flow regime)
Sl ^a	Sand, fine to coarse	Low-angle (<10°) cross-beds	Scour fills, antidunes
Sr ^a	Sand, very fine- to medium-grained	Ripple marks and ripple cross-lamination of all types	Ripples: bar-top, secondary channel flood plain (lower flow regime)
Ss ^a	Sand, fine to coarse, may be pebbly, may contain intraclasts	Broad, shallow scours, including eta cross-stratification	Scour fills
Sh ^a	Sand, medium to very coarse, may be pebbly	Parallel lamination, plane bedding	Planar bed flow (lower and upper flow regime)
Sh(g)	Silt, sand, very fine to very coarse, may be pebbly, may contain pumice-pebble streaks	Plane bedding and very low angle (<10°) bedding, normally graded may fine upward to silt	Hyperconcentrated flow; long-wavelength dunes
Sh(m) ^c	Sand, fine- to very coarse, may be pebbly	Parallel strata (0.5-5 m thick), laterally discontinuous over 1-5 m, gradational contacts between coarse and fine strata	Planar bed flow (upper flow regime), sheetflood deposits
Fl ^a	Sand (very fine to fine), silt, mud	Ripple marks, plane lamination, convolute bedding, burrows, plant rootlets, leaf impressions	Deposit of waning floods, overbank deposits
Fm ^a	Silt, clay	Massive	Overbank or drape deposits
Pp ^b	Mottling in sand, silt or mud, clay ironstones	Pedogenic features	Paleosol
Tms ^b	Tuff-breccia, massive, matrix supported	May show normal grading of lithics and reverse grading of pumice	Pyroclastic flow (ignimbrite)
Ta ^c	Tuff, well sorted	Massive or horizontal bedding, may show evidence of burrowing or root disturbance	Pyroclastic fall (airfall tuff)
Tr ^b	Tuff, well sorted, may be clayey	Massive or (cross-)stratified	Reworked tuff

^a After Miall (1977, 1978b)

^b After Mathisen and Vondra (1983)

^c After Smith (1987)

minor facies. Channel sequences of 10-13 m are most common. Individual beds are between 1-6 m thick. The greatest sandy channel encountered had a width of over 100 m (photo 20, p. 114). The sandbodies may have convex downward, scouring basal contacts, or flat non-scouring

bases; loadcasts are occasionally present. The medium to very coarse sand is poorly rounded and poorly to moderately sorted. Pebbles are present as channel lags (facies Gm(b)), as thin pebble stringers, or scattered throughout the sand. Pebbly sandstones are common. The widespread occurrence of facies Sh and Sl indicates that deposition took place under shallow upper-flow regime conditions, Sh being deposited as horizontally bedded sand and Sl as shallow scour fills (McKee *et al.*, 1967; Miall, 1978b; Rust, 1978).

IV. The sandy unconfined facies association

This facies association is characterized by facies Sh(m), Sh and Sl. The deposits show rapid alternations of discontinuous layers of horizontally stratified to crudely horizontally bedded and very low-angle cross-bedded sandstone and pebbly sandstones. The coarser layers may consist either of very coarse to pebbly sandstone or of conglomerate. The finer layers are mostly medium to very coarse sand. The deposits have non-erosional basal contacts; internal contacts are usually not very erosive either. Individual layers vary between 1 to 13 m in thickness and extent laterally over hundreds of meters. No consistent grading is found in the deposits. Bedding is visible due to segregation of granule-rich and sand-rich horizons (photo 21, p. 114). This segregation is due to deposition under upper-flow regime conditions (Blair, 1987).

The great lateral extent and lack of scouring basal contacts with underlying deposits as well as the great similarity to sheetflood deposits on alluvial fans (Bull, 1972; Nilsen, 1982) indicates that the sediments were deposited by unconfined or broadly confined sheetfloods under upper-flow conditions in very shallow water.

V. The debris flow and hyperconcentrated flow facies association

This facies association comprises debris flow deposits (facies Gms) and intercalated hyperconcentrated flow deposits (Gm(a) and Sh(g)).

The debris flow deposits consist of massive matrix-supported conglomerates which are ungraded, or exhibit normal grading or reverse grading. Grading is often of the coarse-tail type. The maximum size of the majority of the clasts is 5-25 cm, but outsize boulders up to 2.5 m in diameter are also present. The clasts are angular to subrounded and may consist almost entirely of dacite and andesite fragments. However, some very polymict debris flow deposits were found containing up to 48% of Palaeozoic schist fragments. The deposits usually have sharp planar basal contacts. Sometimes these contacts are irregular and scour underlying sediments.

Most debris flow deposits have a limited thickness of 1-2 m, but some very thick debris flows

Table XVII. Lithofacies associations of the Gigante Formation.

Facies ass.	Dominant facies	Minor facies	Interpretation
I	Fm, Fl	Sh, Sl, Sr, Pp	Overbank deposits
II	Gm(b), Sl deposits	Gi, Gt, Sh, Sp, Ss	Conglomeratic fluvial channel
IIIa	Sp, St, Gm(b)	Sh, Sl, Ss	Sandy fluvial channel deposits (lower-flow regime)
IIIb	Sh, Sl	Sp, St, Sr	Sandy fluvial channel deposits (upper-flow regime)
IV	Sh(m), Sh, Sl		Unconfined sheetflood deposits
V	Gms, Sh(g)	Gm(a)	Debris flow and hyperconcentrated flow deposits
VI	Tms	Ta, Tr, Sh, Sl	Ignimbrites and air-fall tuffs

of over 17 m were also encountered (photo 23a, b, p. 116). Often, the debris flow deposits are found associated with deposits of hyperconcentrated flows (facies Sh(g) and Gm(a)), in some places in single-story couplets, at other locations in multi-story sequences up to 70 m thick. In the latter case both sandy and gravelly hyperconcentrated flow deposits may be present. The sandy hyperconcentrated flow deposits have thicknesses varying between <1-1.7 m and the gravelly deposits occur in beds up to 3 m thick. The sandy hyperconcentrated flow deposits are usually normally graded and the thinnest deposits (≤ 1 m) often fine upwards to a silt-rich top. Similar deposits have been described by Ballance (1984) as subaqueous sediment gravity flow deposits and were reinterpreted by Smith (1986) as resulting from rapid deposition of hyperconcentrated flows under conditions of waning flow energy. The top of the hyperconcentrated flow deposits may be pumice-enriched. Thin pumice or gravel lenses are often present at various levels in the deposits, as has been described by Pierson and Scott (1985; see also photo 23c). The sandy deposits show a faint horizontal stratification while the gravels (facies Gm) are massive. Both sandy and gravelly deposits contain little matrix. Sorting of the sandy deposits and the gravels is poor. Basal contacts of both sandy and gravelly deposits are mostly planar and the deposits generally extend over several hundreds of meters.

VI. The ignimbrite and air-fall tuff facies association

This facies association comprises the facies Tms, Ta and Tr. Facies Tms consists of massive matrix supported tuffs and tuff breccias resulting from deposition from pyroclastic flows (ignimbrites). Most deposits have thicknesses of ± 1 m with some exceptions that are up to 4.5 m thick. The deposits have planar, non-scouring bases and consist of pumice clasts with a maximum size of 40 cm and up to 5 cm big rock fragments in a matrix of dacitic glass. None of the ignimbrites was found to be welded.

The majority of the ignimbrites is completely undifferentiated, and pumice clasts and lithic fragments are evenly distributed over the whole lithosome. In some fine-grained deposits well sorted and well rounded pumice pebbles were found in laterally discontinuous lenses and the breccias showed a crude bedding. Most ignimbrites are strongly enriched in lithics. Most lithics are of comagmatic origin, but xenoliths are found as well. In thin section it is visible that the deposits are often crystal-enriched and somewhat fines-depleted.

Only at one location (photo 22, p. 114) three successive tuffs were found that show a clear differentiation in a basal layer, a lithic concentration zone (LCZ) at the base of the main body, and a pumice concentration zone (PCZ) at the top of the main body of the deposit (Sparks *et al.*, 1973; Freundt and Schmincke, 1986; see also fig. 40, chapter X). No surge deposits or dust layers were encountered.

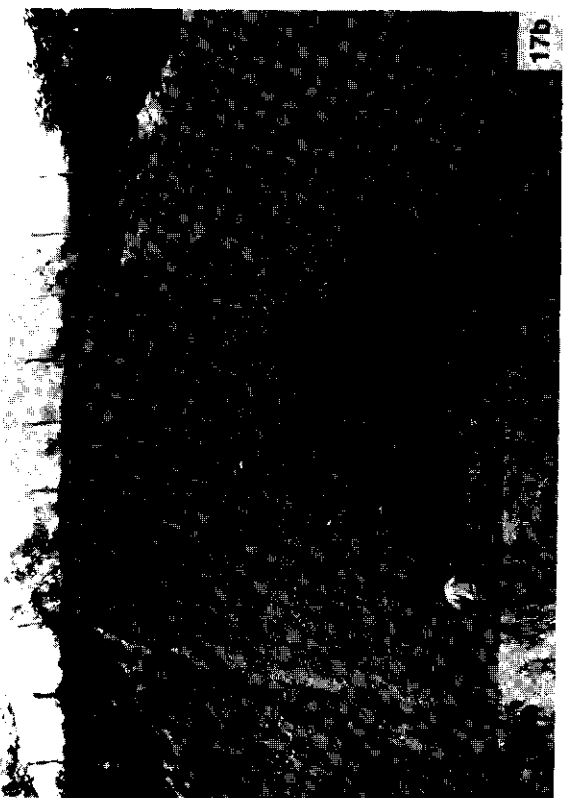
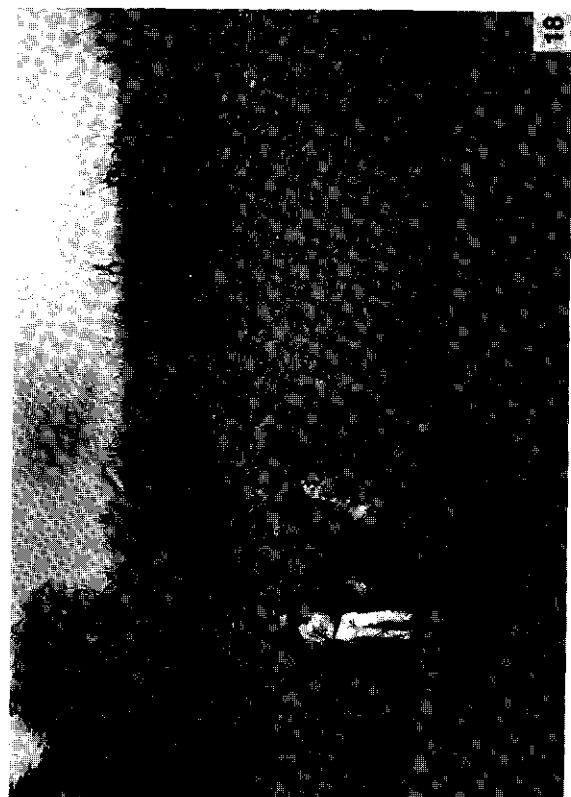
Ta, the air-fall tuff facies, consists of fine-grained crudely horizontally stratified tuff with alternating layers of pumice clasts and phenocrysts, while Tr, the reworked air-fall tuff facies, consists of cross-bedded or low-angle cross-bedded tuff.

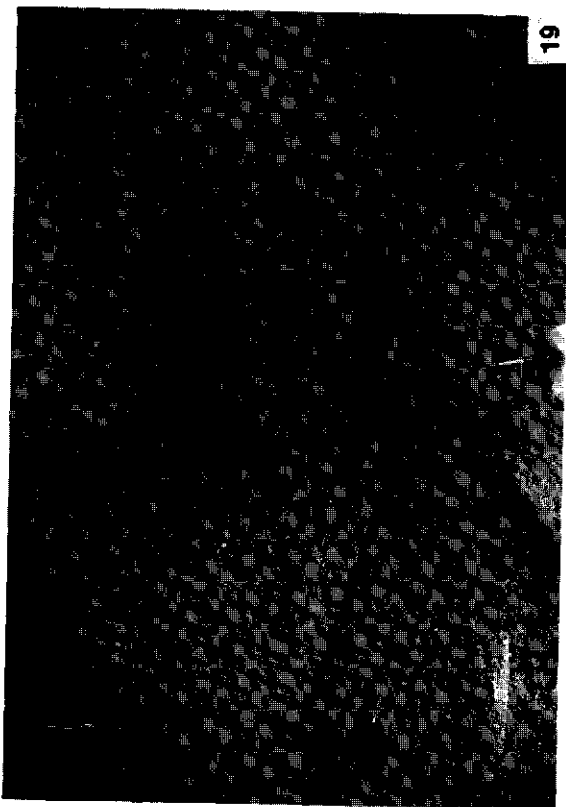
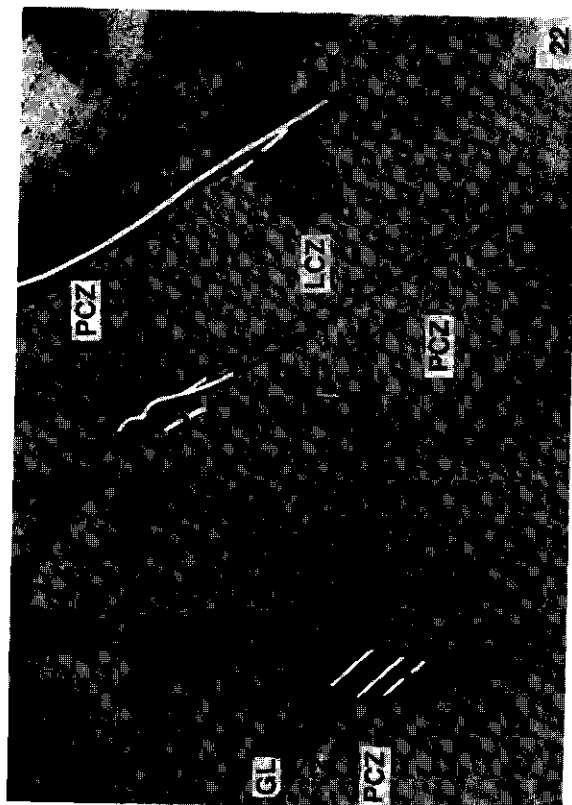
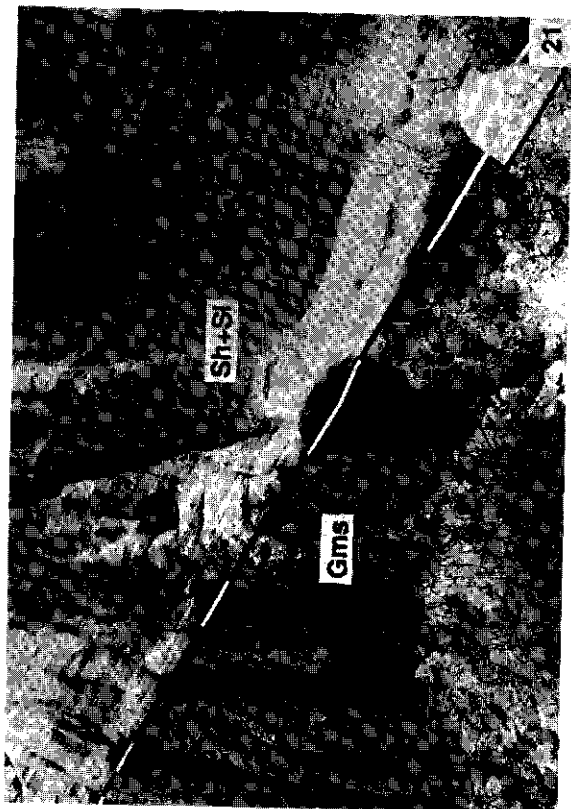
3. Depositional environments

In this section, the deposits of the Gigante Formation are described in terms of the six different facies associations given above. The depositional environments of the three members will be reconstructed with the aid of these facies associations and measured paleocurrent directions.

Photo 17. Examples of the fluvial channel facies association. Photo 17a. Imbricated conglomerates of facies Gm(b) and intercalated sandstone lenses of facies Sh in the Los Altares Member, Q. La Honda section. View of the photo is toward the NNE. Length of hammer is ± 30 cm. Photo 17b. A ± 15 m thick channel deposit in the Neiva Member, near the confluence of the Magdalena and Suaza Rivers. View of the photo is toward the E. Photo 17c. Alternating layers of plane-bedded sandstone and conglomerate in the Neiva Member, Q. Guandinosita section. View of the photo is toward the S.

Photo 18. Outsized andesite clast of ± 2.5 m in a conglomerate, belonging to the fluvial channel facies association. Garzón Member. Photo was taken along the road from Río Loro to Gigante. View of the photo is toward the NW.





3. 1. Paleocurrent directions

Fig. 33 shows the paleocurrent directions measured in the Gigante Formation. Both pebble imbrication measurements (dip of the ab-plane) and measurements on planar and trough cross-bedding were performed. The Neiva and Garzón Members show paleocurrent directions to the north, while the paleocurrent directions measured in the Los Altares Member fan outward from a number of centres in an eastward direction. In the Neiva and Garzón Members the observed variance in paleocurrent directions between beds was very low. The northward paleocurrent directions of the Neiva Member are in contrast to eastward directions presented by Howe (1974). In order to test whether our data were correct, we measured paleocurrent directions for a second time, but the extra data confirmed the northward directions of the Neiva Member.

Table XVIII. Abundances of facies associations of the different members of the Gigante Formation.

Member	Dominant facies associations	Minor facies associations
Neiva	II	I, IIIa, b
Los Altares	Dependent on distality of section: I, IIIb, IV, V	II, VI
Garzón	II, IV I, IIIa, V, VI	

3. 2. Depositional environment of the Neiva Member

Description

The member is characterized by the conglomeratic fluvial channel facies association (II), the sandy channel facies association (IIIa,b) and the overbank facies association (see table XVIII).

Howe (1974) remarked with regard to the Neiva Member deposits that the internal sequence of facies within the lithological units varies greatly. A lack of cyclicity prevails and it is impossible to trace any single unit throughout the basin. Although this is true, it appears that the ratio overbank deposits/sandy channel deposits/gravelly channel deposits remains very constant throughout the basin (table XIX), if one assumes that the unexposed parts of the stratigraphical columns represent overbank deposits.

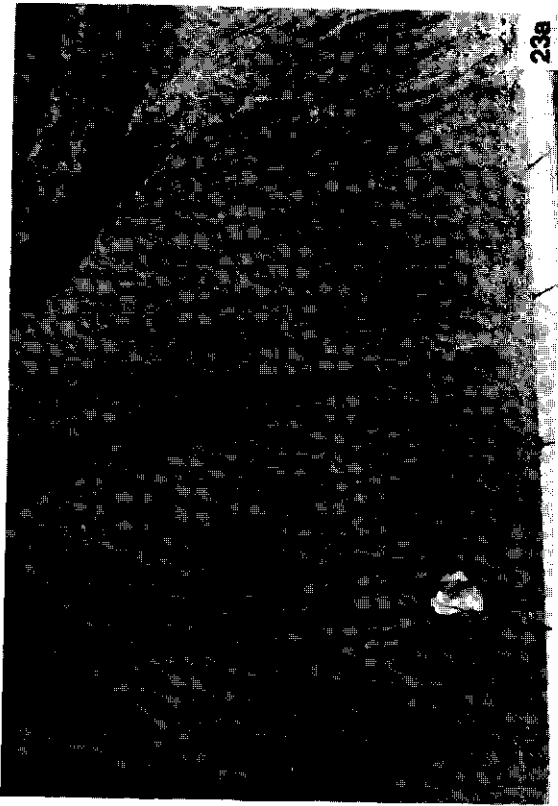
Thick sequences of massive, often imbricated multi-storied conglomerates alternate with units of floodplain deposits and sequences of intercalated conglomerates and sandstones, belonging to both sandy fluvial channel facies subassociations. Channel depths of the conglomerates vary between 1-15 m (photo 17b); channel widths are maximally one hundred meters for the greatest conglomeratic channels. The maximum and average clast size of the conglomerates decrease in a S-N direction (table XIX). The mudstone intervals of the Neiva Member are often poorly exposed or covered altogether. The mudstones have a red-brown color without mottles; paleosol development is lacking.

Photo 19. Trough cross-bedding in pebbly sandstones and sandstones of the Garzón Member in the Q. La Honda section. The deposits belong to facies subassociation IIIa. View of the photo is toward the NNW. Length of hammer is ± 30 cm.

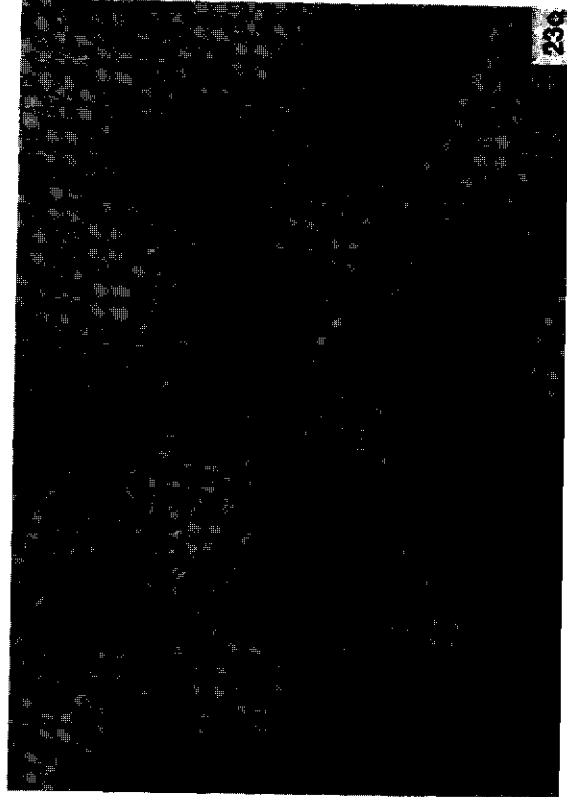
Photo 20. Very large channel in the Los Altares Member, filled with horizontally bedded deposits belonging to subassociation. IIIb. Q. Guandinosita section. View of the photo is toward the ENE. Man, when seated, is ± 1.20 m tall.

Photo 21. Debris flow deposit of facies association V, overlain by an unconfined sheetflood deposit of facies association IV. Los Altares Member, Q. Guandinosita section. View of the photo is toward the NE.

Photo 22. Three superimposed ignimbrite deposits showing a clear differentiation into a ground layer (GL) and a main body with a Lithic Concentration Zone (LCZ) at the base and a Pumice Concentration Zone (PCZ) at the top. Q. La Honda section. View of the photo is toward the N.



23a



23b

Interpretation

The high portion of horizontally bedded and imbricated gravel, the lack of debris flow and hyperconcentrated flow deposits, the consistent paleocurrent directions to the N, and the diminution of the maximum and average pebble size of the conglomerates in a south-north direction (table XIX) suggest deposition by a north-flowing proximal braided river system. The river system responsible for the deposition of the Neiva Member has characteristics of both gravelly and sandy braided river systems described in the literature (Rust, 1975, 1978; Boothroyd and Ashley, 1975, Cant, 1978). The occurrence of sandy, gravelly and overbank deposits points to deposition by a mixed-load river (terminology after Schumm, 1968).

The sudden coarsening upward of the Neiva Member with regard to the underlying Honda Formation suggests that the braided river system developed as a result of uplift in the source area, *i.e.* the Central Cordillera. The northward paleocurrent directions and the diminution of the material to the N suggest that especially the southern part of the Central Cordillera was uplifted, possibly the area where this cordillera merges with the Eastern Cordillera. This area consists mainly of Triassic/Jurassic volcanics and intrusives, which agrees with the composition of the Neiva conglomerates. Some additional erosional material, however, must have come from the part of the Central Cordillera bordering the S. Neiva Basin to the W. It is likely that this material was deposited by channels on alluvial fans and/or by tributaries of the N-flowing braided river system, that joined this latter system under a low angle.

The relatively high portion of overbank deposits may be accounted for by assuming that infilling of the basin kept pace with subsidence and compaction, resulting in preservation of the channel deposits and part of the overbank deposits. This is in accordance with the lack of pedogenic features in the floodplain deposits, suggesting that vertical aggradation was rapid and constant: no indications are found for periods of non-deposition.

Formerly, thick intercalations of overbank deposits were thought to be unusual in the braided environment. However, it has been shown by several authors that a high share of overbank deposits is not necessarily related to high-sinuosity systems, but is dependent on climatic and orogenic factors (Schumm, 1968; Baker, 1978; Friend, 1978; McLean and Jerzykiewicz, 1978; Bridge and Leeder, 1979).

Table XIX. Ratio of gravelly channel deposits, sandy channel deposits and overbank deposits, as well as maximum clast size of the conglomerates in different sections of the Neiva Member.

Section	Overbank Deposits	Sandy Deposits	Gravel Deposits	ϕ average congl. (cm)	ϕ max. congl. (cm)
Q. Las Damas	29.8	27.1	43.1	18.1	45
Cuchilla del Tigre	31.9	28.8	39.3	19.3	25
Q. La Guandinosita	24.7	29.3	46.0	15.2	30
Q. Guandinosita	27.4	29.8	42.8	13.1	30

Photo 23. Photographs of deposits belonging to facies association V. Photo 23a. Very thick, multi-storied sequence of debris flow deposits in the Q. Guandinosita. Man is ± 1.80 tall. Photo 23b. Detail of a plane-bedded sandstone intercalation in the debris flow deposits. Possible explanations for the origin of this layer are given in chapter III, section 2.4. Length of hammer is ± 30 cm. Photo 23c. Crude horizontal stratification with pumice streaks in the Los Altares Member, Q. Guandinosita section. View of all photos is toward the NNE.

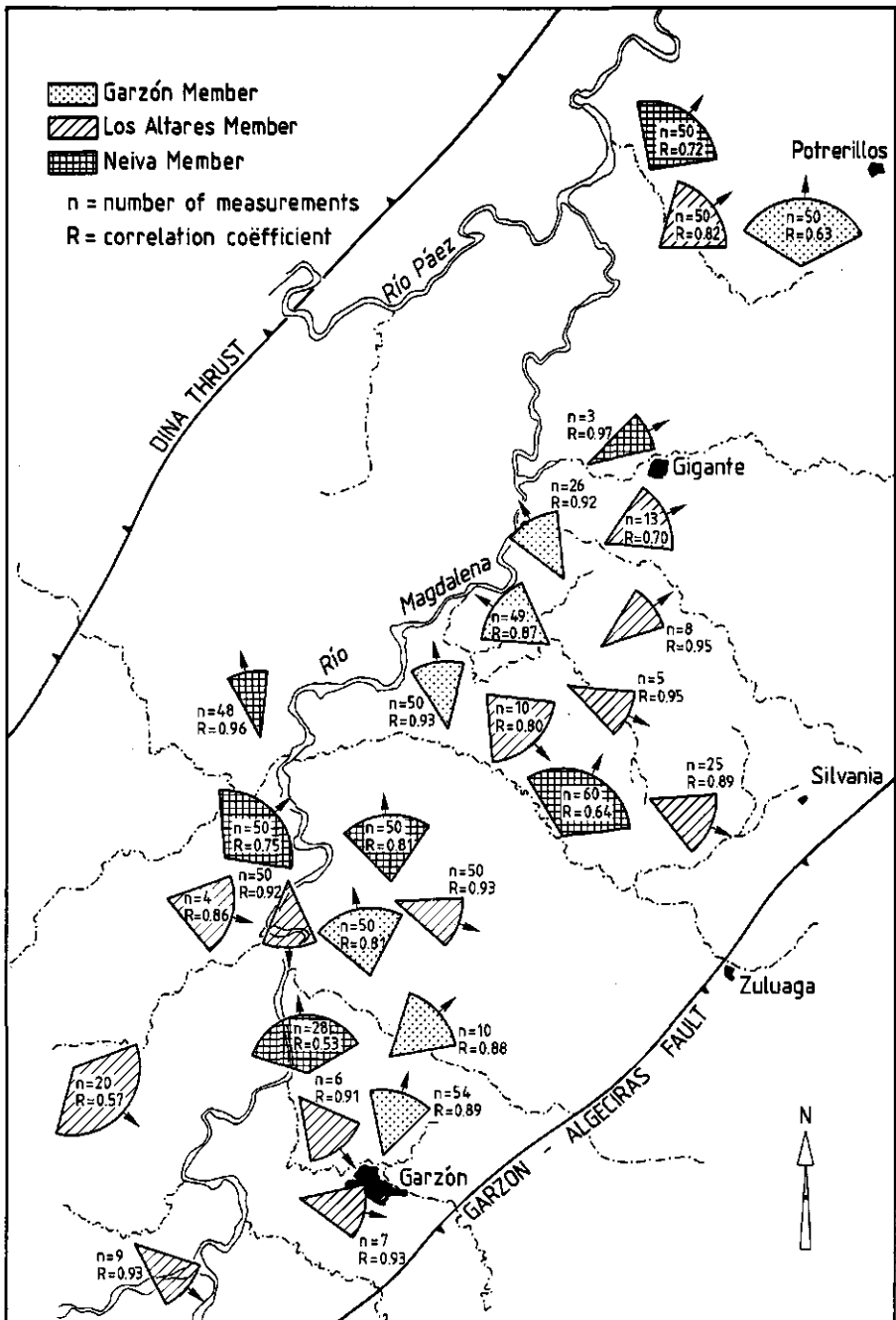


Fig. 33. Paleocurrent directions of the Gigante Formation. Pebble imbrication measurements can be recognized by the greater number of measurements ($20 \leq n \leq 50$); foreset measurements by a much lower number of measurements ($4 \leq n \leq 13$). The width of the fans equals $2s$ (in degrees).

3. 3. Depositional environment of the Los Altares Member

Description

The relative abundances of the different facies associations found in this member are dependent on the position of the stratigraphical section within the basin. In fact, all facies associations are present in variable proportions (table XVIII). Although most sandstone and conglomerate banks seem to form resistant, laterally extensive sheets that vary little in thickness, and many of the individual banks can be followed over several hundreds of meters in scarp facies of hogbacks along strike, Van Houten and Travis (1968) already noted that these banks are in fact composed of "complexly lensing deposits". The lack of marker beds makes it difficult to correlate the different sections.

In the Q. Guandinosita section, the debris flow and hyperconcentrated flow facies association (V) and the sandy unconfined facies association (IV) are dominant. Further to the SE both the sandy unconfined facies association (IV) and the sandy channel facies subassociation IIIb are important, while the amount of overbank deposits (I) increases.

In the lower part of the Q. Guandinosita section, several thick series of superimposed volcanic debris flow deposits (photo 23a) are present. In the middle part of the section, debris flow deposits are found associated with deposits of hyperconcentrated flows (facies Sh(g) and Gm(a)) in multi-story sequences up to 70 m thick. Some of the gravels of facies Gm(a) consist entirely of one or two angular clast types (andesite and/or dacite), contain very little matrix and are well sorted. These gravels are described by Howe (1969) as volcanic pebbles and may have been deposited by grain flows.

In the upper part of the Q. Guandinosita section and in the Quebrada La Honda section, single-story units of debris flow deposits, with or without related hyperconcentrated flow deposits are present; multi-story sequences are lacking.

In the Q. Guandinosita section mudstones are very scarce. The thickness of the mudstone intervals varies between 1-6 m. In the Quebrada La Honda, on the other hand, mudstones make up 26% of the total section. In the lower part of the Los Altares Member the mudstones have a red-brown colour without mottles. Higher up in the member they are usually greyish-white. Few paleosols are developed in the mudstones.

Conglomerates, belonging to facies Gm(b) of the fluvial facies association are mostly found in relatively thin multi-story sequences of 10 m or less in the lower part of the Q. Guandinosita section. The thickness of the beds varies between 2 and 8 m, and the basal contacts are mostly planar or slightly scouring. In some of the more southerly sections (e.g. the Q. Jagualito section, fig. 17, p. 52) thick multi-storied conglomeratic sequences of up to 25 m are present. These sequences often exhibit scouring basal contacts. Individual beds have maximum thickness of 8.5 m and the clasts may be larger than the clasts in the northerly sections, the maximum clast size being 80 cm.

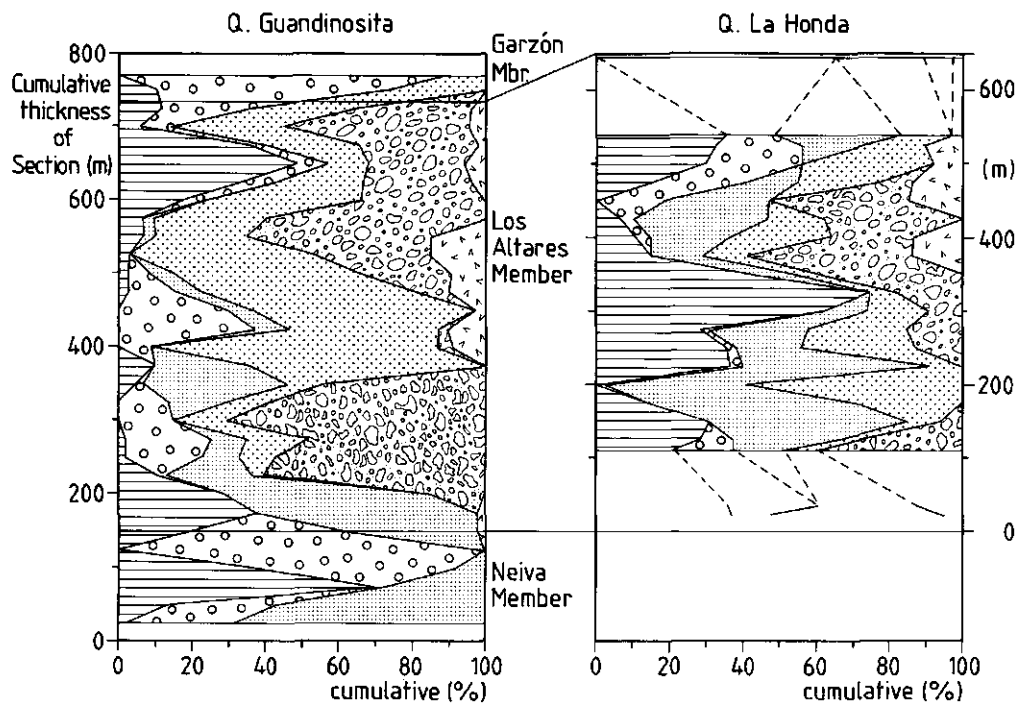
Both in the Q. Guandinosita and the Q. La Honda, thin ignimbrites, airfall tuffs and reworked air-fall tuffs are found scattered throughout the upper part of the Los Altares Member.

Interpretation

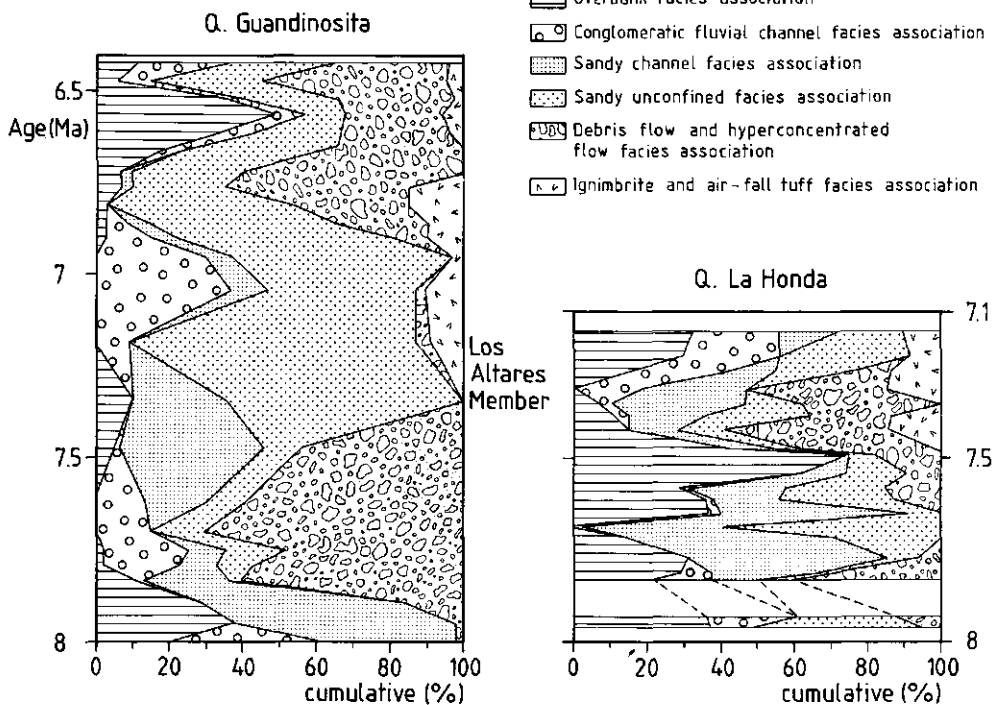
The fanning paleocurrent directions, the predominance of debris flow and hyperconcentrated flow deposits, and the widespread occurrence of facies Sh and Sl, both in sandy channels and as unconfined sheetflood deposits, point to alluvial fan deposition. Also, the great variations between the different stratigraphical sections, both with respect to relative abundances of facies associations and with respect to overall grain size, and the fact that individual banks cannot be correlated from one section to another are typical characteristics of alluvial fan deposits (Bull, 1972; Nilsen, 1982). The volcanic pebbles associated with the debris-flow deposits may perhaps be interpreted as sieve-lobe deposits.

When the relative abundances of the facies associations found in the Quebrada Guandinosita and Q. La Honda sections are plotted against the position within the stratigraphy (fig. 34, above) the differences between the sections are clearly visible. From the figure it may be concluded that the Q. Guandinosita section was deposited on the more proximal part of an alluvial fan because it is dominated by sediments from the debris flow and hyperconcentrated flow facies association, by a greater amount of conglomeratic channels and by unconfined sheetflood deposits. The Q. La Honda deposits were deposited more distally, as is indicated by the higher amount of overbank deposits and the lack of debris flow deposits (Bull, 1972; Nilsen, 1982). A comparison of fig. 34 (above) with the Hornelen Basin in Norway (Gloppen and Steel, 1981) suggests that the deposits of the Q. Guandinosita were laid down in middle fan reaches, while the sediments of the Q. La Honda were deposited in a distal fan setting.

The very high percentage of fresh volcanic matter, both in the conglomerates and the sandstones (chapter V) points to a volcanic origin of the material aggrading on these fans, i.e. to deposition



- Overbank facies association
- Conglomeratic fluvial channel facies association
- Sandy channel facies association
- Sandy unconfined facies association
- Debris flow and hyperconcentrated flow facies association
- Ignimbrite and air-fall tuff facies association



on volcanic aprons resulting directly from volcanic eruptions or from mobilization of loose volcanic debris on the slopes of the volcanoes as a result of heavy rainfall.

No consistent differences in mineralogical composition were found to exist between volcanoclastic sandstones from the sandy fluvial channel infills of subassociation IIIb and the sheetflood deposits. Blair (1987) describes sheetflood deposits of the Roaring River Alluvial Fan in Colorado that are unconfined in proximal reaches but become rechannelized distally. The proximal deposits consist of sand and pebbly sand in (discontinuous) horizontal or slightly inclined beds in which granule-rich and sand-rich horizons are segregated, due to deposition under upper-flow regime conditions. The distal rechannelized deposits show vertically and laterally varying sets of trough-cross-bedded, ripple-bedded and planar-cross-bedded sand and pebbly sand deposited under lower-flow regime conditions.

Although the sandy channel deposits of the Los Altares Member show relatively greater amounts of facies Sh and Sl than the Roaring River fan, it is likely that a mechanism of partial rechannelization played a role here also. This would explain the similarities between the channel sandstones and the unconfined sandstone deposits: both types of sandstones are, in fact, sheetflood deposits, but the first type was rechannelized and the second type was deposited unconfined. Furthermore, it would explain the predominance of unconfined sheetflood deposits in the Q. Guandinosita section, located on the midfan and the approximately equal proportions of unconfined and rechannelized sheetflood deposits in the Q. La Honda section, which was deposited on a more distal part of an apron, where partial rechannelization had taken place (fig. 35).

An explanation for the difference in distality may be that the Q. Guandinosita section is located much nearer to the Dina Thrust, the easternmost fault of the Chusma fault system than the Q. La Honda section (figs. 32, 35). This fault forms the western boundary of the S. Neiva Basin (chapter VI, section 4.3). Along the fault the Honda Formation, underlying the Gigante Formation, is juxtaposed against the Jurassic Saldaña Formation. As the Saldaña Formation is far more resistant to erosion than the Honda Formation, it is likely that a high was present at the east side of the fault. The Los Altares rivers may then have entered the S. Neiva Basin at re-entrants along the fault, forming volcanic aprons at those points (fig. 35).

Nonmarine volcanoclastic sedimentation is characterized by the rapid production of vast volumes of easily erodible material over irregular time intervals combined with nonuniform rates of sediment erosion (Vessell and Davies, 1981). It seems likely that in the northern part of the basin some of the events resulting in the deposition of the Los Altares Member produced sufficiently great quantities of sediment to force the northflowing trunk river, the ancestral Magdalena River, to flow close to the Garzón-Algeciras Fault which delimits the basin from the Garzón Massif (fig. 35). Unfortunately this cannot be checked, because the area directly west of the fault is nowadays covered by younger sediments. Further west, however, in the surroundings of Gigante, the deposits of the Los Altares Member are coarse-grained and proximal and no interfingering of volcanoclastic deposits with "Neiva"-type conglomerates is found above the contact between the two members, suggesting that the paleo-Magdalena river probably flowed further to the east.

In a stratigraphical column from the S of the basin (Quebrada las Damas), interfingering of the Neiva and Altares Members is found up to 500 m above the base of the Neiva Member. In this part of the basin the volcanoclastic deposits of the Los Altares member are much thinner and finer-grained. Deposition took place by sheetfloods and floodplain aggradation on the distal parts of the volcanic aprons grading into the alluvial plain (fig. 17, p. 52). During deposition of the Los Altares Member volcanism had little influence on the sedimentation processes at this location and "Neiva"-type conglomerates were deposited by the major trunk river (fig. 35).

Fig. 34, above. Cumulative percentages of the different facies associations found in the Gigante Formation, plotted against the position within the stratigraphical column. Percentages were calculated over 50 m intervals of the stratigraphical sections and plotted in the middle of the interval. For each subsequent calculation an overlap of 25 m with the underlying interval was taken. Fig. 34, below. Cumulative percentages of the facies associations of the Gigante Formation plotted against interpolated ages.

In the middle of the basin the contact between the two members is poorly exposed, but interfingering is found some km west of the Garzón-Algeciras Fault, indicating that the paleo-Magdalena river here also flowed close to the Garzón Massif during deposition of the Los Altares Member. Further to the W fine-grained volcanoclastic multi-storied sheetflood deposits are found intercalated with conglomeratic fluvial channel deposits and overbank deposits (fig. 17, p. 51-52, section Río Magdalena, section Q. Jagualito). The channel deposits probably represent channels on the distal parts of the volcanic aprons grading into the alluvial plain. Grain size of the deposits is intermediate between the coarse-grained deposits found in the Q. Guandinosita and the fine-grained deposits in the south.

3. 4. *Depositional environment of the Garzón Member*

Description

Like the Neiva Member, this member is characterized predominantly by the conglomeratic fluvial channel facies association (II) and by sheetflood deposits of association IV (table XVIII).

The conglomerates of the Garzón Member contain coarser clasts than the those of the underlying members; in one instance even a boulder of 2.5 m in diameter was found (photo 18, p. 113). Most clasts, however, have a longest axis of less than 50 cm. The conglomerates occur in multi-story sequences up to 40 m thick. The maximum thickness of the individual beds is 15 m. Deposits of the fluvial channel facies association are found to alternate with deposits of the sheetflood facies association. The latter deposits are characterized by horizontally bedded or low-angle cross-bedded blue-grey sandstone beds consisting almost entirely of andesitic and dacitic volcanic fragments.

Paleosols are developed in some of the sandstone bodies (facies Pp). Furthermore, some thin ignimbrite and debris flow intercalations are found in the member.

Interpretation

On the grounds of the same criteria used for the determination of the paleo-environment of the Neiva Member, the member may be interpreted as being deposited by a north-flowing braided river system. In fact, the deposits of the Garzón Member can be considered as the younger deposits of the paleo-Magdalena river, the main distinction with the Neiva Member deposits being that the conglomerates of the Garzón Member contain a much higher share of metamorphic clasts provening from the Garzón Massif (chapter V, section 1.3). Apparently, the massif underwent beginning uplift during deposition of the Garzón Member, and erosional products from the uplifting massif entered the fluvial system. The lower portion of overbank sediments in the Garzón Member as compared to the Neiva Member may be attributed to the higher amount of coarse material which entered the basin as a result of uplift of the Garzón Massif. Uplift culminated during deposition of the overlying Las Vueltas formation, which consists entirely of coarse alluvial fan material provening from the massif (chapter V, section 1.3).

In the east of the region the conglomerates of the Garzón Member are dominated by east-derived components. In the center of the basin, however, both east-derived material from the massif and west-derived volcanoclastics are found. The presence of thin ignimbrites and debris flow intercalations and the occurrence of thick sheetflood deposits consisting almost entirely of fresh volcanic material, indicate that influence of volcanism of the Central Cordillera was still significant, although not as important as during deposition of the Los Altares Member. The greater number of paleosols in this member probably reflects the diminishing influence of volcanism on sedimentation (Smith 1987b) and thus longer pauses in sedimentation between periods of rapid aggradation. It is likely that the somewhat reduced volcanic input on the one hand and erosion of the uplifting Garzón Massif on the other hand forced the paleo-Magdalena River back to its former position in the center of the basin (fig. 35).

The Garzón Member is essentially a strike outcrop. The lack of outcrops further to the west preclude an interpretation of the paleo-environment of this area. Therefore, it remains uncertain whether volcanic aprons were still present in this area, albeit much reduced in size, or whether braided channels, transporting volcanic material and erosional products from the Central Cordillera to the major north-flowing trunk river, flowed on an alluvial plain where

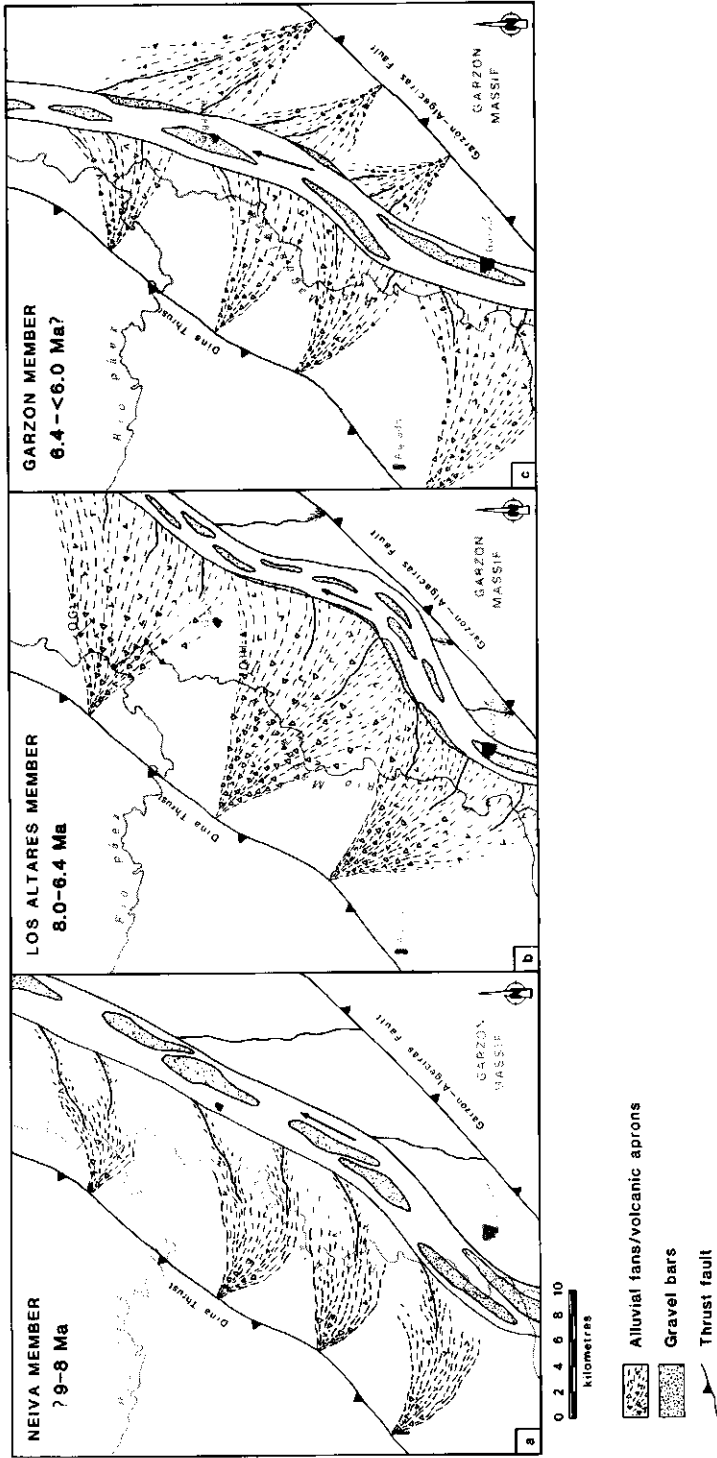


Fig. 35. Reconstruction of the paleogeography at the time of deposition of the different members of the Gigante Formation.

sedimentation was dominated by overbank deposition and sheetflood events. In fig. 35 the first option has been depicted.

4. Discussion

In the case of the Gigante Formation it is unknown where the former volcanoes were located that were responsible for the production of the volcanic and volcanoclastic deposits. Davies *et al.* (1978) give characteristics of fluvial sediments, channel forms and flow conditions for the fluvial systems draining the Fuego volcano in Guatemala. They divided the river systems into three segments, *i.e.* the volcanic highlands, a transition region and the coastal plain. The characteristics of the Los Altares deposits are broadly comparable to those of the sediments from the transition region, which were deposited at a distance of some 30-40 km from the crater. In the case of the Gigante Formation, however, it is likely that the former volcanoes were located at a somewhat greater distance from the southern Neiva Basin, *i.e.* at a distance of some 50-60 km. This would place the former eruptive centres exactly within the present-day main belt of andesitic stratovolcanoes. Considering that during the 1985 eruption of the Nevado del Ruiz in Colombia the debris flows ran between 60-90 km before deposition took place (Naranjo *et al.* 1986), this would still be a realistic assumption.

Unfortunately, more proximal deposits of Gigante age are either lacking or buried under younger volcanic deposits. An exception is formed by a single small stratigraphic section in the Q. el Arrayán, 15 km SW of La Plata, consisting of volcanoclastic deposits that show great similarity to the Los Altares deposits. The deposits are coarser-grained than the deposits found in the S. Neiva Basin. A K-Ar determination on hornblende from an ignimbritic intercalation gave an age of 7.3 ± 0.3 Ma (chapter IX, table XX). This section probably represents a more proximal equivalent of the Los Altares Member. It is likely that part of the volcanoclastic material produced in the proximal areas was transported to the S. Neiva Basin by an ancestral Río Paez and other tributaries of the paleo-Magdalena River. Similar processes are described by Vessell and Davies (1981) in Guatemala, where in a period of three years 5% of all ejecta and 12% of the glowing avalanche deposits on the flanks of the volcano Fuego were remobilized by debris flows in proximal reaches. Almost at the same time large quantities of sediment were introduced into the stream systems, resulting in rapidly aggrading braided bed-load channels in which deposition occurred mainly through flash-floods. The authors estimate that approximately 20-30 years are necessary to remove most of the loose debris from a single eruption from the flanks of the volcano.

In chapter IV (section 2) it has been estimated that the contact between the Los Altares Member and the Neiva Member is 8 Ma old and the contact between the Los Altares Member and the Garzón Member 6.4 Ma old. These average ages and the intertacent K-Ar ages from the Q. Guandinosita and Q. La Honda sections were used to calculate average sediment accumulation rates for both sections. These rates were used in their turn to construct figure 34 (below) from figure 34 (above). In the figure, the cumulative percentages of the different facies associations of the Gigante Formation are plotted against the intrapolated ages. In this way the timing of the sedimentological changes in both sections may be compared. The following may be concluded:

1. Sedimentation rates for the period between 8-6.4 Ma average 0.36 mm/year in the Q. Guandinosita section and 0.42 mm/year in the Q. La Honda section.
2. The sections probably represent different volcanic aprons, because periods of intense volcanoclastic sedimentation do not coincide. This is in accordance with the paleocurrent patterns given in fig. 33, which seem to indicate different fan systems.
3. Main ignimbrite deposition started approximately at the same time in both sections. Possibly, the ignimbrites on both aprons are derived from the same eruption phases. It has already been shown above (section on facies association VI) that three types of ignimbrite deposits are present: undifferentiated deposits with very large pumice clasts, deposits showing a clear

tripartite division in a LCZ, a main body and a PCZ and thin, crudely horizontally bedded ignimbrite deposits with thin pumice lenses. Similar differences within a single ignimbrite deposit are described by Walker *et al.* (1980, 1981) and Wilson and Walker (1982) as occurring in the Taupo ignimbrite in New Zealand and by Schumacher and Schmincke (1990) for the Laacher See volcano ignimbrites. These differences are interpreted by the latter authors as lateral facies changes. According to these authors, the bedded deposits represent a facies developed on the higher parts of the original topography, while the massive deposits and deposits with a tripartite division represent a facies developed in the valleys. A detailed study of the ignimbrite deposits of the Gigante Formation, however, is needed to determine whether the differences between the deposits are lateral facies changes within the same ignimbrite or resulted from different ignimbrite eruptions.

The following observations on the Q.Guandinosita section are of interest:

1. In the lower part of the Q. Guandinosita section confined sheetflood and overbank deposits are replaced by channel conglomerates, and debris flow and unconfined sheetflood deposits. This replacement probably reflects the gradual basinward extension of the volcanic apron due to increasing volcanic activity.
2. The two intervals characterized by intense volcanoclastic sedimentation in the Q. Guandinosita section are approximately of equal duration: they lasted ± 0.5 Ma each.
3. A more or less regular alternation of channel deposits and overbank deposits is visible in fig. 34 (below). It is likely that this alternation represents lateral shifting of the channels on the fan.

5. Paleogeographic reconstruction and conclusions

During deposition of the Neiva Member, uplift of the southern part of the Central Cordillera resulted in deposition of polymictic pebble conglomerates, sandstones and mudstones in the S. Neiva Basin. The river sedimenting the deposits was a braided N-flowing paleo-Magdalena River, that was fed predominantly from the S and to a lesser extent from the west by small alluvial fans and braided tributaries (fig. 35). Deposition took place mainly on longitudinal bars under upper flow regime conditions and by sheetfloods. The channel belt was probably rather wide, channels being separated by bars and areas where floodplain deposition took place.

During deposition of the Los Altares Member, volcanism became much more intense and eruptions of andesitic and dacitic material resulted in the formation of large, partly coalescing volcanic aprons along the reactivated former thrust front of the Central Cordillera (fig. 35). At first volcanic activity resulted mostly in the formation of volcanic debris flows and sheetfloods, but gradually, when the eruptions became more explosive, ignimbrites and air-fall tephra were erupted as well. The former eruptive centres were probably located 15-20 km west of La Plata within the present chain of large andesitic stratovolcanoes.

The large volcanic aprons in the north and center of the southern Neiva Basin forced the paleo-Magdalena river to flow further to the east. In the south, the volcanic influence on sedimentation seems to have been more restricted, either because of the greater distance to the fault front from which the aprons spread out into the basin or because the former eruptive centres were located relatively far to the north and mainly influenced sedimentation processes in the northern part of the study area. Because of the limited volcanic influence in the south, the ancestral Magdalena River kept its original course during deposition of the Los Altares Member and "Neiva" conglomerates are found to interfinger with thin volcanoclastic deposits in that area.

During deposition of the Los Altares Member aggradation was rapid: sedimentation rates on the volcanic aprons averaged 0.36-0.42 mm/year. As in the case of the Deschutes Formation in Oregon (Smith, 1987a), aggradation was at a maximum during volcanic events, but rapidly decreased during intervening periods. In such periods of relative quiescence, braided bed-load channels on the proximal volcanic aprons incised into the volcanoclastic deposits and were either filled by the products of debris flows, hyperconcentrated flows and ignimbrites, or by

polymict pebble conglomerates with a high content of fresh volcanic clasts during the next depositional event. The restricted depth of these channels (< 5m) and their generally non-erosional bases indicate that large depositional events followed each other very rapidly and little time was available for incision of fluvial channels. The same is indicated by the lack of paleosols in the stratigraphy.

On the proximal parts of the volcanic aprons sedimentation was dominated by debris flows, hyperconcentrated flows and unconfined sheetfloods. Distally, where the aprons graded into the alluvial plain of the paleo-Magdalena river, sedimentation was determined by sheetflood and overbank deposition. Here, some paleosols in the upper part of the member are developed as mud-cracked fine-grained layers containing gypsum crystals or laminae, indicating deposition under playa-like conditions.

During deposition of the Garzón Member volcanism became somewhat less intense, as shown by the appearance of paleosols in the sandy overbank deposits and by renewed sedimentation of large amounts of pebble conglomerates with northward paleocurrent directions. Apparently, the braided paleo-Magdalena river retook its former course (fig. 35). The conglomerates have partly an eastern provenance, indicating that erosional products of the uplifting Garzón Massif entered the S. Neiva Basin. Fluvial sedimentation was interrupted at times by the influx of great quantities of blue-grey sands of sheetflood origin and occasionally by a debris flow or ignimbrite, which probably spread out from the much reduced volcanic aprons in the west over the alluvial plain and into the main river system.

Chapter VIII

Tectonics of the S. Neiva Basin

1. Faulting of the basinal sediments

In and alongside the S. Neiva Basin, four types of faults may be distinguished:

1. The steeply westward-dipping Dina Thrust, which forms the limit of the east-verging middle Tertiary foreland fold and thrust belt. The fault has a northeastern trend (Butler, 1983; Butler and Schamel, 1988).
2. The Garzón-Algeciras Fault: the eastern limit of the S. Neiva Basin. This fault is an eastward-dipping high-angle Laramide-style reverse fault, along which right lateral strike-slip movements have taken place (and possibly still are taking place). The fault has a NE-SW trend.
3. Small-scale low-angle thrusts along the Garzón-Algeciras Fault. These low-angle thrusts are only found directly E of Garzón and NE of Gigante.
4. Eastward dipping, high-angle reverse faults, trending toward the NE and NNE, occur within the sediments of the S. Neiva Basin.

ad 1. The Dina Thrust forms the easternmost expression of the Chusma fault system (fig. 5). It has been shown in chapter VI, section 4.3, that the fault is the western limit of the S. Neiva Basin. A similar opinion is found in the thesis of Butler (1983, p. 233-234).

ad 2. Along the fault-trace, Precambrian rocks are juxtaposed against rocks of the upper member of the Gigante Formation (the Garzón Member). It has been argued in chapter II that Early Neogene uplift along the fault (≥ 12 Ma ago) must have been in the order of 4.5 km, while Late Neogene uplift (≤ 6 Ma ago) amounted to some 2.5 km.

Vertical movements on the fault system generally appear to be older than strike-slip movements. Sediments of the upper unit of the Las Vueltas formation and Quaternary alluvial fan sediments (Qaf₂) are found on both sides of the Garzón-Algeciras Fault. They are not offset vertically by this fault. In the upper unit of the las Vueltas formation (Tv₂) near Zuluaga slickensides are found, indicating a horizontal displacement in the direction 40-220°. Evidence of Quaternary wrench-faulting is formed by hanging valleys and shutter-ridges in the surroundings of Zuluaga and Sylvania.

ad 3. A small thrust sheet, consisting mainly of Paleozoic rocks and rocks, belonging to the Jurassic Saldaña Formation, is found along the Garzón-Algeciras Fault east of Garzón (see geological map, appendix 1). The presence of big blocks of sandstone of the Cretaceous Caballos Formation (chapter I, section 3.3) on top of the sheet, as well as oil seepage in the upstream part of the Quebrada Las Damas suggests that Cretaceous rocks also took part in the thrusting. The thrust sheet rests unconformably on folded sediments of the lower two members of the Gigante Formation.

In the north of the S. Neiva Basin a similar thrust sheet consists of Jurassic plutonic and extrusive rocks, as well as rocks from the Paleocene-Cretaceous Guaduas and Guadalupe Formations. These rocks are thrust onto folded sediments of the Los Altares Member of the Gigante Formation.

ad 4. The majority of the faults in the S. Neiva Basin are high-angle reverse faults, found in the folded basinal sediments. The trend and the direction of movement of the faults are identical to those of the Garzón-Algeciras Fault. From the geological map (appendix 1) it can be estimated that the maximum vertical throw on these faults is 150-600 m. The youngest sediments to be affected are the sediments of the Qt_2 terrace along the Quebrada Guandinosita (chapter III, section 2.7, and photo 8). It has been mentioned in chapter III that the eastern part of the terrace was uplifted some 160 m relative to the western part, as a result of activity of the Puerto Seco Fault.

2. Folding of the basinal sediments

Most large-scale folds in the S. Neiva Basin are N- and NE-trending, slightly asymmetrical rather open folds, which plunge toward the N-NE and the S-SW. The smaller folds are generally more asymmetrical and tighter. The fold axes are approximately parallel to the Garzón-Algeciras Fault and the Dina Thrust.

The youngest sediments to be involved in the folding are the sediments from the lower unit of the Las Vueltas formation (Tv_1). In the NW part of the basin, between the Q. La Honda and Q. Las Vueltas, these sediments rest with an angular unconformity of 10-13° on the deposits of the upper member of the Gigante Formation, the Garzón Member (chapter III, section 2.5). In the center of the basin, in the Vereda El Piñal section, the dip of the sediments belonging to the Garzón Member and to the Las Vueltas formation decreases more gradually from old to young.

In the NE of the basin, the Tv_1 sediments are found along (and partly on top of) the thrust sheet consisting of Jurassic plutonic and extrusive rocks.

3. Conclusions

From the above observations the following may be concluded:

1. The formation of two small thrust sheets during the ≤ 6.4 Ma uplift of the Garzón Massif suggests that uplift of the massif occurred along several faults belonging to the Garzón-Suaza fault system (see chapter I, section 3.2), of which the Garzón-Algeciras Fault forms the westernmost expression. Differential faulting during early Neogene uplift was also suggested by the range in apparent apatite fission track ages given in chapter II (section 3.3) and would agree with the opinion of Colletta *et al.* (1990) and Cobbold *et al.* (1990), who interpret the Eastern Cordillera as consisting of a series of sub-parallel thrust faults.

2. Beginning uplift of the Garzón Massif along the Garzón-Algeciras Fault some 6.4 Ma ago (the age of the base of the Garzón Member) coincided with SE-NW compression of the basinal sediments, leading to beginning folding and reverse faulting of these sediments. Quaternary vertical offset of the Qt_2 terrace along the Puerto Seco Fault indicates that SE-NW compression is still going on nowadays.

3. As uplift of the massif intensified, a thrust splay from the Garzón-Algeciras Fault spread out over the deforming deposits in the N of the basin. Erosion of both the thrust sheet and the massif during continued uplift, led to deposition of the lower unit of the Las Vueltas Formation in the north and the center of the basin. This unit was subsequently deformed.

4. At the same time, or perhaps a geologically short time later, a thrust sheet spread out from the massif over the Gigante and Honda deposits in the S of the area, simultaneously overturning these sediments to form an anticlinal structure. In contrast to the northern part of the basin, where the lower unit of the Las Vueltas Formation reaches thicknesses of up to 300 m, little erosional material from the uplifting massif and the thrust sheet appears to have been conserved in the S, probably due to the nearness of the ancestral Magdalena River which eroded the newly-formed sediments.

5. Continued, albeit much reduced tectonic activity of the massif, presumably resulting mainly from intermittent dextral strike-slip faulting along the Garzón-Algeciras Fault and other, more eastward faults of the Garzón-Suaza fault system, led to deposition of the upper unit of the Las Vueltas formation and was probably also responsible for the deposition of younger alluvial fan sediments (Qaf₁ and Qaf₂ on the geological map, appendix 1).

6. Wrench-faulting along the Garzón-Suaza fault system appears to have had little influence on the faults within the basin. It is possible that the Puerto Seco Fault which, according to Guillande (1988), connects with the Garzón-Algeciras Fault further to the NE, underwent some left-lateral strike-slip (chapter IV, section 2). Part of the deposits of the Gualanday Group show horizontal offset and strike-slip is also suggested by lineaments on the fault plane which indicate horizontal movements in a NE-SW direction.

PART 4

DEPOSITS OUTSIDE THE S. NEIVA BASIN

This part of the thesis is dedicated to deposits located outside the S. Neiva Basin. In agreement with Butler (1983) and Butler and Schamel (1988), a distinction is made between the S. Neiva Basin, which is defined here as the part of the Upper Magdalena Valley located between the Garzón-Algeciras Fault and the Dina Thrust, the most westerly fault of the Chusma fault system, and the fold and thrust belt area west of the S. Neiva Basin, which covers the region between the Dina Thrust and the Chusma Thrust (fig. 5, p. 15). This distinction is made because both areas have different depositional histories. On the geological map published by Kroonenberg and Diederix (1982), it can be seen that deposits of the Honda and Gigante Formations are restricted to the S. Neiva Basin: the deposits found in the center of the Tesalia Syncline west of the Dina Thrust, which have been indicated as Honda Formation on the map, belong in fact to the La Cira Formation (H. Diederix, pers. comm.). It is likely that this difference is caused by differences in elevation between the two areas. It has been shown in chapter VI (section 4.3) that subsidence of the S. Neiva Basin commenced during deposition of the Honda Formation, while the fold and thrust belt area remained a high.

The first Neogene deposits to be encountered in both areas, although very limited in the S. Neiva Basin, are the ignimbrite deposits of the Guacacallo Formation, which have a Late Pliocene age (see below). Also, the volcanoclastic terraces along the Río Páez and Río La Plata are found in both areas, extending from the point where the Río Páez enters the fold and thrust belt area to some 10 km N of the confluence of the Páez and Magdalena rivers, E of the Dina Thrust.

The Guacacallo Formation and the volcanoclastic terraces along the Páez and La Plata Rivers are described below in chapters X and XI respectively, because they give information on the Pliocene to Holocene geological history of the region. In the S. Neiva Basin, the period between 6-1 Ma ago is characterized by long periods of non-deposition and erosion, alternating with periods of deposition of alluvial fan sediments belonging to the Las Vueltas formation, which has tentatively been assigned a Latest Miocene to Pliocene age.

In chapter IX, deposits of Gigante age, located outside the S. Neiva Basin, are described. One of these outcrops was encountered at the transition from the Central Cordillera to the fold and thrust belt area; the other one in the Suaza Valley: an intramontane valley, situated within the southern part of the Garzón Massif. These deposits are discussed because they give additional information on the sedimentological and tectonic Upper Miocene history of the region.



Photo 24. Lower part of the section, taken in the Q. El Arrayán. The boy is standing on the dated ignimbrite deposit. In the background the 5 m thick sheetflood deposit is visible. View of the photo is toward the E.

Chapter IX

Deposits of the Gigante Formation outside the S. Neiva Basin¹

1. Introduction

In the Upper Magdalena Valley, deposits of Gigante age are only found at two locations outside the S. Neiva Basin. In this chapter two sections, taken in these deposits at both locations will be described.

One section is located in the Quebrada el Arrayán, 15 km SW of la Plata. Here, deposits of Gigante age crop out at the base of the canyon. The deposits are not folded and are overlain by a ± 300 m thick ignimbrite deposit belonging to the Pliocene Guacacallo Formation (chapter X). The section consists of volcanoclastic deposits that show great similarities in colour and composition to those of the Los Altares Member, although they are coarser-grained than the deposits found in the S. Neiva Basin. The section was taken in order to determine whether the deposits might be a more proximal equivalent of the Los Altares deposits in the S. Neiva Basin.

The other outcrop of Gigante sediments is situated in the Suaza Valley, south of the S. Neiva Basin. At the west side of the Suaza River, ± 600 -700 m of Gigante deposits are found, consisting mainly of thick conglomerate sequences with minor intercalations of sandstones and thin ignimbrite deposits showing some similarity to deposits of the Garzón Member. A 170 m long stratigraphical section could be measured. The section was taken, because it was thought to be of importance with regard to the reconstruction of the tectonic history of the area during deposition of the Gigante Formation.

2. Lithostratigraphy, geochronology and petrology of the deposits

2.1. Quebrada El Arrayán

2.1.1. Description

The lower part of the section in the Quebrada El Arrayán consists of 3 meters of conglomerate, overlain by a ± 1 m thick ignimbrite deposit. The conglomerate is built up entirely of cobbles and boulders of fresh andesite. The ignimbrite thins towards the N (fig. 36; photo 24). A K-Ar determination on hornblende from the ignimbrite gave an age of 7.3 ± 0.3 Ma (table XX). The deposit is overlain by 10 cm of organic clay with plant remains (not indicated in the fig. 36) followed by a 1 m thick volcanic debris flow deposit. The top of the debris flow deposit is partly incised by a 5 m thick sheetflood deposit (photo 24). The pebbles in this deposit are composed of erosional material of Jurassic intrusives. On top of the sheetflood deposit, a 40 cm thick pebble to cobble conglomerate with a similar composition is present. The top of the sequence is formed by a thin ignimbrite deposit.

Both the conglomerate and the thin ignimbrite deposit are deeply incised by a channel, filled with subrounded ignimbrite blocks up to 50 cm in diameter. This channel fill is overlain by a 3.5 m thick ignimbrite with a vitrophyre at its base. It is likely that the ignimbrite, and possibly also the underlying channel fill, already belong to the Guacacallo Formation. The Guacacallo Formation consists of one or more superimposed rhyolitic ignimbrite deposits resulting from deposition of several ignimbrite flows (chapter X).

¹ The K-Ar mineral age determination was performed by Dr. E.H. Hebeda and co-workers, and the zircon fission track age determination by Dr. P.A.M. Andriessen and co-workers.

Table XX. K-Ar hornblende data of an ignimbrite in the Quebrada El Arrayán section

Sample no.	Mineral	K (ppm wt.)	Radiogenic ^{40}Ar (ppb wt.)	Atmospheric ^{40}Ar (% total ^{40}Ar)	Calculated age $\pm \sigma$ (Ma)
MW 542	Hbl	0.41	0.22	77	7.3 \pm 0.3
		0.42	0.21	93	

Unfortunately, no samples could be taken in the upper part of the section to determine the exact position of the contact between the two formations. Some 20 m further to the N, a ± 250 m thick ignimbrite deposit is found with a 5 m thick vitrophyre at its base. This ignimbrite certainly belongs to the Guacacallo Formation.

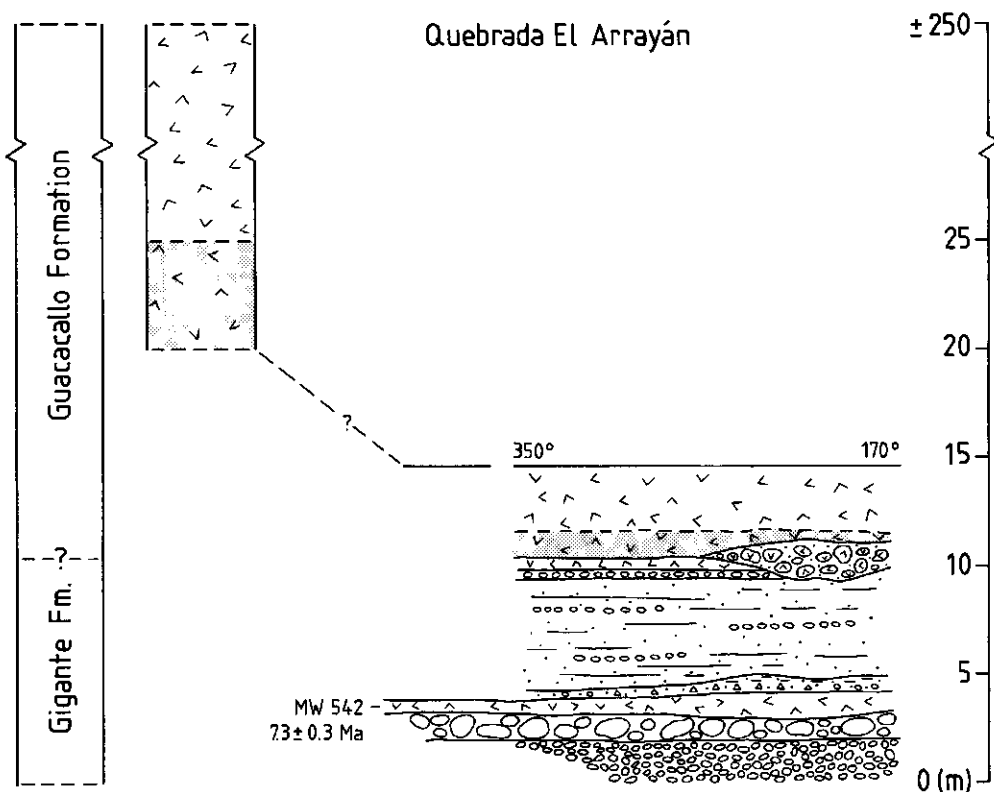


Fig. 36. Stratigraphical section in the Q. El Arrayán, ± 15 km SW of La Plata (see fig. 44 for exact location). For legend, see fig. 16.

2.1.2. Discussion and conclusions

The coarser grain size of the conglomerates in the "Gigante" deposits as compared to that of the conglomerates of the Los Altares Member in the S. Neiva Basin, as well as similarities in colour and composition, and the Upper Miocene age suggest that the assumption that the lower part of the section is a more proximal equivalent of the Los Altares Member is correct.

An alternative interpretation, however, that the age of the ignimbrite is too old and that the deposits in fact form part of the El Carmen formation (chapter X), or belong to the Guacacallo Formation, cannot be excluded completely on the grounds of the fact that the dated ignimbrite contains a rather large amount of xenoliths (*e.g.* fragments of schist), and on the grounds of the apparent conformity between the deposits and the Guacacallo Formation. The second point may be explained by assuming that uplift of the Garzón Massif did not lead to deformation of the sediments (as it did in the S. Neiva Basin), because they were located within a rigid block formed entirely by Jurassic deposits. The first point, however, can only be solved by performing an additional radiometric age determination. For the time being, it is assumed that the sediments represent a proximal equivalent of the Gigante Formation.

2. 2. Suaza Valley: "Picuma conglomerate"

2.2.1. Description

The section in the Suaza Valley was taken at the west side of the Suaza River, ± 4 km S of the town of Suaza. It consists mainly of a series of polymict orthoconglomerates with minor intercalations of volcanoclastic and fluvial sandstones, some siltstones and two ignimbrite deposits (fig. 38), which together are normally called the "Picuma conglomerate". The conglomerates include both well rounded pebble to cobble conglomerate beds and poorly rounded cobble to boulder beds.

A fission-track age determination on zircon from the lower ignimbrite deposit revealed an age of 6.6 ± 1.4 Ma (table XXI). This implies that the section is a time equivalent of the Los Altares Member or the Garzón Member in the S. Neiva Basin. The composition of the conglomerates, however, is very different from that of the Garzón Member. In the Suaza Valley 60-85% of the pebbles and boulders consist of erosional material from the Late Triassic/Jurassic Saldaña Formation and 7-33% of material from the Jurassic Suaza Batholith (fig. 38). The composition of the Suaza conglomerates is less surprising when the regional geology is taken into consideration: both on the east and west sides of the Suaza River the Saldaña Formation crops out extensively and parts of the Suaza Batholith surface (fig. 37). The presence of poorly rounded cobble and boulder conglomerates, consisting for more than 80% of clasts from the Saldaña Formation, suggests that the conglomerates have a local origin. Sedimentological criteria like rounding, sorting and grain size indicate that the conglomerates were deposited in an alluvial fan setting. Although no paleocurrent measurements could be taken, the lack of Precambrian metamorphic clasts in the deposits (fig. 38) implies that the material was mainly derived from the area west of the Suaza Valley.

Table XXI. Zircon fission track analytical data of sample MW 178, "Picuma conglomerate"

Sample	ρ_s^1 ($\times 10^6$ t/cm ²)	ρ_i^2 ($\times 10^6$ t/cm ²)	t^3 ($\times 10^6$ yr)	1σ ($\times 10^6$ yr)	Number of grains	ρ_{glass}^4 ($\times 10^5$ t/cm ²)	Uranium (ppm)	P(χ^2) %
MW 178	2.16 (507)	14.16	6.6 (1662)	1.4	12	200634.5 (3318)	435.0	<1



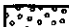


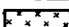
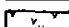

1) ρ_s : density of spontaneous fission tracks; the number of actually counted tracks is given in parenthesis

2) ρ_i : density of induced fission tracks; the number of actually counted tracks is given in parenthesis

3) age calculated according to the Zeta approach with a Zeta value of 308.1; zircon standard used: Fish Canyon with a calculated age of 27.2 ± 3.5 Ma

4) ρ_{glass} : density of fission tracks in standard glass NBS 962; no. of actually counted tracks is given in parenthesis

LEGEND

-  Quaternary deposits
-  Las Vueltas formation
-  Gigante Formation
-  Gualanday Group
-  Cretaceous-Paleocene fms.
-  Jurassic intrusives
-  Saldaña Formation
-  Precambrian
- ★ Fission track sample (MW 178)

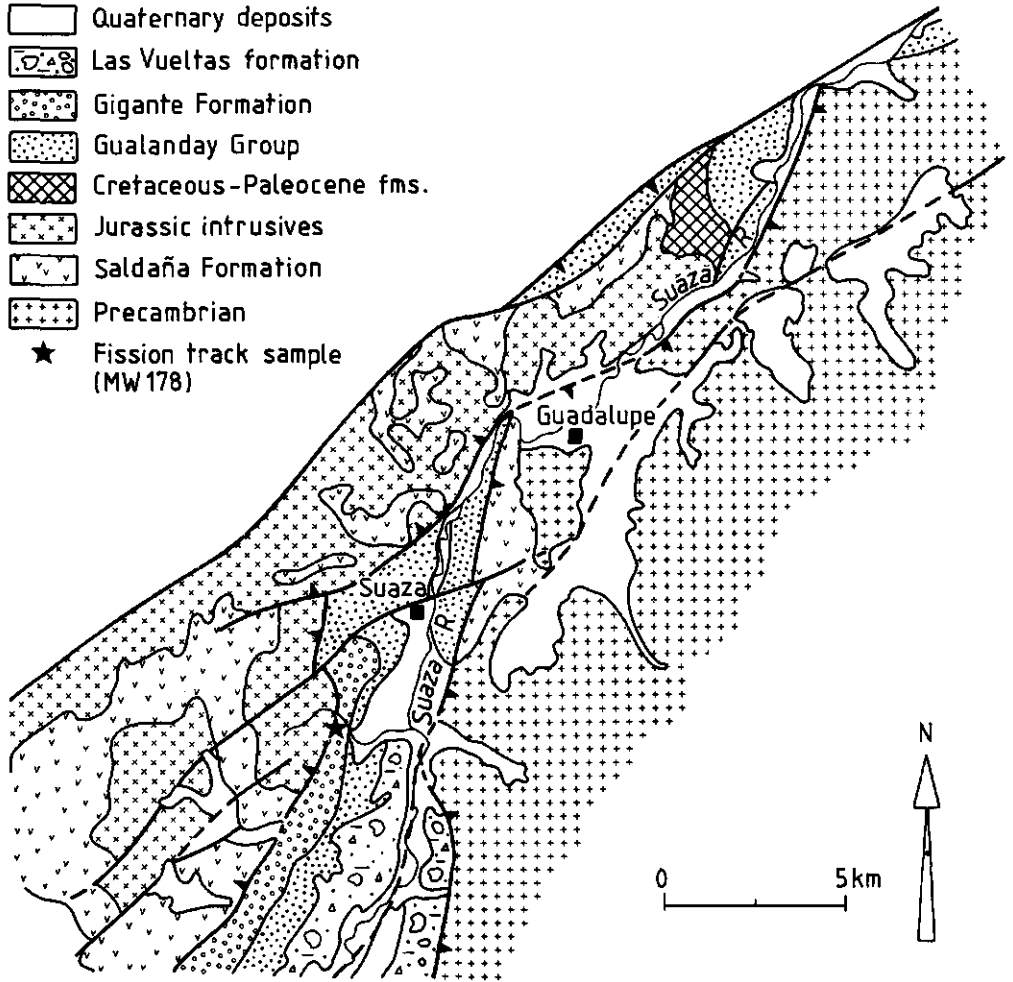
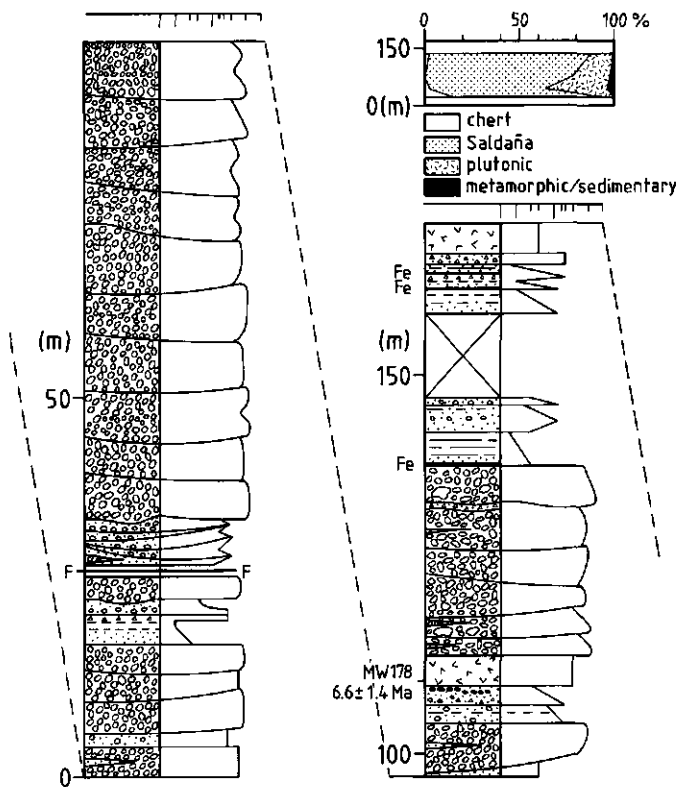


Fig. 37. Geological map of the N part of the Suaza Valley, adapted from maps by Kroonenberg and Diederix (1982) and Diederix and Gomez (in press).

It has already been stated in the introduction (chapter I, section 3.2) that the Suaza Valley is the southernmost one of a series of intramontane basins situated within the Garzón Massif. The valley is located in the area where the Central and Eastern Cordillera converge (fig. 3). In the NW, it is delimited by one of the faults belonging to the Garzón-Suaza fault system. The Gigante sediments occur west of the Suaza River, where they rest unconformably on deposits of the Gualanday Group; the Honda Formation is lacking. Both Gualanday and Gigante sediments are overturned. East of the Suaza River, a lateral equivalent of the Las Vueltas formation is found (fig. 37), consisting of a thick sequence of alluvial fan deposits, composed of poorly sorted and rounded pebble and boulder conglomerates with a very high percentage of Precambrian metamorphic clasts.



Suaza Valley: Picuma conglomerate

Fig. 38. Stratigraphical section of part of the "Picuma conglomerate", Suaza Valley. For legend, see fig. 16.

2.2.2. Conclusions

The data presented above suggest that the Neogene history of this area is similar to that of the Garzón Massif alongside the S. Neiva Basin:

1. The absence of the Honda Formation and the lower part of the Gigante Formation could be explained by uplift of the Garzón Massif. Uplift of the massif ≥ 12 Ma ago probably caused erosion of Honda sediments that had already been deposited. No sediments belonging to the lower part of the Gigante Formation were deposited subsequently, because the area now formed a high.
2. From the fission track age of sample MW 178, it may be concluded that deposition of the "Picuma conglomerate" probably coincided with the second Neogene uplift pulse of the Garzón Massif.
3. The fact that the "Picuma conglomerate" is restricted to the eastern part of the basin and has a western provenance, while the Las Vueltas formation is restricted to the eastern part of the basin and has an eastern provenance, suggests that this second Neogene uplift pulse led to development of local highs and lows, the latter of which acted as sediment traps. Uplift of the

western part of the massif led to accumulation of the "Picuma conglomerate" in the newly formed intramontane basin. The presence of some ignimbrites in the "Picuma conglomerate" may be accounted for by the fact that, due to their mode of transport, ignimbrite flows can surmount barriers of more than 600 m (Fisher and Schmincke, 1984). Uplift of the eastern part of the massif subsequently lead to overturning of the "Picuma conglomerate" and deposition of a lateral equivalent of the Las Vueltas formation.

4. Evolution of local highs and lows within the massif can only be explained by differential faulting on the thrusts forming the Garzón-Suaza fault system.

Chapter X

Deposits W of the S. Neiva Basin: the Guacacallo and El Carmen formations¹

1. Location of the Guacacallo Formation

The Guacacallo Formation forms a plateau that extends over some 1000 km² alongside and west of the Upper Magdalena and La Plata Valleys (fig. 3, p. 12). The formation partly covers the folded and faulted Paleozoic to Oligocene rocks that constitute the Eocene-Oligocene/Miocene fold and thrust belt. It has its greatest extension west of this terrain in the Central Cordillera.

The rhyolitic to rhyodacitic ignimbrites (or ash-flow tuffs) were erupted from a former eruptive centre in the Central Cordillera. Up to the present time it is unknown which caldera acted as source. Kroonenberg *et al.* (1981, 1982) suggested that the ignimbrites were erupted either from the extinct Cutanga (Letrero) caldera, located some 35 km W of San Agustín, or from one of the volcanoes of the Sierra de los Coconucos, or from the Merenberg volcano W of La Argentina (fig. 50). In section 7 of this chapter some attention is given to this problem.

After extrusion, the ignimbrites underwent deep weathering, and a fine dendritic pattern developed (Kroonenberg *et al.*, 1981). The dissection of the plateau led to the typical undulating morphology that nowadays characterizes the ash flow tuffs.

As a result of the very deep weathering, in some places to depths of 10 m, and the generally poor exposure, the study of the Guacacallo Formation was necessarily restricted to isolated outcrops and a few sections. The present study is limited to the ignimbrites found alongside the upper reaches of the Río Magdalena, in the area between Guacacallo and Saladoblanco, and to some outcrops in the area between La Argentina and La Plata.

Two deeply weathered outcrops were found E and N of La Plata in the fold and thrust belt area. The first outcrop is located directly NE of the town of La Plata near the village of San Andrés (fig. 44). Secondly, a very small outcrop is present on the east side of the road Paicol-Tesalia, ± 2 km SW of Tesalia (fig. 3). Due to intensive weathering, no samples were taken at these locations.

Furthermore, a small outcrop was found in the S. Neiva Basin itself, 4 km NE of the town of Tarqui (fig. 3). Here, the ignimbrite is found to rest unconformably on sediments of the Gigante Formation in the center of the Tarqui Syncline (Bok and Veldkamp, 1988; Diederix and Gomez, in press). A sample taken in this outcrop (MW 77) was used for radiometric age dating, the result of which will be discussed below. The outcrop nowadays represents the easternmost occurrence of the ignimbrites.

2. Structure of the ignimbrites

2.1. Distinction between flow units and cooling units

In order to correctly interpret the stratigraphy and field relations of the ignimbrites, it is necessary to make a distinction between flow units, simple cooling units and compound cooling

¹ The K-Ar mineral age determinations given in this chapter were performed by Dr. E.H. Hebeda and co-workers, the zircon fission track age determinations by Dr. P.A.M. Andriessen and co-workers.

units in the sense of Smith (1960). A flow unit is a rock body emplaced by a single pyroclastic flow. When several hot flows are erupted shortly after one another and are deposited on top of each other, they may cool as a single cooling unit. A compound cooling unit forms when there is an interruption in temperature between the successive flows (Fisher and Schmincke, 1984).

The main criterion which is used for distinguishing between simple and compound cooling units is the degree of welding of the deposits. During welding the glass shards and pumice fragments are sintered together, decreasing the porosity. The controls for producing welding in an ignimbrite are the glass viscosity, the porosity and the lithostatic load. The glass viscosity is dependent on the temperature and composition, the lithostatic load on the thickness of the deposit (Cas and Wright, 1987). A cooling unit is marked by a more or less systematic lateral and vertical distribution of welding zones (fig. 39), and thus of bulk density. The top and bottom of cooling units are generally unconsolidated and non-welded, due to rapid cooling against the rock basement and relatively rapid heat conduction and radiation into the atmosphere, respectively. The lower half of a cooling unit is the part of the ignimbrite that experiences maximum welding. At the base of the deposit, where bulk density is at a maximum and porosity is at a minimum, a densely welded zone may develop as a result of high compactional strain. In this densely welded zone, a vitrophyre, the pumice clasts are strongly flattened and compacted to fiamme. Glass shards and fiamme are commonly oriented horizontally and define a planar foliation.

Ash flow tuffs that show such simple welding variations are classified as simple cooling units. Ignimbrites that have several zones of dense and partial welding are classified by Smith (1960) as compound cooling units.

In the partly welded ignimbrites of the Guacacallo Formation it is difficult to establish in the field the exact degree of welding. One of the criteria that may be used, however, is the development of columnar jointing in the deposits, which points to moderate to strong welding (Fisher and Schmincke, 1984). Vitrophyres, found at the base of some of the tuffs, were used to distinguish between different flow units.

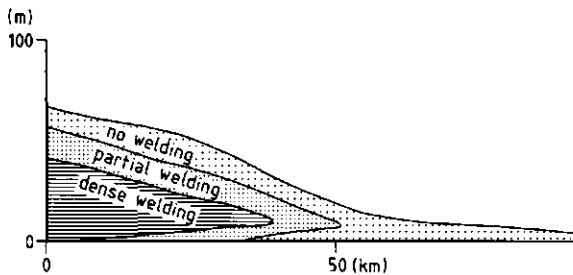


Fig. 39. Vertical distribution of welding zones in an ignimbrite. After Smith (1960).

2. 2. Structure of the flow units

Flow units are generally heterogeneous and may consist of several layers. Viewed from the perspective of flow and emplacement mechanisms, two kinds of deposits may be distinguished: pyroclastic flow deposits, which are usually poorly sorted and massive, and pyroclastic surge deposits which are better sorted, finer-grained, thinner and better bedded than pyroclastic flow deposits (Fisher and Schmincke, 1984). Pyroclastic flows are high-concentration semifluidized bodies, moving with essentially laminar motion (Sparks, 1976), while pyroclastic surges are turbulent low-concentration flows (Sparks and Walker, 1973; Sparks, 1976; Fisher, 1979). Pyroclastic surge deposits include ground surge deposits, underlying the pyroclastic flow deposits and ash clouds deposits that overlie and extend beyond the pyroclastic flow deposits.

The origin of ground surge deposits is still a subject of discussion. According to Wilson (1980), Wilson and Walker (1982) and Freundt and Schmincke (1985) ground surge deposits

are formed as a result of extreme turbulent action at the base of a pyroclastic flow as air is infolded beneath the advancing flow front. Other authors are of the opinion that ground surges are formed separately from the pyroclastic flow (Sparks *et al.*, 1973; Sparks, 1976), possibly from the margin of a collapsing eruption column, while the pyroclastic flow is formed from collapse of the central part of the column (Fisher, 1979).

An idealized sequence of a flow unit (fig. 40) consists from bottom to top of a ground layer, resulting from deposition from the ground surge, a basal layer and a main body, which are both deposited from the pyroclastic flow (ash flow) and a dust layer or ash cloud deposit, which is generated by elutriation of fines from the moving flow (Sparks *et al.* 1973; Fisher, 1979; Freundt and Schmincke, 1986). The main body, furthermore, may ideally be subdivided into a Lithic Concentration Zone (LCZ) at the base, a central zone, and a Pumice Concentration Zone (PCZ) at the top (Freundt and Schmincke, 1986).

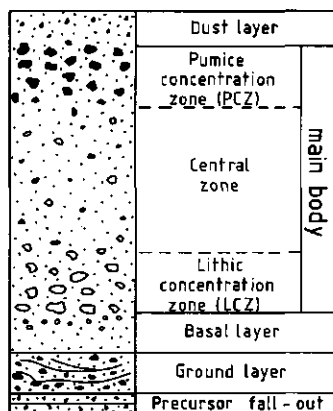


Fig. 40. Idealized sequence of a flow unit, consisting from bottom to top of a ground layer, a basal layer and a main body, which are both deposited from the pyroclastic flow (ash flow), and a dust layer or ash cloud deposit, which is generated by elutriation of fines from the moving flow. Adapted from Sparks *et al.* (1973), Fisher (1979) and Freundt and Schmincke (1986).

The pyroclastic surge and flow deposits may be underlain by fallout tephra (volcanic ash): the precursor fall-out (Fisher, 1979). The precursor fall-out results from an eruption of ash preceding the main eruptive event, *i.e.* the ignimbrite eruption.






In reality, however, a complete vertical sequence of all different layers of a single flow unit will be rarely found, because different kinds of pyroclastic flows produce different sequences. Even in a single flow the sequence may vary due to lateral facies changes.


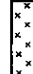
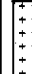
In the immediate surroundings of Guacacallo (fig. 41) and in an outcrop 1 km ESE of Saladoblanco, ground surge deposits underly the pyroclastic flow deposits. The ground surge deposits consist of an unconsolidated mass of angular white pumice fragments and phenocrysts of biotite and feldspar, showing low-angle cross-bedding and horizontal stratification (photo 25). The deposits show a layering in banks of several tens of cm to some meters with convex lower contacts. The bulk of the pumice fragments is concentrated at the base of the deposits. In thin section it is visible that the deposits are not welded. The glass matrix is completely isotropic. These ground surge deposits correspond with "ignimbrite type 1" of Kroonenberg *et al.* (1981).

A volcanic ash layer was found at several locations in the surroundings of Guacacallo, directly underlying the pyroclastic flow and surge deposits (photos 26, 27). This layer apparently represents a precursor fall out.



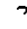

Geological map of the Guacacallo-Saladoblanco area

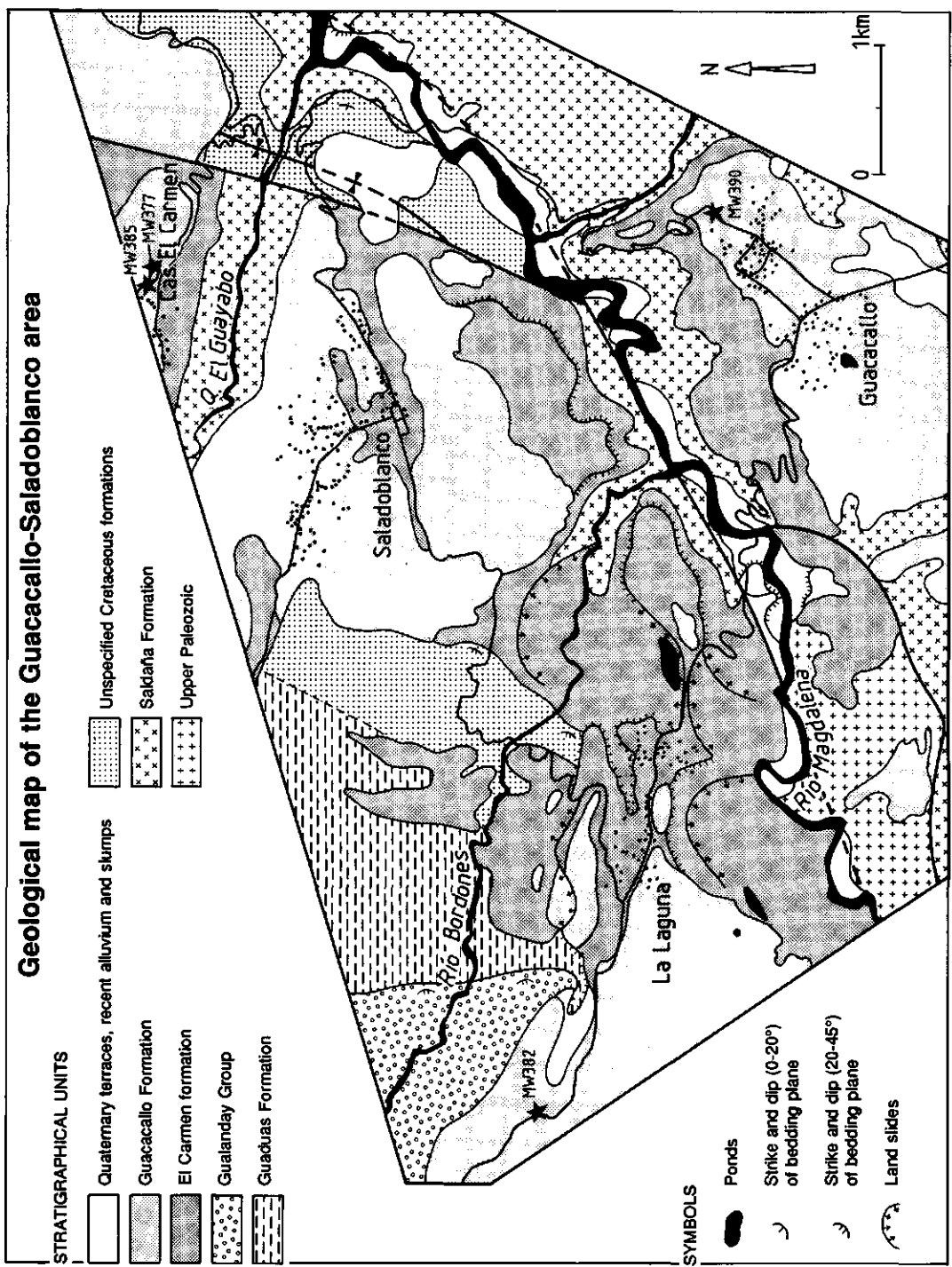
STRATIGRAPHICAL UNITS

-  Quaternary terraces, recent alluvium and stumps
-  Guacacallo Formation
-  El Carmen formation
-  Gualanday Group
-  Guaduas Formation

-  Unspecified Cretaceous formations
-  Saldaña Formation
-  Upper Paleozoic

SYMBOLS

-  Ponds
-  Strike and dip (0-20°) of bedding plane
-  Strike and dip (20-45°) of bedding plane
-  Land slides



The pyroclastic flow deposits of the Guacacallo Formation show little vertical differentiation. No separate basal layer was observed in any of the ignimbrites. A differentiation of the main body into a LCZ and PCZ was only observed in one ignimbrite outcrop, situated 1 km ESE of Saladoblanco. Most deposits contain only small quantities of lithic fragments. Generally, these angular fragments are ≤ 5 cm in size and make up only 1% of the total. Pumice fragments of the same order of magnitude were also found in small quantities in most outcrops. Both pumiceous and lithic fragments are scattered throughout the deposits and no major partings or laterally traceable textural variations are present, suggesting that the ignimbrites were deposited by a turbulent cloud rather than by laminar flow.

The pyroclastic flow deposits are well consolidated, porous and permeable. They exhibit a coarse and irregular joint system that may develop into columnar jointing and have a grey to rose-grey or purple-grey colour. At several locations a horizontal "layering" in banks of approximately 1 m is developed in the deposits. Kroonenberg *et al.* (1981) interpreted this horizontal layering as a stratigraphical phenomenon. Because no changes in the amount of lithics or pumice clasts were recorded at the transitions between the banks, it seems more likely that the layering resulted from horizontal jointing that developed during cooling of the deposit.

The pyroclastic flow deposits correspond with "ignimbrite type 3" of Kroonenberg *et al.* (1981).

The texture of the ignimbrites of the Guacacallo Formation is very similar to that of the Fish Canyon Tuff (Whitney and Stormer, 1985). This tuff is very evenly textured and has a massive appearance. The fragments have sizes of generally less than 1 cm and large pumice blocks are lacking. Within the units there is no noticeable sorting and only minor and gradational variations in grain size. The tuff has a basal vitrophyre up to 10 m thick and is locally underlain by plinian and pyroclastic surge deposits. The ash-flow portion of the outflow sheet is 20-200 m thick and shows minor variations in the degree of welding and subhorizontal jointing. The even texture and the absence of erosional topography or other evidence of a significant cooling break suggest that the tuff forms a single, compound cooling unit (Whitney and Stormer, 1985). It is shown below that the ignimbrites of the Guacacallo Formation also form a compound cooling unit.

3. Stratigraphy and field relations of the Guacacallo Formation

The ignimbrites from the Guacacallo-Saladoblanco area, located in the SE of the ignimbrite plateau, and the La Argentina-La Plata area, situated further to the NE, will be discussed separately because they show some differences in stratigraphy and field relations.

Beside the description of the stratigraphical relations, an attempt is made below to establish the number of flow units and the character of the cooling units on the base of the presence or absence of vitrophyres and columnar jointing (see section 2.1) and on the grounds of stratigraphical criteria like the presence of intercalated alluvial fan deposits.

3.1. Guacacallo-Saladoblanco area

3.1.1. Field relations of the Guacacallo and El Carmen formations

In the Guacacallo-Saladoblanco area, the ignimbrites and air-fall tuffs of the Guacacallo Formation cover an irregular paleotopography, developed in underlying fluvio-volcanic deposits. On the basis of this paleotopography and the presence of paleosols in the fluvio-volcanics, Kroonenberg *et al.* (1981) concluded that they should not be included in the Guacacallo Formation. The present author is of the same opinion. Therefore, the fluvio-volcanics were grouped into a separate informal formation, the El Carmen formation, named

Fig. 41. Geological map of the Guacacallo-Saladoblanco region. Symbols, not indicated in the legend, are explained in appendix 1 (geological map of the S. Neiva Basin).

after the hamlet of El Carmen in the NE of the area, which is the type locality. The El Carmen formation comprises volcanic debris flow deposits, torrential conglomerates, sandy fluvio-volcanic and alluvial fan deposits. The formation is found mainly along the banks of the Río Magdalena and the Río de Bordonos (fig. 41) and to a lesser extent in isolated exposures further away from the river banks. The distribution of rocks of this formation outside the Guacacallo-Saladoblanco area is unknown.

3.1.2. Descriptions

- In the direct surroundings of Guacacallo, along the SE side of the Río Magdalena, the ash flow tuffs are only some tens of meters thick. In several outcrops three different flow units can be distinguished, separated by 2-4 cm thick light-grey clay layers containing some weathered dark minerals. It is probable that these clay layers represent weathered vitrophyres. Locally, a 25-30 cm thick volcanic ash layer underlies the ignimbrites (photos 26, 27).

In this region, the Guacacallo Formation covers fluvial sediments and volcanic debris flow deposits of the El Carmen formation. The fluvial sediments are composed of very poorly sorted pebble and boulder conglomerates (torrential valley fills) and of alternating layers of horizontally stratified, poorly sorted angular conglomerate and pebbly sandstone (alluvial fan deposits). The conglomerates of the alluvial fan deposits contain a high percentage of contemporaneous andesite and dacite clasts beside Paleozoic schists and quartzites, Cretaceous black chert and Jurassic intrusives. In some of these deposits paleosol formation has occurred (photo 26). The pebble and boulder conglomerates are volcanogenic and consist mainly of contemporaneous andesite blocks.

- SW and S of Guacacallo, the ignimbrites of the Guacacallo Formation are overlain by conglomerates. These deposits consist of very poorly sorted pebble and boulder conglomerates with lenses of pebbly sandstone and sandy clay. The conglomerates, of alluvial fan origin, are composed mainly of andesite blocks and fragments ($\pm 80\%$ of the total) with minor quantities of fragments of quartzite, Triassic/Jurassic volcanoclastics and intrusives and Cretaceous rocks. In agreement with Kroonenberg *et al.* (1981), these post-ignimbritic alluvial fan deposits are not included in the Guacacallo Formation.

- WSW of the village of Guacacallo, the ignimbrite cover thickens to some 50 m. In this region the degree of exposure is very low and the precise stratigraphy of the deposits remains unclear. In several outcrops, however, alluvial fan sediments were found intercalated between the ignimbrites.

- NW of Guacacallo, N of the Río Magdalena, the thickness of the ignimbrites gradually increases to the NW to at least 140 m along the road from La Laguna to the Salto de Bordonos (La Laguna section). In the upper part of the section near-perfect columnar jointing is developed and the pumice clasts have been flattened to fiamme (photo 28), pointing to a high degree of welding.

The ignimbrite may well represent a single flow unit because large-scale grain size variations or important changes in texture are absent. The poor degree of exposure, however, precludes a more definite statement.

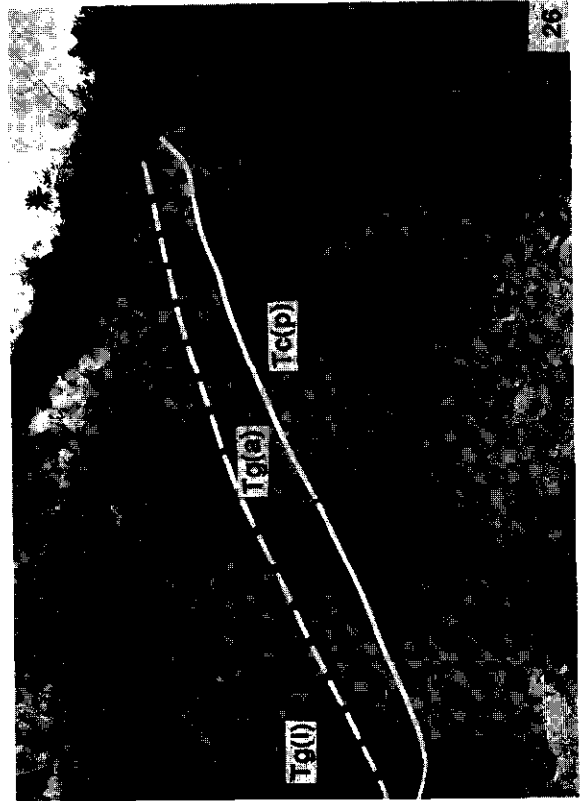
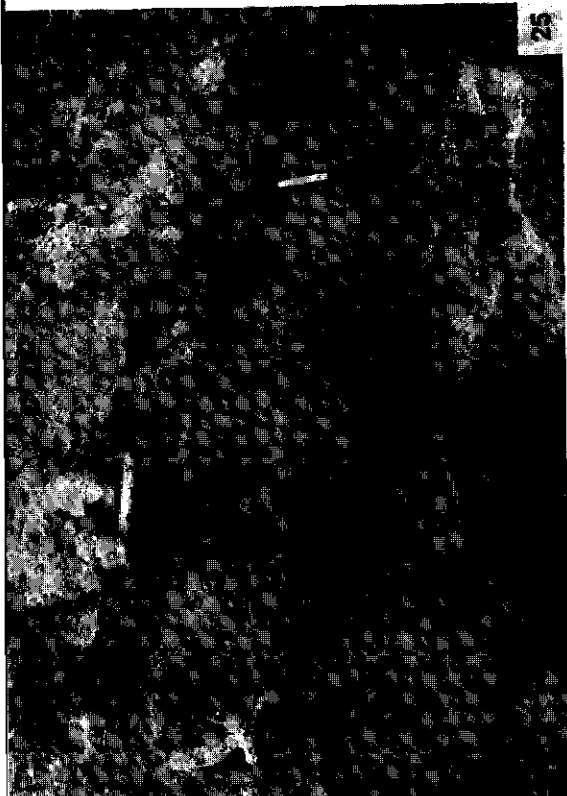
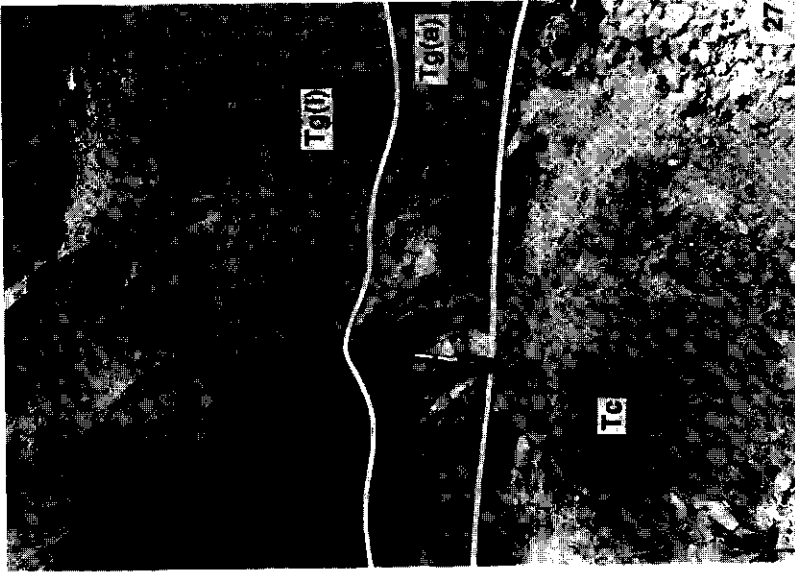
Unfortunately, the base of the ash flow tuff is not exposed. One km further to the E, however, a contact is present between an ignimbrite and a volcanic debris flow deposit of the El Carmen formation. The contact is formed by a 2 cm thick iron-oxide crust; no vitrophyre was encountered. As the outcrop lies topographically 20 m below the lowest exposure of the La Laguna section (sample MW 362c: see fig. 46), it is possible that it represents the base of the section. In that case the total thickness of ignimbrite in this region is about 160 m.

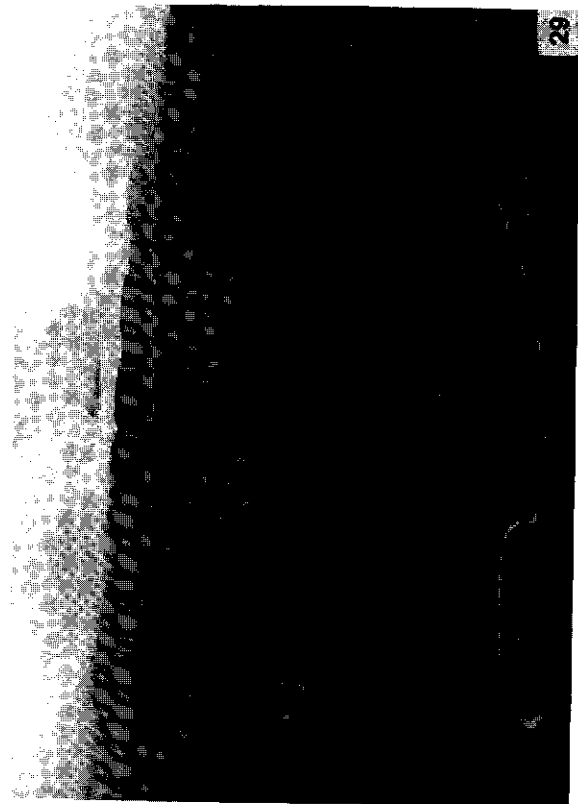
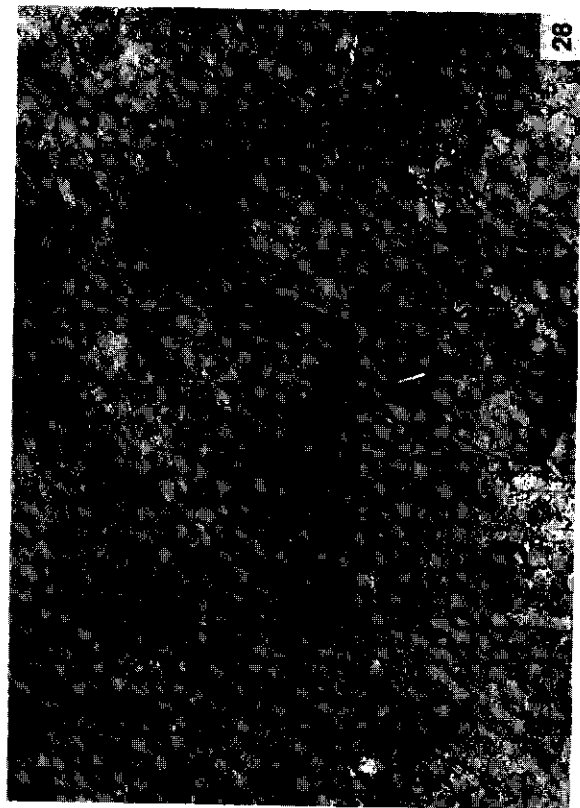
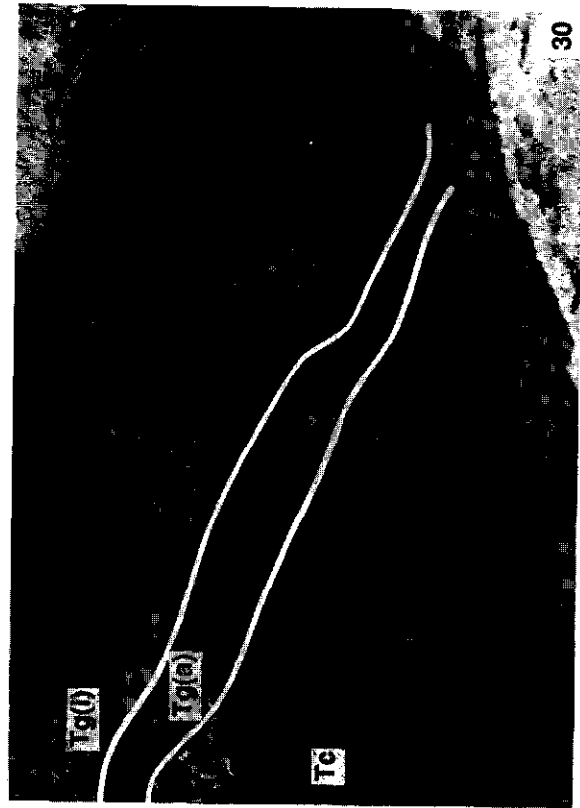
- Along the N bank of the Río Magdalena and along both banks of the Río Bordonos, terraced volcanic debris flow deposits of the El Carmen formation are found (fig. 41), showing large-scale land-sliding. At locations where the terraced deposits are undisturbed by land-sliding, it can be seen that the deposits are characterized by a very planar, undissected surface (photo 29).

Photo 25. Ground surge deposits in the Guacacallo Formation showing low-angle cross-bedding. Photo was taken 1 km WNW of Guacacallo. View of the photo is toward the N. Length of hammer is ± 30 cm.

Photo 26. Contact between fine-grained sediments of the El Carmen formation showing paleosol development (Tc(p)) and the Guacacallo Formation. At the contact, where the hammer stands, a volcanic ash layer (precursor fall-out), indicated as Tg(a), underlies the ignimbrites (Tg(i)). Photo was taken 0.5 km NE of Guacacallo. View of the photo is toward the N.

Photo 27. Contact between pebbly sandstones of the El Carmen formation (Tc) and the Guacacallo Formation (Tg). At the contact a volcanic ash layer, indicated as Tg(a), underlies the ignimbrite deposits (Tg(i)). Photo was taken 0.5 km NE of Guacacallo. View of the photo is toward the N.





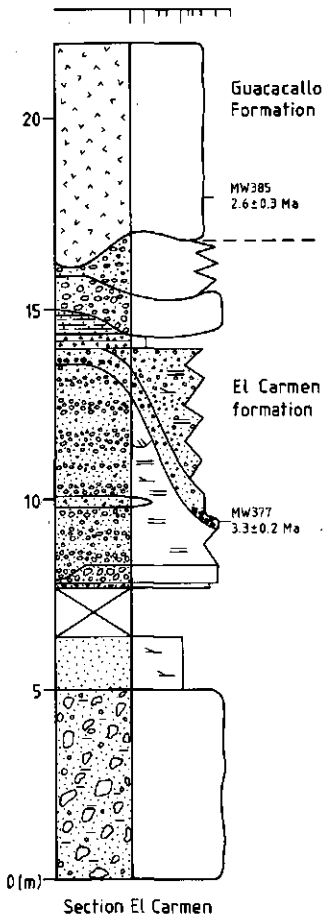


Fig. 42. Section through the El Carmen and Guacacallo fms., SE of the hamlet of El Carmen.

- In the immediate surroundings of La Laguna, two small hills are present: one along the road from La Laguna to the Salto de Bordonos, directly S of La Laguna; the other directly N of La Laguna. Both hills consist of fluvio-volcanic deposits of the El Carmen formation, overlain by ignimbrite deposits of the Guacacallo Formation. Topographically, the fluvio-volcanics are located above the terrace level. These deposits are not planed off, but have a very irregular topography which has been filled by the ash-flow tuffs.

- NW and W of Saladoblanco, ignimbrite deposits are found with a maximum thickness of ± 100 m, filling a very irregular topography in fluviovolcanics of the El Carmen formation (photo 30). Much thinner ignimbrite deposits are present SE of Saladoblanco, where they are draped over terraced, planed off deposits of the El Carmen formation.

On the N side of the Quebrada el Guayabo, SE of the hamlet of El Carmen, a measured section could be taken at the contact between the Guacacallo Formation and the underlying El Carmen formation. This section is depicted in figure 42. No vitrophyre was encountered at the base of the ignimbrite. Because only the lowermost 7 m of the Guacacallo Formation are exposed, the thickness of the flow unit could not be determined. This area is also the type locality of the El Carmen formation, exposed along the road which leads from El Carmen to the main road running between Saladoblanco and Oporapa. At this locality the El Carmen formation consists of ± 140 m of volcanic debris flow deposits, torrential conglomerates, fluvial sandstones and a single thin ignimbrite, together filling a paleotopography in underlying Cretaceous sediments. No measured section was taken, because the deposits are very poorly exposed and may be faulted.

East of El Carmen, the Guacacallo Formation is traversed by a fault. On the east side of the fault, the El Carmen formation is lacking and the Guacacallo Formation directly overlies rocks of Cretaceous age.

3.1.3. Interpretation

From the above observations the following may be concluded:

- The volcanoclastics and volcanics in the Guacacallo-Saladoblanco area may be subdivided into two formations: the El Carmen formation and the Guacacallo Formation.

Photo 28. Fiamme in the middle part of the La Laguna section, 2 km WNW of La Laguna. View of the photo is toward the W. Length of hammer is ± 30 cm.

Photo 29. Planar surface in volcanic debris flow deposits of the El Carmen formation. The planar surface was formed when the Magdalena River eroded a terrace in the deposits. In the background the contact between the terraced debris flow deposits and the Guacacallo Formation is visible. The ignimbrites of the Guacacallo Formation have been fluvially dissected, giving rise to a typical undulating morphology. View of the photo is toward the NNW.

Photo 30. Irregular topography in a torrential conglomerate of the El Carmen formation (Tc), which has been filled by an ignimbrite of the Guacacallo Formation (Tg(i)). At the contact between the two formations a volcanic ash layer, indicated as Tg(a), underlies the ignimbrite. The ignimbrite shows horizontal and vertical jointing. Outcrop is located 1 km WSW of Saladoblanco. View of the photo is toward the WNW.

Photo 31. Columnar jointing in an ignimbrite deposit, pointing to a high degree of welding. Outcrop is located along the road from the Q. la Candelaria to the hamlet of Bellavista. Man is ± 1.80 tall.

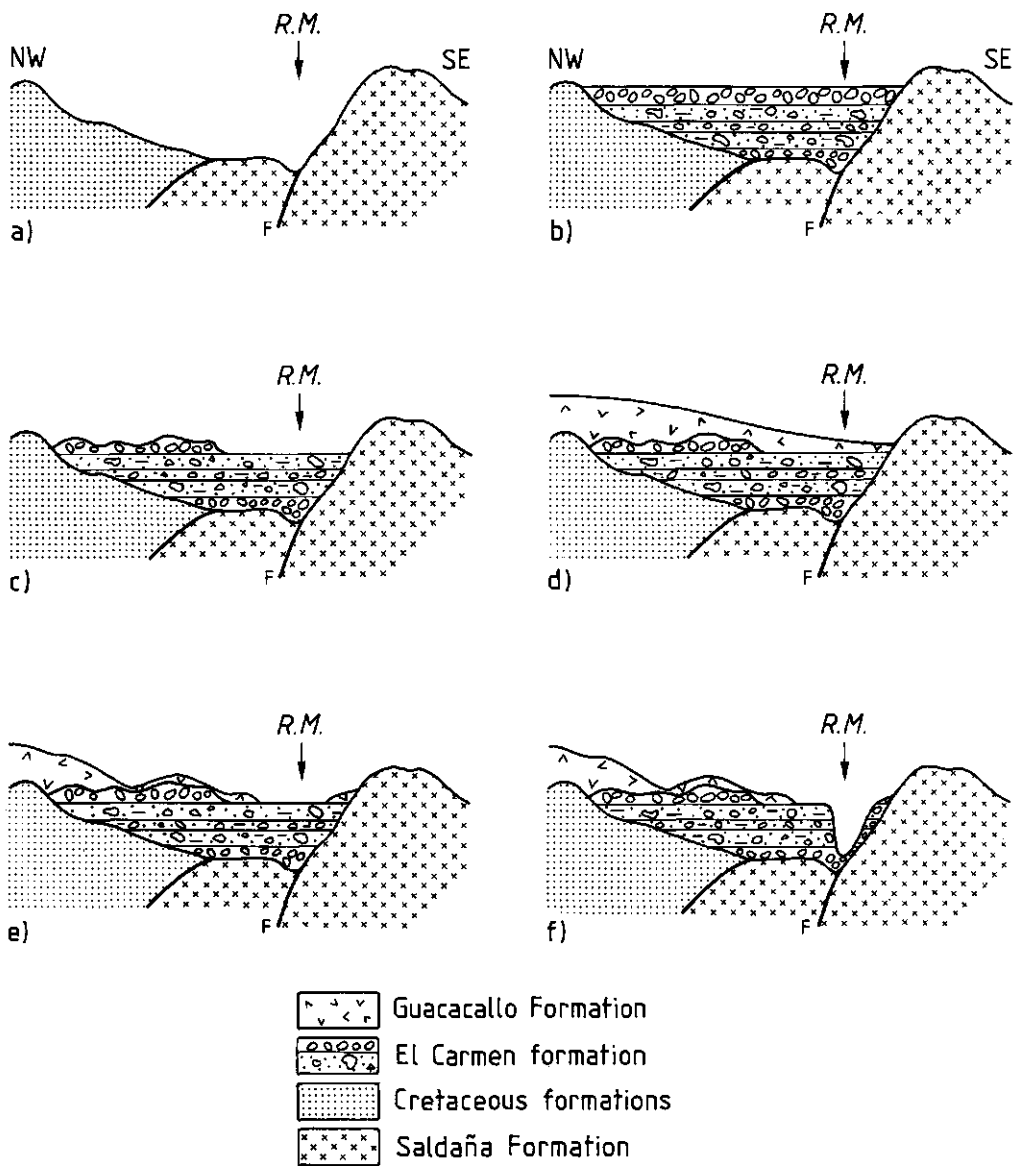


Fig. 43. Reconstruction of the Pliocene to Quaternary depositional history of the Guacacallo-Saladoblanco area. F=fault; R.M.=Río Magdalena.

- The field relations clearly indicate that the El Carmen formation is older than the Guacacallo Formation, which is corroborated by the radiometric age determinations of the deposits (see section 5). This is especially of interest, because there has been some dispute in the past as to the exact age-relationships between the two formations (Tello and Hernández, 1976; Kroonenberg *et al.*, 1981; Kroonenberg and Diederix, 1982).

- In the deposits of the El Carmen formation, two types of fluvial dissection and erosion can be distinguished. In the surroundings of La Laguna and NW of Saladoblanco, the formation shows an irregular paleotopography. Along both banks of the Magdalena River and on the SW side of the Río Bordonos, on the other hand, very planar erosion surfaces have been formed in the fluvio-volcanics.

- The Guacacallo Formation covers the irregular topography as well as the plane fluvial surface formed in the El Carmen formation.

These relations suggest that the volcanic depositional history of the area was as follows (fig. 43):

1. After deposition of the El Carmen formation, the Magdalena River eroded the fluvio-volcanics to a depth where a more resistant layer was reached (probably a very well consolidated volcanic debris flow deposit). At that level it formed a very broad planar surface. Outside the influence area of the Magdalena River a more irregular topography developed in the deposits.

2. The Guacacallo ignimbrites were erupted, filling the paleo-topography in the fluvio-volcanics.

3. Gradually the Magdalena River reoccupied its former position, dissecting the Guacacallo ignimbrites. Because the Guacacallo Formation is much less resistant to fluvial erosion than the El Carmen formation, the river again cut to the level of the resistant layer in the latter formation.

4. Considerable base level lowering of the Río Magdalena, probably in the Pleistocene, caused formation of an erosional terrace in the El Carmen formation. This terrace lies approximately 200-250 m above the present-day level of the Río Magdalena.

5. Destabilization of the terrace scarps, due to this great difference in elevation resulted in large-scale land-sliding of the deposits.

In the Guacacallo-Saladoblanco area several ignimbrite flow units are present. At least the NW part of the area seems to have been covered originally by a very thick ignimbrite that probably consists of a single flow unit. Below this thick flow unit a variable number of much thinner units, each one measuring only a couple of m in thickness, is found. These thinner flow units have different ranges: at some locations three thin flow units are present, while at others they are lacking. The thin flow units may be separated from each other by alluvial fan deposits (surroundings of Guacacallo). This fact and the presence of thin, weathered vitrophyres at the base of several of the units indicate that the flows form a compound cooling unit.

3. 2. *La Argentina-La Plata area*

3.2.1. Introduction

The ignimbrites in this area are partly separated from the ignimbrites in the Guacacallo-Saladoblanco area by the Serranía de las Minas (fig. 50), which is the main divide between the Magdalena Basin and the La Plata Basin. In this range predominantly Triassic/Jurassic and Cretaceous rocks are exposed with minor Paleozoic and Precambrian rocks. The division of the ignimbrites into a northern and a southern realm has some important consequences for the stratigraphical relationships of the Guacacallo Formation.

- In the first place, the deposits of the Guacacallo Formation N of the divide, in the La Argentina-La Plata area, cover a greater elevation interval than in the southern area: in the N they are found between <1370-2000 m; in the S between 1300-1600 m.

- In the second place, the fluvio-volcanic deposits of the El Carmen formation, which in the Guacacallo-Saladoblanco area underlie the Guacacallo Formation, are lacking in the north. The ignimbrites directly overlie Triassic/Jurassic basement rocks of the Saldaña Formation and the La Plata Batholith. In the Quebrada El Arrayán, a tributary of the Río La Plata which is located between La Argentina and La Plata on the W side of the Río La Plata, the ignimbrite deposits

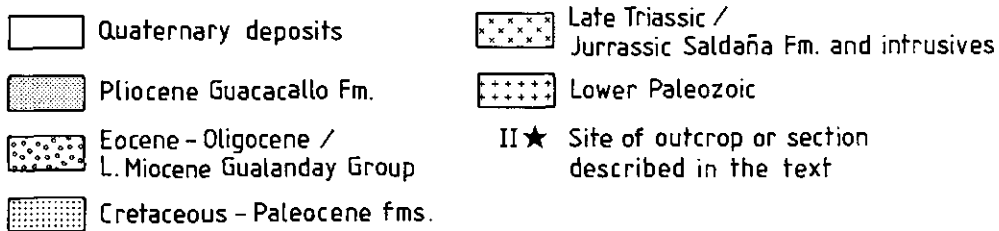
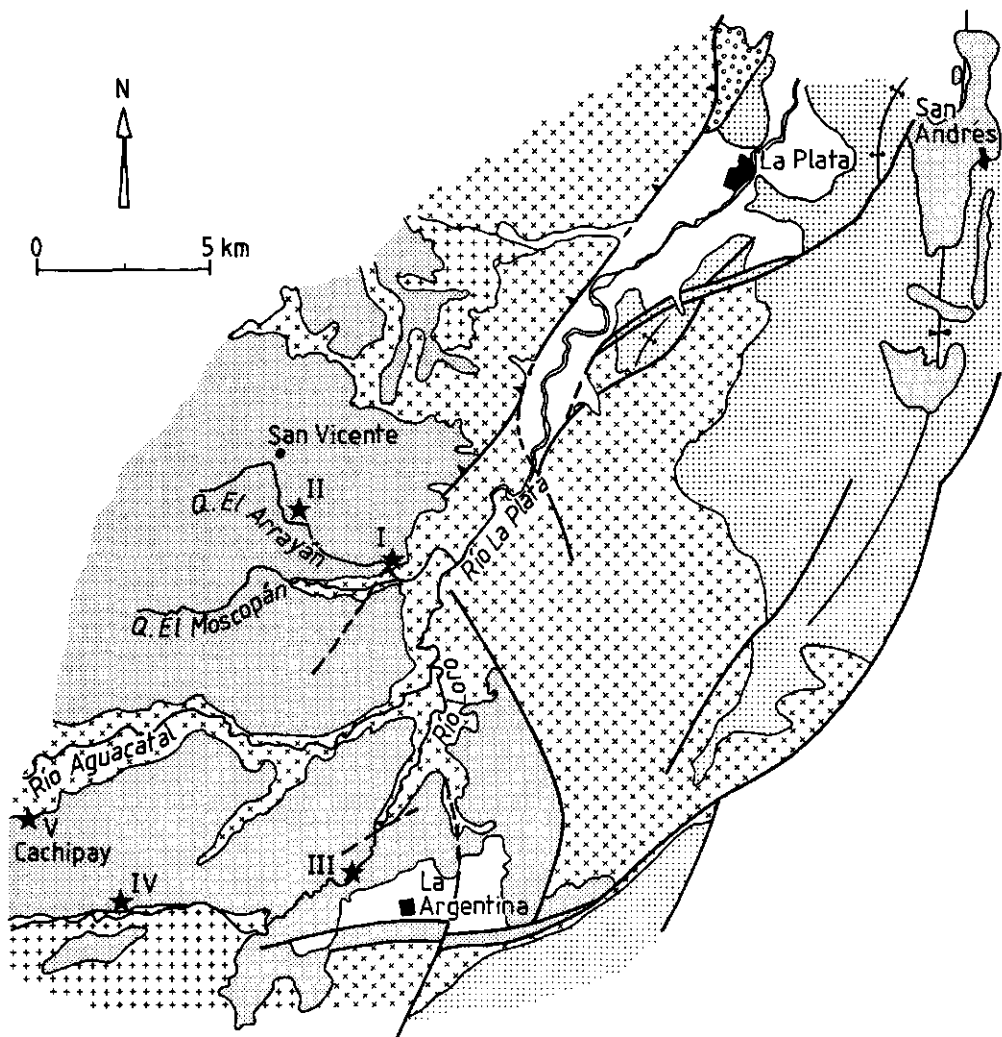


Fig. 44. Geological map of the La Argentina-La Plata area, adapted from maps by Kroonenberg and Diederix (1982) and Diederix and Gomez (in press).

are found to rest unconformably on top of deposits of the Gigante Formation (see chapter IX, section 2.1).

- Another difference between the La-Argentina-La Plata area and the Guacacallo-Saladoblanco area is that few alluvial fan sediments are intercalated between the ignimbrites. Kroonenberg *et al.* (1981) describe conglomeratic intercalations in the ignimbrites along the Río Loro near La Argentina. Unfortunately, the site where these conglomerates should crop out has been completely overgrown in the meantime and could not be located exactly.

3.2.2. Descriptions

Because of the low degree of exposure and the deep weathering of the ignimbrites, it was impossible to construct a geological map of the area and to determine precisely the number of flow units. Only a limited number of outcrops could be studied. The most important outcrops are described below. Their location is indicated in figure 44.

I. The section in the Quebrada el Arrayán has already been discussed in chapter IX. In this quebrada the deposit consists of at least one flow unit with a thickness of ± 250 m. This flow unit has a 5 m thick vitrophyre at its base. Below the vitrophyre a channel is present, filled with ignimbrite blocks. It is likely that the channel fill also forms part of the Guacacallo Formation and represents an older ignimbrite unit that was broken up by fluvial activity, following deposition of ignimbrites elsewhere.

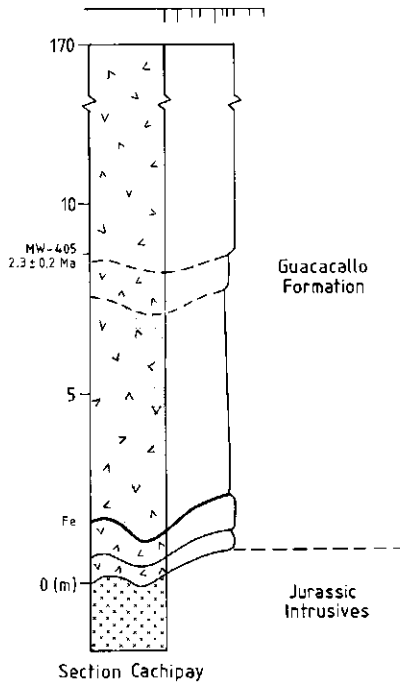


Fig. 45. Stratigraphical section through the lower part of the Guacacallo Formation, Cachipay. For legend, see fig. 16, p. 48.

II. 2.5 km SSE of the hamlet of San Vicente, some 35 m of unwelded ignimbrite are exposed. The deposit contains a relatively large amount of angular lithic fragments compared to other ignimbrite deposits, especially in the middle part of the exposure. Here the ignimbrite is agglomeratic and comprises up to 16 cm big fragments of andesite, dacite, quartz, schist and granite. Pumice fragments and carbonized wood fragments abound throughout the deposit.

No flow unit boundaries were encountered. It could not be determined whether the deposit forms part of the same very thick ignimbrite unit in the Quebrada el Arrayán, some 2.5 km further to the ESE, or may be part of another, younger flow unit overlying it. Topographically, the deposit lies at a higher elevation (± 1700 m) than the flow unit in the Q. El Arrayán, which is situated between 1400-1650 m.

III. Along the road from La Plata to La Argentina, 120 m of ignimbrite are exposed between the point where the road starts its descent to the Río Loro at 1490 m and the bridge at 1370 m. The base of the ignimbrite is not exposed, but occurs ± 200 -250 m below the bridge, according to Kroonenberg *et al.* (1981). If this supposition is correct, the total thickness of ignimbrite at this location amounts to some 320-370 m. It is unclear whether the outcrop consists of a single flow unit, because the degree of exposure is rather poor.

IV. Just E of the hamlet of Belén, a 50 m thick ignimbrite is exposed. No vitrophyres or other indications of limits between flow or cooling units were observed. Unfortunately the outcrop does not reach to the base.

V. In the section Cachipay, 5 km NW of Belén, two thin ignimbrite flow units are observed below a much thicker flow unit with a minimum thickness of 170 m. At the base of the thick flow unit a 6 m thick vitrophyre is present (fig. 45). No vitrophyres were encountered at the base of the two thin flow units.

VI. Five km further to the W, along the road from the Quebrada la Candelaria to the hamlet of Bellavista, a thick ignimbrite deposit is found to rest directly on basement rocks. The base of the flow unit is formed by a several m thick vitrophyre. The minimum thickness of the flow unit is 100 m. In the upper part of the outcrop perfect columnar jointing is developed, pointing to a high degree of welding (photo 31). The position of this outcrop could not be indicated in fig. 44, because it lies further to the west.

3.2.3. Interpretation

From the above it follows that the stratigraphy of the formation in this area is broadly comparable to the stratigraphy in the Guacacallo-Saladoblanco area. Again one thick flow unit appears to be present, underlain by a few thin flow units. In contrast to the Guacacallo-Saladoblanco area, however, an agglomeratic ignimbrite is found, which is either a separate unit or forms the top of the thick flow unit.

Although vitrophyres at the base of the thin units are lacking, the presence of a vitrophyre at the base of the thick ignimbrite unit in the section Cachipay indicates that the flow units form a compound cooling unit. Vitrophyres are probably absent from the lower ignimbrite units, because the units were too thin (the ignimbrites are only ± 1 m thick each), causing neglectable temperature differences between the central part and the base of the tuffs during cooling.

4. Petrography of the Guacacallo Formation

4.1. Welding and devitrification: microscopical and macroscopical observations

Both field observations and thin sections indicate that the thin flow units in the surroundings of Guacacallo and La Laguna, as well as in some of the sections of the La Argentina-La Plata region are unwelded or only very slightly welded.

In the field it is visible that the interiors of the thicker flow units are moderately welded. This is corroborated by the thin sections: only samples from the central part of the thick units show flattened and deformed glass shards and pumice fragments (fiamme) which are occasionally bent around phenocrysts. Both shards and fiamme are oriented horizontally, giving the rock a preferential orientation.

The vitrophyres at the base of the flow units are very strongly welded. In thin section they are characterized by a black matrix of volcanic glass containing phenocrysts, some lithic fragments and black fiamme. The glass shards are strongly deformed and both fiamme and shards define a planar foliation. The matrix is not devitrified. The vitrophyres correspond with "ignimbrite type 2" of Kroonenberg *et al.* (1981).

The majority of the ignimbrite samples is strongly devitrified. Primary devitrification is the process whereby glass shards and pumice fragments within an ignimbrite experience partial or complete recrystallisation to quartz (cristobalite) and alkali feldspar. This process takes place at high temperatures during emplacement, in combination with a slow cooling rate. Devitrification tends to prevail in densely welded ignimbrites, but more-porous tuffs may also be devitrified (Cas and Wright, 1987). In the presently described ignimbrites, primary devitrification of the glass shards has led to the formation of fibrous alkali feldspar and quartz. At the rims of the shards the fibrous crystals are organized in a axiolic structure; in the center of the shards graphic intergrowths of feldspar and quartz occur. The formation of high-temperature quartz shows that even in the unwelded deposits the temperature was high enough and cooling sufficiently protracted to cause primary devitrification of the ignimbrites.

Beside primary devitrification of the tuffs, vapour phase crystallization may occur in ignimbrites as a result of the percolation of hot gases through the deposits during cooling. The vapour phase originates from juvenile glass particles and heated ground water. During compaction and welding, the gasses escape and move upwards, reacting with solid material (Cas and Wright, 1987). As a result of vapour phase crystallization the ignimbrite becomes lithified by crystallization of high temperature vapor phase crystals, *i.e.* silica polymorphs and alkali

feldspar (Fisher and Schmincke, 1984). Vapour phase crystallization is commonly found towards the top of an ignimbrite sheet and may lead to chemical alterations within this part of the deposit. An example is given in section 6.2.

4. 2. *Microscopical description of the ignimbrites*

In thin section the ignimbrites are shown to have a vitrophyric structure. They may be described as vitric crystal-bearing tuffs. The matrix of the rocks consists of X and Y-shaped glass shards grading into small pumice fragments. The predominance of X and Y-shaped shards over shards with intact vesicles indicates that the majority of the vesicles was destroyed during eruption.

Phenocrysts of feldspar (plagioclase), biotite and quartz form between 12-20% of the total volume. Apatite, zircon and opaques are accessories.

The euhedral to subhedral plagioclase crystals, which form 5-15% of the total volume, are up to 3-4 mm in length. Some phenocrysts may be fragmented to elongate, triangular shards. From the fact that these shards lie scattered throughout the deposits, it is clear that fragmentation of the phenocrysts also took place during the eruption and not during cooling and compaction. Beside corrosive embayments the phenocrysts also show dissolution and recrystallisation features. The phenocrysts may contain inclusions of apatite and biotite. They often show a fine-scale oscillatory optical zoning, representing a compositional variation of only 1-3% from the average, which ranges between An₁₈₋₂₄. This composition corresponds to oligoclase.

The biotite phenocrysts, which make up 1-3% of the total volume, vary in length between 2-4 mm. The red to red-brown pleochroitic crystals are generally euhedral and often contain inclusions of plagioclase. Many of the crystals have developed a fine-grained oxide-rich reaction rim of opacite or are completely altered to opacite. As this biotite alteration is common in most sections and outcrops, it is probably a late-depositional phenomenon.

The quartz crystals have a maximum size of 1 mm and form 3-5% of the total volume. These phenocrysts are high temperature bipyramidal crystals, showing extensive corrosive embayments. Cavities are filled with glass.

In a sample (MW 413), taken at the point where the road to La Argentina crosses the Río Loro and in one of the thin flow units from the surroundings of Guacacallo, some small phenocrysts of green to green-brown pleochroitic hornblende were encountered.

Pumice fragments of up to 2 cm in size are present in small but variable quantities. Generally these fragments are not welded and white. In some rocks the pumice fragments are collapsed and welded to fiamme. These elongate fragments are oriented horizontally and have a purplish colour.

In most thin sections $\leq 1\%$ xenoliths are found. Both cognate and non-cognate xenoliths are present. The cognate xenoliths comprise devitrified glass fragments with phenocrysts of biotite and plagioclase, and magma chamber or crater wall fragments consisting of crystals of biotite, plagioclase and opaques with a hypidiomorphic structure. The non-cognate xenoliths include fragments of andesite, slate, schist and intrusives.

5. Geochronology of the Guacacallo Formation

In order to date the Guacacallo Formation, samples were collected at different locations in both areas and used for K-Ar mineral and zircon fission track age determinations. Analytical procedures were identical to those described in chapter II, section 2 and chapter IV, section 1. The results of the K-Ar age determinations are given in table XXII; the results of the fission track analyses are given in table XXIII. Because the ignimbrites from both the Guacacallo-Saladoblanco and the La Argentina-La Plata areas fill a very irregular paleotopography, both the elevation of the samples above sea level and the (estimated or measured) height of the samples above the base of the Guacacallo Formation are indicated in table XXII.

When the calculated K-Ar and fission-track ages of the different samples with their standard deviations and their position in the stratigraphy are considered, it emerges that most samples have ages around 2.5 ± 0.2 to 2.6 ± 0.2 Ma. Although the Guacacallo ignimbrites form a compound cooling unit, it is likely that they were erupted during a single eruptive period. According to Fisher and Schmincke (1984), cooling from emplacement to ambient temperature in a single flow unit takes place in some tens of years, suggesting that cooling of a compound cooling unit will only last a few thousands of years.

Compared with the ages of the other samples, the K-Ar ages of samples MW 408 and MW 413 are somewhat old. When the fission track ages and the standard deviations of samples MW 408 and MW 399 are considered in relation to their K-Ar ages it appears that, although most ages overlap, the fission-track ages are slightly younger. The zircon grains used for the determination

Table XXII. K-Ar mineral data of the Guacacallo and El Carmen formations.

Sample no.	Locality	Elevation of outcrop or section (m)	Height above/below base of Guac. Fm. (m)	Mineral	K (ppm wt.)	Radiogenic ⁴⁰ Ar (ppb wt.)	Atmospheric ⁴⁰ Ar (% total ⁴⁰ Ar)	Calculated age (Ma)
Guacacallo-Oporapa area								
MW 377	El Carmen (Oporapa)	1500	-5	Biotite	6.62	1.48	88	3.3±0.2
MW 385	El Carmen (Oporapa)	1510	2	Biotite	6.62	1.52	88	
MW 382	La Laguna-S. de Bordones	1550	100	Biotite	6.11	1.15	96	2.6±0.3
MW 390	Guacacallo	1400	1	Biotite	6.13	1.07	96	
					6.33	1.15	92	2.4±0.2
					6.24	1.02	90	
					5.93	1.03	93	2.5±0.2
					5.95	1.05	95	
La Argentina-La Plata area								
MW 399	Candelaria-Bellavista	2000	10	Biotite	6.28	1.17	91	2.8±0.2
MW 408	Belén	1980	>100?	Biotite	6.28	1.23	90	
MW 413	Río Loro (La Argentina)	1390	200-250?	Biotite	6.17	1.28	79	2.9±0.2
MW 405	Cachipay	1960	8	Biotite	6.19	1.17	84	
					6.33	1.21	77	2.8±0.1
					6.33	1.23	78	
					6.14	0.98	90	2.3±0.2
					6.14	0.99	93	
S. Neiva Basin								
MW 77	Tarqui	1190	2	Biotite	6.68	1.27	90	2.8±0.2
					6.68	1.36	91	

Table XXIII. Fission track analytical data of zircons from the Guacacallo Formation.

Sample	ρ_s^1 ($\times 10^6$ t/cm^2)	ρ_i^2 ($\times 10^6$ t/cm^2)	t^3 ($\times 10^6$ yr)	1σ ($\times 10^6$ yr)	Number of grains	ρ_{glass}^4 ($\times 10^5$ t/cm^2)	Uranium (ppm)	$P(\chi^2)$ %
Zircon								
MW 385	0.62 (173)	15.45 (2159)	2.3	0.4	10	186782.9 (2883)	509	10
MW 399	0.63 (134)	17.39 (1860)	2.1	0.4	10	186782.9 (2883)	574	15
MW 408	0.80 (149)	19.78 (1837)	2.3	0.4	10	186782.9 (2883)	652	12

1) ρ_s : density of spontaneous fission tracks; the number of actually counted tracks is given in parenthesis

2) ρ_i : density of induced fission tracks; the number of actually counted tracks is given in parenthesis

3) age calculated according to the Zeta approach with a Zeta value of 308.1; zircon standard used: Fish Canyon with a calculated age of 27.2 ± 3.5 Ma.

4) ρ_{glass} : density of fission tracks in standard glass NBS 962; the number of actually counted tracks is given in parenthesis

of the fission track ages of these samples come from very homogeneous populations without reworked grains. In all cases the zircon grains were transparent and rose-coloured, pointing to a volcanic origin. It is likely that the slight differences between the fission track ages and the K-Ar ages on the one hand, and the slightly older ages of samples MW 408 and MW 413 on the other hand, should be attributed to the presence of some small xenoliths in the ignimbrites, which may have had some influence on the K-Ar ages.

An alternative interpretation, *i.e.* that the age differences have time-stratigraphical meaning and that the different ignimbrites of the Guacacallo Formation were erupted over a period of several million of years, separated by periods of erosion and non-deposition, seems unlikely because the samples giving the oldest K-Ar ages are generally located relatively high above the base of the formation (table XXII). Besides, no phenomena indicative of prolonged erosion like paleorelief or paleosol formation were observed in the deposits.

In the section taken just E of the hamlet of El Carmen in the Guacacallo-Saladoblanco area (fig. 42), a K-Ar age was obtained from a pumice concentration just below the contact between the Guacacallo Formation and the El Carmen formation (sample MW 377). The origin of the deposit is unclear. As it lines the walls of a fluvial channel, it is possible that it represents either an air-fall tuff or a thin ignimbrite. The pumice gave an age of 3.3 ± 0.2 Ma. This is the only datable sample obtained from the El Carmen formation: the lower part of the formation could not be dated, because no suitable material was available. The ignimbrite directly overlying the El Carmen formation at this site gave a K-Ar age of 2.6 ± 0.3 Ma and a fission track age of 2.3 ± 0.4 Ma (sample MW 385).

A sample from the only ignimbrite deposit encountered within the S. Neiva Basin (sample MW 77), gave a K-Ar mineral age of 2.8 ± 0.2 Ma, which agrees with the ages of the other tuffs. Therefore, it is clear that the ignimbrite is an isolated remnant of the Guacacallo Formation which apparently covered a much greater area before erosion and fluvial dissection took place.

K-Ar biotite ages of 7.1 ± 0.3 Ma and 3.7 ± 0.2 Ma of the Guacacallo ignimbrites published respectively by Kroonenberg *et al.* (1982) and Murcia and Pichler (1986) appear to be too old. As in the case of samples MW 408 and MW 413, the possibility cannot be excluded that this is due to contamination of the samples with some exotic xenoliths, *e.g.* Paleozoic schist fragments, leading to erroneous ages.

6. Geochemistry of the Guacacallo Formation

6.1. Introduction

The major element chemistry of 29 samples was determined with the aid of XRF analysis. Analytical methods were identical to those described in chapter V, section 2.2.1. Beside samples from isolated outcrops in the Guacacallo-Saladoblanco and La Argentina-La Plata areas, two series of samples from apparently single flow units from both regions were analysed. The first series of samples was collected along the road from La Laguna to the Salto de los Bordonos. Just N of the village of La Laguna, which lies at an elevation of ± 1300 m, the road begins to ascend steadily until it reaches its highest point at ± 1590 m. A thick ignimbrite flow unit is exposed between 1430 and 1590 m (see also section 3.1.2). Samples were taken at elevation intervals of approximately 20 m (fig. 46). The second section was sampled along the road from La Plata to La Argentina between the point where the road starts its descent to the Río Loro and the bridge (fig. 44). Along the river banks, some 120 m of ignimbrite crop out at elevations between 1370 and 1490 m (see also section 3.2.2). Samples were taken every 15-25 m for chemical analysis.

The major reasons for performing major element chemistry were 1) to compare the chemistry of the different groups of samples (both from isolated outcrops and from the sections) in order to investigate whether the ignimbrites from both regions might be compositionally related to one another, 2) to compare the chemistry and the chemical variation of the La Laguna and La Argentina sections in order to determine whether the units may have been erupted from a zoned magma chamber.

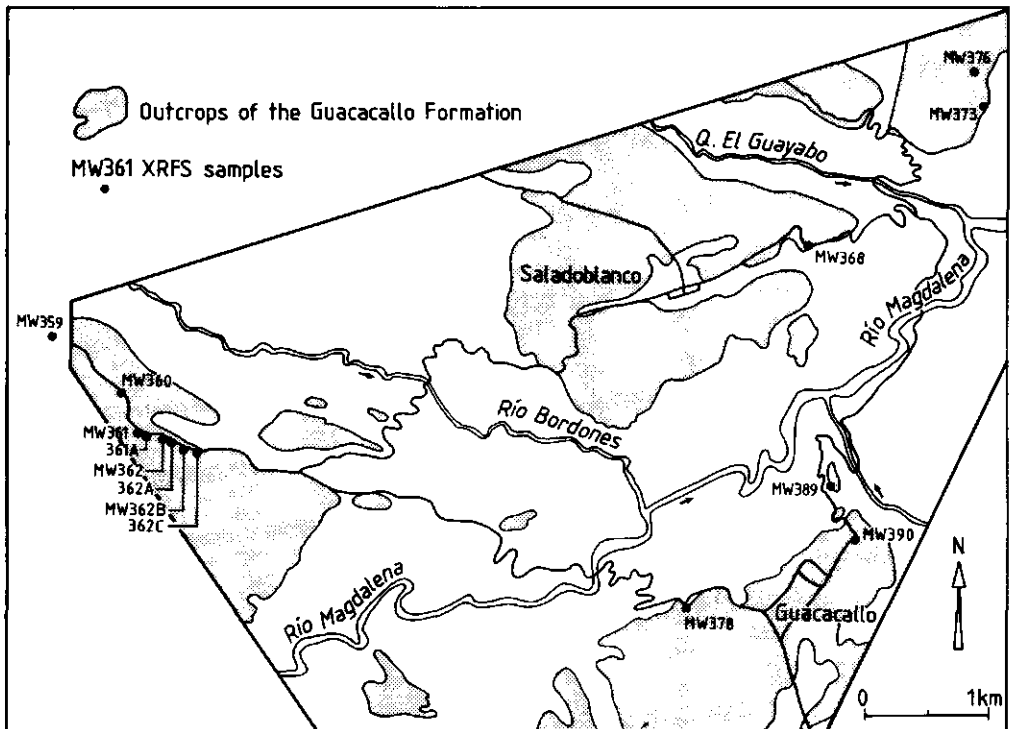


Fig. 46. Location of XRF samples in the Guacacallo-Saladoblanco area.

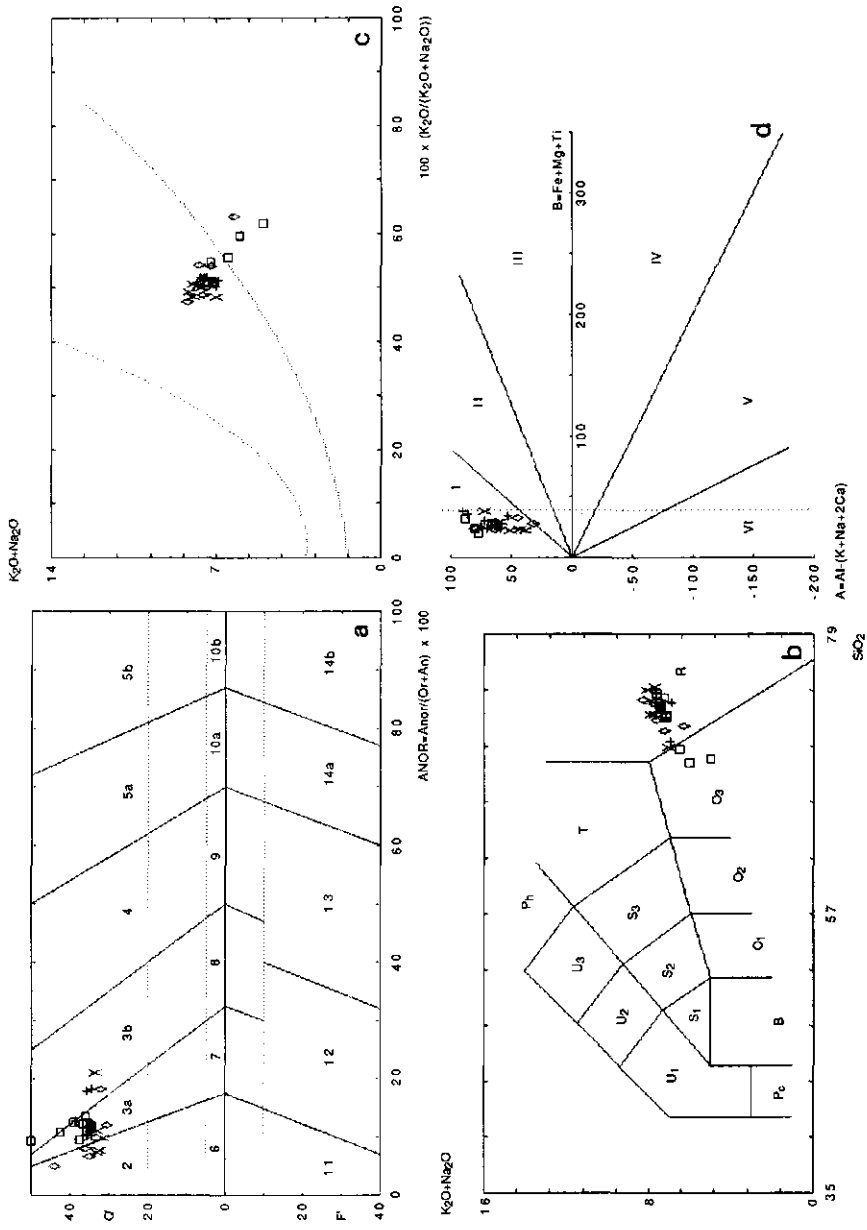


Fig. 47a. Ignimbrites of the Guacacallo Formation in a Q'-ANOR diagram (Streckeisen and Le Maitre, 1979). Fig. 47b. Idem, in a diagram of total alkalis vs. silica (Le Bas *et al.*, 1986). Fig. 47c. "Igneous Spectrum" (Hughes, 1973). Fig. 47d. BA diagram of Debon and Le Fort (1983). Field labels are from the original publications. Symbols are as follows: open squares: La Laguna Section; plus signs: La Argentina Section; diamonds: isolated outcrops in the Guacacallo-Saladoblanco area; crosses: isolated outcrops in the La Argentina-La Plata area.

6.2. Results and discussion

Classification of the ignimbrites

Chemical analyses of all samples are given in appendix 4, together with calculated CIPW norms. These data show that the silica content of the Guacacallo ignimbrites varies from 68.9 to 74.4 percent. In a Q'-ANOR diagram (Streckeisen and Le Maitre, 1979) most samples classify as rhyolites and alkali-rhyolites (fig. 47a). Five samples are rhyodacites. In a diagram of SiO₂ against total alkalis (Le Bas *et al.*, 1986) the majority of the rocks plot in the rhyolite field, while the upper three samples from the La Laguna section plot in the rhyodacite field (fig. 47b).

Origin of the ignimbrites

Comparison of the percentages of oxides and the CIPW norms of the ignimbrites with the average rhyolite composition (Le Maitre, 1976) indicates that the weight percentage of Al₂O₃ is high. In the normative mineral assemblage the weight percentage of corundum is extremely high, reaching values that may be 11 times the value of the average rhyolite. Especially the upper three samples of the section La Laguna give very high corundum values (appendix 4).

In an AFM plot the bulk compositions of all ignimbrite groups fall in the alkali-rich part of the calc-alkaline field (fig. 27, p. 88). Debon and Le Fort (1983) developed a diagram which discriminates between peraluminous and metaluminous rocks. When the Guacacallo ignimbrites are plotted in such a diagram, the rocks are found to belong to the peraluminous domain (fig. 47d). Furthermore, the diagram indicates that the rocks contain less than 7% of dark minerals ($B < 38.8 \text{ gramatoms} \times 10^3$) and should be classified as leucocratic. The position of the ignimbrites in the peraluminous domain and the attitude of the distribution line of the data points in the diagram (*i.e.* the direction of the major evolutionary trend), which in the case of the ignimbrites is vertical, together indicate that the ignimbrites belong to the aluminous association. This association is mainly or completely derived from the anatexis of crustal material.

Average ANKC ratios (Chappell and White, 1974, 1984) for the four groups of samples are given in table XXIV. As the values of all groups, including their standard deviations, are greater than 1.05, the limit between I-type and S-type rocks, it is clear that the ignimbrites formed from

Table XXIV. Average compositions of the four ignimbrite sample groups.

	La Laguna Section x σ (n=6)		La Argent. Section σ (n=7)		Guacacallo- Saladobl. area σ (n=6)		La Argentina- La Plata area σ (n=6)	
	x		x		x		x	
SiO ₂	73.41	0.73	72.93	1.19	72.71	1.05	73.14	1.72
TiO ₂	0.21	0.02	0.23	0.04	0.24	0.02	0.24	0.04
Al ₂ O ₃	14.80	0.60	14.95	0.74	14.45	0.16	14.51	0.63
Fe ₂ O ₃	1.52	0.22	1.76	0.32	1.64	0.56	1.45	0.35
MnO	0.06	0.02	0.04	0.02	0.05	0.01	0.07	0.02
MgO	0.19	0.05	0.23	0.07	0.24	0.05	0.23	0.06
CaO	0.62	0.07	0.72	0.17	0.58	0.26	0.61	0.25
Na ₂ O	3.56	0.17	3.56	0.13	3.51	0.68	3.92	0.19
K ₂ O	3.78	0.12	3.74	0.17	3.92	0.17	3.83	0.22
P ₂ O ₅	0.02	0.00	0.02	0.01	0.03	0.01	0.03	0.01
SiO ₂ /Al ₂ O ₃	4.96	0.24	4.89	0.30	5.03	0.10	5.05	0.30
ANKC	1.35	0.05	1.34	0.06	1.34	0.19	1.25	0.06
Zr (ppm)	135	15	148	42				

a magma with a continental origin, corroborating the results of the BA diagram (fig. 47d). A continental origin of the ignimbrites has already been suggested by various other authors (Schmitt, 1983; Murcia and Pichler, 1986). Such an origin would also account for the enrichment in Al_2O_3 shown by the samples when compared to the average rhyolite composition given by Le Maitre (1976).

Comparison of the chemical characteristics of the four sample groups

For the calculation of the average compositions of the four sample groups, the three samples from the section La Laguna with SiO_2 -contents <70% were left out of consideration. The results are given in table XXIV. Within error, the compositions of the four groups are identical, as are the $\text{SiO}_2/\text{Al}_2\text{O}_3$ ratios and the ANKC ratios.

In order to investigate whether the ignimbrites from both regions might be related to one another, average compositions of the four sample groups were calculated and variation diagrams were drawn in which various oxides are plotted against SiO_2 (fig. 48). The figures clearly indicate that the different groups of ignimbrites show comparable chemical trends, independent of their stratigraphical and regional position. The oxides TiO_2 , Al_2O_3 , Fe_2O_3 and MgO decrease with increasing SiO_2 content, while Na_2O and K_2O increase. Only the behaviour of CaO as a function of the weight percentage of SiO_2 is more variable and unpredictable.

When siliciumoxide is plotted against total alkalis and against $\text{Al}_2\text{O}_3+\text{Fe}_2\text{O}_3+\text{MgO}$, identical trends are found as for the separate oxides, but with a much better correlation coefficient than the one obtained for the separate oxides:

- The correlation coefficients (R^2) for Al_2O_3 , Fe_2O_3 and MgO are 0.632; 0.458 and 0.376 respectively; the R^2 for $\text{Al}_2\text{O}_3+\text{Fe}_2\text{O}_3+\text{MgO}$ equals 0.707.
- The correlation coefficients for the separate alkali-oxides are 0.497 (Na_2O) and 0.490 (K_2O) respectively, the correlation coefficient for a best fit in a diagram of total alkalis against SiO_2 equals 0.617.

This is not the case when SiO_2 is plotted against $\text{Na}_2\text{O}+\text{K}_2\text{O}+\text{CaO}$ or against $\text{Fe}_2\text{O}_3+\text{MgO}+\text{TiO}_2$. The first observation implies that sodium and potassium are completely interchangeable. The relation between SiO_2 and total $\text{Al}_2\text{O}_3+\text{Fe}_2\text{O}_3+\text{MgO}$ might indicate that aluminium, iron and magnesium are also interchangeable in the glass matrix of the ignimbrites. It is unlikely that the relation is caused by the interchangeability of these elements in biotite: from figure 47c and from the volume percentages of phenocrysts found in the thin sections (section 4.2) it is clear that the chemistry of the ignimbrites is completely controlled by the chemistry of the light minerals and the matrix, and that ferromagnesian minerals play a minor role.

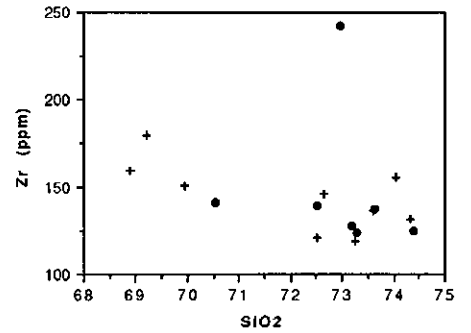
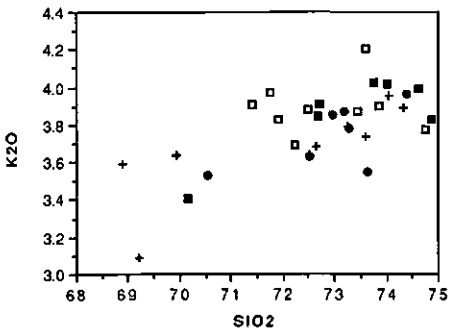
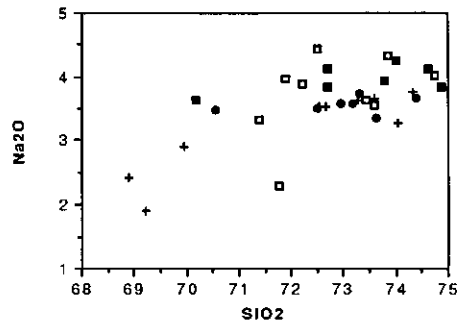
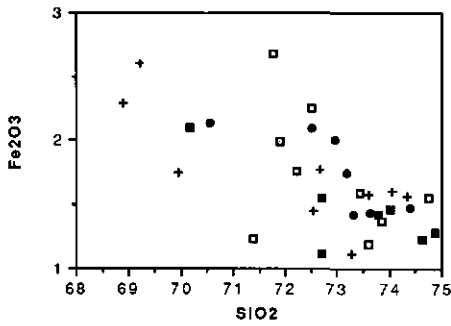
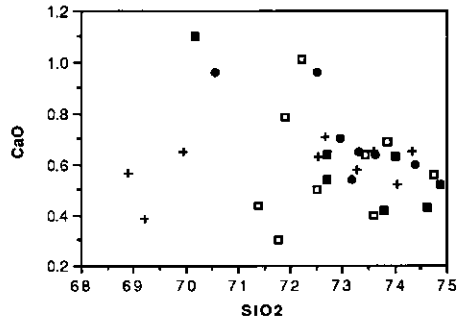
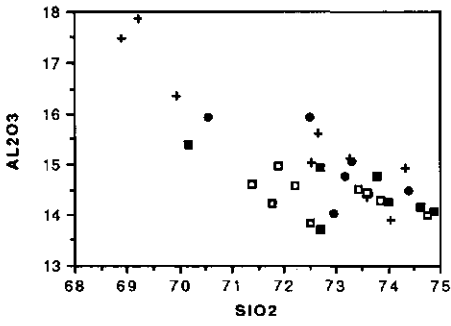
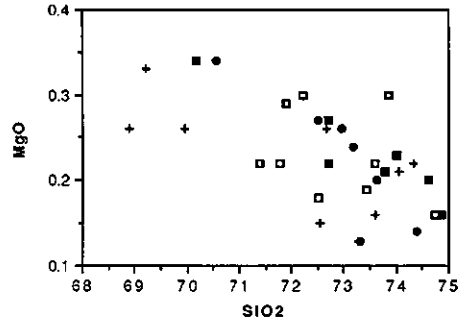
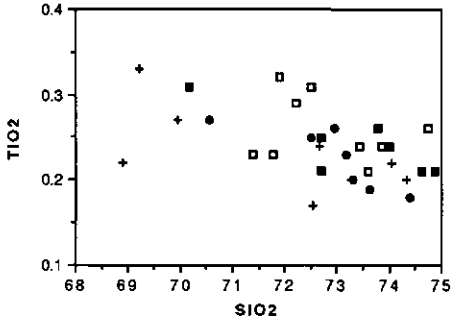
These results and the fact that the different samples show narrow distributions in the Streckeisen/Le Maitre and the Debon/Le Fort diagrams suggest that all ignimbrites are closely related to one another and probably were erupted from the same volcanic entity.

Chemical variation with stratigraphical height: a comparison of the La Laguna and La Argentina sections

In order to investigate whether the ignimbrites may have come from a zoned magma chamber, as described by Hildreth (1979) for the Bishop Tuff, the data of the La Laguna section were plotted against stratigraphical height. Hereby it was assumed that the lowermost sample, sample MW362c (fig. 46), is positioned 20 m above the base of the La Laguna section (section 3.1.2.).

The results are shown in fig. 49 (to the left). Most oxides (SiO_2 , TiO_2 , Fe_2O_3 , MgO , total $\text{Al}_2\text{O}_3+\text{Fe}_2\text{O}_3+\text{MgO}$, Zr) appear to show a more or less systematic variation with the elevation, although the correlation coefficients of the diagrams are rather low. While the weight percentages of siliciumoxide decreases towards the top of the flow unit, the percentages of the ferromagnesian elements, Al_2O_3 , Zr and the total of $\text{Al}_2\text{O}_3+\text{Fe}_2\text{O}_3+\text{MgO}$ increase.

The trend is lacking in the alkali-oxides, which appear to be independent of stratigraphical height. Only in the upper three samples of the La Laguna section, which have a rhyodacitic composition (see above) the alkalis show a correlation with the elevation. When the samples are plotted in the alkali ratio diagram of Hughes (1973) it appears that these rhyodacites plot outside



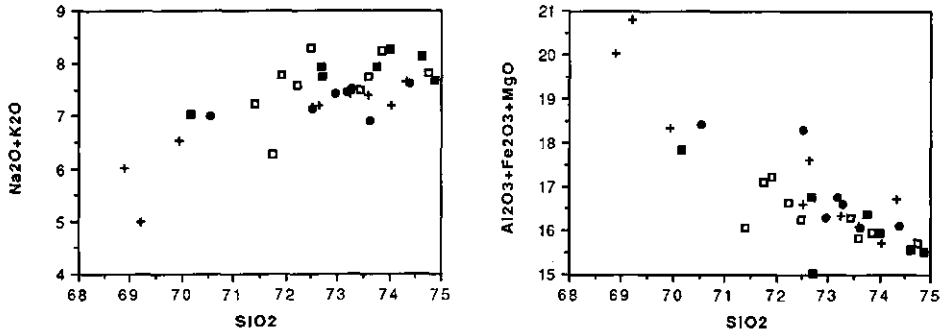


Fig. 48. Variation diagrams of several oxides. The four sample groups are indicated by different symbols.

+ La Laguna
 ● La Argentina
 ■ La Arg.-La Plata
 □ Guac.-Saladobl.

the igneous spectrum and are slightly K-depleted (fig. 47c). As the samples were collected in the upper part of the ignimbrite, it is possible that the K-depletion was caused by degassing processes which took place during cooling of the ignimbrite. Activity of cooled fumaroles at the top of the ignimbrite probably led to vapour-phase crystallization and K-depletion (section 4.1).

When the different oxides of the section La Argentina are plotted against stratigraphic height (assuming that the base of the section lies 250 m below the bridge: see section 3.2.2), no systematical variations with the elevation are observed (fig. 48, to the right). There are four possible explanations for these differences:

1) It has been shown in section 3.2.2 that at the location of the La Argentina section the total ignimbrite thickness probably amounts to some 320-370 m. The great thickness of the ignimbrites along the Río Loro might possibly be explained by assuming that the section represents a small valley fill. The systematical variations of the elements with stratigraphic height may have been lost due to turbulence in the flow when the ignimbrite filled the valley.

2) In thin sections from the part of the section La Argentina located between 1370 and 1380 m, some small hornblende grains were encountered (section 4.2). No hornblende was found in the samples from the La Laguna section. Therefore, the possibility cannot be excluded that the sections represent different flow units. In that case the stratigraphy of the ignimbrites would be much more complicated than has hitherto been assumed.

3) The systematical trends observed in the La Laguna section are illusory. From the diagram of SiO₂ vs. stratigraphic height it is clear that a compositional gap exists between the rhyolitic and rhyodacitic samples. It is possible that the rhyodacitic part of the section was erupted as a small separate flow some time after deposition of the rhyolitic part of the section.

4) In section 2.2 it has been shown that the Fish Canyon Tuff is very similar in texture and structure to the Guacacallo ignimbrites: both tuffs are very homogeneous in structure and texture and both consist of a single compound cooling unit. Samples from the Fish Canyon Tuff showed systematical trends between most elements and SiO₂, which could be accounted for by phenocryst-matrix fractionation, probably due to glass winnowing during eruption and emplacement (Whitney and Stormer, 1985). No significant correlation was found, however, between the elements and stratigraphic height in the section, although calculations of the viscosity, density and size of the parental body indicate that the system should convect with any

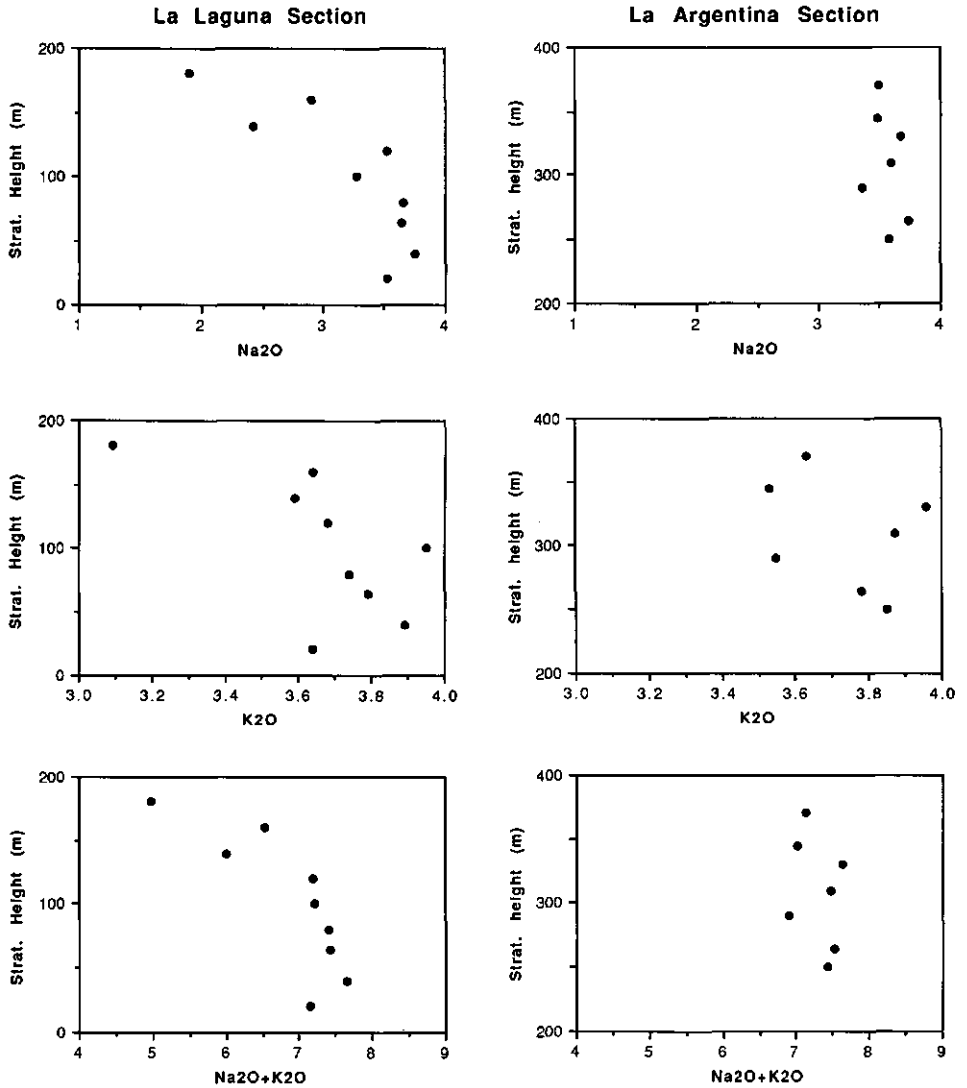
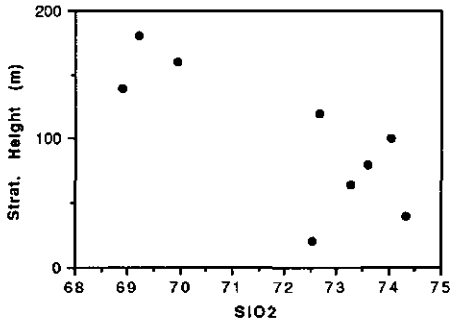
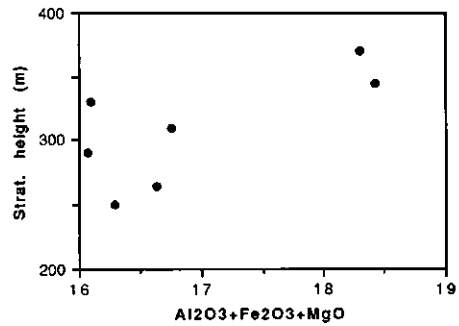
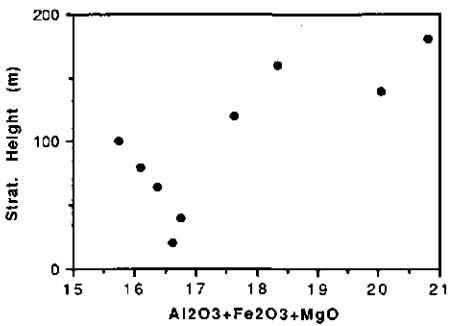
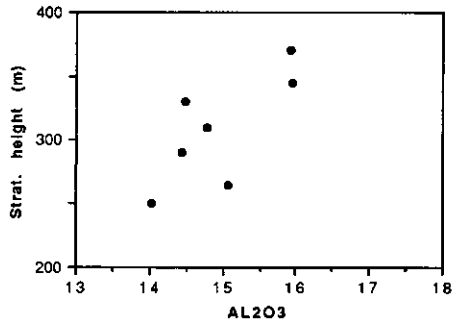
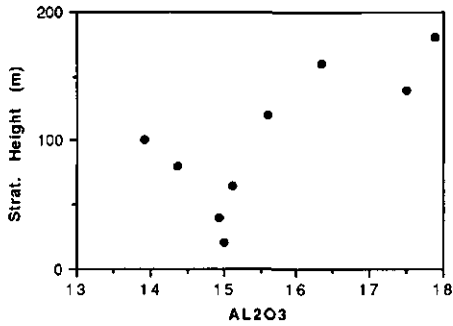
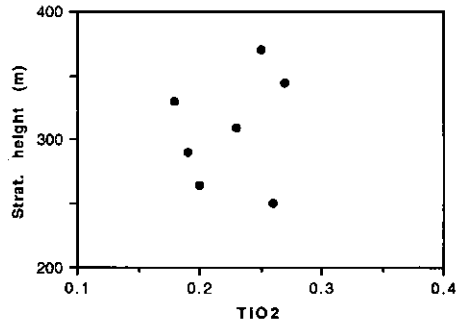
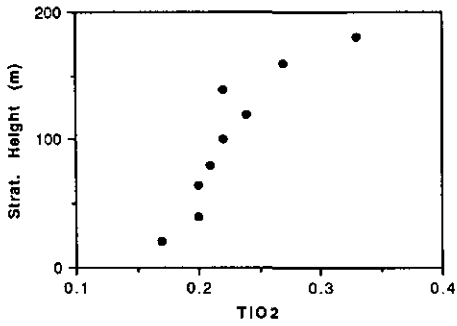
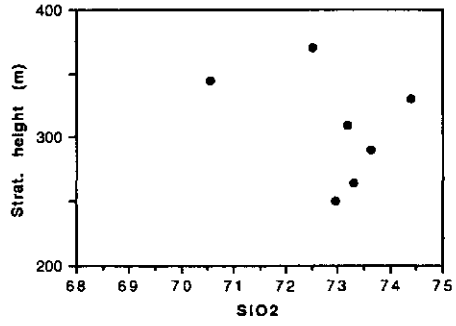


Fig. 49. Plots showing the variation in the weight percentages of several oxides with stratigraphical height. The La Laguna section is given at the left-hand side, the La Argentina section at the right-hand side of the page. The figure is continued on pages 163 and 164.

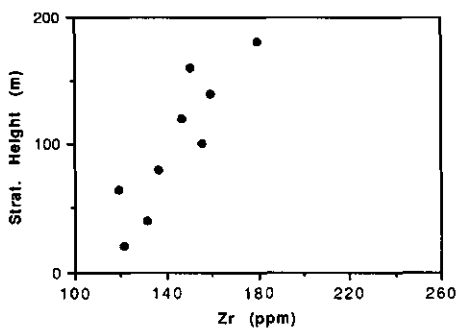
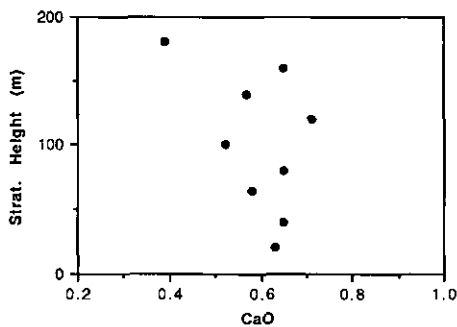
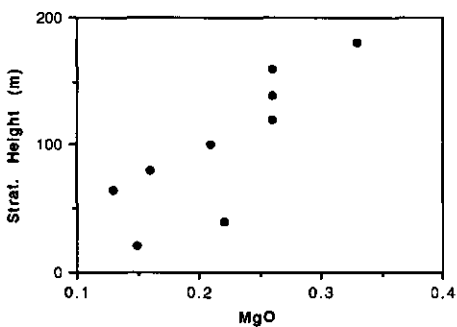
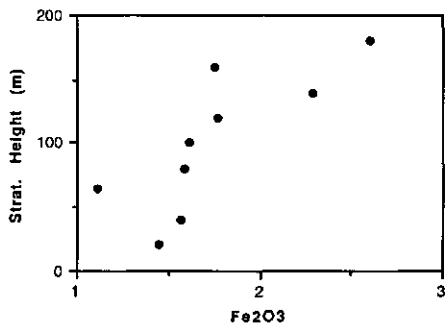
La Laguna Section



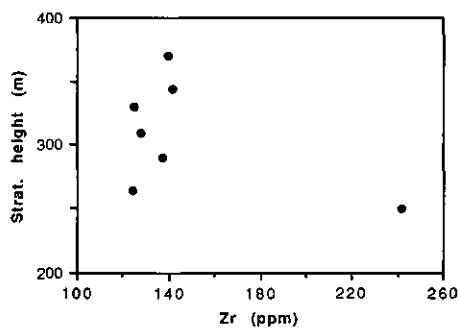
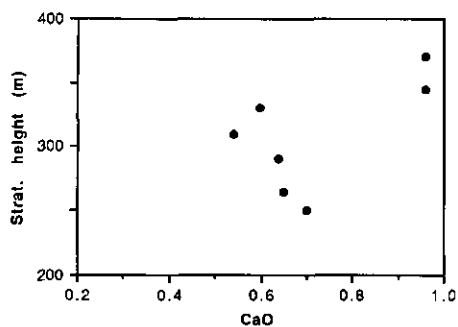
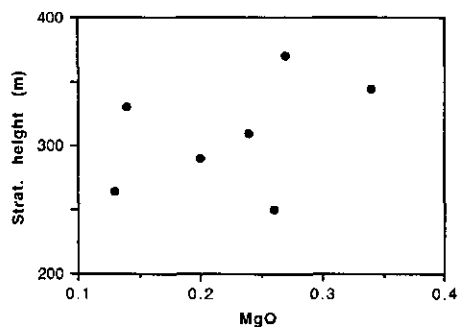
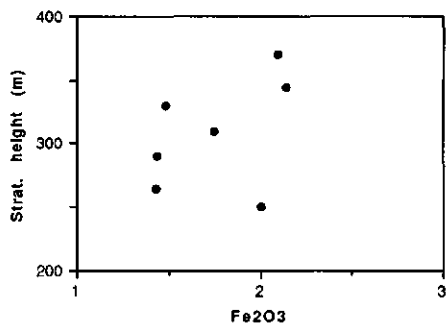
La Argentina Section



La Laguna Section



La Argentina Section



reasonable thermal gradient. The authors explain the homogeneity of the parent magma body by convective mixing in the magma chamber.

An alternative explanation for the lack of zoning of both the Fish Canyon Tuff and the Guacacallo ignimbrites could be that the ignimbrites experienced turbulence during flowage, which destroyed the original chemical gradients. This would also account for the great homogeneity in texture and structure (section 2.2). It is possible that one of the lobes of the flows, in which the La Laguna section is located underwent less turbulence, as a consequence of which some of the original gradients have been conserved.

The data presented above are insufficient to determine which of the above options is correct. Although they do not exclude the possibility that the ignimbrites of the Guacacallo Formation were erupted from a zoned magma chamber, additional major and trace element data from phenocrysts, matrix and whole rock samples are needed to test this hypothesis.

7. Possible sources of the ignimbrites

In the introduction, the question has been raised as to the source of the ignimbrites. Kroonenberg *et al.* (1981, 1982) suggested several volcanoes and calderas that could have acted as source, like the extinct Cutanga (Letrero) caldera, located some 35 km W of San Agustín, or one of the volcanoes of the Sierra de los Coconucos, or the Merenberg volcano W of La Argentina (fig. 50).

The Merenberg Volcano may be rejected on the grounds of the small diameter of the caldera, which is only 1.5 km wide (Kroonenberg *et al.*, 1981) and on the grounds of its major element chemistry: the Merenberg lavas should be classified as quartz-normative tholeiit-hawaiites (Schmitt, 1983).

With regard to the volcanoes of the Sierra de los Coconucos it should be noted that, again, these volcanoes have very small crater diameters, which makes the eruption of some 100 km³ of ignimbrite from one of them extremely improbable. The major element chemistry of the Puracé, which is one of the volcanoes of the Sierra de los Coconucos, also indicates that this volcano may be rejected as possible source of the ignimbrites. On the basis of the CIPW norms, the lavas from this volcano are classified as quartz-latitude andesites (Murcia, 1982; Schmitt, 1983), plotting in field 9 of the double triangle QAPF of Streckeisen (1976). Since these rocks evolve from basaltic magmas, a common origin with the ignimbrites is impossible.

The Cutanga Caldera, on the other hand, has a base of 15 km in diameter and a caldera diameter varying between 4-6 km (Kroonenberg *et al.*, 1981). Furthermore, it is aligned in a N-S direction with some other volcanoes (fig. 50). This alignment is very roughly parallel to the general trend of the subduction zone. The northernmost volcano along this alignment is the Sotará, which is still active and is situated approximately 20 km N of the Cutanga Caldera. The Sotará Volcano consists of 3 more or less concentric calderas, the outermost of which has a diameter of ± 4.5 km (Acevedo and Cepeda, 1982). The major element chemistry and normative mineral values of the extrusives of the Sotará Volcano show some similarities to those of the ignimbrites. In the double triangle QAPF of Streckeisen the rocks plot in the fields of the alkali-rhyolites, dacites and quartz-latitude andesites (Acevedo and Cepeda, 1982; Schmitt, 1983). As in the case of the Guacacallo ignimbrites, the volcanics show relatively high values of normative corundum. According to Schmitt, the alkali-rhyolites cannot have been differentiated from the calcalkaline lavas, but must have been formed by anatexis of crustal material. The nearness of the Sotará Volcano to the extinct Cutanga Caldera and the alignment of both raises the question whether the lavas of the latter may not have had a chemistry comparable to that of the Sotará. Both this possibility and the large diameter of the caldera suggest that the Cutanga Caldera is a conceivable candidate for the source of the ignimbrites.

There are, however, some facts which might argue against this hypothesis. If the Cutanga caldera was the source of the ignimbrites, the Argentina-La Plata area was located more distally as compared to the Guacacallo-Saladoblanco area. In that case it is strange that:

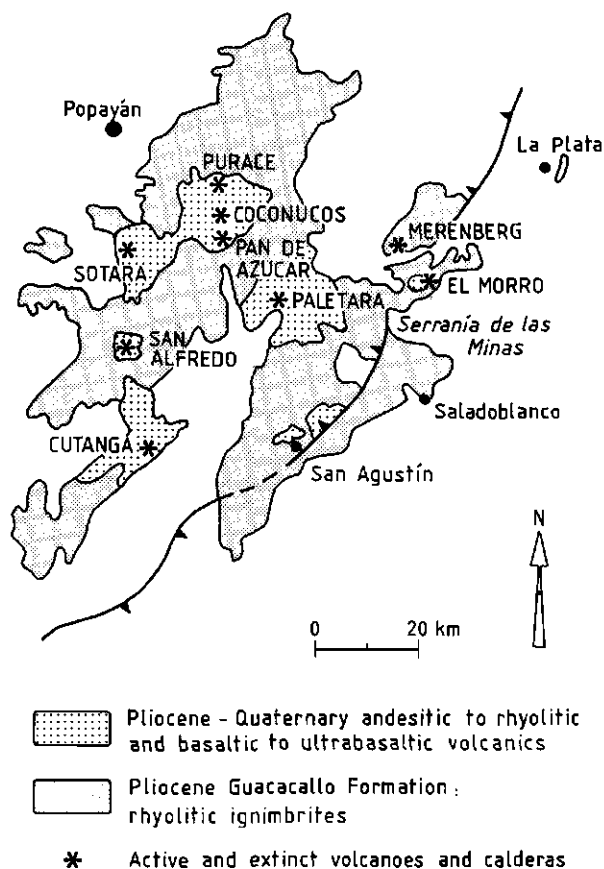


Fig. 50. Extension of the Guacacallo Formation and location of the most important volcanoes and calderas. Adapted from the geological map of Colombia at a scale of 1 : 1,200,000 by Geotec (1988).

- 1) the ignimbrites reach their greatest thickness in the La Argentina-La Plata area: in the surroundings of the Quebrada el Arrayán they have a thickness of at least 250-300 m.
- 2) the ignimbrites cover a greater elevation difference in the distal part of their deposition area (1370-2000 m) than in the more proximal part (1300-1600 m).
- 3) an agglomeratic ignimbrite is found only in the La Argentina-La Plata area (section 3.2.2).

It is possible, however, that the differences in thickness of the ignimbrite cover may be due to differences in erosion rates between the two areas, for example as a result of faulting. In the surroundings of Guacacallo most outcrops are extensively traversed by small faults. The almost complete disappearance of the ignimbrite cover from the S. Neiva Basin (section 1) also indicates that erosion may locally have played an important role. The sole occurrence of an agglomeratic ignimbrite in the upper part of the ignimbrite deposits of the La Argentina-La Plata area, furthermore, might be explained by the assumption that this ignimbrite was formed by a separate, relatively late pyroclastic flow which resulted from partial caldera collapse and

ran from the Cutanga Caldera in a NE direction. This would also explain the fact that the NE part of the caldera wall is breached (Kroonenberg *et al.*, 1981). From the above it is clear that the distribution of the ignimbrites does not undermine the possibility that the Cutanga Caldera was the eruptive center of the ignimbrites.

8. Conclusions

1. Major element analyses indicate that the magma producing the ignimbrites of the Guacacallo Formation probably formed from anatexis of crustal material.
2. It is feasible that the ignimbrites of the Guacacallo Formation erupted from a zoned magma chamber. Additional chemical data, however, are needed to prove or disprove this hypothesis.
3. The most likely source of the ignimbrites is the extinct Cutanga Caldera, located some 60 km WSW of La Laguna.
4. In the Guacacallo-Saladoblanco region, the Guacacallo ignimbrites unconformably overlie fluvio-volcanic deposits of the El Carmen Formation. In the La Argentina-La Plata region, on the other hand, the ignimbrites rest immediately on bedrock material. No younger deposits were encountered in the area.
5. The age of the El Carmen formation is ≥ 3.3 Ma. The age of the ignimbrites is approximately 2.3-2.7 Ma. The ignimbrite flows form together a compound cooling unit which must have been erupted and cooled in a geologically short period.
6. After deposition of the Guacacallo Formation, the area was subjected to fluvial erosion and incision. The main phase of fluvial incision resulted in the formation of an erosional terrace, located some 200-250 m above the present-day bottom of the Magdalena River.
7. An erosional remnant of the Guacacallo Formation NE of Tarqui, found unconformably on top of deposits belonging to the Gigante Formation, indicates that the formation originally extended deep into the S. Neiva Basin. Large-scale erosion after 2.5 ± 0.2 Ma led to a significant reduction in size of the distribution area of the ignimbrites.
8. The fact that in the western part of the S. Neiva Basin no deposits are found that are intermediate in age between the Gigante Formation and the Guacacallo Formation suggests that this area mainly underwent erosion in the period between ≤ 6 and 2.5 ± 0.2 Ma.

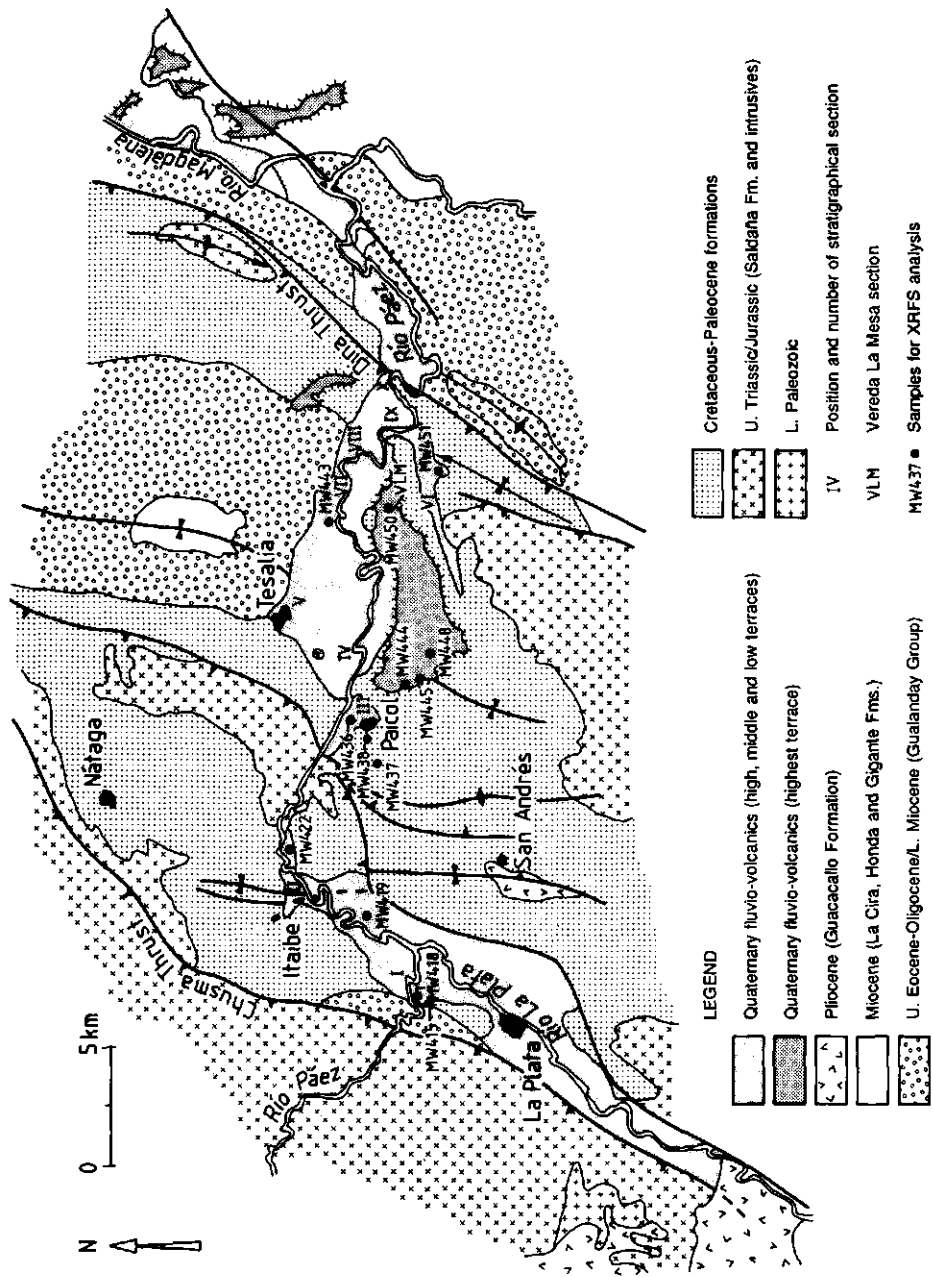


Fig. 51. Geological map of the Río Páez area, adapted from maps by Van Kampen (1986), Bos and Lansu (1987), Baltissen and Geijer (1987) and Diederix and Gomez (in press). Locations of stratigraphical sections and XRF/S samples are also indicated.

Chapter XI

The volcanoclastic terraces along the Río Páez and downstream part of the Río La Plata¹

1. Introduction

In this chapter the volcanoclastic terraces along the Páez River and the downstream part of the La Plata River are treated. These terraces are of interest in the reconstruction of the geological history of the S. Neiva Basin, although they are located W of the Dina Thrust, and therefore outside the sedimentation area of the Honda, Gigante and Las Vueltas formations. As is shown below, the terraces can be correlated with similar terraces along the Río Magdalena within the S. Neiva Basin. Furthermore, NE of La Plata the stratigraphical relation between the terraces and ignimbritic deposits of the Guacacallo Formation could be clarified. In this way the deposits along the La Plata and Páez rivers can be used to link the young geological history of the ignimbrite terrain in the west to the geological history of the S. Neiva Basin in the east.

A previous investigation of the terraces was performed by students of the Agricultural University of Wageningen (Van Kampen, 1986; Bos and Lansu, 1987; Baltissen and Geijer, 1987). The investigation was extended by the author of this thesis.

2. Location and field relations

Young volcanoclastic terraces are found along the lower reaches of the La Plata River up to some 10 km S of the town of La Plata, and along part of the Páez River, between the point where it emerges from the Central Cordillera, west of the Chusma Thrust, down to the confluence with the Magdalena River some 35 km further to the east (fig. 51).

Terraces are lacking east of the village of Itaibe, 5 km north of the confluence of the Páez and La Plata rivers. Here, the course of the Páez River changes abruptly from NNE to W. At this point, the valley suddenly narrows and the Páez River has formed a canyon in Late Triassic/Jurassic and Cretaceous rocks (fig. 51).

The terraced deposits have not been deformed tectonically and are found unconformably on top of older deposits: the Late Triassic/Jurassic Saldaña Formation, Jurassic intrusives, Cretaceous formations and Tertiary rocks, belonging to the Guaduas Formation and the Gualanday Group. Northeast of La Plata, eroded remnants of the Guacacallo Formation are found along the eastern margin of the La Plata Valley in the surroundings of the village of San Andrés (fig. 51). As these remnants are found at much higher elevations than the terraces along the La Plata and Páez rivers, it is clear that they are older than the terraces. The same may be concluded from a small outcrop of the Guacacallo Formation near Tesalia (chapter X, section 2), which is found to protrude through the plane surface of the "high" terrace (see below).

¹ The K-Ar mineral age determinations given in this chapter were performed by Dr. E.H. Hebeda and co-workers.

3. Stratigraphy of the terraces

Several terrace levels may be distinguished:

1. Erosional remnants of the highest terrace level are situated some 275-300 m above the present-day streambed of the Páez River, approximately 215-225 m above the next terrace level. The remnants are only present at two locations: directly E of the village of Paicol in the Vereda la Mesa and some 10 km ESE of the village of Tesalia. The terrace is an erosional terrace, formed in a sequence of volcanic debris-flow and other volcanoclastic deposits, called the "Paicol Breccia" by Van Houten (1976).

2. The high terrace is situated 115-60 m above the present river bottoms of the La Plata and Páez rivers and has a very great extension. In contrast to the highest terrace, it has been little affected by later fluvial dissection. The terrace has been formed in a sequence of volcanic debris flow and fluvio-volcanic deposits.

3. The middle terrace is situated 80-50 above the streambeds of the La Plata and Páez rivers. This terrace level does not have a very great extension and is lacking in many places (*e.g.* fig. 53, sections VII to X). The terrace is also formed in volcanic debris flow and other volcanoclastic deposits.

4. The low terraces. Three terrace levels are found below the middle terrace level. These levels are situated respectively 50-20, 45-15 and 10-2 m above the present-day streambeds of the La Plata and Páez rivers. The terraces are developed in volcanoclastic conglomerates and sandstones. The terraces are taken together as the "low terraces" and are not indicated separately in the figures.

3. 1. Stratigraphy of the highest terrace

Vereda la Mesa

Because of the generally poor exposure, the composition of the sediments making up the highest terrace is not completely clear. Most of the sequence appears to be formed by volcanic debris flow deposits and torrential conglomerates, sandy fluvio-volcanics being restricted to the lower part of the unit where they form a minor component. Beside tuffaceous sandstones and pebbly sandstones, a sandy deposit was encountered containing a very large pumice block which was used for K-Ar dating (see section 4, sample MW 548).

The pebbles and boulders of both the volcanic debris flow deposits and the torrential conglomerates consist of andesitic lava and may well have the same origin. In both types of deposits sorting is very poor, but the torrential conglomerates are slightly better rounded. It is possible that the conglomerates were formed by diluted debris flows and should be considered as hyperconcentrated flow deposits.

A single section could be taken in the western remnant of the terrace near Paicol (see fig. 51 for location). Although the section only comprises ± 4 m of sediment, it clearly shows that sandy fluvio-volcanic intercalations are found in the lower part of the terrace deposits. The section is depicted in fig. 52.

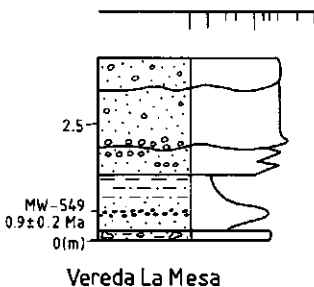


Fig. 52. Stratigraphy of fluvio-volcanic deposits, exposed in the highest terrace west of Paicol. For legend, see fig.16, p. 48.

Quaternary volcanoclastic terraces along the Páez River

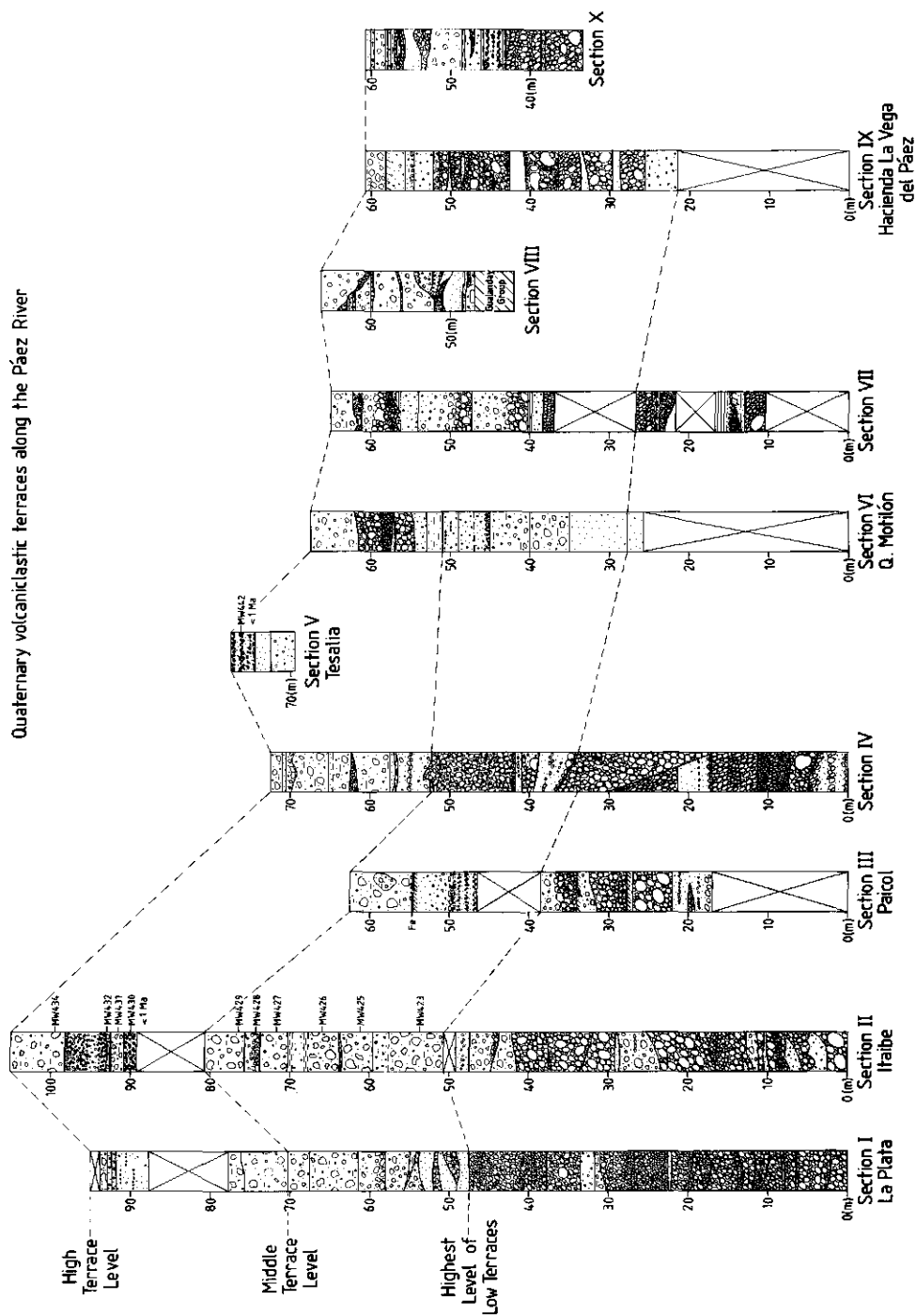


Fig. 53. Ten measured sections, taken along the Río Páez and downstream part of the Río La Plata. Position of sections is given in fig.51. Legend of sections is given in fig.16. The broken lines indicate the position of the different erosional terrace levels.

Stratigraphy of the outcrop 10 km ESE of the village of Tesalia

The degree of exposure of the easternmost erosional remnant of the highest terrace is very low. In the southernmost, lowest part of the remnant a single outcrop in a debris flow deposit was encountered. The pebbles and boulders within the deposit consisted almost entirely of andesite clasts with very little xenolithic material. The deposit had a thickness of ≥ 7 m. The total thickness of the remnant is ≤ 100 m.

3. 2. Stratigraphy of the high, middle and low terraces

Ten measured sections were taken in the deposits of the high, middle and low terraces along the La Plata and Páez Rivers, which have been depicted in fig. 53 in a downcurrent direction (from west to east). In the sections, the following points are noteworthy:

- In the La Plata region the upper part of sections I and II (the La Plata and Itaibe sections) consists almost entirely of debris flow deposits and torrential conglomerates (photos 32, 33), with minor intercalations of sandy fluvio-volcanics.

The lower part of the sections consists of fluvial deposits (conglomerates and sandstones). The fluvial conglomerates contain a high portion of pebbles and boulders originating from contemporaneous volcanism.

- The predominance of debris flow deposits decreases in a downstream direction along the Páez River. The bulk of the downstream sections is formed by finer-grained fluvio-volcanics (photos 34, 37). These sediments comprise poorly rounded to well rounded, poorly sorted polymict fluvial conglomerates beside sandstones, pebbly sandstones and minor silt and sandy silt intercalations. The conglomerates consist of clasts from Paleozoic schists, Saldaña volcanics, Jurassic intrusives and contemporaneous volcanics.

The lower part of the sections again consists mainly of polymict conglomerates and sandstones. The conglomerates are well rounded and poorly sorted and often show pebble imbrication (photo 38). They contain a relatively high share of unaltered andesite pebbles originating from contemporaneous volcanism.

- From N to S along the La Plata River, the total thickness of the sections and the total thickness of the debris flow deposits decreases. In the La Plata section only the upper 15 m are formed by debris flow deposits and the total thickness of the section comprises 95 m.

- One of the volcanoclastic sediments, a sandstone layer containing very large amounts of dacitic pumice pebbles, could be followed over the entire study area. In the Itaibe section the pumice clasts have a maximum size of 20 cm. The pebbles are well rounded and moderately sorted. Further downstream a similar deposit was encountered in the Tesalia section. Here, the pumice clasts are concentrated in separate layers which alternate with layers of sand. Again, the maximum size of the clasts is 20 cm. In section X an identical deposit was found, again with pumice clasts of up to 20 cm in diameter.

- In some sections (middle part of section III, upper part of section VI) very poorly sorted and well-rounded matrix-supported polymict conglomerates are present that fine upward to pebbly sandstone (photo 35). This type of conglomerate generally contains up to 40% of clasts originating from contemporaneous volcanism. In other sections (VII, VIII) debris flow deposits are found, containing a lower portion of contemporaneous volcanic clasts. The deposits pinch out rapidly over short distances and alternate with thin fluvial channel deposits, filled with poorly rounded material (photo 36).

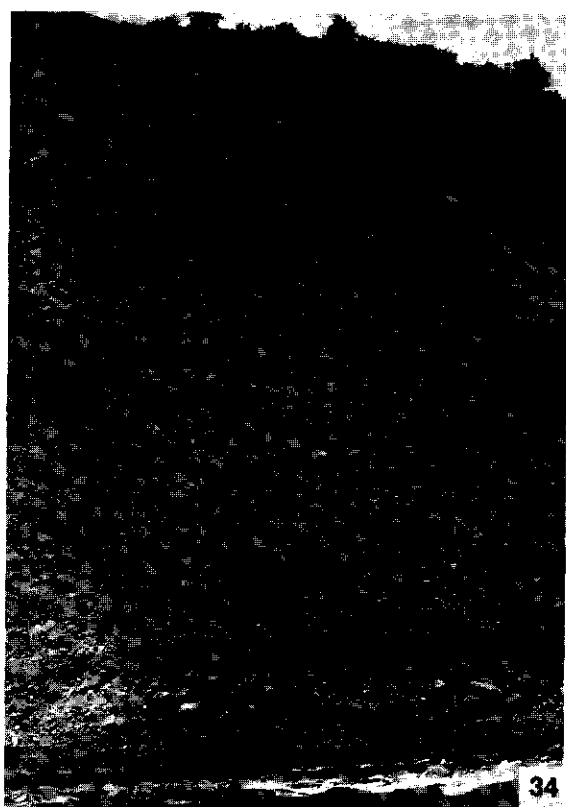
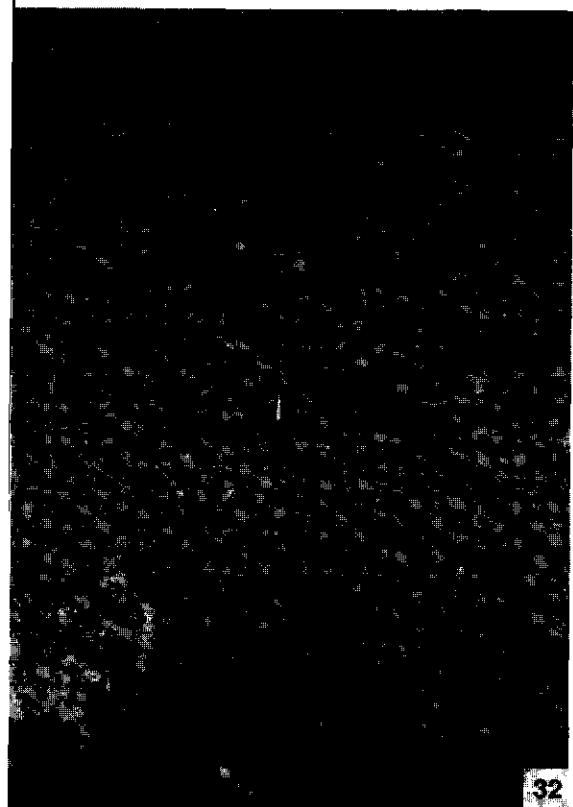
3. 3. Interpretation

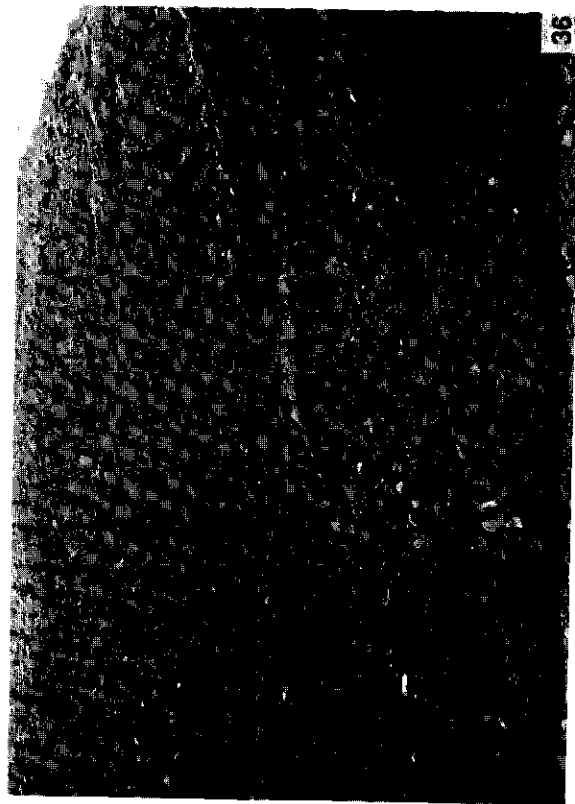
1. During the fieldstudy it became clear that the high, middle and low terrace levels are erosional terraces, which were formed during several stages of fluvial degradation in a

Photo 32. Debris flow deposit in the upper part of the Itaibe section, overlain by a poorly rounded and sorted conglomerate (torrential conglomerate?). View of the photo is toward the W. Length of hammer is ± 30 cm.

Photo 33. Torrential conglomerate or volcanic debris flow deposit in the upper part of the Itaibe section. The conglomerate consists entirely of fresh andesite boulders and pebbles. View of the photo is toward the W.

Photo 34. Section IV. Deep fluvial channel cut into underlying fluvial conglomerates. Both the channel-fill conglomerates and the underlying conglomerates are poorly sorted, and moderately rounded. View of the photo is toward the NNE.





single sequence of fluvio-volcanic deposits, termed the "Páez Breccia and Conglomerate" by Van Houten (1976). In several large outcrops along the Páez River the complete stratigraphy of the deposits is visible in the river banks. The deposits continue uninterruptedly from one terrace level to the next: no erosional unconformities were seen between deposits found in the different terraces. This can also be seen in fig. 53. Section VI contains a very large channel fill, formed by a channel which has cut deeply into the underlying sediments. The boundary between the low terraces and the middle terrace, however, does not coincide with the channel, but lies higher in the section. It is clear, therefore, that there is no relation between the terrace boundaries and the sedimentary sequence. This is in accordance with the opinion of Van Houten (1976), but in contrast to the view of Cepeda *et al.* (1986) who consider the terraces to be depositional terraces (see their figure 4). A schematic profile through the deposits, illustrating the interpretation given above is given in fig. 54.

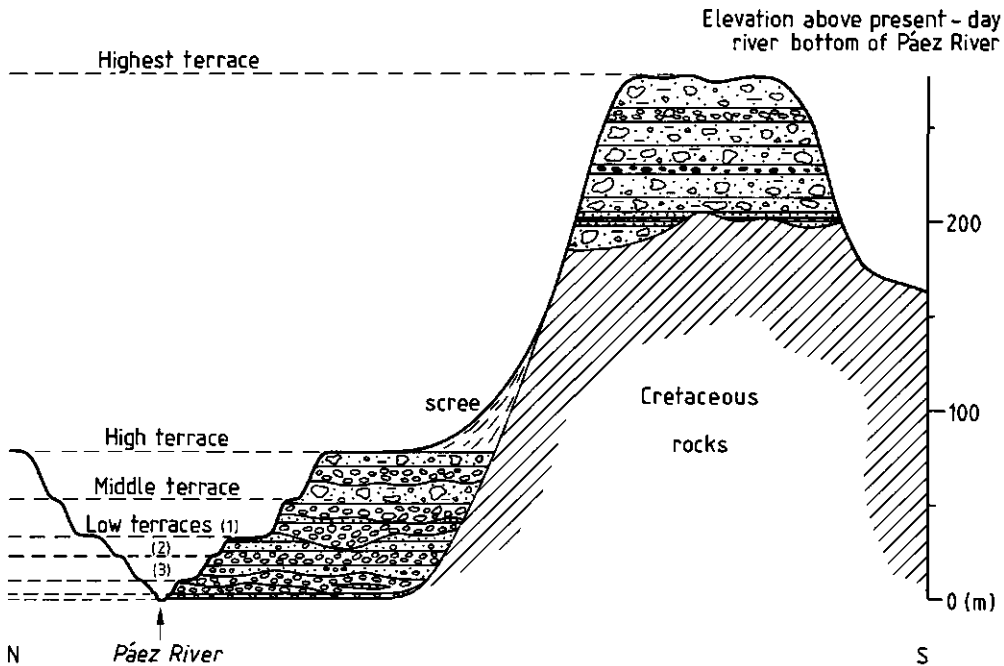


Fig. 54. Schematic profile through the different sequences of fluvio-volcanic deposits, showing the position of the terrace levels. The profile crosses the Vereda La Mesa approximately at the longitude of sample MW 448 (see fig. 51).

Photo 35. Poorly sorted and rounded polymict conglomerates in section VII, fining upward to pebbly sandstone. It is possible that these deposits were laid down by hyperconcentrated flows. View of the photo is toward the N. Man is ± 1.80 tall.

Photo 36. Deposits of section VIII, showing strong channeling and rapid changes in bank thickness. It is likely that these deposits have an alluvial fan origin. View of the photo is toward the S.

Photo 37. Fluvio-volcanic conglomerates and sandstones of section IX. View of the photo is toward the SSW. Length of hammer is ± 30 cm.

Photo 38. Fluvio-volcanic conglomerates and sandstones found in the lower part of the "Páez Breccia and Conglomerate". The photo was taken in one of the lower terraces of section III. View of the photo is toward the W.

2. The fact that the lower part of the sections consists of moderately to well rounded, imbricated fluvio-volcanic conglomerates and sandstones, while the upper part of the sections generally consists of alternations of debris-flow deposits and poorly rounded torrential conglomerates, suggests that volcanic activity was minimal when the lower part of the sections was deposited and the fluvial system was little influenced by it. As volcanism gradually intensified, larger amounts of volcanic products entered the river system and typical volcanoclastic sediments were deposited.

The same is true of the "Paicol Breccia", where fine-grained fluvio-volcanic sediments are also mostly restricted to the lower part of the deposits, while the upper part is dominated by volcanic debris flow deposits and torrential conglomerates.

3. Radiometric age determinations on hornblende from samples taken in the Tesalia and Itaibe sections (see section 4 of this chapter) suggest that the pumice deposits, encountered in sections II, V and X, resulted from the same eruptive event. The fact that the size of the pumice pebbles does not decrease in a downstream direction may be explained by its buoyancy, the number of clast collisions being much smaller when pebbles are transported while floating than when they are moved by rolling and/or saltation.

4. It is possible that the sediments from the middle part of section III and the upper part of section IV originated from hyperconcentrated flow processes. The relatively high portion of non-cognate clasts may have been caused either by erosion of underlying rocks by the original debris flows or by admixing of fluvial deposits during transport, when the flows were already more diluted.

5. The poor sorting and rounding of the deposits in sections VII and VIII, the high portion of non-cognate clasts, and the fact that they occur in irregular layers that pinch out rapidly over short distances, suggest that they have a local alluvial fan origin. It is likely that these fans originated N of the Páez River in the older geological formations. The admixture with fresh andesite clasts may be caused by partial reworking of the fans at the points where they entered the ancestral Páez River.

6. The differences between the sections suggest the following paleo-geography during deposition of the "Páez Breccia and Conglomerate": in the center of the area the wide Páez Valley was gradually filled with fluvio-volcanics, laid down by the ancestral Páez River. An erosional remnant of the "Paicol Breccia" formed a high to the south. At the N-side of the Páez Valley another high was present, formed by outcrops of older rocks. Erosion of these rocks led to the formation of alluvial fans, which entered the paleo-Páez River from the N.

7. The thickness of the "Páez Breccia and Conglomerate" not only decreases from west to east (in a downstream direction along the Río Páez), but also from N to S, *i.e.* from the point where the Páez River emerges from the Central Cordillera and enters the Páez Valley to the southernmost extension of the deposits along the La Plata River. This observation suggests that the fluvio-volcanics along the downstream part of the La Plata River were also deposited by the Río Páez.

4. Geochronology of the deposits

K-Ar mineral age determinations were carried out on biotite separates of two samples from the highest terrace and on hornblende separates of two samples from the high terrace. The results are given in table XXV. The analytical procedures used for the K-Ar determinations are described in chapter IV, section 1.

Sample MW 549 was collected in a pumice concentration in a tuffaceous sandstone in the highest terrace, just E of Paicol (fig. 51: La Mesa section). The sample gives an age of 0.9 ± 0.2

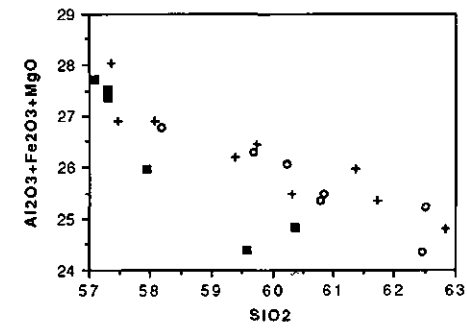
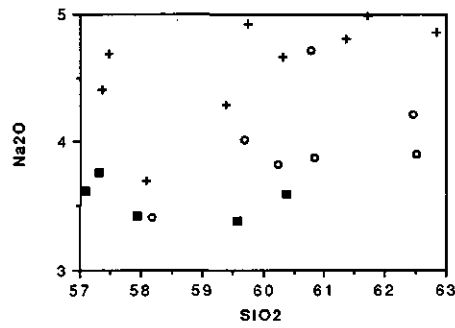
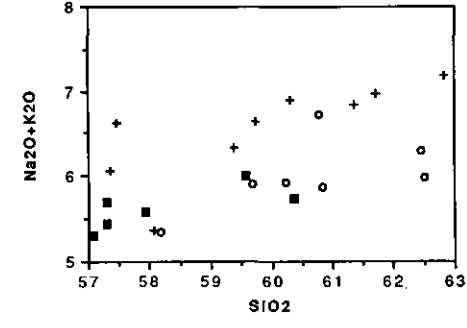
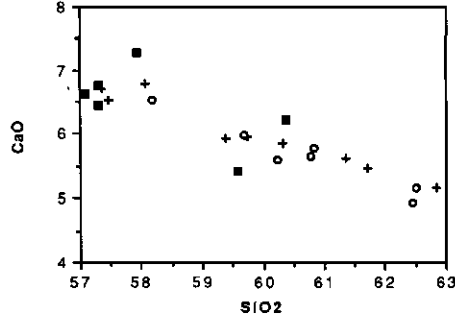
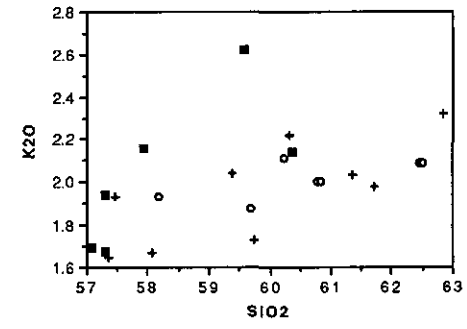
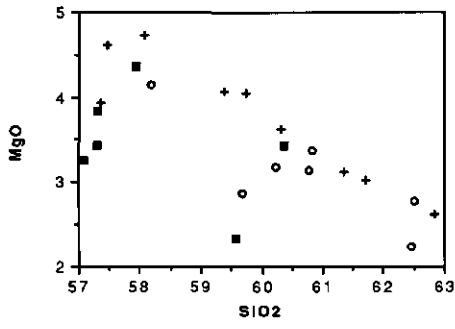
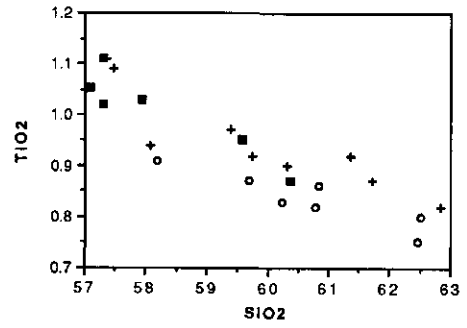
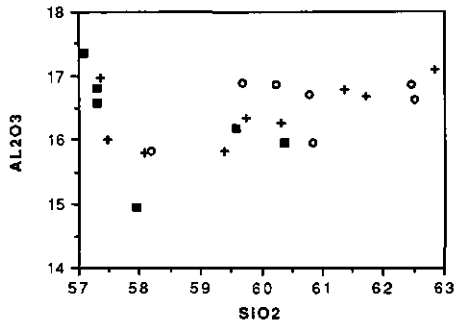
Table XXV. K-Ar mineral data of some volcanoclastic deposits along the Páez and La Plata Rivers.

Sample no.	Mineral	K (ppm wt.)	Radiogenic ⁴⁰ Ar (ppb wt.)	Atmospheric ⁴⁰ Ar (% total ⁴⁰ Ar)	Calculated age (Ma)
Highest terrace					
MW 548	Biot	6.43	0.54	96.1	1.1±0.2
		6.43	0.46	98.1	
		6.43	0.41	97.4	
MW 549	Biot	5.82	0.36	99.2	0.9±0.2
		5.82	0.48	96.8	
		5.82	0.29	97.6	
High terrace					
MW 430	Hbl	0.40	0.01	99.7	< 1
MW 442	Hbl	0.41	0.01	99.5	< 1

Ma. Sample MW 448 was collected from the already mentioned big pumice clast, located in a sandy layer approximately halfway between the eroded top of the highest terrace and the plane top of the high terrace (see section 3.1). This sample gives an age of 1.1 ± 0.2 Ma. The average of these ages is 1.0 ± 0.2 Ma. This is much younger than the biotite age of 3.7 ± 0.2 Ma, given by Van Houten (1976). Because Van Houten does not indicate in what kind of deposit his sample was taken, it is difficult to evaluate the meaning of that age. It is unlikely, though, that the sample was collected in an andesite lava clast, because these clasts generally do not contain sufficient biotite for K-Ar dating. The two samples that were dated during the present study were both analyzed in triplicate (table XXV). Both the results of the different analyses performed on each sample and the ages of the two samples agree very well with each other. For these reasons it is assumed here that our data is the correct one. Even if the pumice clasts, which were used for the present analyses, had been situated on the flanks of a volcano for some time before being incorporated into the terrace sediments, this would only imply that the pumice ages are maximum ages and that the terrace sediments may in fact be somewhat younger.

Within error, the ages of the deposits are identical to the ages obtained for the high terrace along the Río Magdalena at the latitude of Gigante. Hornblende from two pumice samples taken in this terrace along the road from Gigante to El Hobo gave an average age of 0.8 ± 0.3 Ma (chapter IV, section 2). Therefore, it is likely that the Qt₂ terrace (see geological map, appendix 1) is a lateral equivalent of the highest terrace along the Río Páez, which agrees with the elevation of the terrace above the present-day streambed of the Río Magdalena (70-90 m). This is in accordance with the opinion of Van Houten (1976), who also suggested that the "Paicol Breccia" might be a lateral equivalent of the deposits of the high terraces along the Río Magdalena.

Samples MW 442 and MW 430 were collected in the deposits of the high terrace. Sample MW 430 was collected in a pumice concentration within a sandy deposit of the Itaibe section. Sample MW 442 was collected in a pumice layer within a tuffaceous sandstone of the Tesalia section (figs. 50, 53). Both samples are younger than 1 Ma (table XXV). The large error is caused by the low K-content of the hornblende. An age of less than 1 million years for the deposits that make up the high terrace, however, is younger than the plagioclase age of 1.8 ± 0.2 Ma given by Van Houten (1976) for these deposits. For the same reasons as the ones given above it is assumed that the age presented here is the correct one.



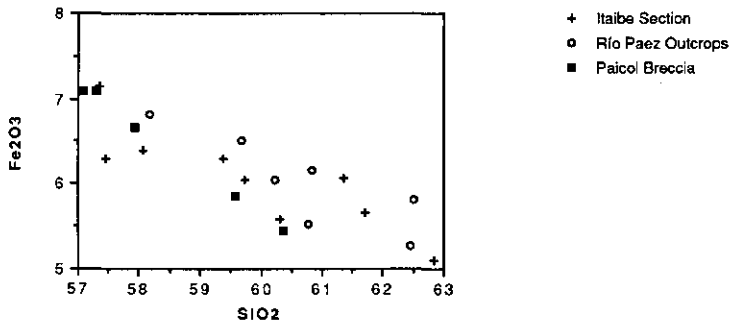


Fig. 55. Variation diagrams for several oxides. The three sample groups are indicated by different symbols.

5. Geochemistry of the deposits

The major element chemistry of 22 andesite lava blocks, collected in different volcanic debris flow deposits from the "Paicol Breccia", the Itaibe section (section II) and isolated outcrops in the high, middle and low terraces along the Río Páez, was determined with the aid of XRFS analysis. Analytical procedures for XRFS analysis are described in chapter V, section 2.2.1. Chemical analyses of all samples, together with calculated CIPW norms, are given in appendix 5.

Both in the normative Q'-ANOR diagram (Streckeisen and Le Maitre 1979) and in a diagram of total alkalis against SiO_2 (Le Bas *et al.*, 1986), the samples classify as andesites and trachyandesites (figs. 56a, b). In the BA diagram of Debon and Le Fort (1983), the samples plot in the metalluminous terrain (fig. 56d), which agrees with the fact that they plot in the calc-alkaline field in an AFM diagram (fig. 27, p. 88).

Because the andesite blocks might well have experienced alteration when lying on the flanks of the volcano before being incorporated in the debris flows, the samples were plotted in the alkali ratio diagram of Hughes (1973). From this figure, it is clear that the andesite blocks did not undergo potassium or sodium alteration (fig. 56c).

In order to determine whether the volcanic deposits of the "Paicol Breccia" are chemically related to those from the lower terrace levels (the "Páez Breccia and Conglomerate") or, in other words, whether they may have come from the same source, Harker diagrams were drawn for various oxides (fig. 55). The diagrams clearly indicate that the andesite lava blocks from the different debris flows found in the high, middle and low terraces are related to one another, as most of the different oxides of the samples show linear chemical trends. The oxides TiO_2 , Fe_2O_3 , MgO and CaO decrease with increasing SiO_2 content. The trends of Al_2O_3 and the alkalis are unclear, because the data points are strongly scattered. It seems, however, that the weight percentage of K_2O increases with increasing SiO_2 content, which is what would be expected in calc-alkaline lavas.

The samples from the "Paicol Breccia" have a slightly more basic chemistry than those from the "Páez Breccia and Conglomerate". Although they appear to give similar trends as those from the "Páez Breccia and Conglomerate", the data points of several oxides (Al_2O_3 , MgO , CaO , K_2O) are generally more strongly scattered. This observation suggests that the samples from the highest terrace may not have come from a single volcano, but may be heterogenous. It is possible that much reworked, older material was incorporated in the debris flows when they followed the channel of the Río Páez, or when they entered the Páez Valley. This could also explain the K-Ar age given by Van Houten, which is higher than our data (1976; see section 4 of the present chapter). It is possible that the age of 3.8 Ma given by this author was obtained from an older rock fragment that was reworked by one of the Paicol debris flows.

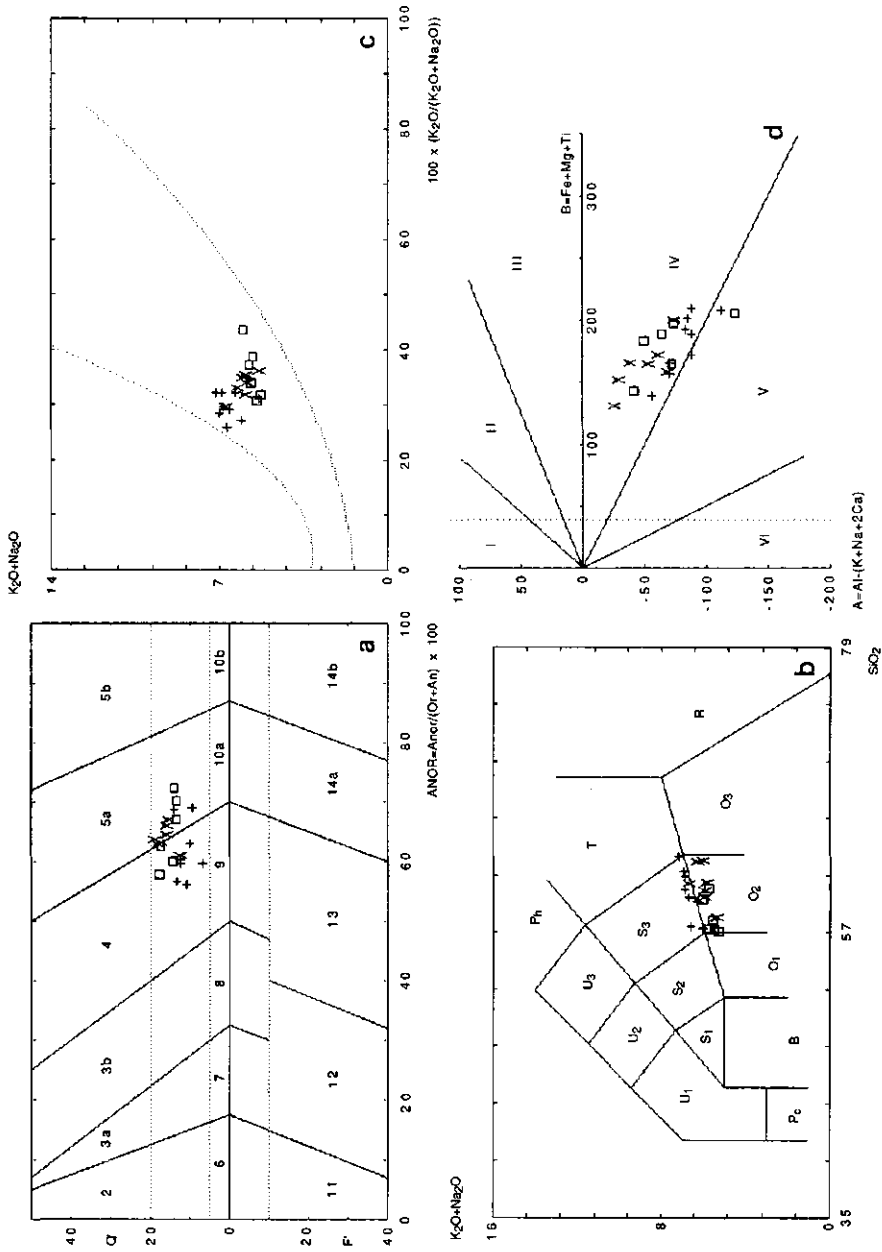


Fig. 54a. Classification of the debris flow blocks in a Q'-ANOR diagram (Streckeisen and Le Maitre, 1979). Fig. 54b. Idem, in a diagram of total alkalis vs. silica (Le Bas *et al.*, 1986). Fig. 54c. "Igneous Spectrum" (Hughes, 1973). Samples plotting outside the funnel-shaped area are alkali-altered. Fig. 54d. BA diagram of Debon and Le Fort (1983). Field labels are from the original publications. Symbols are as follows: open squares: "Paicol Breccia"; plus-signs: Itaibe Section; crosses: isolated outcrops along the Rto Páez.

6. Conclusions

From the field relations, the K-Ar age determinations and the major element chemistry, the following geological history may be reconstructed:

1. The deposition of the Guacacallo ignimbrites in the La Plata area was followed by a period of fluvial erosion and dissection.
2. Approximately one million years ago, some 75 m of volcanic debris flows and torrential conglomerates filled the E-W trending ancestral Páez Valley. As no comparable deposits are found along the Río La Plata further south, it is probable that the debris flows followed the channel of the Río Páez, which suggests that the Nevado del Huila may have been the source of the volcanic material.
3. During renewed fluvial erosion and channel incision the highest terrace was cut into the fluvio-volcanic deposits and the underlying Cretaceous rocks (fig. 54).
4. Some hundreds of thousands of years later, renewed volcanic activity caused several surges of volcanic material to fill the Páez Valley and northernmost part of the La Plata Valley. During inter-eruptive periods fluvial sediments and reworked volcanics were deposited. The total thickness of the deposits ranges from 120 m in the surroundings of Itaibe to some 50 m along the lower reaches of the Río Páez. Along the Río Magdalena the deposits thin even further from ± 20 -25 m along the Quebrada Guandinosita to a few meters in the surroundings of El Hobo. The fact that the deposits thin toward the E and the S suggests that the volcanic debris flows again followed the channel of the Río Páez and spread southward into the La Plata Valley and eastward into the Páez Valley.
5. It is likely that the Nevado del Huila again was the source of the volcanic material. This would also explain the great similarities in major element chemistry between the debris flow deposits of the highest terrace and those of the lower terraces.
6. When fluvial degradation commenced, the Páez and La Plata rivers cut down to their former bottoms, forming five erosional terrace levels in the sediments (fig. 54).

PART 5

SYNTHESIS

Chapter XII

Overview of the geological history of the S. Neiva Basin and adjacent areas

In section 1 of this chapter, the structural geological patterns observed in the S. Neiva Basin (chapter VIII) are integrated with the geological history of the area, as reconstructed from the radiometrical, stratigraphical and sedimentological investigations, and with the Neogene uplift history of the Garzón Massif. It is shown, furthermore, that the geological histories of the adjacent areas (the region west of the S. Neiva Basin and the Suaza Valley) concur with the interpretation given below (section 3).

In the last section of this chapter, uplift of the Garzón Massif and the geological history of the S. Neiva Basin are considered in the light of the plate tectonic setting.

1. Tectonics and sedimentation in the S. Neiva Basin

- Foreland folding and thrusting of the Chusma fault system ended with deposition of the upper conglomerate of the Gualanday Group and the La Cira Formation at the end of the Oligocene or earliest Miocene.

- Subsidence of the area west of the Chusma fault system started during the Lower Miocene, probably more than 16 Ma ago, with deposition of the Honda Formation. This subsidence followed the last phase of thrusting of the Chusma fault system. The Dina Thrust, the most eastward fault of this system, formed the limit between the subsiding area to the east and the fold and thrust belt region to the west. Further to the east, the subsiding area was probably bordered by a range of very low, isolated hills: erosional remnants of the Garzón Massif, which had been uplifted between 100 and 80 Ma ago.

- In the period between >16 Ma and approximately 12 Ma (deposition of sequences A and B of the Honda Formation), the subsidence rate of the area was not yet very great. Deposition was determined by volcanic activity of the Central Cordillera volcanic arc: sediments were laid down on distal volcanic aprons and by braided river systems, flowing toward the east. The range of low hills in the east did not form a serious obstacle to these eastward-flowing rivers, although it is possible that they followed locally a more northward course (compare Van Houten and Travis, 1968, fig. 12C).

- The Neiva Basin started to form around 12 Ma when the Garzón Massif and the Central Cordillera experienced simultaneous uplift. Uplift of the massif resulted in the presence of a continuous mountain range at the site of the former isolated low hills. The uplifting mountains

to the east and the west of the basin caused rapid subsidence of the basin floor and the deposition of increasingly coarse material from the west (sequence C of the Honda Formation).

The continuing eastward paleocurrent directions and the lack of erosional material from the Garzón Massif in the basinal sediments suggest that the uplifting massif had little influence on the depositional processes in the basin. Several factors, which will be discussed below, may have caused this phenomenon.

- After 12 Ma ago, tectonic activity of both the Central Cordillera and the Garzón Massif waned. The sediments, deposited during this period (sequence D of the Honda Formation) exhibit eastward and northward paleocurrent directions, suggesting that the main drainage of the area gradually shifted to the N, due to the presence of the uplifted Garzón Massif along the eastern border of the basin.

- Activity of the Central Cordillera volcanic arc was resumed some 10-9 Ma ago, during beginning deposition of the Gigante Formation (Neiva Member). Renewed uplift of the Central Cordillera caused deposition of coarse clastic material in the basin. The decrease of the pebble size to the north and the northward paleocurrent directions suggest that uplift occurred mainly in the southern part of the Central Cordillera, *i.e.* in the area where this cordillera merges with the Garzón Massif.

- Between 8 and 6.4 Ma ago activity of the Central Cordillera volcanic arc reached a maximum and great quantities of volcanic and volcanoclastic material were dumped into the S. Neiva Basin (deposition of the Los Altares Member). The influx of material was so great that the north-flowing paleo-Magdalena River was forced to a more eastward position by eastward extending volcanic aprons and now flowed immediately west of the Garzón Massif.

- Around 6.4 Ma ago a new phase of uplift of the Garzón Massif commenced. As the massif rose, first slowly and then more rapidly, increasing quantities of metamorphic pebbles and boulders entered the basin from the east. During beginning uplift of the massif, the ancestral Magdalena River reoccupied its former position in the center of the basin. The pebble and sandstone composition of the sediments (Garzón Member of the Gigante Formation) indicate that material came both from the east and the west and that the Central Cordillera volcanic arc was still active, albeit not as active as during the previous period.

- Uplift of the massif culminated ≤ 6 Ma ago. During uplift strong SE-NW compression of the basinal sediments occurred, causing folding and reverse faulting. Newly formed erosional material from the massif (lower unit of the Las Vueltas formation) was deformed immediately after deposition, forming a small angular unconformity with the underlying sediments. Uplift of the massif probably took place along several faults of the Garzón-Suaza fault system and not just along the Garzón-Algeciras Fault. Both high-angle and low-angle thrusting occurred and at several places along the basin margin the basinal sediments were overthrust by small thrust sheets, splaying from the fault zone.

- Uplift of the massif and folding of the basinal sediments ended after deposition of the lower unit of the Las Vueltas formation. Since then, the Garzón-Suaza fault system has experienced intermittent dextral strike-slip faulting, leading to the formation of several generations of alluvial fans (the oldest of which is formed by the upper unit of the Las Vueltas formation), which consist entirely of material with an eastern provenance. These fans were deposited horizontally and lie with an angular unconformity on the deformed older sediments. Strike-slip deformation of young Quaternary sediments along the Garzón-Algeciras Fault indicates that horizontal movements are still occurring along the fault system. Very little wrench-faulting is recorded along the reverse faults within the S. Neiva Basin, so it appears that this type of faulting is mainly restricted to the massif.

- In the S. Neiva Basin, the period between ≤ 6 Ma and ± 1 Ma ago (*i.e.* the period after deposition of the lower unit of the Las Vueltas formation and before sedimentation of the terrace deposits along the Magdalena River) is characterized by a scarcity of deposits: only the alluvial fan sediments along the western front of the Garzón Massif date from this period. In the west of the basin, NE of the village of Tarqui, an erosional remnant of the Guacacallo Formation, which overlies the Gigante Formation with an erosional unconformity (chapter X), suggests that very little deposition took place in that area between 6.4 Ma and ≤ 2.5 Ma ago. Basinwide, this period appears to be characterized mainly by erosion, following deformation of the basinal sediments.

- Quaternary reverse faulting of the sediments within the S. Neiva Basin indicates that NW-SE compression still plays a role.
- During the Quaternary, several terrace levels developed in the sediments along the Río Magdalena. The oldest terrace remnants, which are located in the very east of the basin 500 m above the present-day level of the Magdalena River, were probably formed by two tributaries of the Magdalena River, i.e. the Río Loro and the Q. de Garzón (chapter III, section 2.7), because it does not seem to be very probable that after uplift of the Garzón Massif ≤ 6 Ma ago, the Magdalena River still flowed so far to the east.

2. Possible causes for the scarcity of erosional products from the Garzón Massif in the sediments of the Honda Formation

It has been mentioned in the previous section that during deposition of sequence C of the Honda Formation no erosional material from the Garzón Massif appears to have entered the S. Neiva Basin, although uplift of the massif occurred during this period, ≥ 12 Ma ago. There are several possible explanations for this phenomenon:

a. On radar photos of the massif it can be seen that main present-day drainage is toward the east. A slight tilting of the massif toward the east during uplift would account for the observed drainage pattern and for the lack of erosional products of the massif in the S. Neiva Basin. This interpretation, however, does not explain why erosional material from the massif did enter the basin during the next uplift phase, ≤ 6.4 Ma ago.

b. The presence of intramontane basins within the massif has already been mentioned several times. These basins are aligned along faults, belonging to the Garzón-Suaza fault system. Although it is known from the literature that at least some of the basins have a strike-slip origin (e.g. the Pitalito Basin; Bakker, 1990), it is possible that others were formed as a result of Neogene differential uplift along faults of the Garzón-Suaza system, and acted as sediment traps. The strong overlap of the apatite FT ages of the Garzón Massif, however, argues against differential uplift (chapter II, section 3.3). Besides, most of these basins are rather small, so it is likely that erosional material from the massif would still have entered the S. Neiva Basin, even if the basins acted as sediment traps during uplift of the massif.

c. During deposition of the Honda Formation the floor of the S. Neiva Basin was tilted towards the east, and the depocenter was situated immediately west of the massif. If this hypothesis is correct, the Honda sediments directly west of the Garzón Massif should contain a much higher share of erosional products from the massif and should exhibit northward paleocurrent directions. Unfortunately, these sediments are very poorly exposed and could not be studied in great detail. Still, this explanation appears to be the most probable of the three, although it does not agree with the opinion of Butler (1983) that the basin axis was located in the center of the basin during deposition of the Honda Formation.

Eastward tilting of the valley floor possibly ended when the southern part of the Central Cordillera was uplifted during deposition of the Neiva Member.

3. Geological histories of the areas outside the S. Neiva Basin

3.1. The area west of the S. Neiva Basin

From the data given in chapters IX, X and XI it is clear that very little deposition took place in the foreland fold and thrust belt area between the moment that maximum deformation of the Chusma fault system had ended (probably the Lower Miocene), and the moment that deposition of the El Carmen formation commenced ≥ 3.3 Ma ago. Apart from a small outcrop of the Gigante Formation in the Q. El Arrayán, no sediments are known from the intervening period. It appears to be unlikely that a lot of sediment is buried below the thick cover of the Guacacallo Formation: deep canyon incisions show that the Guacacallo and El Carmen formations cover

rocks of the Jurassic and Cretaceous periods unconformably. Therefore, it is probable that the entire area between the Central Cordillera and the S. Neiva Basin formed a high in Upper and Middle Miocene times, which agrees with the suggestion done in chapter VI, section 4.3.

The occurrence of the El Carmen and Guacacallo formations west of the S. Neiva Basin, dated at ≥ 3.3 Ma to ≤ 2.5 Ma, as well as the presence of volcanoclastic terraces along the Magdalena and Páez Rivers, dated at ≤ 1 Ma, shows that at the latitude of the S. Neiva Basin the Central Cordillera volcanic arc was active from ≥ 3.3 Ma onward. The lack of volcanic and volcanoclastic deposits, both in the S. Neiva Basin and in the area west of the basin, dating between ≤ 6 Ma and ≥ 3.3 Ma suggests that no volcanic activity took place during that period. As this period coincides with the second Neogene uplift pulse of the Garzón Massif and with maximum deformation of the basinal sediments, the lack of volcanic activity may perhaps be explained by low-angle subduction of the Benioff zone some 200 km to the west. This point is further discussed below.

3. 2. *The Suaza Valley*

In chapter IX it has been mentioned that in the Suaza Valley sediments of the Gigante Formation, probably of the Garzón Member, unconformably overlie deposits of the Gualanday Group, while sediments of the Honda Formation are lacking. It was suggested that uplift of the area ≥ 12 Ma ago lead to erosion of the Honda Formation and the lower part of the Gigante Formation, and that the ≤ 6.4 Ma uplift of the Garzón Massif involved differential faulting, causing development of local sediment traps.

The geological history of the S. Neiva Basin as reconstructed in section 1 of this chapter strengthens these hypotheses. Furthermore, the following point is of interest:

- The Suaza Valley, which is faultbounded on both sides (fig. 37, p. 136), deepens from a few hundreds of meters in the SSW to 3 km in the NNE (B. Colletta, pers. comm.). The fault which delimits the Suaza Basin to the east is a lateral offshoot of the Garzón-Algeciras Fault, *i.e.* the Garzón-Suaza Fault.

The geometry of the basin is comparable to that of the Pitalito Basin, a strike-slip basin, which deepens from 300 m in the W to 1.2 km in the E, and is bounded on its N-side by the lateral continuation of the Garzón-Algeciras Fault (Bakker, 1990). This author calculated an age of 4.5 Ma for the basin, assuming that the sedimentation rate within the basin has remained constant in time.

The comparable geometries of the basins and the fact that both are delimited by faults belonging to the Garzón-Suaza fault system suggest that the Suaza Valley may well have been subjected to strike-slip movements from the Pliocene onward.

4. Uplift of the Garzón Massif in the light of the plate tectonic setting

4. 1. *Strike-slip movements*

Both with regard to the age of the initiation of strike-slip and with regard to the fault systems that are accomodating the strike-slip movements there is disagreement in the literature. According to Case *et al.* (1971), right-lateral displacement in the central and southern part of the Colombian Andes is concentrated on the Dolores Megashear (fig. 57), which separates nuclear South America from an area of oceanic crust. Observations of shallow and intermediate-depth seismicity and focal mechanisms, however, led Pennington (1981) to the conclusion that the Dolores Megashear is inactive and that right-lateral strike-slip movements are accomodated by the Eastern Andean Frontal Fault Zone, a system of faults along the eastern front of the Colombian Andes, which continues into Ecuador and Venezuela (Boconó Fault; see fig. 57). This fault zone separates the Andean block to the W from the S.American craton (the Guiana shield) to the E. According to Pennington (1981), Kellogg (1984) and Mann and Burke (1984), the Andean block is moving to the NNE with regard to the South American continent.

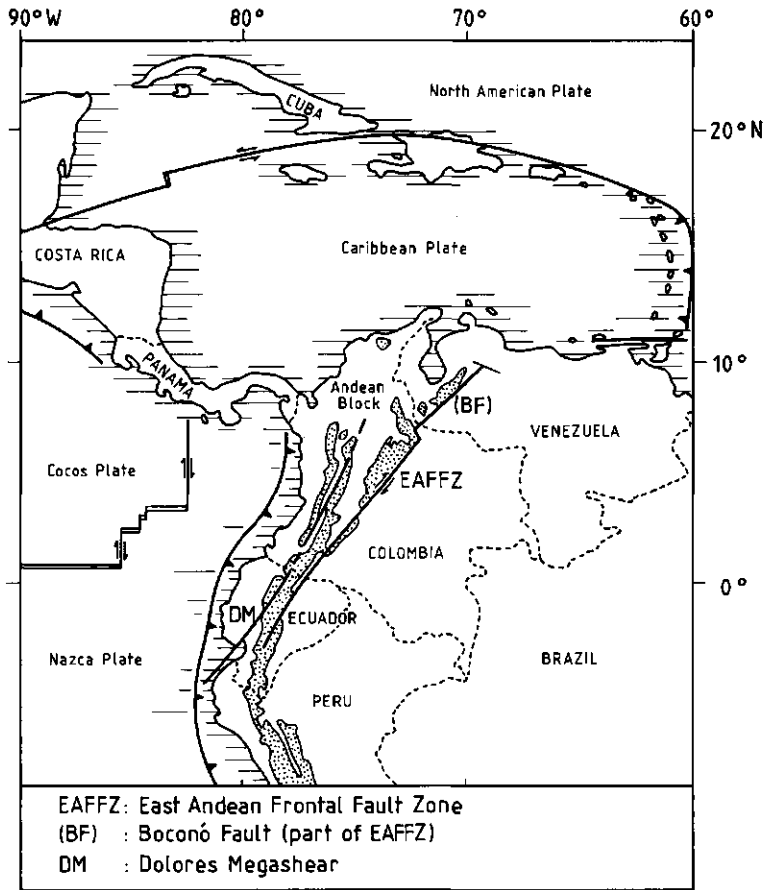


Fig. 57. Main tectonic features of NW South America and neighbouring areas. The plate boundaries near the northern edge of the Andean block and the southern Caribbean are still unclear. Adapted from Pennington (1981).

Pennington (1981) attributed the detachment of the Andean block from South America to the collision of the Carnegie Ridge with the Colombia-Ecuador trench. In view of the fact that subduction of aseismic ridges generally appears to have little influence on the subduction process (see section 4.2), the suggestion by Kellogg (1984) appears to be more likely. This author supposes that the Andean block became detached from the South American Plate when the Panama volcanic arc (the isthmus of Panama) collided with South America as a result of eastward motion of the Caribbean Plate. This event started around 7 Ma and was completed 3 Ma ago (Keigwin, 1978; Sykes *et al.*, 1982; Mann and Burke, 1984), suggesting that strike-slip movements on the East Andean Frontal Fault Zone must have commenced in the Pliocene. This is in agreement with the data obtained during the present study: it has been shown above that strike-slip movements along the Garzón-Suaza fault system commenced during deposition of the upper unit of the Las Vueltas formation, which has an estimated Pliocene age. A Pliocene age for the initiation of strike-slip, furthermore, agrees with the inferred age of the Pitalito Basin of 4.5 Ma (Bakker, 1990; see also section 3.2 of this chapter) and with the geologic history of the Suaza Valley.

The suggestion by Meissnar *et al.* (1976), that lateral strike-slip displacements in SW Colombia started some 60 Ma ago, is not supported by any other evidence and appears to be incorrect.

4. 2. Uplift of the massif in relation to igneous activity

When the ages of the two Neogene uplift phases of the Garzón Massif are compared with the ages of the volcanically active periods, the following facts are noteworthy:

- At the latitude of the S. Neiva Basin, volcanic activity decreased during deposition of sequence B of the Honda Formation and ceased altogether during uplift of the Garzón Massif ≥ 12 Ma ago (deposition of sequence C).
- Very restricted volcanic activity took place at the end of the deposition of the Honda Formation and during deposition of the Neiva Member around ± 10 Ma to 8 Ma ago.
- Volcanism reached a maximum during deposition of the Los Altares Member, between 8 Ma and 6.4 Ma ago.
- Beginning uplift of the Garzón Massif coincided with deposition of the Garzón Member and with a gradual decline of volcanism.
- During deposition of the lower unit of the Las Vueltas formation, maximum uplift of the massif concurred with complete cessation of volcanism ≤ 6 Ma ago.
- Volcanic activity was resumed ≥ 3.3 Ma ago with the deposition of the El Carmen formation, and is still taking place nowadays (*e.g.* the Puracé volcano is active at present).

These facts show that volcanism ceased during periods of uplift of the massif and was resumed during periods of tectonic quiescence. Apparently, Laramide-style uplift is contemporaneous with absence of activity of the volcanic arc further to the west, a notion which is supported by the literature. Both in the Western United States (Cross and Pilger, 1978; Cross, 1986) and in Argentina (Jordan *et al.*, 1983a, b; Jordan and Allmendinger, 1986; Strecker *et al.*, 1989) Laramide-style, basement-cored uplift of rigid blocks along reverse faults (the Colorado Plateau and the Sierras Pampeanas respectively) are described, coinciding with cessation of igneous activity. In the Western United States these events occurred in the Mesozoic to early Cenozoic; in Argentina the processes commenced during the late Cenozoic and are still going on today. Like the Colombian Andes, these regions form part of a non-collisional orogenic system in an ocean/continent subduction setting. In both cases, Laramide-style uplift and cessation of volcanism are explained by low-angle subduction of the Benioff zone further to the west.

According to Cross and Pilger (1982) four interdependent factors are responsible for the variation in geometry and angle of the subducting oceanic plate, *i.e.*:

1. Rapid absolute upper-plate motion toward the trench and active overriding of the subducted plate.
2. Rapid relative plate convergence.
3. Subduction of intraplate island-seamounts chains, aseismic ridges and oceanic plateaus.
4. The age of the subducting plate.

Recent research has shown that point 3 is probably relatively unimportant, although aseismic ridge subduction may lead to an extra reduction in dip angle (Strecker *et al.*, 1989; Wortel, 1986). The most important of the four controls summarized above is probably the age of the subducting lithosphere (Wortel, 1986).

Although low-angle subduction appears to be the mechanism, responsible for the cessation of activity of the volcanic arc, it is probably not the only factor which determines the style of mountain-building in the hinterland. Seismological data show that the Benioff zone along the coast of South America may be subdivided into different segments, some of which are currently experiencing low-angle subduction (the subducting plate dipping 5-10°) while others are being subducted at an angle of 30-35°. Present-day low-angle subduction of the oceanic plate is found to occur in Peru at latitudes between 2-15°S and in Chile/Argentina between 27-33°S. In the upper plate, these segments correspond with gaps in the distribution of active volcanoes. North

upper plate, these segments correspond with gaps in the distribution of active volcanoes. North and south of these zones steeply-dipping segments occur, characterized by volcanism in the upper plate (Hall and Wood, 1985).

Several authors (Barazangi and Isacks, 1976; Pilger, 1981; Cross and Pilger, 1982; Jordan *et al.*, 1983a, b; Hall and Wood, 1985) have shown that, along strike, the Andes may also be described in terms of different segments, which vary in structural geology and morphology. Although the segment boundaries partly coincide with variations in the geometry of the subducting plate, suggesting that this is one of the main controls on the style of mountain building, other segment boundaries, however, have no apparent relation to structures on the Nazca Plate which are being subducted, and may instead represent fundamental and long-lasting structures of the continent (Jordan *et al.*, 1983a; Hall and Wood, 1985). This idea is supported by Strecker *et al.* (1989), who showed that uplift in the Sierras Pampeanas in Argentina should be regarded as the result of thermal uplift and shortening in an overall compressional stress regime in a region with inherited zones of structural weakness.

It is likely that Neogene uplift of the Garzón Massif was also influenced by both factors: flat subduction processes and crustal predisposition to a certain style of uplift. Several arguments plead for such an interpretation:

1. Butler and Schamel (1988) suggested that the style and configuration of the structures of the middle Tertiary foreland fold and thrust belt west of the Neiva Basin are controlled by a polygonal array of pre-existing mechanical anisotropies in the pre-Cretaceous basement. In the northern part of the Chusma fault system these anisotropies led to the development of N-S trending, moderately dipping basement-rooted thrusts, which flatten upward into detachment surfaces and splay upward into the pre-Miocene sedimentary cover, forming trailing imbricate fans. Alongside the southern portion of the Neiva Basin, the same basement faults are steeper, trend to the NE and cut directly up through the sedimentary cover without forming associated imbricate thrusts. According to Butler and Schamel, the interplay of Oligocene crustal shortening with pre-existing basement weaknesses created a transitional terrain with features of both thin-skinned thrust belts and thick-skinned Laramide-style crustal uplifts. Although this terrain is located west of the Garzón Massif, it is very probable that comparable inherited zones of basement weakness exist within the massif.

2. The geometry of the subducting plate at the latitudes of the Garzón Massif and the Eastern Cordillera during the Late Miocene-Pliocene is, of course, unknown. A geophysical study by Meissner *et al.* (1976), however, revealed that a series of minor earthquakes, concentrated at depths between 35-100 km, was recorded below the Western and Eastern Cordilleras in the southern half of Colombia, beside earthquakes, defining the present-day position and angle of the subducting slab. According to these authors, it is possible that the minor quakes are caused by the presence of old oceanic material from former subduction processes, as they appear to define a flat-lying broken-off segment of oceanic lithosphere. If a subduction rate of 9 cm/yr is assumed (the average rate of subduction over the last 10 Ma, according to Pardo-Casas and Molnar, 1987), this segment must have commenced subduction some 7-6 Ma ago and must have stopped being subducted ± 3 Ma ago. This argument pleads for low-angle subduction between the upper Miocene to Pliocene, both below the Garzón Massif and the Eastern Cordillera further to the N.

References

- Abbey, S. 1980. Studies in "Standard samples" for use in the general analysis of silicate rocks and minerals. Part 6: 1979 edition of "usable" values. *Geol. Surv. Canada Pap.* 80 (14), pp. 30.
- Acevedo, A.P. and Cepeda, H. 1982. El Volcán Sotará: Geología y geoquímica de elementos mayores. *Pub. Geol. Esp. Ingeominas* 10, 19-30.
- Allen, J.R.L. 1963. The classification of cross-stratified units with notes on their origin. *Sedimentology* 2, 93-114.
- Allen, J.R.L. 1978. Studies in fluvial sedimentation: An exploratory quantitative model for the architecture of avulsion-controlled alluvial suites. *Sed. Geol.* 21, 129-147.
- Alvarez, J. 1981. Determinación de la edad Rb-Sr en rocas del Macizo de Garzón, Cordillera Oriental, Colombia. *Geol. Norandina* 4, 31-38.
- Alvarez, J. and Cordani, U.G. 1980. Precambrian basement within the septentrional Andes: age and geological evolution (abstract). *26th Congr. Geol. Int. Paris* 1, 10.
- Alvarez, J. and Linares, E. 1985. Una edad K/Ar del Macizo de Garzón, Departamento del Huila, Colombia. *Geol. Norandina* 9, 31-33.
- Anderson, T.A. 1970. Geology of the lower Tertiary Gualanday Group, Upper Magdalena Valley, Colombia. *PhD Thesis, Princeton University*, pp 86.
- Anderson, T.A. 1972. Paleogene Nonmarine Gualanday Group, Neiva Basin, Colombia, and Regional Development of the Colombian Andes. *Bull. geol. Soc. Am.* 83, 2423-2438.
- Andriessen, P.A.M. 1978. Isotopic age relations within the polymetamorphic complex of the island of Naxos (Cyclades, Greece). *ZWO Laboratorium voor Isotopen-Geologie, Amsterdam, Verh.* 3, pp. 71.
- Andriessen, P.A.M. and Bos, A. 1986. Post-Caledonian thermal evolution and crustal uplift in the Eidfjord area, western Norway. *Norsk Geologisk Tidsskrift* 66, 243-250.
- Andriessen, P.A.M., Helmens, K., Hooghiemstra, H., Riezebos, P.A. and Van der Hammen, T. in prep. Pliocene-Pleistocene chronology of the sediments of the basin of Bogotá, Eastern Cordillera, Colombia.
- Aspden, J.A. and McCourt, W.J. 1985. A Middle Mesozoic Oceanic Terrane in the Central Cordillera of Western Colombia. *Geol. Norandina* 9, 19-26.
- Aspden, J.A., McCourt, W.J. and Brook, M. 1987. Geometrical control of subduction-related magmatism: the Mesozoic and Cenozoic plutonic history of Western Colombia. *J. geol. Soc. London* 144, 893-905.
- Baker, V.R. 1978. Adjustment of fluvial systems to climate and source terrain in tropical and subtropical environments. In: *Fluvial Sedimentology* (Edited by Miall, A.D.), *Can. Soc. Petrol. Geol. Mem.* 5, 211-230.
- Bakker, J. 1990. Tectonic and climatic controls on Late Quaternary sedimentary processes in a neotectonic intramontane basin (the Pitalito Basin, South Colombia). *PhD Thesis, Agricultural University of Wageningen*, pp. 160.
- Ballance, P.F. 1984. Sheet-flow dominated gravel fans of the non-marine middle Cenozoic Simmler Formation, central California. *Sed. Geol.* 38, 337-359.
- Baltissen, G. and Geijer, J. 1987. A geomorphological survey of the downstream part of the river Páez Valley, Tesalia, El Huila. *Unpublished report of the Agricultural University of Wageningen*, pp. 39.
- Barazangi, M. and Isacks, B.L. Spatial distribution of earthquakes and subduction of the Nazca plate beneath South America. *Geology* 4, 686-692.
- Beaumont, C. 1981. Foreland basins. *Geoph. J. Roy. Astron. Soc.* 65, 291-329.
- Beerbower, J.R. 1964. Cyclothem and cyclic depositional mechanisms in alluvial plain sedimentation. In: *Symposium on Cyclic Sedimentation* (Edited by Merriam, D.F.), *Bull. State Geol. Surv. Kansas* 169, 31-42.
- Beets, D.J., Maresch, W.V., Klaver, G.Th., Mottana, A., Bocchio, R., Beunk, F.F. and Monen, H.P. 1984. Magmatic rock series and high-pressure metamorphism as constraints on the tectonic history of the southern Caribbean. In: *The Caribbean-South American plate boundary and regional tectonics*. (Edited by Bonini, W.E. and others), *Mem. geol. Soc. Am.* 162, 95-130.
- Beltrán, N. and Gallo, J. 1968. The Geology of the Neiva Sub-Basin, Upper Magdalena Basin, southern portion. In: *Geological field-trips Colombia 1959-1978* (Edited by Geotec), *Col. Soc. Petrol. Geol. Geophys.*, 253-275.

- Benjamin, M.T., Johnson, N.M. and Naeser, C.W. 1987. Recent rapid uplift in the Bolivian Andes: Evidence from fission-track dating, *Geology* 15, 680-683.
- Blair, T.C. 1987. Sedimentary processes, vertical stratification sequences, and geomorphology of the Roaring River Alluvial Fan, Rocky Mountain National Park, Colorado. *J. Sed. Petrol.* 57 (1), 1-18.
- Blakey, R.C. and Gubitosa, R. 1984. Controls of sandstone body geometry and architecture in the Chinle Formation (Upper Triassic), Colorado Plateau. *Sed. Geol.* 38, 51-86.
- Bok, A.M. and Veldkamp, E. 1988. Geomorphological study in the area Tarqui-Altamira (Huila). *Unpublished report of the Agricultural University, Wageningen*, pp. 26.
- Boothroyd, J.C. and Ashley, G.M. 1975. Processes, bar morphology, and sedimentary structures on braided outwash fans, northeastern Gulf of Alaska. In: *Glaciofluvial and glaciolacustrine sedimentation* (Edited by Jopling, A.V. and McDonald, B.C.), *Soc. Econ. Pal. Mineral. Spec. Publ.* 23, 193-222.
- Bos, P. and Lansu, A. 1987. A geomorphological survey of the Páez Valley between La Plata and Paicol, Huila, Colombia. *Unpublished report of the Agricultural University of Wageningen*, pp. 50.
- Bourgeois, J., Toussaint, J.-F., Gonzalez, H., Azema, J., Calle, B., Desmet, A., Murcia, L.A., Acevedo, A.P., Parra, E. and Tournon, J. 1987. Geological history of the Cretaceous ophiolitic complexes of Northwestern South America (Colombian Andes). *Tectonophysics* 143, 307-327.
- Bridge, J.S. and Leeder, M.R. 1979. A simulation model of alluvial stratigraphy. *Sedimentology* 26, 617-644.
- Briggs, N.D., Naeser, C.W. and McCulloh, T.H. 1981. Thermal history of sedimentary basins by fission-track dating (abstract), *Nucl. Tracks* 5, 235-237.
- Brook, M. 1984. New radiometric age data from S.W. Colombia. *Ingeominas Misión Británica (British Geological Survey), Cali, Colombia Report* 10, pp. 25.
- Bull, W.B. 1972. Recognition of alluvial-fan deposits in the stratigraphical record. In: *Recognition of ancient sedimentary environments* (Edited by Rigby, J.K. and Hamblin, W.K.), *Soc. Econ. Pal. Mineral. Spec. Publ.* 16, 63-83.
- Butler, J.W. 1942. Geology of the Honda district, Colombia. *Am. Ass. Petrol. Geol. Bull.* 26, 793-837.
- Butler, K.R. 1983. Andean-type foreland deformation: Structural development of the Neiva Basin, Upper Magdalena Valley, Colombia. *PhD Thesis, University of North Carolina*, pp 272.
- Butler, K.R. and Schamel, S. 1988. Structure along the eastern margin of the Central Cordillera, Upper Magdalena Valley, Colombia. *J. South. Am. Earth Sci.* 1 (1), 109-120.
- Cant, D.J. 1978. Development of a facies model for sandy braided river sedimentation: Comparison of the South Saskatchewan River and the Battery Point Formation. In: *Fluvial Sedimentology* (Edited by Miall, A.D.), *Can. Soc. Petrol. Geol. Mem.* 5, 627-639.
- Case, J.E., Duran, L.G., Lopez, A. and Moore, W.R. 1971. Tectonic Investigations in Western Colombia and Eastern Panama. *Bull. geol. Soc. Am.* 82, 2685-2712.
- Cepeda, H., Mendez, R., Murcia, A. and Vergara, H. 1986. Mapa preliminar de riesgos volcánicos potenciales del Nevado del Huila. Texto explicativo. *Unpublished report of Ingeominas, Medellín*, pp. 19.
- Chappell, B.W. and White, A.J.R. 1974. Two contrasting granite types (expanded abstract). *Pacific Geology* 8, 173-174.
- Chappell, B.W. and White, A.J.R. 1984. I- and S-type granites in the Lachlan Fold Belt, southeastern Australia. In: *Geology of granites and their metallogenic relations*, (Edited by Keqin, X. and Guangchi, T.), Science Press, Beijing, 87-101.
- Cifelli, R.L. and Guerrero Díaz, 1989. New remains of *Prothoatherium colombianus* (Lioterna, Mammalia) from the Miocene of Colombia. *J. Vert. Paleont.* 9 (2), 222-231.
- Cobbing, E.J. 1976. The geosynclinal pair at the continental margin of Peru, *Tectonophysics* 36, 157-165.
- Cobbing, E.J. 1978. The Andean geosyncline in Peru, and its distinction from Alpine geosynclines, *J. geol. Soc. London* 135, 207-218.
- Cobbold, P., Richard, P. and Ulloa, C. 1990. Cenozoic thrusting and wrenching in the Cordillera Oriental, Colombia: Field data and experimental insights (abstract). *Symposium International "Géodynamique Andine"*, Grenoble, 215.
- Colletta, B., Hébrard, F., Letouzey, J., Werner, Ph. and Rudkiewicz, J.-L. 1990. Tectonic style and crustal structure of the Eastern Cordillera (Colombia) from a balanced cross-section (unpublished abstract). *Symposium International "Géodynamique Andine"*. Grenoble.
- Cross, T.A. 1986. Tectonic controls of foreland basin subsidence and Laramide style deformation, western United States. In: *Foreland Basins* (Edited by Allen, P.A. and Homewood, P.), *Int. Ass. Sed. Spec. Publ.* 8, 15-39.
- Cross, T.A. and Pilger, R.H., Jr. 1978. Constraints on absolute motion and plate interaction inferred from Cenozoic igneous activity in the western United States, *Am. J. Sci.* 278, 865-902.
- Cross, T.A. and Pilger, R.H., Jr. 1982. Controls of subduction geometry, location of magmatic arcs, and tectonics of arc and back-arc regions. *Bull. geol. Soc. Am.* 93, 545-562.
- Crough, S.T. 1983. Apatite fission-track dating of erosion in the eastern Andes, Bolivia, *Earth Planet. Sci. Lett.* 64, 396-397.

- Cuatrecasas, J. 1958. Aspectos de la vegetación natural de Colombia. *Rev. Acad. Col. Cienc. Ex. Fis. Nat.* **10** (40), 221-264.
- Dalrymple, G.B. and Lanphere, M.A. 1969. *Potassium-Argon dating. Principles, Techniques and Applications to Geochronology*. W.H. Freeman and Company, San Francisco, pp. 240.
- Davies, D.K., Vessell, R.K., Miles, R.C., Foley, M.G. and Bonis, S.B. 1978. Fluvial transport and downstream sediment modifications in an active volcanic region. In: *Fluvial Sedimentology* (Edited by Miall, A.D.), *Can. Soc. Petrol. Geol. Mem.* **5**, 61-83.
- Debon, F. and Le Fort, P. 1983. A chemical-mineralogical classification of common plutonic rocks and associations. *Trans. Roy. Soc. Edinburgh: Earth Sci.* **73**, 135-149.
- Diederix, H and Gomez, H. in press. Mapa geológico del Sur del Departamento del Huila, escala 1: 100,000. Revista CIAF.
- Dott, R.H. 1964. Wacke, greywacke and matrix - what approach to immature sandstone classification? *J. Sed. Petrol.* **34** (3), 625-632.
- Duncan, R.A. and Hargraves, R.B. 1984. Plate tectonic evolution of the Caribbean region in the mantle reference frame. In: *The Caribbean-South American plate boundary and regional tectonics*, (Edited by Bonini, W.E. and others), *Mem. geol. Soc. Am.* **162**, 81-93.
- Fabre, A. and Delaloye, M. 1982. Intrusiones básicas cretácicas en las sedimentitas de la parte central de la Cordillera Oriental, *Geol. Norandina* **6**, 19-28.
- Fisher, R.V. 1979. Models for pyroclastic surges and pyroclastic flows. *J. Volc. Geoth. Res.* **6**, 305-318.
- Fisher, R.V. and Schmincke, H. -U. 1984. Pyroclastic Flow Deposits, chapter 8, 187-230. In: *Pyroclastic rocks*. Springer-Verlag Berlin, pp. 472.
- Fitzgerald, P.G. and Gleadow, A.J.W. 1988. Fission-track geochronology, tectonics and structure of the Transantarctic Mountains in northern Victoria Land, Antarctica, *Chem. Geol. (Isot. Geosci. Sect.)* **73**, 169-198.
- Folk, R.L. 1968. *Petrology of sedimentary rocks*, Hemphill Publishing Co., Austin, pp. 170.
- Freundt, A. and Schmincke, H.-U. 1985. Lithic-enriched segregation bodies in pyroclastic flow deposits of Laacher See volcano (East Eifel, Germany). *J. Volc. Geoth. Res.* **25**, 193-224.
- Freundt, A. and Schmincke, H.-U. 1986. Emplacement of small-volume pyroclastic flows at Laacher See (East-Eifel, Germany). *Bull. Volcanology* **48**, 39-59.
- Friend, P.F. 1978. Distinctive features of some ancient river systems. In: *Fluvial Sedimentology* (Edited by Miall, A.D.), *Can. Soc. Petrol. Geol. Mem.* **5**, 531-542.
- Friend, P.J. 1983. Towards the field classification of alluvial architecture or sequence. In: *Modern and ancient fluvial systems* (Edited by Collison, J.D. and Lewin, J.), *Int. Ass. Sed. Spec. Publ.* **6**, 345-354.
- Galloway, W.E. 1981. Depositional architecture of Cenozoic Gulf coastal plain fluvial systems. In: *Recent and ancient nonmarine depositional environments. Models for exploration* (Edited by Ethridge, F.G. and Flores, R.M.), *Soc. Econ. Pal. Mineral. Spec. Publ.* **31**, 127-157.
- Geotec Ltda. 1988. Mapa geológico de Colombia, escala 1: 1,200,000, elaborated by Cediel, F and Cacaes, C. Two sheets.
- Gleadow, A.J.W. and Brooks, C.K. 1979. Fission track dating, thermal histories and tectonics of igneous intrusions in East Greenland, *Contrib. Mineral. Petrol.* **71**, 45-60.
- Gleadow, A.J.W. and Duddy, I.R. 1981. A natural long-term track annealing experiment for apatite, *Nucl. Tracks* **5**, 169-174.
- Gleadow, A.J.W. and Fitzgerald, P.G. 1987. Uplift history and structure of the Transantarctic Mountains: new evidence from fission track dating of basement apatites in the Dry Valleys area, southern Victoria Land, *Earth Planet. Sci. Lett.* **82**, 1-14.
- Gleadow, A.J.W., Duddy, I.R., Green, P.F. and Hegarty, K.A. 1986. Fission track lengths in the apatite annealing zone and the interpretation of mixed ages, *Earth Planet. Sci. Lett.* **78**, 245-254.
- Gleadow, A.J.W., Duddy, I.R., Green, P.F. and Lovering, J.F. 1986. Confined fission track lengths in apatite: a diagnostic tool for thermal history analysis, *Contrib. Mineral. Petrol.* **94**, 405-415.
- Gleadow, A.J.W., Hurford, A.J. and Quaife, R.D. 1976. Fission track dating of zircon: Improved etching techniques, *Earth Planet. Sci. Lett.* **33**, 273-276.
- Gloppen, T.G. and Steel, R.J. 1981. The deposits, internal structure and geometry in six alluvial fan-fan delta bodies (Devonian-Norway) - A study in the significance of bedding sequence in conglomerates. In: *Recent and ancient nonmarine depositional environments: Models for exploration* (Edited by Ethridge, F.G. and Flores, R.M.), *Soc. Econ. Pal. Mineral. Spec. Publ.* **31**, 49-69.
- Green, P.F. 1980. On the cause of the shortening of spontaneous fission tracks in certain minerals, *Nucl. Tracks* **4**, 91-100.
- Green, P.F., Duddy, I.R., Gleadow, A.J.W. and Tingate, P.R. 1985. Fission-track annealing in apatite: Track length measurements and the form of the Arrhenius plot. *Nucl. Tracks* **10** (3), 323-328.

- Green, P.F., Duddy, I.R., Laslett, G.M., Hegarty, K.A., Gleadow, A.J.W. and Lovering, J.F. 1989. Thermal annealing in fission tracks in apatite 4. Quantitative modelling techniques and extension to geological timescales. *Chem. Geol. (Isot. Geosci. Sect.)* 79, 155-182.
- Guillande, R. 1988. Evolution Meso-Cenozoique d'une vallée intercordilleraïne andine: La Haute Vallée du Río Magdalena (Colombie). *PhD thesis, University of Paris 6*, 358 p.
- Gustavson, T.C. 1978. Bed forms and stratification types of modern gravel meander lobes, Nueces River, Texas. *Sedimentology* 25, 401-426.
- Hall, M.L. and Wood, C.A. 1985. Volcano-tectonic segmentation of the northern Andes. *Geology* 13, 203-207.
- Halpern, M. 1973. Regional Geochronology of Chile South of 50° Latitude, *Bull. geol. Soc. Am.* 84, 2407-2422.
- Harms, J.C. and Fahnstock, R.K. 1965. Stratification, bedforms and flow phenomena (with an example from the Rio Grande). In: *Primary sedimentary structures and their hydrodynamic interpretation* (Edited by Middleton, G.V.), *Soc. Econ. Pal. Mineral. Spec. Publ.* 12, 84-115.
- Harrison, T.M., Armstrong, R.L., Naesser, C.W. and Harakal, J.E. 1979. Geochronology and thermal history of the Coast Plutonic Complex, near Prince Rupert British Columbia, *Can. J. Earth Sci.* 16, 400-410.
- Helmens, K. Andriessen, P.A.M. and Riezebos, P.A. 1990. Chapter 9: Absolute chronology. In: K.Helmens. Neogene-Quaternary geology of the High Plain of Bogotá (Eastern Cordillera, Colombia) (stratigraphy, paleoenvironments and landscape evolution) pp. 133-141. *PhD Thesis, University of Amsterdam*, pp. 202.
- Heward, A.P. 1978. Alluvial fan sequence and megasequence models; with examples from Westphalian D - Stephanian B coalfields, Northern Spain. In: *Fluvial Sedimentology* (Edited by Miall, A.D.), *Can. Soc. Petrol. Geol. Mem.* 5, 669-702.
- Hildreth, W. 1979. The Bishop Tuff: Evidence for the origin of compositional zonation in silicic magma chambers. *Bull. geol. Soc. Am. Spec. Paper* 180, 43-75.
- Hooghiemstra, H. 1984. Vegetational and climatic history of the high plain of Bogotá, Colombia: a continuous record of the last 3,5 million years. *PhD Thesis, University of Amsterdam*. Also published as *Dissertationes Botanicae* 79, J. Cramer, Vaduz, pp. 368.
- Howe, M.W. 1969. Geologic studies of the Mesa Group (Pliocene?), Upper Magdalena Valley, Colombia. *PhD Thesis, Princeton University*, pp. 67.
- Howe, M.W. 1974. Nonmarine Neiva Formation (Pliocene?), Upper Magdalena Valley, Colombia: Regional Tectonism. *Bull. geol. Soc. Am.* 85, 1031-1042.
- Hughes, C.J. 1973 (for 1972). Spilites, keratophyres, and the igneous spectrum. *Geol. Mag.* 109 (6), 513-527.
- Hurfurd, A.J. 1986. Cooling and uplift patterns in the Lepontine Alps South Central Switzerland and an age of vertical movement on the Insubric fault line, *Contrib. Mineral. Petrol.* 92, 413-427.
- Hurfurd, A.J. and Green, P.F. 1983. The Zeta age calibration of fission-track dating, *Chem. Geol. (Isot. Geosci. Sect.)* 1, 285-317.
- Hurfurd, A.J. and Green, P.F. 1982. A user's guide to fission track dating calibration, *Earth. Planet. Sci. Lett.* 59, 343-354.
- Ingeominas 1988. Mapa geológico de Colombia, escala 1: 1,500.000. Bogotá, Colombia, two sheets.
- Ingeominas 1989. Mapa geológico generalizado del Departamento del Huila, escala 1: 400.000. Bogotá, Colombia. One sheet.
- Irving, E.M. 1975. Structural evolution of the northernmost Andes of Colombia, U.S. Geol. Surv. Prof. Pap. 846, 1-42.
- Jackson, R.G. II 1978. Preliminary evaluation of lithofacies models for meandering alluvial streams. In: *Fluvial Sedimentology* (Edited by Miall, A.D.), *Can. Soc. Petrol. Geol. Mem.* 5, 543-576.
- Jäger, E., Niggli, E. and Wenk, E. 1967. Rb-Sr Altersbestimmungen an Glimmern der Zentralalpen. *Beitr. Geol. Karte Schweiz, Nf Liefg.* 134, Kümmerly and Frey, Bern.
- Jaramillo, J. 1978. Determinación de las edades de algunas rocas de la Cordillera Central de Colombia por el método de huellas de fisión (abstract). *Segundo Congreso Colombiano de Geología, Bogotá*, 19-20.
- Jordan, T.E. 1981. Thrust loads and Foreland Basin Evolution, Cretaceous, Western United States. *Am. Ass. Petrol. Geol. Bull.* 65 (12), 2506-2520.
- Jordan, T.E. and Allmendinger, R.W. 1986. The Sierras Pampeanas of Argentina: A modern analogue of Laramide deformation. *Am. J. Sci.* 286, 737-764.
- Jordan, T.E., Isacks, B.L., Allmendinger, R.W., Brewer, J.A., Ramos, V.A. and Ando, C.J. 1983a. Andean tectonics related to geometry of subducted Nazca plate. *Bull. geol. Soc. Am.* 94, 341-361.
- Jordan, T.E., Isacks, B.L., Ramos, V.A. and Allmendinger, R.W. 1983b. Mountain building in the Central Andes. *Episodes* 3, 20-26.
- Kamp, P.J.J. 1989. Fission track analysis reveals character of collisional tectonics in New Zealand, *Tectonics* 8 (2), 169-195.
- Keigwin, L.I.D. 1978. Pliocene closing of the Isthmus of Panama, based on biostratigraphic evidence from nearby Pacific Ocean and Caribbean Sea cores. *Geology* 6, 630-634.

- Kellogg, J.N. 1984. Cenozoic tectonic history of the Sierra de Perijá, Venezuela-Colombia, and adjacent basins, In: *The Caribbean-South American plate boundary and regional tectonics*, (Edited by Bonini, W.E. and others), *Geol. Soc. Am. Mem.* 162, 239-261.
- Kohn, B.P., Shagam, R., Banks, P.O. and Burkley, L.A. 1984. Mesozoic-Pleistocene fission-track ages on rocks of the Venezuelan Andes and their tectonic implications, In: *The Caribbean-South American plate boundary and regional tectonics*, (Edited by Bonini, W.E. and others), *Mem. geol. Soc. Am.* 162, 365-384.
- Kroonenberg 1980. Mármoles y rocas calcosilicatadas en el Macizo de Garzón cerca de la Jagua, Huila, Colombia. *Geol. Norandina* 2, 11-16.
- Kroonenberg, S.B. 1982a. A Grenvillian granulite belt in the Colombian Andes and its relation to the Guiana Shield, *Geol. Mijnb.* 61, 325-333.
- Kroonenberg, S.B. 1982b. Litología, metamorfismo y origen de las granulitas del Macizo de Garzón, Cordillera Oriental (Colombia), *Geol. Norandina* 6, 39-46.
- Kroonenberg, S.B. and Diederix, H. 1982. Geology of South-Central Huila, Uppermost Magdalena Valley, Colombia. *21st Annual Field Conference, Col. Soc. Petrol. Geol. Geoph. Guide Book* 1-39.
- Kroonenberg, S.B., León Silvestre, L.A.L., do N. Pastana, J.M. and Pessoa, M.R. 1981. Ignimbritas Pliopleistocénicas en el Suroeste del Huila, Colombia y su influencia en el desarrollo morfológico. *Revista CIAF* 6 (1-3), 293-314.
- Kroonenberg, S.B., Pichler, H. and Diederix, H. 1982. Cenozoic alkalibasaltic to ultrabasic volcanism in the uppermost Magdalena Valley, Southern Huila Department, Colombia. *Geol. Norandina* 5, 19-26.
- Kroonenberg, S.B., Pichler, H. and Schmitt-Riegraf, C. 1987. Young Alkalibasaltic to Nephelinitic Volcanism in the Southern Colombian Andes - Origin by Subduction of a Spreading Rift? *Zentralblatt für Geol. Paldont.* I (7/8), 919-936.
- Laslett, G.M., Green, P.F., Duddy, I.R. and Gleadow, A.J.W. 1987. Thermal annealing of fission tracks in apatite 2. A quantitative analysis, *Chem. Geol. (Isot. Geosci. Sect.)* 65, 1-13.
- Le Bas, M.J., Le Maitre, R.W., Streckeisen, A. and Zanettin, B. 1986. A chemical classification of volcanic rocks based on the total Alkali-Silica diagram. *J. Petrol.* 27 (3), 745-750.
- Le Maitre, R.W. 1976. The chemical variability of some common igneous rocks. *J. Petrol.* 17, 589-637.
- Lundberg, J.G., Machado-Allison, A. and Kay, R.F. 1986. Miocene Characid Fishes from Colombia: Evolutionary Stasis and Extirpation. *Science* 234, 208-209.
- Mann, P. and Burke, K. 1984. Neotectonics of the Caribbean. *Rev. Geoph. Space Phys.* 22 (4), 309-362.
- Mathisen, M.E. and Vondra, C.F. 1983. The fluvial and pyroclastic deposits of the Cagayan Basin, Northern Luzon, Philippines - an example on non-marine volcanoclastic sedimentation in an interarc basin. *Sedimentology* 30, 369-392.
- Mattson, P.H. 1984. Caribbean structural breaks and plate movements. In: *The Caribbean-South American plate boundary and regional tectonics*, (Edited by Bonini, W.E. and others), *Mem. geol. Soc. Am.* 162, 131-152.
- McCourt, W.J., Aspden, J.A. and Brook, M. 1984. New geological and geochronological data from the Colombian Andes: continental growth by multiple accretion. *J. geol. Soc. London* 141, 831-845.
- McGowen, J.H. and Garner, L.E. 1970. Physiographic features and stratification types of coarse-grained point bars: Modern and ancient examples. *Sedimentology* 14, 77-111.
- McKee E.D., Crosby, E.J. and Berryhill, H.L. 1967 Flood deposits, Bijou Creek, Colorado. *J. Sed. Petrol.* 37, 829-851.
- McLean, J.R. and Jerzykiewicz, T. 1978. Cyclicity, tectonics and coal: Some aspects of fluvial sedimentology in the Brazeau-Paskapoo Formations, Coal Valley area, Alberta, Canada. In: *Fluvial Sedimentology* (Edited by Miall, A.D.), *Can. Soc. Petrol. Geol. Mem.* 5, 441-468.
- Meissnar, R.O., Flueh, E.R., Sibane, F. and Berg, E. 1976. Dynamics of the active plate boundary in southwest Colombia according to recent geophysical measurements. *Tectonophysics* 53, 115-136.
- Mégard, F. 1984a. The Andean orogenic period and its major structures in central and northern Peru, *J. geol. Soc. London* 141, 893-900.
- Mégard, F. 1984b. Structure and Evolution of the Peruvian Andes. In: *Anatomy of Mountain Ranges*, (Edited by Shaer, J.P. and J. Rodgers, J.), Princeton University Press, 179-210.
- Mégard, F., Noble, D.C., McKee, E.H. and Bellon, H. 1984. Multiple pulses of Neogene compressive deformation in the Ayacucho intermontane basin, Andes of central Peru, *Bull. geol. Soc. Am.* 95, 1108-1117.
- Miall, A.D. 1977. A review of the Braided-River Depositional Environment. *Earth-Science Reviews* 13, 1-62.
- Miall, A.D. 1978a. Tectonic setting and syndepositional deformation of molasse and other nonmarine-paralic sedimentary basins. *Can. J. Earth Sci.* 15, 1613-1632.
- Miall, A.D. 1978b. Lithofacies types and vertical profile models in braided river deposits: a summary. In: *Fluvial Sedimentology* (Edited by Miall, A.D.), *Can. Soc. Petrol. Geol. Mem.* 5, 597-604.
- Miall, A.D. 1980. Cyclicity and the facies model concept in fluvial deposits. *Bull. Can. Petrol. Geol.* 281, 59-80.
- Miall, A.D. 1985. Architectural-element analysis: A new method of facies analysis applied to fluvial deposits. In: *Recognition of fluvial depositional systems and their resource potential* (Edited by Flores, R.M., Ethridge,

- F.G., Miall, A.D., Galloway, W.E. and Fouch, F.D.), *Soc. Econ. Pal. Mineral., Lecture Notes for Short Course 19*, 33-81.
- Mooney, W.D. 1980. An East Pacific-Caribbean ridge during the Jurassic and Cretaceous and the evolution of western Colombia. In: *The origin of the Gulf of Mexico and the early opening of the central North Atlantic Ocean.* (Edited by Pilger Jr., R.H.), *Houston Geological Society Continuing Education Series*, School of Geoscience, Louisiana State University, Baton rouge, 55-74.
- Murcia, A. 1982. El vulcanismo Plio-Cuaternario de Colombia: Depósitos piroclásticos asociados y mediciones isotópicas de $^{87}\text{Sr}/^{86}\text{Sr}$, $^{143}\text{Nd}/^{144}\text{Nd}$ y $\delta^{18}\text{O}$ en lavas de los volcanes Galeras, Puracé y Nevado del Ruiz. *Pub. Geol. Esp. Ingeominas* 10, 1-17.
- Murcia, A. and Pichler, H. 1986. Geoquímica y dataciones radiométricas de las ignimbritas cenozoicas del SW de Colombia. *Revista CIAF* 11 (1-3), 270.
- Myers, J.S., Vertical crustal movements of the Andes in Peru. *Nature* 254 (5502), 672-674, 1975.
- Naeser, C.W. 1978. Fission track dating, *U.S. Geol. Surv. Open File Rep.*, 76-190.
- Naeser, C.W. 1981. The fading of fission tracks in the geologic environment - data from deep drill holes (abstract), *Nucl. Tracks* 5, 248-250.
- Naranjo, J.L., Sigurdsson, H., Carey, S.N. and Fritz, W. 1986. Eruption of the Nevado del Ruiz Volcano, Colombia, On 13 November 1985: Tephra Fall and Lahars. *Science* 233, 961-963.
- Nikonov, A.A. 1989. The rate of uplift in the Alpine mobile belt, *Tectonophysics* 163, 267-276.
- Nilsen, T.H. 1982. Alluvial Fan Deposits. *Am. Ass. Petrol. Geol. Mem.* 31, 49-86.
- Omar, G.I., Steckler, M.S., Buck, W.R. and Kohn, B.P. 1989. Fission-track analysis of basement apatites at the western margin of the Gulf of Suez rift, Egypt: evidence for synchronicity of uplift and subsidence, *Earth Planet. Sci. Lett.* 94, 316-328.
- Pardo-Casas, F. and Molnar, P. 1987. Relative motion of the Nazca (Farallon) and South American plates since Late Cretaceous time. *Tectonics* 6 (3), 233-248.
- Parrish, R.R. 1983. Cenozoic thermal evolution and tectonics of the Coast Mountains of British Columbia 1. Fission track dating, apparent uplift rates, and patterns of uplift, *Tectonics* 2 (6), 601-631.
- Parrish, R.R. 1985. Some cautions which should be exercised when interpreting fission track and other data with regard to uplift rate calculations (abstract), *Nucl. Tracks* 10, 425.
- Pennington, W.D. 1981. Subduction of the Eastern Panama Basin and Seismotectonics of Northwestern South America. *J. Geoph. Res.* 86 (B11), 10753-10770.
- Pierson, T.C. and Scott, K.M. 1985. Downstream Dilution of a Lahar: Transition from Debris Flow to Hyperconcentrated Streamflow. *Water Resources Research* 21 (10), 1511-1524.
- Priem, H.N.A., Andriessen, P.A.M., Boelrijk, N.A.I.M., de Boorder, H., Hebeda, E.H., Huguett, A., Verdurmen, E.A.Th. and Verschure, R.H. 1982. Geochronology of the Precambrian in the Amazonas region of southeastern Colombia (Western Guyana Shield). *Geol. Mijnb.* 61, 229-242.
- Priem, H.N.A., Boelrijk, N.A.I.M., Hebeda, E.H., Verdurmen, E.A.Th. and Verschure, R.H. 1971. Isotopic ages of the Trans-Amazonian acidic magmatism and the Nickerie Metamorphic Episode in the Precambrian basement of Suriname, South America. *Bull. geol. Soc. London* 82, 1667-1680.
- Priem, H.N.A., Kroonenberg, S.B., Boelrijk, N.A.I.M. and Hebeda, E.H. 1989. Rb-Sr and K-Ar evidence for the presence of a 1.6 Ga basement underlying the 1.2 Ga Garzón-Santa Marta granulite belt in the Colombian Andes, *Precambrian Res.* 42, 315-324.
- Ramos, A. and Sopena, A. 1983. Gravel bars in low-sinuosity streams (Permian and Triassic, central Spain). In: *Modern and Ancient Fluvial systems* (Edited by Collinson, J.D. and Lewin, J.), *Int. Ass. Sed. Spec. Publ.* 6, 301-312.
- Ruiz, E. 1977. Estudio morfopedológico de la cuenca superior oriental del alto valle del Río Magdalena, sector Garzón-Gigante, Depto. Huila. *Thesis, University Pasteur/IGAC, Bogotá*, pp. 120.
- Rust, B.R. 1975. Fabric and structure in glaciofluvial gravels. In: *Glaciofluvial and glaciolacustrine sedimentation* (Edited by Jopling, A.V. and McDonald, B.C.), *Soc. Econ. Pal. Mineral. Spec. Publ.* 23, 238-248.
- Rust, B.R. 1978. Depositional models for braided alluvium. In: *Fluvial Sedimentology* (Edited by Miall, A.D.), *Can. Soc. Petrol. Geol. Mem.* 5, 605-625.
- Schmincke, H.-U. 1964. Petrology, paleocurrents, and stratigraphy of the Ellensburg Formation and interbedded Yakima Basalt flows, southcentral Washington. *PhD thesis, John Hopkins University, Baltimore*, pp. 426.
- Schmincke, H.-U. 1967. Graded lahars in the type sections of the Ellensburg Formation, south-central Washington, *J. Sed. Petrol.* 37 (2), 438-448.
- Schmitt, C. 1983a. Petrologische Untersuchungen junger Vulkanite in Südkolumbien. *PhD Thesis, University of Tübingen*, pp. 207.
- Schmitt, C. 1983b. Young volcanism in the Cordillera ranges of Southern Colombia. *Zbl. Geol. Paläont.* I (3/4), 318-328.
- Schumacher, R. and Schmincke, H.-U. 1990. The lateral facies of ignimbrites at Laacher See volcano. *Bull. Volcanology* 52 (4), 271-286.

- Schumm, S.A. 1968. Speculations Concerning Paleohydrologic Controls of Terrestrial Sedimentation. *Bull. geol. Soc. London* 79, 1573-1588.
- Setoguchi, T. and Rosenberger, A.L. 1985. Some new Ceboid Primates from the La Venta, Miocene of Colombia. *Memorias del VI Congreso Latinoamericano de Geología, Bogotá* 1, 287-298.
- Shagam, R., Kohn, B.P., Banks, P.O., Dasch, L.E., Vargas, R., Rodríguez, G.I. and Pimentel, N. 1984. Tectonic implications of Cretaceous-Pliocene fission-track ages from rocks of the circum-Maracaibo Basin region of western Venezuela and eastern Colombia. In: *The Caribbean-South American plate boundary and regional tectonics*, (Edited by Bonini, W.E. and others), *Mem. geol. Soc. Am.* 162, 385-412.
- Smith, G.A. 1986. Coarse-grained nonmarine volcanoclastic sediment: Terminology and depositional process. *Bull. geol. Soc. London* 97, 1-10.
- Smith, G.A. 1987a. The influence of explosive volcanism on fluvial sedimentation: The Deschutes Formation (Neogene) in Central Oregon. *J. Sed. Petrol.* 57 (4), 613-629.
- Smith, G.A. 1987b. Sedimentology of volcanism-induced aggradation in fluvial basins: examples from the Pacific Northwest, U.S.A. In: *Recent developments in Fluvial sedimentology* (Edited by Ethridge, F.G., Flores, R.M. and Harvey, M.G.), *Soc. Econ. Pal. Soc. Econ. Pal. Mineral. Spec. Publ.* 39, 217-228.
- Smith, N.D. 1970. The braided stream depositional environment: comparison of the Platte River with some Silurian clastic rocks, north-central Appalachians. *Bull. geol. Soc. London* 81, 2993-3014.
- Smith, R.L. 1960. Zones and zonal variations in welded ash flows. *U.S. Geol. Survey Prof. Paper* 354F, 149-159.
- Sparks, R.S.J. 1976. Grain size variations in ignimbrites and implications for the transport of pyroclastic flows. *Sedimentology* 23, 147-188.
- Sparks, R.S.J., Self, S. and Walker, G.P.L. 1973. Products of ignimbrite eruptions. *Geology* 1, 115-118.
- Steel, R.J. 1976. Devonian basins of western Norway - Sedimentary response to tectonism and to varying tectonic context. *Tectonophysics* 36, 207-224.
- Steel, R.J. and Aasheim, S.M. 1978. Alluvial sand deposition in a rapidly subsiding basin (Devonian, Norway). In: *Fluvial Sedimentology* (Edited by A.D. Miall) *Can. Soc. Petrol. Geol. Mem.* 5, 385-412.
- Stibane, F. and Forero, A. 1969. Los afloramientos del Paleozoico en La Jagua (Huila) y Río Nevado (Santander del Sur). *Geol. Colombiana* 6, 33-66.
- Streckeisen, A. 1976. To each plutonic rock its proper name. *Earth Sci. Rev.* 12, 1-33.
- Streckeisen, A. and Le Maitre, R.W. 1979. A Chemical Approximation to the Modal QAPF Classification of the Igneous Rocks. *N. Jb. Miner. Abh.* 136 (2), 169-206.
- Strecker, M.R., Cervený, P., Bloom, A.L. and Malizia, D. 1989. Late Cenozoic tectonism and landscape development in the foreland of the Andes: Northern Sierras Pampeanas (26°-28°S), Argentina. *Tectonics* 8 (3), 517-534.
- Sykes, L., McCann, W.R. and Kafka, A.L. 1982. Motion of Caribbean Plate during last 7 million years, and implications for earlier Cenozoic movements. *J. Geophys. Res.* 87, 10656-10676.
- Takemura, K. and Danhara, T. 1983. Fission-track age of pumices included in the Gigante Formation, North of Neiva, Colombia. *Kyoto University Overseas Research Reports of New World Monkeys* 3, 13-15.
- Tello, H. and Hernández, T. 1976. Investigación geológica en el Parque Arqueológico de San Agustín (Huila). *BSc thesis, Universidad Nacional de Colombia*, pp. 30.
- Thomas, R.G., Smith, D.G., Wood, J.M., Visser, J., Calverley-Range, E.A. and Koster, E.H. 1987. Inclined heterolithic stratification - Terminology, description, interpretation and significance. *Sed. Geol.* 53, 123-179.
- Thouret, J.C. 1988. La Cordillère Centrale des Andes de Colombie et ses bordures: morphogenèse Plio-Quaternaire et dynamique actuelle et récente d'une cordillère volcanique englacée. *PhD Thesis, Université Joseph Fourier, Grenoble* I.
- Uyeda, S. and Watanabe, T. 1970. Preliminary report of terrestrial heat flow study in the South American continent; Distribution of geothermal gradients, *Tectonophysics* 10, 235-242.
- Van der Hammen, T. and Cleef, A.M. 1986. Development of the High Andean Páramo Flora and Vegetation. In: *High-altitude Tropical Biogeography*, (Edited by Vuilleumier, F. and Monasterio, M.), Oxford University Press, 153-200.
- Van Houten, F.B. 1976. Late Cenozoic volcanoclastic deposits, Andean foredeep, Colombia. *Bull. geol. Soc. Am.* 87, 481-495.
- Van Houten, F.B. and Travis, R.B. 1968. Cenozoic deposits, Upper Magdalena Valley, Colombia. *Am. Ass. Petrol. Geol. Bull.* 52, 675-702.
- Van Kampen, M. 1986. Geomorphologisch onderzoek in de Vallei van de Río Paez rondom Paicol, Huila, Colombia. *Unpublished report, Agricultural University of Wageningen*, pp. 53.
- Vessell, R.K. and Davies, D.K. 1981. Nonmarine sedimentation in an active fore arc basin. In: *Recent and ancient nonmarine depositional environments: models for exploration* (Edited by Ethridge, F.G. and Flores, R.M.), *Soc. Econ. Pal. Mineral. Spec. Publ.* 31, 31-49.
- Wagner, G.A. 1979. Correction and interpretation of fission track ages. In: *Lectures in Isotope Geology*, (Edited by Jäger, E. and Hunziker, J.C.), 170-177.

- Wagner, G.A. 1988. Apatite fission-track geochrono-thermometer to 60°C: projected length studies, *Chem. Geol. (Isot. Geosci. Sect.)* 72, 145-153.
- Wagner, G.A., Gleadow, A.J.W. and Fitzgerald, P.G. 1989. The significance of the partial annealing zone in apatite fission-track analysis: Projected track length measurements and uplift geochronology of the Transantarctic Mountains, *Chem. Geol. (Isot. Geosci. Sect.)* 79, 295-305.
- Wagner, G.A., Reimer, G.M. and Jäger, E. 1977. Cooling ages derived by apatite fission-track, mica Rb-Sr and K-Ar dating: The uplift and cooling history of the Central Alps, *Inst. Geol. Mineral. Univ. Padova Mem.* 30, 27 pp.
- Walker, G.P.L., Heming, R.F. and Wilson, C.J.N. 1980. Low-aspect ratio ignimbrites. *Nature* 283, 286-287.
- Walker, G.P.L., Wilson, C.J.N. and Frogatt, P.C. 1981. An ignimbrite veneer deposit: the trail marker of a pyroclastic flow. *J. Volcanol. Geotherm. Res.* 9, 409-421.
- Weiske, F. 1926. Memoria detallada de los estudios del Río Magdalena, obras proyectadas para su arreglo y resumen del presupuesto. *Comp. Estud. Geol. Ofic. Colombia* 4, 15-124.
- Wellman, S.S. 1968. Stratigraphy, petrology, and sedimentology of the nonmarine Honda Formation (Miocene), Upper Magdalena Valley, Colombia. *PhD Thesis, Princeton University*, pp 250.
- Wellman, S.S. 1970. Stratigraphy and Petrology of the Nonmarine Honda Group (Miocene), Upper Magdalena Valley, Colombia. *Bull. geol. Soc. Am.* 81, 2353-2374.
- Whitney, J.A. and Stormer Jr., J.C. 1985. Mineralogy, petrology and magmatic conditions from the Fish Canyon Tuff, Central San Juan Volcanic Field, Colorado. *J. Petrol.* 26 (3), 726-762.
- Wilson, C.J.N. 1980. The role of fluidization in the emplacement of pyroclastic flows: an experimental approach. *J. Volcanol. Geotherm. Res.* 8, 231-249.
- Wilson, C.J.N. and Walker, G.P.L. 1982. Ignimbrite depositional facies: the anatomy of a pyroclastic flow. *J. geol. Soc. London* 139, 581-592.
- Winkler, H.G.F. 1979. *Petrogenesis of metamorphic rocks*, Springer Verlag, New York, chapter 5: A key to determine metamorphic grades and major reaction-isograds or isograds in common rocks, 239-250.
- Wortel, M.J.R. 1986. Spatial and temporal variations in the Andean subduction zone. *J. geol. Soc. London* 141 (5), 783-791.
- Zaun, P.E. and Wagner, G.A. 1985. Fission-track stability in zircons under geological conditions, *Nucl. Tracks* 10 (3), 303-307.
- Zeitler, P., Tahirkheli, R.A.K., Naeser, C.W. and Johnson, N.M. 1982. Unroofing history of a suture zone in the Himalaya of Pakistan by means of fission track annealing ages, *Earth Planet. Sci. Lett.* 57, 227-240.

Appendix 2

Lithology and mineralogy of the fission track samples of chapter II.

Sample no.	Lithology	Composition ¹
Section Guadalupe-Florencia		
MW 59	Charnockitic/charno-enderbitic granulite	Brown hornblende; brown biotite; plagioclase; rich in K-feldspar
MW 58	Charnockitic granulite	Chloritized biotite; plagioclase; perthite; K-feldspar; quartz
MW 57	Gabbro-noritic granulite	brown hornblende; Ti-rich biotite; orthopyroxene; clinopyroxene; rich in plagioclase (labradorite, andesine); quartz
MW 56	Quartz diorite	Sericitized hornblende and plagioclase; microgranitic groundmass
MW 54	Enderbitic/charno-enderbitic granulite	Biotite; amphibole; orthopyroxene; plagioclase; K-feldspar, quartz
MW 53	Charnockitic granulite	Biotite; hornblende; perthite
Section Tres Esquinas		
SK 490	Gabbro-noritic granulite	Brown hornblende; orthopyroxene; clinopyroxene; plagioclase; no quartz
MW 74	Charnockitic granulite	Retrograde metamorphosed; primary minerals: plagioclase; K-feldspar (perthite); quartz; secondary minerals: biotite; epidote
MW 73	Noritic granulite	Retrograde metamorphosed; primary minerals: biotite, hornblende; quartz; orthopyroxene; plagioclase (andesine); secondary minerals: biotite; amphibole
MW 72	Biotite granite	Biotite; feldspar; quartz
MW 75	Calcsilicate rock	Hornblende; scapolite; plagioclase; K-feldspar; titanite
MW 76	Calcsilicate rock	Phlogopite; K-feldspar; diopside
Neiva-San Vicente del Caguán		
JF 1	Biotite gneiss	Chloritized biotite; plagioclase; K-feldspar; granate
JF 3	Biotite gneiss	Ti-rich biotite; plagioclase (microcline); quartz; granate

¹ accessory minerals are not listed

Lithological and mineralogical classification of the K-Ar and fission track samples from the Honda and Gigante Formations (chapters IV and VIII).

Sample no.	Classification	Degree of reworking and composition ¹
Honda Formation		
MW 216	Air-fall tuff	Biotite; hornblende; augite; plagioclase
MW 165	Air-fall tuff	Slightly reworked; biotite; hornblende; plagioclase; pumice fragments
Gigante Formation		
MW 104	Lapilli stone (ignimbrite)	Biotite; hornblende; plagioclase; quartz; pumice fragments; lithic fragments
MW 105	Dacite clast from ignimbrite	Biotite; hornblende; plagioclase; quartz
MW 110	Lithic crystal tuff (ignimbrite)	Slightly reworked; biotite; hornblende; plagioclase; quartz
MW 126	Crystal tuff (ignimbrite)	Hornblende; plagioclase; hypersthene; pumice fragments; lithic fragments
MW 146	Ignimbrite clast from debris flow deposit	Reworked; biotite; hornblende; plagioclase; quartz; pumice fragments; lithic fragments
MW 154	Lithic crystal tuff (ignimbrite)	Hornblende; plagioclase; quartz; pumice fragments; lithic fragments
MW 157	Crystal tuff (ignimbrite)	Biotite; hornblende; plagioclase; quartz; pumice fragments; lithic fragments
MW 202	Ignimbrite clast from ignimbrite clast concentration in sandstone	Reworked?; biotite; hornblende; plagioclase; quartz
MW 179	Pumice clast from pumice concentration in sandstone	Biotite; hornblende; augite; plagioclase; quartz
MW 195	Pumice clast from pumice concentration in sandstone	Biotite; hornblende; plagioclase; quartz
MW 206	Pumice clast from pumice concentration in sandstone	Biotite; hornblende; plagioclase; quartz
MW 537	Weathered air-fall tuff	White clay, contains zircon grains
MW 542 (Q. El Arrayán)	Lapilli stone (ignimbrite?)	Hornblende; plagioclase; quartz; pumice fragments; lithic fragments
MW 178 (Suaza Valley)	Crystal tuff (ignimbrite)	Biotite; hornblende; plagioclase; quartz; pumice fragments; lithic fragments

¹ accessory minerals are not listed

Lithology of the K-Ar and fission track samples from the El Carmen and Guacacallo formations (chapter IX), as well as from the volcanoclastic terraces along the Río Páez and Río Magdalena (chapters IV and X).

Sample no.	Classification	Composition ¹
El Carmen formation		
MW 377	Crystal tuff (ignimbrite/air-fall tuff?)	Biotite; hornblende; plagioclase; pumice fragments; lithic fragments
Guacacallo Formation		
MW 385	Vitric tuff (ignimbrite)	Biotite; plagioclase; quartz; pumice fragments; lithic fragments
MW 382	Vitric tuff (ignimbrite)	Biotite; plagioclase; quartz; pumice fragments; lithic fragments
MW 390	Vitric tuff (ignimbrite)	Biotite; plagioclase; quartz; pumice fragments
MW 399	Vitric tuff (ignimbrite)	Biotite; plagioclase; quartz; pumice fragments
MW 408	Vitric tuff (ignimbrite)	Biotite; plagioclase; quartz; pumice fragments; lithic fragments
MW 413	Vitric tuff (ignimbrite)	Biotite; plagioclase; quartz; pumice fragments
MW 405	Vitric tuff (ignimbrite)	Biotite; plagioclase; quartz; pumice fragments; lithic fragments
MW 77	Vitric tuff (ignimbrite)	Biotite; plagioclase; quartz; lithic fragments
Río Páez Terraces		
<u>Highest terrace</u>		
MW 548	Pumice clast	Biotite; hornblende; plagioclase; quartz
MW 549	Pumice clast	Hornblende; plagioclase; quartz
<u>High terrace</u>		
MW 430	Pumice clast	Biotite; hornblende; plagioclase; quartz
MW 442	Pumice clast	Biotite; hornblende; plagioclase; quartz
Río Magdalena Terraces		
<u>High terrace</u>		
MW 100	Pumice clast	Biotite; hornblende; plagioclase; quartz
MW 101	Pumice clast	Biotite; hornblende; plagioclase; quartz

¹ accessory minerals are not listed

Appendix 3

Gigante Formation: Major element data of ignimbrites.

Sample Section Member	MW 104	MW 110	MW 115	MW 119	MW125	MW 126	MW 154	MW 157	MW 188	MW 178
	QQt Alt.	QQt Alt.	QQt Alt.	QQt Alt.	QQt Alt.	QQt Alt.	QLH Alt.	QLH Garz.	Alt.	Suaza Garz.?
SiO2	59.97	63.91	62.17	62.13	59.31	61.25	62.86	60.72	61.55	64.38
TiO2	0.59	0.40	0.53	0.55	0.61	0.54	0.59	0.64	0.61	0.56
Al2O3	14.77	17.96	17.35	16.41	16.48	18.09	16.48	18.08	16.67	14.59
Fe2O3	4.81	3.07	3.85	3.97	4.73	3.81	4.57	5.06	4.66	4.24
MnO	0.10	0.05	0.06	0.07	0.08	0.09	0.08	0.09	0.07	0.07
MgO	2.77	1.54	1.85	2.08	3.20	1.54	2.57	2.38	2.76	1.96
CaO	3.99	5.07	4.63	4.51	4.73	5.05	4.63	4.87	4.79	3.46
Na2O	1.88	4.20	3.91	3.49	3.33	3.81	3.71	3.80	3.41	2.81
K2O	1.66	1.46	1.99	2.39	1.91	2.73	2.00	1.90	1.88	2.63
P2O5	0.22	0.12	0.19	0.20	0.17	0.15	0.19	0.21	0.19	0.24
BaO	0.07	0.10	0.10	0.12	0.09	0.12	0.11	0.13	0.12	0.13
L.I.	8.93	1.76	3.36	3.13	5.42	2.69	2.09	2.00	3.15	4.09
Total (%)	99.76	99.64	99.99	99.05	100.06	99.87	99.88	99.88	99.86	99.16
Q	33.74	21.55	20.38	21.38	19.26	16.43	20.90	18.37	21.41	29.82
Or	10.81	8.82	12.18	14.74	11.94	16.62	12.10	11.48	11.50	16.37
Ab	17.52	36.34	34.27	30.82	29.80	33.21	32.13	32.89	29.87	25.04
An	20.22	24.92	22.51	21.99	23.64	24.80	22.24	23.31	23.31	16.43
Hy	7.60	3.92	4.77	5.41	8.43	3.95	6.55	6.06	7.12	5.14
Hm	5.30	3.14	3.99	4.14	5.00	3.93	4.68	5.18	4.82	4.47
Ap	0.57	0.29	0.47	0.49	0.43	0.37	0.46	0.51	0.47	0.60
Il	0.24	0.11	0.13	0.16	0.18	0.20	0.18	0.20	0.16	0.16
C	3.47	0.55	0.83	0.38	0.78	0.05	0.26	1.45	0.80	1.48
Ru	0.53	0.35	0.48	0.49	0.55	0.45	0.51	0.55	0.55	0.51
C.I.	25.55	27.67	25.85	25.78	29.55	27.57	26.83	27.56	28.30	20.03
D.I.	65.54	67.27	67.66	67.32	61.77	66.31	65.38	64.20	63.58	72.71

Gigante Formation: Major element data of pumice.

Sample Section Member	MW 105	MW 126	MW 187	MW 179	MW 91	MW 195	MW 206
	QQt Alt.	QQt Alt.	Alt.	QQt Alt.	Alt.	QID-B Alt.	Alt.
SiO2	61.23	62.40	65.27	64.08	59.02	62.99	59.97
TiO2	0.45	0.49	0.51	0.51	0.69	0.51	0.68
Al2O3	16.77	17.52	16.45	15.53	16.12	16.18	15.76
Fe2O3	3.01	3.83	3.78	3.67	5.52	3.75	5.05
MnO	0.10	0.10	0.07	0.07	0.09	0.07	0.11
MgO	2.20	1.42	1.96	1.92	2.34	2.09	2.63
CaO	4.49	5.06	4.19	4.01	4.31	4.12	4.45
Na2O	3.73	3.30	3.24	3.22	2.10	3.44	2.36
K2O	1.15	3.01	3.28	3.07	2.58	3.43	2.97
P2O5	0.17	0.16	0.27	0.20	0.26	0.20	0.29
BaO	0.16	0.13	0.15	0.13	0.11	0.17	0.10
L.I.	6.65	2.08	1.75	3.57	6.43	2.71	4.74
Total (%)	100.11	99.50	100.92	99.98	99.57	99.66	99.11
Q	24.34	19.71	22.96	23.59	26.81	19.21	23.59
Or	7.28	18.28	19.57	18.84	16.39	20.94	18.61
Ab	33.82	28.70	27.68	28.29	19.10	30.07	21.18
An	22.68	24.72	19.21	19.30	21.15	19.19	21.40
Hy	5.87	3.63	4.93	4.97	6.26	5.38	6.95
Hm	3.23	3.94	3.82	3.81	5.93	3.87	5.36
Ap	0.43	0.39	0.65	0.49	0.66	0.49	0.73
Il	0.23	0.22	0.15	0.16	0.21	0.15	0.25
C	1.75	0.02	0.60	0.10	2.86	0.00	1.34
Tn	0.00	0.00	0.00	0.00	0.00	0.40	0.00
Ru	0.36	0.39	0.44	0.45	0.63	0.28	0.59
C.I.	26.80	27.27	22.66	22.78	25.54	22.96	26.27
D.I.	67.20	66.71	70.81	70.83	65.15	70.23	64.73

Gigante Formation: Major element data of volcanic debris flow blocks.

Sample Section Member	MW 164 QQt Alt.	GB 6 QQt Alt.	GB 7 QQt Alt.	MW 109 QQt Alt.	MW 116 QQt Alt.	GB 15 QQt Alt.	MW 121 QQt Alt.	MW 85 Alt.	MW 93a Alt.	MW 205 Alt.
SiO ₂	61.19	64.51	62.37	65.84	63.08	63.35	63.56	63.94	62.18	61.74
TiO ₂	0.62	0.44	0.47	0.45	0.49	0.57	0.56	0.65	0.72	0.73
Al ₂ O ₃	15.71	15.71	16.71	15.69	17.89	16.08	16.47	16.23	16.86	16.22
Fe ₂ O ₃	4.37	3.23	3.38	3.30	3.71	4.45	4.34	5.10	4.83	5.39
MnO	0.08	0.04	0.07	0.05	0.06	0.07	0.07	0.10	0.09	0.10
MgO	2.10	1.45	1.67	1.46	1.65	2.27	2.36	2.16	1.32	2.75
CaO	4.79	3.31	3.84	3.91	4.83	4.14	4.57	4.68	4.53	5.45
Na ₂ O	2.49	3.20	4.30	4.13	4.25	3.56	3.89	3.69	3.42	4.53
K ₂ O	2.11	1.65	1.30	1.72	1.64	2.30	2.04	2.39	2.51	2.16
P ₂ O ₅	0.22	0.12	0.15	0.17	0.15	0.19	0.18	0.19	0.34	0.24
BaO	0.16	0.10	0.09	0.11	0.10	0.12	0.11	0.10	0.12	0.10
L.I.	5.46	4.42	4.92	3.25	2.66	2.50	0.87	0.69	3.03	1.59
Total (%)	99.30	98.18	99.27	100.08	100.51	99.60	99.02	99.92	99.95	101.00
Q	27.60	32.74	23.44	26.01	20.15	22.81	20.74	21.09	22.69	13.83
Or	13.31	10.41	8.15	10.51	9.91	14.01	12.29	14.25	15.32	12.85
Ab	22.49	28.91	38.59	36.13	36.78	31.06	33.57	31.49	29.89	38.59
An	23.83	16.69	19.17	18.90	23.51	19.89	21.88	20.84	20.92	17.66
Hy	5.58	3.86	4.41	3.76	4.20	5.83	5.99	5.43	3.40	4.80
Hm	4.66	3.45	3.59	3.41	3.80	4.59	4.43	5.14	4.99	5.43
Ap	0.56	0.30	0.38	0.42	0.36	0.46	0.43	0.45	0.83	0.57
Il	0.18	0.09	0.16	0.11	0.13	0.15	0.15	0.22	0.20	0.22
Di	0.00	0.00	0.00	0.00	0.00	0.00	0.00	0.00	0.00	4.53
C	1.23	3.13	1.70	0.34	0.72	0.68	0.00	0.00	1.13	0.00
Tn	0.00	0.00	0.00	0.00	0.00	0.00	0.03	0.93	0.00	1.53
Ru	0.57	0.42	0.41	0.41	0.43	0.51	0.48	0.16	0.64	0.00
C.I.	27.74	19.40	22.26	21.54	26.45	23.98	26.08	24.64	23.30	25.55
D.I.	64.62	75.19	71.88	72.99	67.57	68.56	66.60	66.82	69.03	65.27

ANKC-values of all samples

Sample	ANKC	Sample	ANKC	Sample	ANKC
MW 110	1.01	MW 126	0.98	GB 6	1.21
MW 115	1.02	MW 187	1.00	GB 7	1.08
NW 119	1.00	MW 179	0.98	MW 109	1.00
MW 126	0.99	MW 195	0.96	MW 116	1.02
MW 154	0.99	MW 206	1.04	GB 15	1.02
MW 157	1.06			MW 121	0.98
MW 188	1.02			MW 85	0.95
				MW 93a	1.11
				MW 205	0.82

Appendix 4

Itaibe section: Major element data of volcanic debris flow blocks.

Sample	MW 423	MW 425	MW 426	MW 427	MW 428	MW 429	MW 431	MW 432	MW 434
SiO ₂	60.31	59.39	57.35	57.47	61.36	62.84	61.71	59.73	58.06
TiO ₂	0.90	0.97	1.11	1.09	0.92	0.82	0.87	0.92	0.94
Al ₂ O ₃	16.26	15.92	16.97	16.00	16.78	17.10	16.69	16.36	15.80
Fe ₂ O ₃	5.58	6.30	7.14	6.30	6.06	5.09	5.65	6.05	6.39
MnO	0.10	0.11	0.12	0.11	0.09	0.09	0.10	0.10	0.11
MgO	3.63	4.08	3.93	4.61	3.12	2.62	3.02	4.05	4.72
CaO	5.86	5.93	6.71	6.53	5.62	5.17	5.46	5.97	6.79
Na ₂ O	4.67	4.29	4.41	4.69	4.81	4.86	4.99	4.92	3.70
K ₂ O	2.22	2.04	1.65	1.93	2.03	2.32	1.98	1.73	1.67
P ₂ O ₅	0.28	0.27	0.34	0.29	0.28	0.29	0.27	0.28	0.37
BaO	0.10	0.10	0.09	0.11	0.11	0.13	0.11	0.10	0.12
L.I.	0.76	1.19	0.50	0.31	0.13	0.11	0.26	0.39	1.18
Total (%)	100.67	100.49	100.32	99.44	101.31	101.44	101.11	100.60	99.85
Q	9.74	10.80	8.17	5.75	11.29	12.62	11.32	8.68	11.87
Or	13.14	12.15	9.77	11.52	11.87	13.54	11.61	10.21	10.01
Ab	39.58	36.59	37.41	40.07	40.26	40.63	41.90	41.58	31.76
An	16.88	18.03	21.69	17.07	18.00	17.78	17.16	17.42	21.88
Hy	6.29	7.76	7.63	7.87	5.90	5.28	5.53	7.36	9.42
Hm	5.59	6.35	7.16	6.36	5.99	5.03	5.61	6.04	6.48
Ap	0.66	0.64	0.81	0.69	0.66	0.68	0.63	0.66	0.89
Il	0.21	0.24	0.26	0.24	0.19	0.19	0.21	0.21	0.24
Di	5.97	5.35	4.71	8.04	3.85	2.51	4.16	5.85	5.41
Tn	1.94	2.09	2.40	2.39	1.99	1.74	1.84	1.98	2.03
C.I.	27.25	28.82	31.75	30.62	25.99	23.99	25.21	28.44	33.90
D.I.	62.46	59.54	55.35	57.34	63.42	66.79	64.84	60.47	53.65

Río Páez, isolated outcrops: Major element data of volcanic debris flow blocks.

Sample	MW 415	MW 418	MW 419	MW 422	MW 436	MW 443	MW 451
SiO ₂	60.84	60.22	59.69	62.46	62.52	58.19	60.77
TiO ₂	0.86	0.83	0.87	0.75	0.80	0.91	0.82
Al ₂ O ₃	15.96	16.86	16.90	16.86	16.62	15.83	16.70
Fe ₂ O ₃	6.16	6.04	6.51	5.27	5.82	6.81	5.53
MnO	0.10	0.11	0.11	0.09	0.09	0.11	0.10
MgO	3.37	3.18	2.88	2.24	2.77	4.14	3.14
CaO	5.77	5.59	5.99	4.92	5.15	6.53	5.64
Na ₂ O	3.88	3.82	4.02	4.21	3.90	3.41	4.72
K ₂ O	2.00	2.11	1.88	2.09	2.09	1.93	2.00
P ₂ O ₅	0.26	0.29	0.35	0.26	0.28	0.31	0.27
BaO	0.10	0.11	0.10	0.13	0.11	0.10	0.11
L.I.	0.14	0.91	0.66	0.75	0.39	0.83	0.11
Total (%)	99.44	100.07	99.96	100.03	100.54	99.10	99.91
Q	15.54	14.86	14.15	17.36	17.90	13.70	11.37
Or	11.91	12.59	11.20	12.45	12.34	11.62	11.85
Ab	33.09	32.63	34.28	35.92	32.98	29.39	40.05
An	20.39	22.84	22.69	21.11	21.66	22.60	18.53
Hy	6.97	7.72	6.39	5.63	6.89	8.50	5.93
Hm	6.21	6.10	6.56	5.31	5.82	6.94	5.55
Ap	0.62	0.69	0.84	0.62	0.66	0.75	0.64
Il	0.22	0.24	0.24	0.19	0.19	0.24	0.21
Di	3.21	0.59	1.82	0.00	0.00	4.32	4.12
Tn	1.85	1.75	1.85	1.26	1.44	1.96	1.74
Ru	0.00	0.00	0.00	0.14	0.11	0.00	0.00
C.I.	28.48	28.84	28.99	25.05	26.49	32.87	26.81
D.I.	60.54	60.07	59.62	65.73	63.22	54.70	63.27

Vereda La Mesa: Major element data of volcanic debris flow blocks.

Sample	MW 437	MW 438	MW 444	MW 445	MW 448	MW450
SiO ₂	57.09	57.30	60.37	57.29	57.92	59.58
TiO ₂	1.05	1.11	0.87	1.02	1.03	0.95
Al ₂ O ₃	17.35	16.80	15.96	16.58	14.96	16.19
Fe ₂ O ₃	7.10	7.10	5.44	7.10	6.66	5.86
MnO	0.11	0.12	0.09	0.08	0.16	0.13
MgO	3.25	3.44	3.43	3.83	4.36	2.33
CaO	6.64	6.46	6.23	6.77	7.27	5.41
Na ₂ O	3.62	3.76	3.59	3.76	3.42	3.39
K ₂ O	1.69	1.94	2.14	1.68	2.16	2.62
P ₂ O ₅	0.37	0.49	0.31	0.32	0.36	0.41
BaO	0.09	0.13	0.12	0.10	0.14	0.15
L.I.	1.53	1.07	0.06	1.39	0.95	1.91
Total (%)	99.89	99.72	98.61	99.92	99.39	98.93
Q	12.71	11.81	15.64	11.61	12.06	17.10
Cr	10.16	11.63	12.84	10.08	12.98	15.98
Ab	31.16	32.28	30.85	32.32	29.43	29.60
An	26.55	23.58	21.45	23.77	19.41	21.90
Hy	7.80	7.88	6.81	7.91	6.76	5.94
Hm	7.22	7.20	5.53	7.21	6.77	6.05
Ap	0.89	1.18	0.75	0.77	0.87	1.00
Il	0.24	0.26	0.20	0.17	0.35	0.29
Di	0.95	1.75	4.03	3.84	9.24	0.11
Tn	2.31	2.43	1.92	2.32	2.12	2.04
C.I.	32.97	30.85	30.24	33.15	33.39	26.17
D.I.	54.04	55.72	59.33	54.01	54.48	62.68

Appendix 5

Guacacallo-Saladoblanco area: Major element data of ignimbrites.

Sample	MW 368	MW 373	MW 376	MW 378	MW 389	MW 390
SiO ₂	72.23	73.85	73.44	71.77	71.39	73.60
TiO ₂	0.29	0.24	0.24	0.23	0.23	0.21
Al ₂ O ₃	14.59	14.29	14.52	14.22	14.62	14.44
Fe ₂ O ₃	1.76	1.37	1.60	2.68	1.23	1.19
MnO	0.06	0.05	0.06	0.03	0.05	0.07
MgO	0.30	0.30	0.19	0.22	0.22	0.22
CaO	1.01	0.69	0.64	0.30	0.44	0.40
Na ₂ O	3.89	4.34	3.62	2.30	3.33	3.55
K ₂ O	3.69	3.90	3.87	3.97	3.91	4.20
P ₂ O ₅	0.03	0.04	0.02	0.04	0.03	0.03
BaO	0.18	0.18	0.18	0.18	0.14	0.18
L.I.	1.08	0.63	1.42	3.81	4.15	1.71
Total (%)	99.11	99.88	99.80	99.75	99.74	99.80
Q	33.38	31.97	36.34	43.54	37.37	36.33
Or	22.31	23.28	23.31	24.54	24.22	25.37
Ab	33.67	37.09	31.22	20.36	29.54	30.70
An	4.93	3.19	3.10	1.28	2.08	1.83
C	2.49	1.79	3.32	5.95	4.38	3.47
Hy	1.51	1.24	1.21	2.23	1.11	1.08
Mt	1.08	0.87	0.98	1.54	0.76	0.74
Il	0.56	0.46	0.46	0.46	0.46	0.41
Ap	0.07	0.10	0.05	0.10	0.07	0.07
C.I.	5.46	3.72	3.44	1.69	2.49	2.22
D.I.	91.84	94.13	94.19	94.39	95.52	95.87

La Argentina-La Plata area: Major element data of ignimbrites.

Sample	MW 392	MW 396	MW 399	MW 405	MW 408	MW 410
SiO ₂	74.88	72.70	72.69	74.61	73.77	70.16
TiO ₂	0.21	0.21	0.25	0.21	0.26	0.31
Al ₂ O ₃	14.08	13.72	14.93	14.15	14.77	15.40
Fe ₂ O ₃	1.28	1.11	1.55	1.23	1.42	2.10
MnO	0.06	0.07	0.06	0.06	0.09	0.10
MgO	0.16	0.22	0.27	0.20	0.21	0.34
CaO	0.52	0.64	0.54	0.43	0.42	1.10
Na ₂ O	3.85	3.84	4.11	4.13	3.93	3.63
K ₂ O	3.83	3.91	3.84	3.99	4.02	3.40
P ₂ O ₅	0.02	0.05	0.03	0.03	0.03	0.02
BaO	0.19	0.17	0.20	0.17	0.18	0.20
L.I.	0.87	2.44	1.09	0.80	1.30	2.21
Total (%)	99.95	99.08	99.56	100.01	100.40	98.97
Q	36.72	34.89	32.93	34.32	34.54	33.95
Or	22.90	23.97	23.11	23.82	24.03	20.83
Ab	32.97	33.70	35.42	35.31	33.64	31.85
An	2.48	2.95	2.53	1.96	1.91	5.52
C	2.74	2.21	3.16	2.35	3.30	3.94
Hy	0.95	1.05	1.32	0.99	1.12	2.00
Mt	0.79	0.70	0.97	0.78	0.89	1.25
Il	0.40	0.41	0.48	0.40	0.50	0.61
Ap	0.05	0.12	0.07	0.07	0.07	0.05
C.I.	2.76	3.35	3.01	2.31	2.28	6.14
D.I.	95.33	94.76	94.62	95.80	95.51	90.57

Section La Laguna: Major element data of ignimbrites.

Sample Elevation (m)	MW 362c 1430	MW 362b 1450	MW 362a 1475	MW 362 1490	MW 361a 1510	MW 361 1530	MW 360 1550	MW 359a 1570	MW 359 1590
SiO ₂	72.53	74.34	73.26	73.60	74.04	72.66	68.89	69.94	69.20
TiO ₂	0.17	0.20	0.20	0.21	0.22	0.24	0.22	0.27	0.33
Al ₂ O ₃	15.02	14.95	15.12	14.36	13.91	15.60	17.49	16.34	17.88
Fe ₂ O ₃	1.45	1.57	1.11	1.58	1.61	1.77	2.29	1.75	2.60
MnO	0.07	0.05	0.07	0.09	0.04	0.04	0.04	0.04	0.48
MgO	0.15	0.22	0.13	0.16	0.21	0.26	0.26	0.26	0.33
CaO	0.63	0.65	0.58	0.65	0.52	0.71	0.57	0.65	0.39
Na ₂ O	3.52	3.76	3.64	3.66	3.27	3.52	2.43	2.90	1.90
K ₂ O	3.64	3.89	3.79	3.74	3.95	3.68	3.59	3.64	3.09
P ₂ O ₅	0.02	0.02	0.02	0.02	0.02	0.02	0.02	0.02	0.01
BaO	0.18	0.18	0.20	0.17	0.18	0.17	0.18	0.18	0.26
L.I.	1.83	0.79	1.07	0.88	1.18	1.38	3.13	2.37	3.86
Total (%)	99.21	100.62	99.19	99.12	99.15	100.05	99.11	98.36	100.33
Q	37.33	35.75	36.70	36.80	39.10	36.46	40.59	38.69	45.72
Or	22.15	23.09	22.93	22.56	23.89	22.10	22.18	22.47	19.01
Ab	30.67	31.95	31.53	31.61	28.32	30.27	21.49	25.64	16.74
An	3.08	3.11	2.81	3.16	2.51	3.45	2.82	3.23	1.95
C	4.32	3.44	4.12	3.22	3.44	4.66	9.01	6.79	11.17
Hy	1.20	1.28	1.15	1.24	1.30	1.50	2.15	1.57	3.40
Mt	0.87	0.96	0.68	0.96	0.97	1.06	1.28	1.02	1.34
Il	0.33	0.38	0.04	0.41	0.43	0.46	0.44	0.54	0.65
Ap	0.05	0.05	0.05	0.05	0.05	0.05	0.05	0.05	0.02
C.I.	3.35	3.49	3.04	3.44	2.88	3.91	3.29	3.71	2.55
D.I.	94.46	94.23	95.27	94.18	94.75	93.49	93.27	93.59	92.64
Zr (ppm)	121	131	119	136	156	147	159	151	180

Section La Argentina: Major element data of ignimbrites.

Sample Elevation (m)	MW 600a 1370	MW 600b 1385	MW 600c 1410	MW 600d 1430	MW 600e 1450	MW 600f 1465	MW 600g 1490
SiO ₂	72.97	73.29	73.62	73.18	74.38	70.55	72.52
TiO ₂	0.26	0.20	0.19	0.23	0.18	0.27	0.25
Al ₂ O ₃	14.03	15.07	14.43	14.77	14.48	15.94	15.93
Fe ₂ O ₃	2.00	1.43	1.44	1.75	1.48	2.14	2.10
MnO	0.04	0.02	0.03	0.08	0.03	0.03	0.06
MgO	0.26	0.13	0.20	0.24	0.14	0.34	0.27
CaO	0.70	0.65	0.64	0.54	0.60	0.96	0.96
Na ₂ O	3.57	3.74	3.36	3.59	3.67	3.48	3.50
K ₂ O	3.85	3.78	3.55	3.87	3.96	3.53	3.63
P ₂ O ₅	0.03	0.02	0.02	0.01	0.02	0.02	0.02
BaO	0.16	0.17	0.18	0.17	0.16	0.16	0.20
L.I.	1.01	0.99	1.29	0.98	0.76	2.14	1.31
Total (%)	98.88	99.49	98.95	99.41	99.86	99.56	100.75
Q	36.13	35.90	39.59	36.28	36.56	34.82	35.70
Or	23.31	22.73	21.54	23.30	23.67	21.48	21.64
Ab	30.95	32.21	29.19	30.95	31.41	30.31	29.88
An	3.36	3.15	3.13	2.66	2.88	4.77	4.67
C	2.86	3.76	4.05	3.79	3.15	4.84	4.59
Hy	1.60	0.94	1.23	1.50	1.03	1.94	1.76
Mt	1.22	0.87	0.85	1.07	0.91	1.27	1.24
Il	0.51	0.39	0.37	0.45	0.35	0.53	0.48
Ap	0.07	0.05	0.05	0.02	0.05	0.05	0.05
C.I.	3.82	3.38	3.48	3.09	3.13	5.38	5.15
D.I.	93.25	94.60	94.37	94.31	94.79	91.44	91.80
Zr (ppm)	242	124	137	128	125	141	139